



Dissertation

Multi-Scale 3D Modeling and Parametrization of the Resource Forest Based on Airborne and Terrestrial Laser Scanning

Ausgeführt zum Zwecke der Erlangung des akademischen Grades eines
Doktors der technischen Wissenschaften (Dr.techn.)

Unter der Leitung von
Univ.-Prof. Dipl.-Ing. Dr.techn. Norbert Pfeifer

und der Mitbetreuung von
Dipl.-Ing. Dr.techn. Markus Hollaus

E 120.7
Department für Geodäsie und Geoinformation
Forschungsgruppe Photogrammetrie

Eingereicht an der Technischen Universität Wien
Fakultät für Mathematik und Geoinformation

von

Dipl.-Ing. Lothar Eysn

Matrikelnummer: 9926553
Schönbrunnerstrasse 16/15
1050 Wien
Österreich

.....
Unterschrift

Wien, am 30.November 2015



Dissertation

**Multi-Scale 3D Modeling and Parametrization of
the Resource Forest Based on Airborne and
Terrestrial Laser Scanning**

A thesis submitted in fulfillment of the academic degree of
„Doktor der technischen Wissenschaften (Dr.techn.)“^{*)}

under the supervision of
Univ.-Prof. Dipl.-Ing. Dr.techn. Norbert Pfeifer

and co-supervision of
Dipl.-Ing. Dr.techn. Markus Hollaus

E 120.7
Department of Geodesy and Geoinformation
Research Group Photogrammetry

Research conducted at TU Wien
Faculty of Mathematics and Geoinformation

by

Dipl.-Ing. Lothar Eysn

Matriculation number: 9926553
Schönbrunnerstrasse 16/15
1050 Vienna
Austria

Vienna, 30 November 2015

*) comparable to the Doctor of Engineering Sciences

A handwritten signature in black ink, appearing to read 'Lothar Eysn', is written above a horizontal dotted line.

Signature

Supervisor/Reviewer: Prof. Dr. Norbert Pfeifer
Department of Geodesy and Geoinformation
Research Group Photogrammetry
Vienna University of Technology
Gußhausstraße 27-29, 1040 Vienna, Austria.
E-Mail: Norbert.Pfeifer@geo.tuwien.ac.at

Reviewer: Prof. Dr. Juha Hyypä
Finnish Geospatial Research Institute (FGI)
Centre of Excellence in Laser Scanning Research
Geodeetinrinne 2, 02430 Masala, Finland
E-Mail: juha.coelast@gmail.com

Co-supervisor: Dr. Markus Hollaus
Department of Geodesy and Geoinformation
Research Group Photogrammetry
Vienna University of Technology
Gußhausstraße 27-29, 1040 Vienna, Austria.
E-Mail: Markus.Hollaus@geo.tuwien.ac.at

Erklärung zur Verfassung der Arbeit

Author's Statement

Hiermit erkläre ich, dass ich diese Arbeit selbstständig verfasst habe, dass ich die verwendeten Quellen und Hilfsmittel vollständig angegeben habe und dass ich die Stellen der Arbeit - einschließlich Tabellen, Karten und Abbildungen -, die anderen Werken oder dem Internet im Wortlaut oder dem Sinn nach entnommen sind, auf jeden Fall unter Angabe der Quelle als Entlehnung kenntlich gemacht habe.

I hereby declare, that I independently drafted this manuscript, that all sources and references used are correctly cited and that the respective parts of this manuscript including tables, maps and figures - which were included from other manuscripts or the internet, either semantically or syntactically -, are made clearly evident in the text and all respective sources are correctly cited.

Dipl.-Ing. Lothar Eysn
Schönbrunnerstraße 16/15
A-1050 Wien
Österreich



.....
(Unterschrift / Signature)

Table of Contents

Danksagung	ii
Kurzfassung	iv
Abstract	vi
List of Publications	viii
Abbreviations	x
1 Introduction	1
1.1 Statement of the research problem.....	2
1.2 Context of the scientific publications.....	3
2 Level of Detail Concept	4
2.1 Introduction.....	4
2.2 Levels.....	5
3 Objectives	10
4 Summary of the scientific publications	13
4.1 Article I: Forest Delineation Based on Airborne LIDAR Data.....	14
4.2 Article II: Crown coverage calculation based on ALS data.....	15
4.3 Article III: Forest Gap Delineation Based on ALS Data Using α -Shapes.....	16
4.4 Article IV: A Benchmark of Lidar-Based Single Tree Detection Methods Using Heterogeneous Forest Data from the Alpine Space.....	17
4.5 Article V: A Practical Approach for Extracting Tree Models in Forest Environments Based on Equirectangular Projections of Terrestrial Laser Scans.....	18
5 Discussion and Conclusion	20
5.1 Forest delineation.....	20
5.2 Crown Cover.....	21
5.3 Forest Gaps.....	22
5.4 Single tree extraction.....	22
5.5 High resolution tree models.....	23
5.6 General Conclusions.....	24
5.7 Key findings.....	26
Bibliography	27
Appendix A - Scientific Articles	31

Danksagung

Die Verfassung einer Dissertation und der damit verbundene Lebensabschnitt sind wie eine Schifffahrt auf dem Meer. Sonnige Tage auf glatter See bringen Weitblick, Ruhe und lassen Kraft für neue Aufgaben schöpfen. Stürmische Tage hingegen verwandeln die See in ein raues Fahrwasser, auf dem man schnell den Horizont aus den Augen verliert, dass eine stetige Neuorientierung erfordert und dem Fahrer sein ganzes Können abverlangt um nicht vom Kurs abzuweichen oder gar unterzugehen. Gut, dass man diese Reise nicht alleine antritt und von einem Netzwerk aus wunderbaren Menschen umgeben ist, die einem mit Wissen und Taten zur Seite stehen ...

Ich bedanke mich...

- ... bei Professor Kraus, der mir mit seinen hingabevollen Vorträgen den Fachbereich der Photogrammetrie schmackhaft gemacht hat.
- ... bei Norbert Pfeifer, der mich stets unterstützt hat, viele inspirierende Anstöße gab und mir die Möglichkeit eröffnete, im Wissenschaftlichen Umfeld der Photogrammetrie tätig zu werden.
- ... bei Markus Hollaus für all sein Vertrauen, seine Unterstützung und die Zeit, die er in mich investiert hat.
- ... bei Juha Hyypä für die Begutachtung dieser Arbeit.
- ... bei den Teams der Gruppen OPALS, IT, Sekretariat, Management, EODC und Fernerkundung sowie bei allen anderen KollegInnen, die immer ein offenes Ohr und gute Laune hatten.
- ... bei meinen Zimmerkollegen Philipp und Christian sowie meinen PhD Buddies Markus („der Nichttechniker“), Eva, Milutin und Werner für die lustigen, interessanten und manchmal verrückten Stunden. Danke für die schönen Momente auf Dienstreisen, für die tiefgehenden Gespräche und die manchmal ausufernden, wilden Partys.
- ... bei meinen neuen KollegInnen in der MA41 für die nette Aufnahme in ihr Team.

Spezieller Dank gilt den vielen lieben Menschen aus meinem privaten Umfeld. Ihr habt mich durch gute wie auch schlechte Zeiten getragen. Eure Freundschaft, Bindung und Unterstützung ist unglaublich wichtig und schön. An dieser Stelle alle Namen zu nennen würde Seiten füllen und so erlaubt mir bitte, den Dank pauschal auszusprechen.

Größter Dank gilt...

- ... meiner Frau Daniela, die mich in allen Phasen der letzten Jahre begleitet und bestärkt hat. Sie ist mein Fels in der Brandung und ohne sie wäre diese Dissertation wohl nie entstanden.
- ... den Familien Eysn und Rauchwarter für ihre Fürsorge und den endlosen Support.

Ich möchte diese Danksagung mit einem Motto beschließen, das mich während der letzten Jahre durch meine wissenschaftlichen Tätigkeiten begleitet hat:

DREAM IT – WISH IT – LIVE IT – DO IT

but

WHEN NOTHING GOES RIGHT – GO LEFT

Diese Arbeit wurde teilweise durch die Projekte LASERWOOD (Klima- und Energiefonds – Neue Energien 2020, 822030), ChangeHabitats2 (Marie Curie-FP7-People-2009-IAPP), 3DVeglab (ESA STSE AO/1-6529/10/I-NB), NEWFOR (European Territorial Cooperation „Alpine Space“, 2-3-2-FR), sowie durch die Technische Universität Wien finanziert.

Kurzfassung

Ungefähr ein Drittel der Landfläche der Erde ist durch Wald bedeckt. Der Wald erfüllt Ökologische und Ökonomische Funktionen für Mensch und Tier und dient als Ressource und Habitat. Die Domäne der Forstwirtschaft und Forstwissenschaft beschäftigt sich mit der Erhaltung und Bewirtschaftung der Wälder und ihrer Funktionen. Eine wesentliche Aufgabe ist dabei die Analyse von Zuständen und Prozessen im Wald. Dazu werden unter anderem Modelle des Waldes benötigt. Als unterstützende Maßnahme zur Analyse und Lösung von verschiedenen Fragestellungen aus forstbezogenen Anwendungen können Daten und Produkte aus den Domänen der Fernerkundung und Photogrammetrie verwendet werden. Neue Fernerkundungstechnologien, wie zum Beispiel Flugplattform getragenes Laserscanning (ALS) oder terrestrisches Laserscanning (TLS) ermöglichen die Erfassung von detaillierten 3D Informationen über das Kronendach von Waldbeständen sowie die Erfassung einzelner Bäume. Basierend auf diesen Daten können verschiedene Modelle der hohen Vegetation extrahiert und beschrieben werden. Diese Modelle weisen unterschiedliche Granularität auf, und modellieren die Vegetation in einem größeren oder geringeren Ausmaß. Die Granularität hängt hauptsächlich von der Zielanwendung, der Qualität der Eingangsdaten sowie dem gewünschten Zielmaßstab ab. Anwendungen, wie beispielsweise die Abgrenzung von Waldgebieten, die Erkennung von einzelnen Bäumen oder die Gewinnung von Informationen über einzelne Bäume oder Waldbestände können von Laserscandaten sowie den daraus extrahierten Modellen profitieren.

Die Ziele dieser Dissertation sind (i) die Analyse und Weiterentwicklung von Methoden, die Vegetation auf mehreren Skalen modellieren und (ii) die Extraktion von Vegetationsparametern basierend auf Daten des Laserscannings. Dazu gehört die Entwicklung von ALS basierten Verfahren für die Abgrenzung von Waldflächen und Waldlücken, sowie die Schätzung von Parametern und Positionen einzelner Bäume. Außerdem wird ein TLS basiertes Verfahren zur 3D-Modellierung von Stämmen und Zweigen einzelner Bäume entwickelt. Zusätzlich wird ein geometrisch getriebenes Levels of Detail Konzept für die Modellierung hoher Vegetation vorgestellt. Das an bestehende Modellierungskonzepte der Stadtmodellierung angelehnte Konzept besteht aus sechs Stufen, und ermöglicht eine Modellierung der Ressource Wald mit unterschiedlicher Granularität. Die ersten drei Stufen beschreiben die Vegetation ausschließlich in 2D oder 2.5D. Sie können zur Modellierung von Waldflächen, Waldbeständen oder individuellen Objekten verwendet werden. Die letzten drei Stufen ermöglichen eine Modellierung von individuellen Objekten im 3D-Raum. Die Beschreibung generischer Modelle (z.B. Ellipsoid oder Alpha-Hülle auf einer Stange) sowie detaillierter Modelle von Strukturelementen (z.B. Stamm, Äste) einzelner Bäume wird in diesen Stufen ermöglicht.

In fünf Forschungsartikeln wurden drei Stufen des Modellierungskonzeptes näher studiert. Die vorliegenden Studien wurden bereits in mehreren begutachteten Fachzeitschriften und Konferenzbeiträgen publiziert. Artikel I, II und III untersuchen das Potenzial von ALS für (i) eine Wald - Nichtwald Klassifizierung / Abgrenzung, (ii) die Ermittlung des

Überschirmungsgrades und (iii) die Abgrenzung und Klassifizierung von Waldlücken. Die vorgestellten Methoden liefern automatische, reproduzierbare und objektive Ergebnisse bei großer Flächenleistung und zeigen hohes Potenzial für die untersuchten Anwendungen. Artikel IV untersucht das Potenzial von acht ALS basierten Einzelbaum Detektionsmethoden basierend auf einem heterogenen Datensatz von ALS Daten und Forstinventurdaten aus dem Alpenraum. Artikel V untersucht ein Verfahren zur Extraktion von Baumstruktur und Volumetrischen Modellen auf Basis von TLS Daten. Auf Grundlage der vorgelegten Studien konnte nachgewiesen werden, dass Laser-Scanning ein leistungsfähiges Werkzeug zur Erfassung und mehrskaligen Modellierung von hoher Vegetation ist.

Aus dieser Dissertation ergeben sich vier Schlüsselergebnisse:

1. Die Modellierung und Quantifizierung von hoher Vegetation impliziert die Notwendigkeit für Modelle mit unterschiedlicher Granularität. Diese Modelle können in verschiedenen Detaillierungsgraden definiert und kategorisiert werden. Die vorgeschlagenen Modelle ermöglichen die Beschreibung von aggregierter Informationen mehrerer Objekte bis hin zu einer detaillierten Beschreibung einzelner Objekte. Die Beschreibung einzelner Strukturteile von Bäumen (z.B. Stamm, Äste, Nadeln/Blätter) in Stufe 5 stellt die höchstmögliche Modellierungsstufe dar.
2. Laser Scanning (ALS oder TLS) ist eine leistungsfähige 3D Erfassungsmethode, und stellt eine gute Datenquelle für die Modellierung der Ressource Wald in verschiedenen Skalen dar. Alle vorgeschlagenen Modellierungsstufen können aus Laserscandaten abgeleitet werden. Einschränkungen des Laser Scannings ergeben sich aus der begrenzten Sichtbarkeit von Objekten, den physikalischen und geometrischen Einschränkungen der Messmethode sowie der Geometrie in der Datenerfassung. Die Zielanwendung und der Maßstab des gewünschten Modells definieren, welche Art von Laserscanning Daten zu favorisieren sind.
3. Mit steigendem Detaillierungsgrad sinkt die allgemeine Qualität der Ergebnisse. Die beste Genauigkeit konnte für "einfache" Modelle wie beispielsweise im Modell der Stufe 0 ermittelt werden.
4. Die im Bereich der Forstwirtschaft und Forstwissenschaft verwendeten Definitionen sind vielfach nicht rein geometrisch, was jedoch für die Nutzung von Laserscandaten von Vorteil wäre. Bis jetzt sind viele der existierenden Definitionen nicht vollständig mit der Genauigkeit von Laserscanning kompatibel.

Abstract

Forests cover nearly a third of the world's total land area, fulfil ecological and economical functions for humans and animals, and can be seen as a resource and habitat. The domain of Forestry is concerned with the maintenance and management of forests and its functions. A fundamental task is analyzing states and processes within the forest. To do so, models of the forest are required. Data and products from the domains Remote Sensing and Photogrammetry can help to tackle different questions in forestry related applications. New remote sensing technologies as for example airborne or terrestrial laser scanning enable the acquisition of detailed 3D information about the forests canopy or single trees. These data can be used to extract different models that describe tall vegetation. The models can have different granularity and model the vegetation to a greater or lesser extent. The granularity mainly depends on the target application, the quality of the input data and the desired scale. Applications as, for example, the delineation of forested areas, the detection of single trees or the extraction of detailed information about single trees or forest stands can benefit from laser scanning data and the models extracted from it.

The objectives of this dissertation are the analysis and further development of methods to model vegetation at multiple scales and the extraction of vegetation parameters based on laser scanning data. This includes further development of airborne laser scanning based methods for delineating forested areas and forest gaps as well as estimating single tree parameters and positions. Furthermore, methods for terrestrial laser scanning based 3D modeling of stems and branches of single trees are developed. In addition, inspired by the modeling concept used in city modeling, a geometrically driven Level of Detail concept for tall vegetation is proposed. It consists of six levels, which describe the resource forest with different granularity. The first three levels model the vegetation exclusively in 2D or 2.5D and can be used to model e.g. forest area, forest stands or individual objects. The last three levels enable modeling in 3D space. They can be used to extract generic models of single trees (e.g. ellipsoid on stick, alpha hull on stick) or detailed models describing the structural elements of trees (e.g. stem and branches).

Three Levels are further investigated and evaluated in five research articles. The present studies have already been incorporated in several peer-reviewed journals and conference papers. Article I, II and III investigate the potential of airborne laser scanning for being used (i) in a forest – non-forest classification / delineation, (ii) to extract the criterion of crown coverage and (iii) to delineate and classify forest gaps. The presented automatic methods show high potential, as they deliver repeatable and objective results for large areas at low processing cost. Article IV investigates the potential of eight airborne laser scanning based single tree detection methods using a unique heterogeneous dataset from the Alpine Space. Finally, Article V investigates a method for extracting tree topology and volumetric models based on terrestrial laser scanning data. The presented studies prove, that laser scanning, either performed airborne or terrestrial, is a powerful tool to capture and model vegetation across multiple scales.

The dissertation results in four key findings:

1st Modeling and quantifying tall vegetation implies the need for models with different granularity. These models can be defined and categorized in different Levels of Detail. The models range from aggregated information to detailed information about individual objects. Level 5, which describes a model of structural tree parts (e.g. stem, branches, needles), is the highest possible modeling level.

2nd Laser scanning (ALS or TLS) is a powerful 3D mapping tool and a good data source for modeling the forest environment at different scales. All suggested modeling levels can be obtained from laser scanning data. Some limitations occur due to a limited visibility of objects, physical and geometrical constraints of laser scanning and limitations in the acquisition geometry. The target application and the scale of the desired model define, which type of laser scanning data are in favor.

3rd With increased LoD the overall quality of the results decreases. The best result could be obtained for “simpler” models as for example the Level 0 models.

4th The definitions used in the domain of Forestry are not purely geometric, but this would be advantageous for exploiting laser scanning data. Up to now, many of the existing definitions are not fully compatible with the exactness of laser scanning data.

List of Publications

This thesis is based on the work contained in the following papers, referred to by Roman numerals in the text:

- I L. Eysn, M. Hollaus, K. Schadauer, N. Pfeifer: "Forest Delineation Based on Airborne LIDAR Data"; *Remote Sensing*, 4 (2012), 3; 762 - 783. (peer reviewed journal paper)
Online available at: <http://www.mdpi.com/2072-4292/4/3/762>
- II L. Eysn, M. Hollaus, K. Schadauer, A. Roncat: "Crown coverage calculation based on ALS data"; *Proceedings of the 11th International Conference on LiDAR Applications for Assessing Forest Ecosystems (Silvilaser 2011)*, Hobart, Australia; 2011-10-16 - 2011-10-20; 10 pages. (reviewed conference paper)
Online available at: http://publik.tuwien.ac.at/files/PubDat_202289.pdf
- III L. Eysn, M. Hollaus, W. Mücke, M. Vetter, N. Pfeifer: "Waldlückenerfassung aus ALS Daten mittels α -Shapes"; *Talk: Dreiländertagung - 30. Wissenschaftlich-Technische Jahrestagung der DGPF*, Wien; 2010-07-01 - 2010-07-03; in: "Publikationen der Deutschen Gesellschaft für Photogrammetrie, Fernerkundung und Geoinformation e.V.", Band 19 (2010), 9 pages. English Translation: Forest Gap Delineation Based on ALS Data Using α -Shapes. (conference paper)
Online available at: http://publik.tuwien.ac.at/files/PubDat_189897.pdf
- IV L. Eysn, M. Hollaus, E. Lindberg, F. Berger, J. Monnet, M. Dalponte, M. Kobal, M. Pellegrini, d. Lingua, D. Mongus, N. Pfeifer: "A Benchmark of Lidar-Based Single Tree Detection Methods Using Heterogeneous Forest Data from the Alpine Space"; *Forests*, 6 (2015), 5; 1721 - 1747. (peer reviewed journal paper)
Online available at: <http://www.mdpi.com/1999-4907/6/5/1721>
- V L. Eysn, N. Pfeifer, C. Ressler, M. Hollaus, A. Grafl, F. Morsdorf: "A Practical Approach for Extracting Tree Models in Forest Environments Based on Equirectangular Projections of Terrestrial Laser Scans"; *Remote Sensing*, 5 (2013), 11; 5424 - 5448. (peer reviewed journal paper)
Online available at: <http://www.mdpi.com/2072-4292/5/11/5424>

All papers are reproduced with the permission of the publishers.

The contribution of Lothar Eysn to the papers included in this thesis was as follows:

- I Developed the delineation method, implemented the workflow, performed the analyses and validation, and wrote the major part of the manuscript.
- II Developed the tree-triples approach, implemented the workflow, performed the analyses and validation, and wrote the major part of the manuscript.
- III Developed and implemented the forest gap delineation method, performed the analyses, and wrote the major part of the manuscript.
- IV Planned and organized the experiment, developed and implemented the matching method, performed the analyses, and wrote the major part of the manuscript.
- V Planned and managed the field experiment, developed parts of the modeling approach, implemented parts of the workflow, processed the terrestrial laser scanning data, performed the analyses and validation of the models, and wrote the major part of the manuscript.

The studies of the Articles I to III were carried out during the project LASERWOOD, funded by the Klima- und Energiefonds – Neue Energien 2020 (ID: 822030). This project was dealing with the extraction of forest related parameters from airborne laser scanning data. One work package included studies regarding the extraction of forest area and forest gaps.

The study of Article IV was carried out in the framework of the project NEWFOR, funded by the European Territorial Cooperation „Alpine Space“ (ID: 2-3-2-FR). The main objective of the NEWFOR project was the improvement of mountain forest accessibility for a better efficiency of wood harvesting and transport in a context of sustainable forest management and wood industry.

The study of Article V was performed within the ESA funded project 3DVeglab (ID: ESA STSE AO/1-6529/10/I-NB). One of the main goals of this project was to model a forest stand from TLS data at a very high level of detail. The virtual scene was used to calculate ray tracing in forest environments simulating the signal paths of future Sentinel satellites.

Abbreviations

2D	Two-Dimensional
2.5D	Two-and-a-Half-Dimensional
3D	Three-Dimensional
ALS	Airborne Laser Scanning
CC	Crown Cover
CHM	Canopy Height Model
DBH	Diameter at Breast Height
DSM	Digital Surface Model
DTM	Digital Terrain Model
EO	Earth Observation
GIS	Geographic Information System
GPS	Global Positioning System
GNSS	Global Navigation Satellite System
LIDAR	Light Detection and Ranging
LOD	Level of Detail
nDSM	Normalized Digital Surface Model
NFI	National Forest Inventory
RMSE	Root Mean Square Error
RPAS	Remotely Piloted Aircraft System
RS	Remote Sensing
TLS	Terrestrial Laser Scanning

1 Introduction

The increased technologization of the society changed, and still changes, its way of living as well as its demands and needs in a modern world. One rising demand is the need for up to date geometrical and analytical representations of the society's environment, whereat representations of the natural- and built environment can be 2D models (maps), 3D models or extracted parameters originating from descriptive models. Such models and parameters show great potential for being used in a wide range of applications and for supporting processes in the daily business of different domains as, for example, industry, public sector or research. A prominent example using such data are digital globes such as Google Earth [1,2], NASA World Wind [3] or Web-based visualization platforms [4,5], which opened up a large field of new possibilities and applications as they provide an easy and accessible way of visualizing and distributing all sorts of data in a geographical context.

Depending on the application, the natural and built environment can be modeled at multiple scales, which means that the abstraction process of modeling the real world is carried out to a fewer or greater extend. Therefore, models of different scale show different levels of detail (LOD). This LOD concept is already established and close to standardization in selected fields (e.g. 3D city modeling, cartography), where technical details and terminology are well defined. Different data models are established to tackle the task of geometrically and semantically modeling the environment. Two examples, which were officially established as Open GIS standards by the Open Geospatial Consortium (OGC) [6] in 2008 [7,8], are the City Geography Markup Language (CityGML) [9-12] and the Keyhole Markup Language (KML) [13]. The CityGML standard introduces a five step LOD structure for city and landscape modeling, addressing, beyond others, the thematic areas Buildings, Landuse and Vegetation. For the field of building modeling in urban areas a rather clear understanding of the different LODs and the related complexity of the models exists, which implies that this field is well developed. This can be seen in analogy to the ongoing building information modeling (BIM) trend [14]. However, the field of vegetation modeling is still developing and up to now, no clear definitions regarding modeling vegetation objects exists in the standards. Therefore the requested model complexity within each LOD remains unclear.

Contrary to this situation, a huge trend in vegetation modeling is visible in the domain of forestry, forest management and forest research. The domain of forestry is the science and craft of maintaining and managing forests with respect to timber, water, wildlife, recreation and other values [15,16]. Forests cover nearly a third of the world's total land area [17] and therefore advanced tools are prerequisite to handle this demanding task. The number of published research articles regarding modeling the resource forest and extracting forest parameters from it is increasing. A great variety of modeling approaches addressing different forestry related questions can be found in the literature, which can be categorized into area-based approaches and single tree based approaches [18]. This trend is mainly driven by two aspects, which are (i) an increased demand for models and parameters for sustainable management of forest stands and the resource forest in general (e.g. precision forestry [18]),

and (ii) the continuous development of Earth observation (EO) methods coupled with an increased availability of extensive remote sensing (RS) data.

The use of RS data has a long tradition in the domain of forestry and has been a valuable source of information over the course of the past few decades in mapping and monitoring forest activities. The field of remote sensing began with fully manual methods of analysis applied to aerial photographs, but has since gone to rely on new data and methods [19]. One of these rather new RS methods is the technology of laser scanning (often referred to as Lidar), which is an active measuring technology that enables sampling and discretizing of objects in 3D space using coherent light. Laser scanning can be carried out spaceborne, airborne or terrestrially, which results in different acquisition constellations and consequently different levels of data quality and density. For example, spaceborne lidar is able to deliver information about the canopy's top heights and volume [20,21], while airborne laser scanning (ALS) additionally offers information about single objects and their structure inside the canopy [22-25]. Terrestrial laser scanning (TLS) delivers detailed information about the structure of single trees and their foliage [26,27]. However, this dispersion of laser scanning data is promising in terms of gaining deeper knowledge about the resource / habitat forest by parametrizing and modeling this environment at different LOD.

The goal of this thesis is to bring together the aspects of modeling vegetation at different LOD with the advantages of laser scanning in forests. The thesis is carried out cumulative, bringing together five published articles regarding this topic. In chapter 1 an introduction and the statement of the research problem are presented. In chapter 2, a level of detail concept for modeling forest environments is proposed while chapter 3 outlines the detailed objectives of this thesis. Chapter 4 includes a summary of the research articles. Finally, a discussion and conclusion is drawn in chapter 5. The scientific Articles are presented in Appendix A.

1.1 Statement of the research problem

Is laser scanning a suitable tool for modeling vegetation across a range of scales? This leads to a number of more detailed questions. What are the coarsest and the finest scales to investigate? How can modeling be performed at a specific scale? For answering the first question ("which scales?") a suggestion will be made in chapter 2. It is strongly linked to the LOD concept of CityGML. For answering the second question ("how to model?") individual methods will be developed and/or investigated. Concerning the publication of research articles, these models build the core of this thesis. These include (i) the delineation of forested areas and forest gaps based on ALS data, (ii) the identification of single trees based on ALS data, and (iii) the modeling of wooden tree parts based on TLS data. Beside the geometric modeling task, different forest parameters (e.g crown coverage) are extracted and investigated.

An important aspect of this thesis is to show the potential of laser scanning for modeling forests at different LOD and to discuss the benefits and drawbacks of the presented methods.

1.2 Context of the scientific publications

This thesis and the contained scientific publications are presented in the context of Earth observation, Photogrammetry and monitoring in Forestry. A strong aspect of multi-scale forest vegetation modeling is the acquisition and interpretation of RS (laser scanning) data and the consequent extraction of geometrical models from it. This task is strongly related to EO and Photogrammetry, as RS is a subcategory of EO and geometrically modeling is in the domain of Photogrammetry. Parameters, extracted from the models or the raw data itself, are of interest for the Forestry domain. The whole process of abstracting the real world to models of different LOD is important for the field of environmental modeling.

EO is the gathering of information about planet Earth's physical, chemical and biological systems via RS technologies supplemented by ground based observations (in-situ measurements), encompassing the collection, analysis and presentation of data [28,29]. RS embraces all methods of remotely acquiring information about the Earth's surface by means of measurement and interpretation of electromagnetic radiation either reflected from or emitted by it. Photogrammetry allows to reconstruct the position, orientation, shape and size of objects from pictures as for example laser scanning images [30]. The domain of forestry is concerned with the maintenance and management of forests for timber, water, wildlife, recreation and other values [15].

2 Level of Detail Concept

2.1 Introduction

Analyzing states and processes of vegetation often requires models of the vegetation. Such analysis may include estimating forest biomass [31,32], habitat assessment [33], ray tracing for satellite data simulation [34], landscape planning and analysis [5,35], but also visualization in city modeling [36]. The model of the vegetation is prescribed by the application and may reach from very simple models, e.g. paraboloids or “ellipsoids on sticks” [37], to detailed modeling of each leaf [38].

The “Level Of Detail” concept allows modeling through scale space, in the sense of – continuously [39] or stepwise [10] – looking at a phenomenon from very far away to “close up”, from aggregated information to individual objects. Phenomena in vegetation occur at a variety of scales, thus different models of vegetation are in use. Different LOD are also necessary in city modeling [10]. Starting from level 0 to level 4 increased detail is added in the CityGML [10] framework: 0) orthophoto, 1) block model of each building (e.g. building footprint and building height), 2) main roof structure and facade images, 3) detailed roof structure and geometric model of the facade (windows, etc.), 4) architectural model of the interior. Essentially, the level of detail measure indicates how much detail is included in the model element.

The abbreviation LOD is also used in the context of BIM, but has a different meaning as it describes the level of development of a model element. In essence, level of detail can be thought of as input to the element, while level of development is a measure of reliability of the output [40].

In this thesis, research having different level of detail is conducted, and since there is no clear definition to LOD in forestry, a possible definition used in this thesis is depicted here in Chapter 2. The proposed LOD scheme refers to the LOD concept of CityGML. A geometrically driven level concept is suggested, providing, however, means for the necessary biological or environmental description at each level in order to make it useful in a specific application. The restriction to tall vegetation is stated in the sense of the tree and tall shrub layer, but does not include the herbaceous layer or fungi. The suggested description of vegetation is independent of a data acquisition method. It is applicable to purely artificial models “growing” the trees from a set of parameters, models reconstructed from Earth observation data from different platforms, terrestrial to satellite, and also to combined models [41-44].

Defining these levels shall allow better communication between producers and users of vegetation models.

2.2 Levels

Following the concept of CityGML, six different LOD are proposed for vegetation models. The quality of the data, e.g. accuracy, precision, and reliability are not prescribed for the specific levels. Furthermore, descriptions at a certain level may also have different accuracy. Thus, a specific quality is rather associated with each single parameter of the descriptions. It is proposed, however, to introduce a quality for each parameter. Deviations need to be clearly communicated in order to prevent inappropriate use of the data.

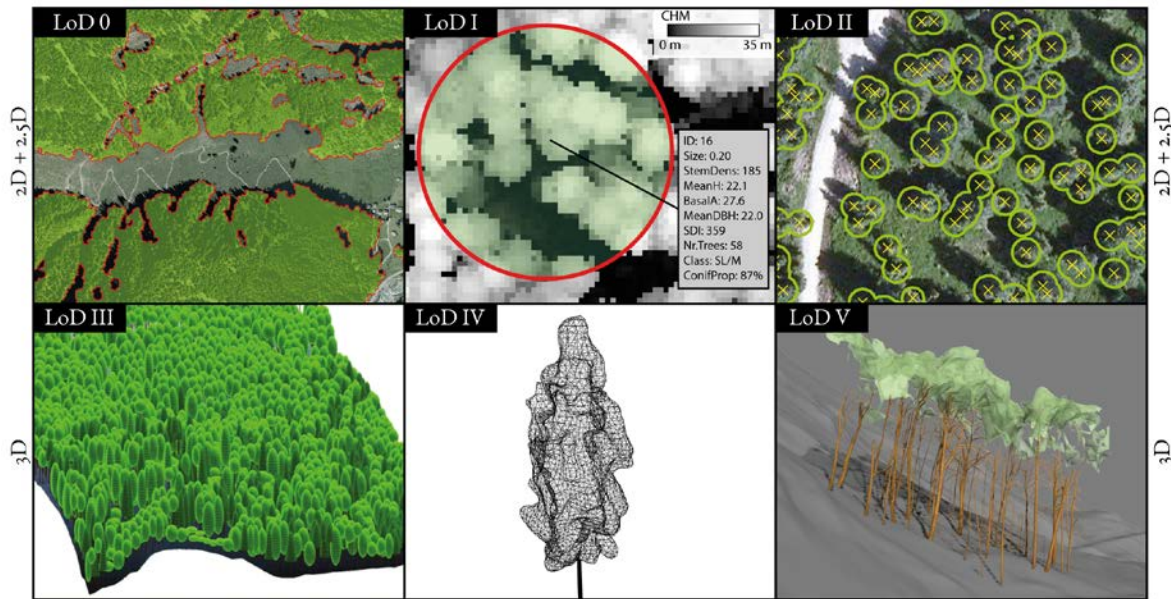


Figure 1: Graphical examples of the different levels. LOD 0 shows a forest mask polygon. LOD 1 shows a forest Inventory plot with metadata obtained by an inventory and RS data. LOD 2 shows single tree positions and estimated crowns approximated as circles. LOD 3 shows a modeled forest scene using generic single tree models (Image Reference: [45]). LOD 4 shows the model of a single tree crown modeled with an alpha-shape. LOD 5 shows a forest scene with volumetric models of the wooden tree parts. Additionally the CHM and DTM is visualized in 3D.

2.2.1 Level 0

Level 0 provides a 2D outline of an area consisting of tall vegetation, separating it from regions without. The modeling result is the so called forest mask which gives information on the location and spatial extent of forested areas. The geometrical localization and geometry of the objects is more important than its implied vegetation properties. The formal model includes a region polygon and an identifier. The geometric primitives are polygons with one exterior boundary and zero or more interior boundaries. The identifier is required to enable linking of statistical information.

In Article I, a method for obtaining level 0 models from ALS data is presented and discussed (see 4.1). A special focus on the interior boundaries is given in Article III (see 4.3).

2.2.2 Level 1

Level 1 provides information about forested areas, aggregated beyond the individual plant. From a geometric point of view, level 1 provides (i) 2D information on location and spatial extent of objects and (ii) 2.5D [46] or 3D information regarding the vegetation's vertical characteristics (e.g. local heights). From a user perspective, additional information about the vegetation properties (e.g. number of stems per hectare) on the spatial units should be of high importance at this aggregation level. Therefore, this is considered as more relevant than an exact geometrical localization. The vegetation properties are stored in attributes, whereat the aggregation of the data can be a classification, statistical measures or links to external data. An object identifier is mandatory to set up a unique link between geometry and attributes. It provides a link to an external database (e.g. Esri Shape), which allows additional entries.

Level 1 allows modeling a stand. The granularity is not prescribed, so multiple forest stands may be aggregated to one. This level can, however, also be used to model a plot, which has a location and an average tree height. Aggregated geometric information beyond the proposed elements, e.g. an average crown diameter, can be linked to the object using the identifier. Such a model is appropriate to describe the information collected by forest inventories.

Location and spatial extent are described by the outline of the element, e.g. "the vegetation". This may be the boundary of a forest stand or the circle of a sample plot. The geometric primitives are points or polygons with one exterior boundary and zero or more interior boundaries. The 2.5D or 3D information, complementing the 2D geometric information, can be one height value, for example the average height of the dominant (typically the topmost) vegetation layer, or a reference to a canopy height model (CHM), also called normalized digital surface model (nDSM). The height information can be either stored with the geometry (polygon is set to a certain z-value) or can be linked with an attribute.

The vegetation properties can be described by a set of categories, comprising the tree species, a formal description of the vertical and horizontal structure [47] and other stand characteristics like for example site indices, age classes, wood quality or insect diseases [47,48]. Species information should be at an aggregated level (e.g. conifer, deciduous, mixed, or unknown) but may also be more detailed if for example the main tree species are named. Regarding the horizontal structure a classification (e.g. densely stocked, sparsely stocked) or statistical measures should be given (e.g. number of stems per hectare; stand density indices; crown cover percentage [49]). This also applies to information regarding the vertical vegetation structure [50]. A classification (e.g. single-layered, dual-layered or multi-layered) or statistical measures (e.g. number of layers; mean height of the living crown) can be stored within the attributes. The same applies for other stand characteristics (e.g. mean diameter at breast height (DBH)).

In addition, quality measures regarding the geometry or attribute information can be given. A quality measure of the vegetation outline may include both, accuracy of acquisition as well as intended generalization. Other quality measures could be for example the threshold for applied classifications or the caliper threshold used in the forest inventory to limit the minimum DBH to be mapped.

In Article II, the extraction of the vegetation property crown coverage (horizontal structure) based on ALS data is presented and discussed (see 4.2). In Article IV, statistical forest inventory measures are presented and used to classify the benchmarking results (see 4.4).

2.2.3 Level 2

In level 2, vegetation objects are modeled in 2D or 2.5D at the level of individuals. Single trees or shrubs become independent models with assigned geometries and attributes. The description of these objects are, however, very generic. Like in level 0 and level 1, location, geometry and properties of the objects are important. The objects are modeled as points or polygons with additional attribute information. In case of a point based representation of an object (e.g. a single tree), the geometrical localization is described by a coordinate tuple (2D case) or triple (2.5D case). This point-wise representation is common in forest inventories, where single tree information is condensed and assigned to a spatial reference per tree. Quality information as for example the semantic of the point (e.g. it represents the highest crown point or the stem point above ground) and the relative and absolute spatial accuracy should be presented.

Vegetation properties are stored to the spatial reference. These can be described by a set of categories, comprising the tree species, a formal description of the vertical tree structure [47] and other tree characteristics. Common properties determined in forest inventories are geometrically driven measures as for example tree height and DBH. 2D Crown shape metrics providing information about approximating geometrical primitives (e.g. circle or ellipse with axis and orientation information) or supplementary 3D metrics regarding the vertical structure of the tree or tree crown might be added. In addition to the point-wise model, the crown can be modeled as 2D polygon, following the crowns outer edge, or approximating the crown as circle or ellipse.

The most important not geometrically interpretable parameter is the species, thus complementing the above parameters. The tree species attribute should follow standardized botanical species classifications as for example described by Carl Linnaeus [51]. Other attributes may act as a formal description of the tree's structure, condition and environment.

In Article IV, LOD 2 models are used to model forest inventory data. The point-based representation of single trees is used in the matching procedure between FI data and ALS derived tree positions (see 4.4).

2.2.4 Level 3

In contrast to LOD 2, this level models the vegetation in 3D space. The models represent single trees and provide a rather generic description of the reality. Trees are represented as geometrical primitives on sticks (e.g. ellipsoids on sticks), whereat the primitive represents the crown and the stick represents a stem. An object based identifier links attributes to the 3D objects. Crown shape metrics are used to describe the geometrical primitives (e.g. sphere, cone, ellipsoid, half ellipsoid or paraboloid). The crown shape descriptor includes parameters describing the orientation, height and how pointed it is (e.g. major axis, minor axis, azimuth of crown ellipse). The geometrical location and extent of the stick is described by (i) a 3D point defining the stem axis at the forest floor and (ii) a starting height of the crown. The stick is always modeled vertically.

Like in LOD 2, quality measures regarding the location of the stem, metrics regarding the crown or other vegetation properties (e.g. FI data) are stored in attributes. Their content acts as a formal description of the tree's structure, condition and environment.

level 3 can be used to visualize a forest stand and its corresponding forest inventory data in 3D space. The model detail is still low, but the spatial distribution of objects and the shape of the crowns illustrate the spatial composition of the forest patch. Supplementary information about the objects properties add to the geometrical representation.

2.2.5 Level 4

Level 4 is the first level, where object characteristics, as for example the vertical distribution of a tree crown, are modeled in 3D. This means, that the individual shape of the tree and its crown are explicitly modeled in 3D space. Therefore, in level 4 the deviations from the generic level 3 models are incorporated. Trees are modeled with a stem object and a crown object. Because of the increased LOD, stem and crown objects may consist of multiple objects, but they still generalize the reality to a high extent.

The stem can be modeled as a skeleton or a volumetric object. In case of a skeleton, a 3D polyline or axis is defined by two or more 3D points. In the volumetric case, simple geometrical models (e.g. frustum) or complex models (e.g. axis buffered by radii obtained from a stem curve) are used. The crown is represented by a geometric model of the crown hull, understood as a surface. For example, this can be obtained by an alpha shape, derived from a 3D triangulation [50,52]. Alternatively, stacked polygons, obtained from height slides of the crown, can be used. An object identifier links attributes to the 3D objects. The attributes may contain information about the tree's structure, condition and environment.

Depending on the level of detail of the crowns alpha shape, the volumetric model of the crown is already the most detailed volumetric representation possible. Further modeling will turn the volumetric model into a description of single foliage objects (see LOD 5).

The LOD 4 model is especially useful for 3D visualizations (e.g. in low level environmental models). The models are useful to perform a classification of tree types. The characteristics of a set of trees can be useful to classify stands or to derive habitat quality measures.

2.2.6 Level 5

The individual elements of the vegetation objects are modeled at a high LOD. The modeling process is strongly data driven. Therefore, the input data must be very accurate and detailed. Mainly TLS data or data collected by RPAS based scanning are used to model this level. Complex tree topology is represented as a network (skeleton), following the real structure with minimum generalization. The foliage is represented by individual elements.

The stem and branching network is described as a graph, consisting of line elements or curves as edges and vertices at structural changes in the real object. Local radius information or fitted elliptical elements, obtained at the location of the vertices, are used to extrude the skeleton to a volumetric model. The foliage is represented as independent geometric objects. Patches of needles/leaves or single needles or leaves are modeled. Ellipsoids, hyperboloids or planar faces are used as geometrical representatives. In contrast to geometrically driven LOD 5 models, fine scaled voxel models might be used to represent the objects. If this is the case, patches of corresponding voxels need to be aggregated to become objects.

All modeled objects have their own identifier. Attributes containing information about e.g. the local branch radius or the ID of the whole tree/shrub can be linked. Beside the geometrical properties and descriptive properties, physical properties can be assigned to the modeled

objects. Examples are parameters regarding surface reflectivity or roughness. Physical properties are common in the domain of radiative transfer modeling.

The introduction of quality measures help to treat the quality of the model. Quantitative (e.g. deviations of fitted objects) and qualitative (e.g. completeness of the modeled object) statistical measures should be used.

In Article V, LOD 5 models are extracted from terrestrial laser scanning data. Beside the extraction of the branching structure, statistical attributes are presented (see 4.5).

3 Objectives

The objective of this thesis is to further develop the methods to model vegetation at multiple scales and to extract vegetation parameters based on laser scanning data. This includes further development of ALS based methods for delineating forested areas and forest gaps as well as estimating single tree parameters and positions. Furthermore, methods for TLS based 3D modeling of stems and branches of single trees are developed.

The specific objectives as well as the novelties of the approaches for the Articles I-V are:

I Forest Delineation Based on Airborne LIDAR Data:

- (a) Investigate the potential of ALS for classifying forested areas.
- (b) Develop statistical methods to estimate tree crowns based on ALS data.
- (c) Develop, implement and validate a method to automatically delineate forested areas based on operational ALS data using clearly defined geometrical criterions. Use flexible criterions to meet the needs of different forest definitions.

Novelty of the approach:

Development of a robust method for delineating forested areas based on four clearly defined criterions. The method can be adapted to different forest definitions. Artificial objects are automatically removed. The crown coverage check is based on a network of detected single trees (tree triples approach). The tree crown diameters of single trees are estimated based on tree heights and local altitude. The relating function can be set up from ALS data or NFI data.

II Crown coverage calculation based on ALS data:

- (a) Investigate the potential of ALS for deriving crown coverage.
- (b) Develop and validate a method to automatically calculate crown coverage based on ALS data and NFI data.
- (c) Detect single trees and estimate their crowns based on a relation obtained from NFI data

Novelty of the approach:

Obtaining information about local crown coverage by using ALS data. A network of detected single trees and estimated crowns is used to obtain the local crown coverage (tree triples approach). In contrast to moving window approaches this method overcomes the reference size problem.

III Forest Gap Delineation Based on ALS Data Using α -Shapes:

- (a) Analyze the potential of ALS for delineating and classifying forest gaps.
- (b) Develop a method for delineating the forest area.
- (c) Develop a method to reveal forest gaps from ALS data.

Novelty of the approach:

ALS data based delineation of forest gaps using α -shapes. Classification of the detected gaps based on the gap size.

IV A Benchmark of Lidar-Based Single Tree Detection Methods Using Heterogeneous Forest Data from the Alpine Space:

- (a) Investigate the potential of different ALS based single tree detection methods.
- (b) Set up a heterogeneous dataset of existing ALS data and NFI data from different areas in the Alpine Space.
- (c) Develop, implement and validate a method to automatically match different single tree detection results to ground truth data.
- (d) Develop and apply statistical methods to analyze the matching results.

Novelty of the approach:

The first single tree detection benchmark ever being performed for study areas within the Alpine Space. Usage and release of a freely available dataset for future studies. Development of a clearly defined matching procedure.

V A Practical Approach for Extracting Tree Models in Forest Environments Based on Equirectangular Projections of Terrestrial Laser Scans:

- (a) Investigate the potential of TLS based 2D maps for revealing tree skeletons and volumetric models.
- (b) Develop a concept for the field experiment
- (c) Develop and validate methods to automatically create TLS based 2D maps and to semi-automatically extract 3D tree skeletons and volumetric models based on these maps.

Novelty of the approach:

Development and application of a method for extracting detailed 3D tree models based on 2D maps derived from TLS data. A large number of trees (e.g. a whole forest stand) can be modeled. The method was successfully applied to a forest stand of 90 trees.

VI An additional objective was to formalize the representation of forest models at different scales within a LOD concept:

This objective developed during the work at the individual papers (and levels, respectively). In contrast to the LOD concept in building modeling, no concept was available so far for the domain of 3D forest modeling. It should be clearly stated, that this is a concept and not yet a standard.

Novelty of the LOD concept:

Five levels of detail for forest models are formalized and linked to the presented Articles. The formalization should help to categorize future approaches and may act as a guideline for the modeling community.

4 Summary of the scientific publications

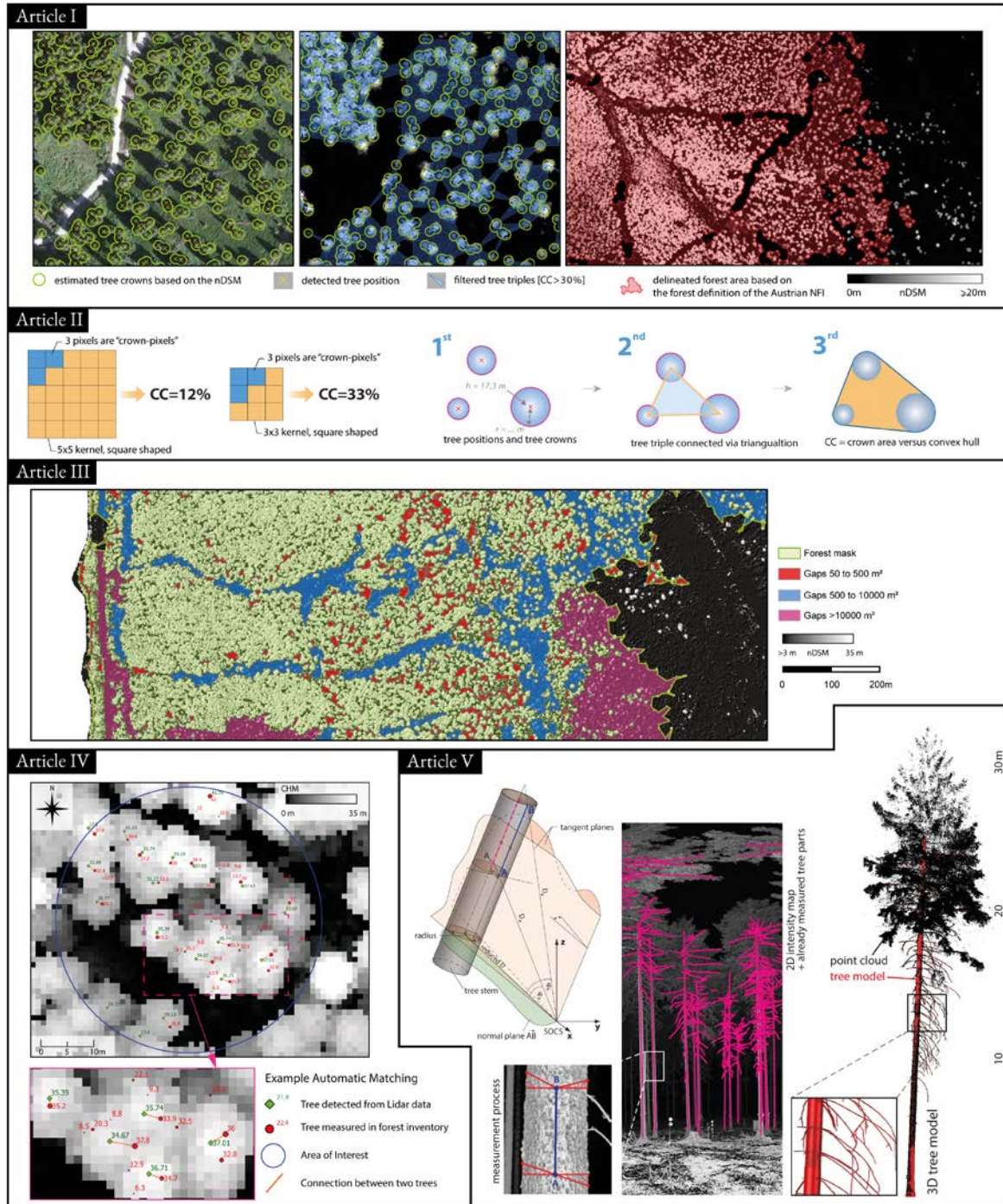


Figure 2: Graphical Abstract of the Scientific Articles.

4.1 Article I: Forest Delineation Based on Airborne LIDAR Data

Article I investigates the delineation of forested areas based on ALS data. This task can be linked to LOD 0 of the proposed LOD scheme. The paper was published on 20th of March 2012 in the MDPI Journal Remote Sensing.

The delineation of forested areas is a critical task, as the resulting maps are a fundamental input for a broad field of applications and users (e.g. governmental authorities). The results determined from these applications are highly dependent on the fundamental input parameters size and position of the delineated areas. To classify an area as forest or non-forest, different forest definitions are available. A common classification method is the interpretation of aerial images, either performed manually or automatically. Shadowing effects and the subjectivity of human interpreters limit this task. An automatic delineation based on ALS data can overcome these limitations in most cases. A mandatory criterion in forest definitions is the criterion of crown coverage (CC), which lacks a clear geometrical definition. Thus current forest delineations differ and tend to be non-comparable because of different settings for checking the criterion of CC in the delineation process.

This paper evaluates a new approach for the automatic delineation of forested areas based on ALS data with a novel method for calculating crown cover. The delineation method relies on four geometrical criteria, which are subsequently checked against ALS data. The method can be applied to different forest definitions. Land use is not considered. In this study, the criteria minimum area, height, crown cover and width of the Austrian national forest inventory (NFI) are used. The method uses rasterized ALS data to bypass extensive pure ALS point cloud processing. Two base products, a canopy height model (CHM) and a digital terrain model (DTM) are used for the delineation. Additionally a slope adaptive echo ratio (sER) map, describing the local point cloud distribution, is used for the elimination of artificial objects.

The hierarchy for checking the criteria of the forest definition is defined as follows: (i) min. height, (ii) min. crown cover, (iii) min. area and (iv) min. width. The minimum height criterion is considered by applying a height threshold on the CHM heights. Artificial objects e.g. buildings can be removed in a pre-processing step using the sER map. The criterion CC is checked with the tree triples method, that uses a triangulated network of single trees and checks three neighboring trees at a time. The single trees are detected using a local maximum search based on the CHM. The crown areas are estimated using a transfer function describing a relation between tree height and crown radii. Parameters included in the transfer function are obtained by using terrestrial measurements of the NFI or by extracting information of clearly separable trees from the ALS data itself. Areas fulfilling the criteria height and CC are checked against the area criterion by using standard GIS queries. Too small gaps are filled while too small forest areas are removed. The width criterion is applied by using morphologic operations (open, close) based on the intermediate result fulfilling the criteria height, CC and area. Narrow forested areas that do not fulfill the criterion are removed. An iterative process of checking minimum area and width is applied. A final forest mask, considering the mentioned criteria, is delineated by using all previously described processing steps.

The approach was applied and analyzed for two study areas in Tyrol, Austria which mainly consist of coniferous trees. A loosely stocked forest at the upper timberline and a fragmented forest on the hillside were studied. The method delivers repeatable and objective results and provides a beneficial tool for operational applications. Compared to a manually delineated forest mask (manually delineated based on an orthophoto and CHM), the method delivers a Kappa of 0.92 and an overall accuracy of 96%. The tree triples approach provides a clearly defined reference size for calculating CC and overcomes limitations of other calculation methods (e.g. smoothing effects, dependency of the kernel size and shape using a moving window approach) especially in loosely stocked forests. A detailed study regarding the calculation of crown coverage with different approaches is published in Article II. The delineation results proof the high potential of this method for being used as a modeling approach for revealing LOD 0 models of forests over large areas.

4.2 Article II: Crown coverage calculation based on ALS data

Article II introduces a novel ALS based crown coverage approach and investigates the effect of a variation of the reference size in moving window approaches. This task can be linked to LOD 2 of the proposed LOD scheme as single tree crowns are modeled to obtain the amount of crown coverage. The paper was published in October 2011 in the Proceedings of the International Silvilaser 2011 conference.

Considering different forest definitions forest land can, for example, be composed of tree crowns, forest gaps, forest streets or harvested areas. This complex land cover class “forest” is often difficult to derive from remotely sensed data with high accuracy on a reliable and comprehensible way. One significant parameter of forest definitions is CC, which defines the percentage of the ground covered by tree crowns. Furthermore, CC is an important parameter to describe the forest structure or the compactness of a forests canopy. However, the calculation of CC relies on the definition of a reference ground area (e.g. size and shape). Unfortunately, the size and shape of the reference area is not clearly defined in most of the forest definitions which makes the CC often to a doubtful criterion. ALS, as an active remote sensing technique, is not influenced by shadowing effects or different sun illumination conditions and is able to deliver reliable information even for small forest gaps. Therefore, rasterized ALS data (e.g. nDSM) provides an excellent data source for calculating CC.

In this contribution, two methods for deriving CC from ALS data are investigated. Method 1 is a novel, geometrically unambiguously approach based on a network of detected single trees. Method 2 consists of a moving window (MW) approach based on rasterized ALS data. The basic assumption of Method 1 is to define CC as a relation between the sum of the crown areas of three neighboring trees (tree triple) at a time and the area of their convex hull. The crown diameters are assessed using empirical functions describing the relation between the tree height and the crown diameter. These functions are calibrated based on NFI data. The tree heights are extracted from the nDSM whereas the tree positions are detected with a local maxima filter. A Delaunay triangulation is used to set up the network of tree triples. Method 2 is based on a MW approach, which basically locally checks the relation between crown pixels

and the total area of the moving window's kernel. To decide whether a pixel is covered by tree crowns or not, a height threshold is applied to the nDSM. The local CC value is obtained by relating the reference area to the tree crown covered area. To demonstrate the effect of different parameters for kernel shapes and -sizes on the resulting CC maps, multiple variations of these two parameters have been analyzed for the MW approach. The results of methods 1 and 2 are compared to each other by investigating the sum of areas fulfilling different CC thresholds.

Both methods are applied to three different test sites in Tyrol, Austria. The investigated areas show mainly coniferous forests with different structures and amounts of forested land. A loosely stocked forest at the upper timberline, a fragmented forest on the hillside and a dense forest consisting of different age classes are investigated. It could be shown, that a decrease of the forest density leads to an increased effect of different CC thresholds on the found forest area. Especially at loosely stocked forests, different MW kernel sizes and CC thresholds lead to a high variation of the found areas. This can be linked to limitations of the MW approach which are (i) a high correlation between the resulting areas and the used kernel size and (ii) blurring effects appearing especially at sharp edges (e.g. forest borders) that introduce errors. However, this study shows the high potential of ALS data for assessing CC for large areas. A clear geometrical definition for the calculation of CC is necessary since CC is a fundamental criterion in most forest definitions and the results of the MW method are geometrically ambiguously. The proposed tree triples method can overcome these limitations.

4.3 Article III: Forest Gap Delineation Based on ALS Data Using α -Shapes

Article III presents a method for automatically delineating and classifying forest gaps based on ALS data. This task can be linked to LOD 0 of the proposed LOD scheme. The paper was published on 1st of July 2010 in the Proceedings of the Annual scientific technical conference of the German society of Photogrammetry and Remote Sensing.

ALS is an active remote sensing technique and is well suited for acquiring data in forested areas. Local vegetation height information, obtained from a point cloud, is a fundamental input for deriving different forestry related parameters as for example the location and characteristics of forest gaps within delineated forested areas. Up to now, a manual or semi-automatically delineation of forested areas is performed by using orthophotos, where shadowed areas can limit the delineation of the forest border and forest gaps. At these areas, ALS shows great potential and, in most cases, is an advantage compared to a manual interpretation of orthophotos.

The stand structure and composition of a forest depends on different dynamic processes and may change over time. Structure plays an important role for the protective function of forests, whereas structural changes can alter the protective potential of the forest. Therefore, constant monitoring of structural elements as for example forest gaps is mandatory for applications in the field of disaster prevention. Another aspect of a changing stand structure is the potential

loss of biodiversity, caused by rapid deforestation or fragmentation and degradation of stands. In this context, an automatic delineation of forest gaps is important for the evaluation of structural changes with respect to biodiversity studies.

In the presented study, a fully automatic method for extracting forest gaps based on ALS data is presented. The delineation of forested areas and forest gaps is performed by combining raster operations with point-based α -Shape detection. A forest mask is extracted by sequentially checking three geometrically defined criteria of a forest definition. A height criterion is checked by detecting single trees higher than a certain threshold. The CC is checked by deriving an α -Shape of the detected positions, whereas a maximum possible distance between two trees at a time is used as alpha value. The area criterion is checked by using standard GIS tools. The forest gaps are delineated by height thresholding the nDSM and detecting local clumps of pixels fulfilling the threshold. The detected clumps (gaps) are classified into three classes representing different sizes. α -Shapes are derived for each class and the alpha value is varied between the classes. For small forest gaps, a small alpha value is used which results in a high level of detail for this class. For the other classes an increased alpha value is used to gain a stronger generalization of the gap polygons and to overcome small objects inside the gaps.

The method is applied to a 5 km² large forest area located in Tyrol, Austria. Three gap classes were extracted from the data, representing forest gaps between 50 m² and 500 m² (class 0), between 500 m² and 1 ha (class 1) and gaps greater than 1 ha (class 2). The extracted forest masks and forest gaps show a good agreement with visually interpretable objects in the Orthophoto. The presented method enables an objective, repeatable delineation of forest area and forest gaps based on ALS data. The fully automatically method shows high potential for an area-wide application.

4.4 Article IV: A Benchmark of Lidar-Based Single Tree Detection Methods Using Heterogeneous Forest Data from the Alpine Space

In Article IV, the performance of different ALS based single tree detection methods is investigated and tested. A heterogeneous dataset from the Alpine Space is used as reference. A method for matching field inventory data to trees detected from remotely sensed data is introduced. The forest scenes were modeled in LOD 2. The study should help to guide the choice of method when performing single tree detection for different forest types in the Alpine space. The paper was published on 15th of May 2015 in the MDPI Journal Forests.

Large area tasks as, for example, obtaining information about forested areas are already operational in forest management as the use of remote sensing data and related methods has become close to a standard. In contrast, terrestrial forest inventories are still obligatory and will probably never be fully replaceable by automatic methods. Data fusion of information obtained from remote sensing data with inventory data can help to reduce the costs of time consuming in-situ inventories. Additionally the spatially limited information of the inventory

could be linked to larger areas. The identification of single trees and their parameters is an important task for analysing large forested areas with respect to forest management or harvesting activities. Parameters as for example the spatial distribution of trees, tree heights and stem diameters, the amount of stems per hectare or information about tree crowns as for example a total crown length are of interest. In case of a terrestrial inventory these parameters are obtained from measurements based on the single tree level. To obtain such detailed information from remotely sensed airborne data many studies on single tree detection were carried out from the research community, resulting in many different algorithms / methods developed in different countries and institutions.

The research project NEWFOR (www.newfor.net) brings together fourteen institutions from six countries within the Alpine space working in the field of forestry and remote sensing. The project aims at enhancing the wood supply chain within the Alpine space to improve forest timber evaluation and mobilization using new remote sensing technologies. One objective of the project is to test established as well as new methods that are capable to extract single tree information based on remote sensing data. For this reason a single tree detection benchmark based on airborne laser scanning data was carried out.

Eight single tree detection methods were applied to a unique dataset originating from different regions of the Alpine space, covering different study areas, forest types and structures. The evaluation of the different detection results was carried out in a clear and reproducible way by automatically matching the detection results to forest inventory data. Quantitative statistical parameters as for example percentages of correctly matched trees as well as Omission and Commission errors are presented. The benchmarking results are prepared in different Levels of Information, starting with investigations based on the detection method. Additionally investigations per forest type and an overall performance of the benchmark are presented. The best matching rate was obtained for single layered coniferous forests. Trees in lower height layers were challenging for all tested methods. The overall performance shows a matching rate of 47 % (RMS) which is comparable to results of other benchmarks performed in the past [53,54]. Future studies should investigate automated absolute georeferencing between FI data and ALS data (co-registration) as well as an automated classification of FI plots in different forest types (e.g., single-/multi-layered forests) based on the ALS data. This would help to overcome the manual steps performed in Article IV.

4.5 Article V: A Practical Approach for Extracting Tree Models in Forest Environments Based on Equirectangular Projections of Terrestrial Laser Scans

Article V presents a method for extracting tree topology and volumetric models based on TLS data. The proposed method was applied to TLS data of a whole forest stand in Northern Germany. The extracted models can be linked to LOD 5 of the proposed LOD scheme. The paper was published on 24th of October 2013 in the MDPI Journal Remote Sensing.

Extracting 3D tree models based on high-density TLS point clouds with automatic, semi-automatic or manual methods is a challenging task as trees are complex, individual objects. An increasing amount of publications in this research field show the demand for tree reconstruction methods based on TLS data. Current TLS devices enable the sampling of objects at a high spatial resolution. The resulting point clouds show high potential for a detailed reconstruction of tree stems and branches. These models are a fundamental input for e.g. stem volume assessment or setting up virtual forest scenes. A completely automated reconstruction of a tree is often limited by imperfect point clouds, consisting of occlusions, data gaps and varying point density. Beside purely point cloud driven automatic extraction methods (e.g. region growing algorithms), tree models can be semi-automatically created by locally fitting geometrical primitives as for example cylinders. This task is challenging and time consuming, especially because the interpreter has to navigate through dense point clouds and the selection of subsets for cylinder fitting can be tricky.

In this article a semi-automatic method for extracting coniferous and deciduous tree models based on projected 2D maps of the TLS point cloud is presented. Equirectangular projections (EP) based on the observation angles of the scan are created, thereby displaying the distance (range map, RM) and intensity information (intensity map, IM) detected by the scanning device. The so-called tree structure elements (e.g. stems and branches) are clearly interpretable in the IM and RM. These easily navigable maps provide a good basis for extracting trees by digitizing the axis of the structure elements and assigning their respective local diameter by depicting it from 2D measurements in the maps. EP derived from multiple scan positions around the trees are used to complete occluded sections. Erroneous measurements, arising from moving tree parts (e.g. branches affected by wind), or by imperfections in the relative orientations of the scans, are overcome because the extraction of the tree structure is performed using single maps instead of a merged point cloud of individual scans. The digitized 2D skeletons are transformed to 3D space and furthermore extruded to 3D models.

The method was applied to a dense TLS dataset acquired in a managed forest close to Dresden, Germany. In total 90 coniferous trees were reconstructed with their stem and branches as visible in 34 single scans. The quality of the modeled trees was tested on five randomly picked sample trees. A validation of horizontal slices of the stems by investigating residuals between tree model and scan data shows values in the order of ± 1.7 cm. Additionally the models were tested for completeness and correctness by investigating the 3D deviations between tree model and point cloud. This was performed for the wooden and defoliated parts of the tree. Standard deviations of the 3D deviations of approximately 1.0 cm were found. The single trees were modeled up to three quarters of the total tree height. Data occlusions towards the tree tops were limiting the reconstruction. Partly occluded branches in the lower section and groups of trees could be successfully modeled using the stepwise approach. In total, approximately 38.000 cylinders with a minimum diameter of 7 mm were modeled to represent the complete stand. In comparison to other approaches, the number of reconstructed trees is higher (by factor 3) than the number of scans. The results demonstrate the feasibility of extracting tree models semi-automatically based on 2D maps with a very high degree of completeness. The extracted tree models were used to set up a virtual forest scene for radiative transfer modeling.

5 Discussion and Conclusion

5.1 Forest delineation

The study presented in Article I investigates the potential of ALS for being used in a forest – non-forest classification. The automatic delineation of forested areas based on rasterized ALS data shows high potential as the method delivers repeatable and objective results at low processing cost. Four common geometrical criteria of forest definitions are checked by the algorithm. The method can be applied to different national and international forest definitions. ALS data enable easy access to local object heights. Therefore, the height criterion check is straightforward. A removal of artificial objects in a pre-processing step is mandatory, and can be performed by using knowledge about the local spatial 3D distribution of ALS points. The proposed crown coverage method uses a network of single trees in a tree-triples configuration and works most efficient for loosely stocked areas, where single tree crowns are clearly interpretable. These areas are the most critical with respect to the crown cover criterion. Compared to area based approaches (e.g. kernel operations), the single tree based method overcomes limitations such as smoothing effects or dependency of the kernel size and shape (see 5.2). The estimation of tree crown diameters based on the local tree height shows consistent results, especially at the upper timberline. The area check enables bridging of small gaps inside the forest as well as the removal of small isolated forest patches. The width check eliminates too narrow forest patches as for example single tree bands along rivers in most cases. With this approach, different aspects of forest definition can be considered, but not land use. Land use cannot be obtained from ALS data and even very high resolution aerial imaging requires manual interpretation to make a step from land cover to land use. Existing GIS data sources may be more helpful, but this requires future research.

ALS data are well suited for the delineation of forested areas because the data are (i) acquired top down and provide a detailed 3D representation of large areas, and (ii) the acquisition is performed with an active sensor, which means that the acquisition is independent of the sunlight conditions. This is an advantage in shadowed areas. Due to the principle of ALS, information about the canopy's top heights, structural information as well as information about the forest floor can be gained. Structural 3D information inside the canopy is not of interest for the delineation task. Therefore, rasterized ALS data can be used to simplify the delineation task to a 2.5D problem. Depending on the local forest characteristics, an overall forest area accuracy of up to 96% could be achieved. This value was found by comparing the results to reference data. This comparison investigates the forest area and not the positional accuracy of the forests outer edges. This could be addressed in future studies. The positional (horizontal) accuracy of ALS data is within approximately ± 10 cm and common rasterized products derived from it show a spatial resolution of 1.0 x 1.0 m. Since the proposed delineation method uses these rasterized products, the positional accuracy of the forests outer edges is believed to be within this accuracy range.

5.2 Crown Cover

The study presented in Article II explores the potential of ALS for deriving Crown cover using an area-based and a single tree based method. Crown cover is one of the most important and critical criterions in national and international forest definitions. Beside its key role in a forest / non-forest classification, CC is an important measure, obtained and used in forest inventories and landscape ecology. The presented tree triples approach was developed to meet the needs of common forest definitions and to be used in the context of a forest / non-forest classification based on ALS data. CC information used in forest inventories and landscape ecology is typically on a higher level. For example, CC in different canopy height layers is of interest. Thus, high resolution data (e.g. TLS data, mobile ground-based or UAV lidar data) of the crown structure and more sophisticated methods are needed to meet the needs of these applications.

The tree triples approach solves the CC problem by setting up a tree network and checking the constellation of three trees and their corresponding crowns at a time. The modeling path for obtaining CC turns from 3D (detecting tree positions and heights) to 2D (approximating tree crowns as circles) to analytical geometry (relating crown areas to the convex hull). The CC criterion itself is only inherent 2D. Therefore it is related to analytical geometry. The use of rasterized ALS data (e.g. the CHM) allows the reduction of the CC problem from 3D to 2D.

For example, a 2D map of vertically projected tree crowns can be deduced from the CHM. The simplified LOD 2 crown model, approximating crowns as circles, is appropriate for the target application. The CHM and the DTM are very useful input data to perform the single tree detection. Sparsely stocked areas are the most critical with respect to forest delineation. Especially at these areas, good results are obtained with the tree triples method. In dense forests, the detection of single trees is critical and the detection quality can be hampered by an ambiguous canopy situation. With respect to forest delineation, this problem can be neglected. The CC thresholds of common forest definitions are not significant at dense areas. The estimation of tree crowns based on the tree height shows consistent results at the, related to CC, critical area at the upper timberline. The transfer function between tree height and crown radius can be calibrated based on FI data or based on samples extracted from ALS data. Using the CHM, a localized calibration of this function can be performed. This is an advantage compared to NFI data which is spatially limited due to the inventory design. In Article I, CHM based functions were successfully calibrated for a fragmented forest and a loosely stocked forest. A validation of the estimated crown area with a reference crown area, obtained by a height cut of the CHM, shows a good agreement. The difference between the reference and the estimated crowns are +10% at a maximum.

The presented CC method introduces a clear geometrical definition for the calculation of CC. Moving window based approaches lack this clear definition and provide differing results due to their high dependency on the kernel size and shape. The origin of this shortcoming can be justified by an unclear crown coverage definition. Especially at loosely stocked areas (e.g. at the upper timberline), different kernel sizes and CC thresholds lead to different results. Here, the tree triples method shows an advantage.

5.3 Forest Gaps

The study presented in Article III highlights the potential of ALS data for automatically extracting and classifying forest gaps. ALS is a powerful tool to obtain detailed information about the forests canopy. The top down acquisition method, combined with active object illumination is well suited to collect data about forest gaps for large areas. Small gaps inside forested areas are often shadowed and therefore hard to interpret in aerial imagery. The CHM overcomes this problem and provides a clear view on the canopy's inner gaps. Additionally local height information and a good representation of the canopy's outer edges are provided. The delineation process itself is basically a 2D task, performed on a height cut CHM. The height information of the CHM is a prerequisite, to identify areas not covered by tree crowns. These areas are delineated with 2D polygons. Depending on the target application, the polygons can be generalized to a certain extent. Beside the geometrical representation of a gap, a classification of the gaps is of interest. The classification can be based on the polygon geometry (e.g. location, size and shape) or can be based on geometrical characteristics inside the gap. For example the vertical vegetation structure within a gap might be used to characterize and furthermore classify a gap. Information about vegetation structure can be obtained with e.g. ALS.

The automatic gap extraction based on the CHM shows advantages compared to a manual delineation based on Orthophotos. The results are objective, reproducible and can be obtained for large areas at low cost. With respect to gap change monitoring across multiple epochs, these qualities are mandatory.

From a technical point of view, the description of the gap modeling workflow is clearly defined. In contrast, the theoretical definitions, used for defining forest gaps, are very generic and suffer from low precision. Clearer definitions are needed. In general, the LOD 0 model is appropriate for modeling forest gaps. The representation with 2D polygons and additional attributes adds to forest polygons found in forest delineation.

5.4 Single tree extraction

The study presented in Article IV investigates the performance of eight different ALS based single tree detection algorithms by comparing them to ground truth data (forest inventory data) from the Alpine Space. The heterogeneous dataset reveals the limitations of the tested detection algorithms, especially at different forest types. In general, all tested methods achieve comparable results for the matching rates, but do differ for the extraction rates and omission/commission rates. The tree extraction rates show a higher variation than the estimated tree heights. This is reasonable, because in ALS data, the vertical component of a tree crown is better identifiable than the location of a possible stem. A local maxima detection method applied to a canopy height model using variable-sized moving windows is rated as the best performing algorithm. Complex multi-layered forests were challenging for all tested methods. A point cloud clustering-based method gained the best results for trees in subdominant layers, which is rated as an advantage over raster-based methods. The best detection results were obtained for single-layered coniferous forests.

The inventory data and the detection results were modeled in LOD 2, which was appropriate for this benchmark. The generalization of single tree objects to 2.5D points helped to simplify the matching task between detection results and ground truth data. Further statistical processing of the matching results also benefited from the reduction of complexity.

ALS is a powerful tool for mapping and characterizing single trees. The ability of mapping the tree crown's vertical distribution is an advantage over classical photogrammetry. The acquisition of ALS data is, in most cases, carried out top down. Therefore, the uppermost canopy is represented the best in the data. Unfortunately, the link between the characteristics of the tree crown (size and shape) and the location of the tree stem can be very weak. Especially trees with a very flat or distributed crown are problematic. Dominated trees in lower layers are also problematic. In contrast to ALS, the forest inventory measurements of tree stems are carried out on the ground. The difference in the mapping principle of ALS versus the forest inventory is a limiting factor. The overall performance of the benchmark shows a matching rate of 47 % (Root Mean Square), which is comparable to results of other benchmarks performed in the past [54]. The low value was expected. The dataset used in this benchmark shows very complex forest scenes in the alpine space. Trees with a DBH larger than 10 cm had to be extracted, which introduces small and subdominant trees. Limitations in the data acquisition in multi layered forests as well as the limitations of CHM based single tree detection methods add to the low overall performance.

5.5 High resolution tree models

In Article V, a method for modeling LOD 5 tree models based on terrestrial laser scanning data is presented and applied to a TLS dataset of an old dense coniferous forest. In total, 90 LOD 5 tree models were successfully generated by a human interpreter. The axis and corresponding radii of wooden tree parts (e.g., branching and stem structure) were extracted by semi-automatically digitizing them in 2D maps. These maps, derived from geometrical and physical TLS information, enable simple 2D navigation in the digitization process. This is an advantage over other semi automatically methods (e.g. pipe fitting) which require navigation in 3D. The tree models are incrementally completed step by step, based on single scan information of multiple scan positions. Imperfections of a merged point cloud, caused by remaining registration errors, noise or e.g. moving branches which were influenced by wind, are mitigated in most cases because of the proposed digitization method. Bridging of gaps can be performed by the operator in the digitization process. The result of the digitization process are topologically correct tree skeletons which are finally extruded to volumetric models by using the radii information stored for each axis segment.

In general, the quality of the TLS data is a very important factor and is strongly correlated with the resulting quality of the tree models. This includes the quality of the orientation between scans, the gained point density on the object side and visibility of the objects itself. For the upper tree parts, the visibility during the data acquisition and distortions in the 2D maps (originating from the chosen projection) are additional limitations. Summarizing, with other existing approaches [42], the proposed method shares the limitation of reduced visibility in the upper tree parts due to the scan position, it provides better handling of registration errors and wind distortions in the point cloud.

A quality assessment of the extracted models shows, that the trees could be modeled up to three quarters of the total tree height. Because of the problematic TLS situation in the upper canopy section, this is a good result. Scans taken from low flying drones may help to overcome the limitations in this section. The use of knowledge from a human interpreter results in a high completeness and correctness of the LOD 5 models. The validation of the stem section and other wooden parts shows a good agreement with the TLS data.

TLS is a good method for acquiring detailed information about forests. Beside the visibility problem in the upper canopy, the data shows a high level of detail and is an ideal source for extracting LOD 5 models. In Article V, branches with a diameter of 7 mm could be modeled. “Classical” ALS, carried out several hundred meters above ground, delivers too less detail with respect to LOD 5. Additionally the footprint of such systems is too large to capture small elements (e.g. small branches) in the canopy. A new ALS segment are low flying RPAS with powerful scanners with a small laser footprint [55,56]. These systems can acquire very detailed information within the canopy and are, beside TLS, could become the future data source for LOD 5 tree models.

5.6 General Conclusions

The level of detail is a matter of observation distance and the level of generalization when looking at a phenomenon. The real situation in a forest has no levels of detail, but by modeling we make a selection of aspects to consider for describing reality. This leads to a set of models, which can be grouped differently. Here, the level of detail (LOD) concept was used to set the models in relation to each other by their geometric content.

Modeling and quantifying the resource forest implies the need for LOD. The act of introducing the levels is arbitrary, as the different LOD's are an aggregated snapshot of the complex reality. Modeling the resource forest is a manifold process. In this process, the proposed LOD scheme might be too inaccurate or generic. If this is the case, the classification of a modeling task into the proposed scheme can be ambiguous. Assigning a modeling task or its products to multiple levels can help to overcome this limitation.

The proposed modeling scheme is geometrically driven. Therefore the proposed models have a strong geometrical aspect, but may also contain thematic information. In case of LOD 0, the observations of ALS fit perfectly to the desired final model, which is mainly driven by geometrical information (e.g. tree heights and spatial distribution). In contrast, the modeling of single tree positions based on ALS is critical, as the observations of ALS only indirectly contain this information. All LOD may contain geometrical as well as thematic information. The type of information may change between different LOD. In LOD 1, for example, the amount of trees per hectare is presented as a statistical value. In LOD 2 this information is turned into geometry. The trees are presented as individual objects.

Laser scanning, whether it is ALS or TLS, is a powerful tool to three dimensionally map the forest environment. Laser scanning is capable to deliver multi-target information and can map vegetation structure inside the canopy. This is an advantage over aerial imagery or point clouds

created with image matching methods. The resulting data is suitable to be used for vegetation modeling purposes across a range of different scales. All proposed LOD can be achieved by using laser scanning data. Limitations of ALS are (i) a limited mapping of the lower canopy layers (e.g. sub-dominant trees) due to the top down acquisition geometry (ii) a limitation in the object size that can be mapped due to a rather large laser footprint and a limited range resolution and (iii) in most cases too low point densities. The main limitations of TLS are (i) the labor intensive orientation of single scans, (ii) the decreasing visibility of objects with increased range (Topmost crown is not covered in TLS data) and (iii) the low ground coverage (large area acquisitions are hardly possible). The small footprint of TLS enables mapping and modeling of small tree objects. Due to the physical and geometrical constraints of laser scanning, LOD 5 is the highest possible modeling level.

From a processing perspective, fully automatic laser scanning based modeling methods are well suited for all proposed LOD. Especially for the large area applications, a human interpreter would be confronted with a too challenging modeling situation. Examples are forest delineation in loosely stocked forests or the extraction of crown coverage. Positive aspects of the automatic modeling methods are repeatability, objectivity and efficiency. For LOD 5 modeling, manual interaction of a human interpreter is useful. Especially the bridging of gaps in the TLS data, knowledge about tree topology and a constant quality check during the modeling process are positive aspects. Subjectivity and low efficiency are negative aspects. LOD 0 to LOD 2 models can be extracted from rasterized laser scanning data, which allows a reduction of the input data during processing. LOD 3 to LOD 5 models mainly rely on dense 3D point cloud data. This means, that an increased LOD leads to a higher processing cost.

There is no clear line, when to use ALS data or TLS data for the different LOD models. In general, the application as well as the scale of the desired model defines, if ALS data or TLS data is in favor. For large area applications (e.g. forest delineation) the used models tend to be simpler or less detailed. In this domain, ALS data are a good input. The desired LOD are LOD 4 down to LOD 0. Small area applications (e.g. high resolution tree models) rely mainly on detailed TLS data, but the visibility issues of TLS can be limiting (e.g. representation of tree tops). In theory, downscaled TLS data could be used for large area applications and models down to LOD 0, but it would be very inefficient and challenging. Vice versa, the use of ALS data is only possible up to LOD 4. The main limiting factors of ALS for being used as a data source for LOD 5 models are the large laser footprint and a too low point density. Between the two segments of ALS and TLS, emerging technologies as for example mobile laser scanning inside the forest (e.g. TLS mounted on an all-terrain vehicle) or RPAS borne laser scanning [56] exist. These methods can help to overcome the above mentioned limitations.

In general, with increased LoD the overall quality of the results decreases. The best accuracy could be obtained for “simpler” models as for example the LOD 0 models. A reason for this are clearly defined goals (e.g. stated in a forest definition) and the fact, that reference data are partly available for the lower levels. In contrast, reference data are hardly available for LOD 5 models.

The definitions used in the domain of Forestry are not purely geometric, but this would be advantageous for exploiting laser scanning data. Up to now, many of the existing definitions are not compatible with the exactness of laser scanning data. The quantitative nature of laser scanning requires exact definitions. For this reason, own definitions as for example the novel crown cover definition became necessary.

In this Dissertation, a broad range of modeling approaches regarding the resource forest is presented. The domain of laser scanning and environmental modeling is rapidly developing. Powerful new sensors, platforms and applications will ensure further development within the domain of laser scanning in the future. Since laser scanning is proven as a powerful tool to three dimensionally map and model the resource forest, the domain of Forestry will benefit from these developments and will make a great step towards the idea of precision forestry [18].

5.7 Key findings

1st Modeling and quantifying tall vegetation implies the need for models with different granularity. These models can be defined and categorized in different levels of detail. The models range from aggregated information to detailed information about individual objects. Level 5, which describes a model of structural tree parts (e.g. stem, branches, foliage), is the highest possible modeling level using TLS data.

2nd Laser scanning, whether it is airborne or terrestrial laser scanning, is (i) a powerful 3D mapping tool and (ii) a good data source for modeling the forest environment at different scales. All suggested modeling levels can be obtained from laser scanning data. Some limitations occur due to a limited visibility of objects, physical and geometrical constraints of laser scanning and limitations in the acquisition geometry. The target application and the scale of the desired model define, which type of laser scanning data is in favor.

3rd With increased LoD the overall quality of the results decreases. The best accuracy could be obtained for “simpler” models as for example the level 0 models.

4th The definitions used in the domain of Forestry are not purely geometric, but this would be advantageous for exploiting laser scanning data. Up to now, many of the existing definitions are not fully compatible with the exactness of laser scanning data.

Bibliography

1. Google Inc. Google Earth Ver. 7.1. <https://www.google.com/earth/> (last access: June 2015).
2. Sheppard, S.R.J.; Cizek, P. The Ethics of Google Earth: Crossing Thresholds From Spatial Data To Landscape Visualisation. *Journal of Environmental Management* **2008**, *90*, 2102-2117.
3. National Aeronautics and Space Administration (NASA). NASA World Wind 2.0. <http://worldwind.arc.nasa.gov/java/> (last access: June 2015).
4. Magistrat der Stadt Wien. Vienna GIS. <http://www.wien.gv.at/stadtplan/en/> (last access: June 2015).
5. Krooks, A.; Kahkonen, J.; Lehto, L.; Latvala, P.; Karjalainen, M.; Honkavaara, E. WebGL Visualisation of 3D Environmental Models Based on Finnish Open Geospatial Data Sets. *ISPRS-International Archives of the Photogrammetry, Remote Sensing and Spatial Information Sciences* **2014**, *1*, 163-169.
6. OGC. Open Geospatial Consortium standards. <http://www.opengeospatial.org/standards/> (last access: June 2015).
7. Open Geospatial Consortium Inc. (OGC). OGC Adopts CityGML Encoding Standard. <http://www.opengeospatial.org/pressroom/pressreleases/899> (last access: August 20 2008)
8. Open Geospatial Consortium Inc. (OGC). OGC Approves KML as Open Standard <http://www.opengeospatial.org/pressroom/pressreleases/857> (last access: April 14 2008)
9. Gröger, G.; Kolbe, T.H.; Czerwinski, A.; Nagel, C. OpenGIS City Geography Markup Language (CityGML) Implementation Specification. Version 1.0: 08-007. 2008.
10. Kolbe, T.H. Representing and Exchanging 3D City Models with CityGML. In *3D Geo-Information Sciences*, Springer: Berlin Heidelberg, 2009; pp 15-31.
11. Gröger, G.; Plümer, L. The Interoperable Building Model of the European Union. In *Geoinformation for Informed Decisions*, Abdul Rahman, A.; Boguslawski, P.; Anton, F.; Said, M.N.; Omar, K.M., Eds. Springer International Publishing: 2014; pp 1-17.
12. Gröger, G.; Plümer, L. CityGML - Interoperable Semantic 3D City Models. *ISPRS Journal of Photogrammetry and Remote Sensing* **2012**, *71*, 12-33.
13. Wilson, T. OGC KML, Version 2.2.0, International OGC Standard. Open Geospatial Consortium: 2008.
14. Eastman, C.; Eastman, C.M.; Teicholz, P.; Sacks, R. *BIM Handbook: A Guide To Building Information Modeling For Owners, Managers, Designers, Engineers and Contractors*. John Wiley & Sons: 2011.
15. Lillesand, T.; Kiefer, R.W.; Chipman, J. *Remote Sensing and Image Interpretation*. Seventh edition ed.; John Wiley & Sons: 2014; p 768.
16. Foresters, S.o.A. The Dictionary of Forestry - Definition Forestry. <http://dictionaryofforestry.org/dict/term/forestry> (last access: July 2015).

17. United Nations Environment Programme (UNEP), F., UNFF. *Vital Forest Graphics - Forest Definition and Extent*; 2009; pp 75 p., ISBN 978-992-975-106264-106267.
18. Holopainen, M.; Vastaranta, M.; Hyypä, J. Outlook for the Next Generation's Precision Forestry in Finland. *Forests* **2014**, *5*, 1682.
19. Franklin, S.E. *Remote Sensing for Sustainable Forest Management*. CRC Press: 2001.
20. Simard, M.; Pinto, N.; Fisher, J.B.; Baccini, A. Mapping Forest Canopy Height Globally With Spaceborne Lidar. *Journal of Geophysical Research: Biogeosciences* **2011**, *116*.
21. Wulder, M.A.; White, J.C.; Nelson, R.F.; Næsset, E.; Ørka, H.O.; Coops, N.C.; Hilker, T.; Bater, C.W.; Gobakken, T. Lidar Sampling for Large-Area Forest Characterization: A Review. *Remote Sensing of Environment* **2012**, *121*, 196-209.
22. Hyypä, J.; Holopainen, M.; Olsson, H.; . Laser Scanning in Forests. *Remote Sensing* **2012**, *4*, 2919-2922.
23. Holmgren, J. Prediction of Tree Height, Basal Area and Stem Volume in Forest Stands Using Airborne Laser Scanning. *Scandinavian Journal of Forest Research* **2004**, *19*, 543-553.
24. Hyypä, J.; Hyypä, H.; Leckie, D.; Gougeon, F.; Yu, X.; Maltamo, M. Review of Methods of Small - Footprint Airborne Laser Scanning for Extracting Forest Inventory Data in Boreal Forests. *International Journal of Remote Sensing* **2008**, *29*, 1339-1366.
25. Næsset, E.; Gobakken, T.; Holmgren, J.; Hyypä, H.; Hyypä, J.; Maltamo, M.; Nilsson, M.; Olsson, H.; Persson, Å.; Söderman, U. Laser Scanning of Forest Resources: The Nordic Experience. *Scandinavian Journal of Forest Research* **2004**, *19*, 482-499.
26. Dassot, M.; Constant, T.; Fournier, M. The Use of Terrestrial LiDAR Technology in Forest Science: Application Fields, Benefits and Challenges. *Annals of Forest Science* **2011**, *68*, 959-974.
27. Liang, X.; Kankare, V.; Yu, X.; Hyypä, J.; Holopainen, M. Automated Stem Curve Measurement Using Terrestrial Laser Scanning. *IEEE Transactions on Geoscience and Remote Sensing* **2014**, *52*, 1739-1748.
28. Wikipedia. Earth observation. http://en.wikipedia.org/wiki/Earth_observation (last access: April 2015).
29. European Commission - Joint Research Centre. Earth observation. <https://ec.europa.eu/jrc/en/research-topic/earth-observation> (last access: June 2015).
30. Kraus, K. *Photogrammetry: Geometry From Images And Laser Scans*. Walter de Gruyter: Berlin, 2007; Vol. 2nd Edition.
31. Hollaus, M.; Dorigo, W.; Wagner, W.; Schadauer, K.; Höfle, B.; Maier, B. Operational wide-area stem bolome estimation based on airborne laser scanning and national forest inventory data. *International Journal of Remote Sensing* **2009**, *30*, 5159-5175.
32. Hollaus, M.; Wagner, W.; Schadauer, K.; Maier, B.; Gabler, K. Growing stock estimation for alpine forests in Austria: a robust lidar-based approach. *Canadian Journal of Forest Research* **2009**, *39*, 1387-1400.
33. Guisan, A.; Zimmermann, N.E. Predictive Habitat Distribution Models In Ecology. *Ecological modelling* **2000**, *135*, 147-186.
34. Kötz, B.; Schaeppman, M.; Morsdorf, F.; Bowyer, P.; Itten, K.; Allgöwer, B. Radiative Transfer Modeling Within A Heterogeneous Canopy For Estimation Of Forest Fire Fuel Properties. *Remote Sensing of Environment* **2004**, *92*, 332-344.

35. Ross, L.; Bolling, J.; Döllner, J.; Kleinschmit, B. Enhancing 3D City Models with Heterogeneous Spatial Information: Towards 3D Land Information Systems. In *Advances in GIScience*, Sester, M.; Bernard, L.; Paelke, V., Eds. Springer Berlin Heidelberg: 2009; pp 113-133.
36. Lafarge, F.; Descombes, X.; Zerubia, J.; Pierrot-Deseilligny, M. Automatic Building Extraction from DEMs using an Object Approach and Application to the 3D-city Modeling. *ISPRS Journal of Photogrammetry and Remote Sensing* **2008**, *63*, 365-381.
37. Morsdorf, F.; Meier, E.; Kötz, B.; Itten, K.I.; Dobbertin, M.; Allgöwer, B. LIDAR-Based Geometric Reconstruction of Boreal Type Forest Stands at Single Tree Level For Forest And Wildland Fire Management. *Remote Sensing of Environment* **2004**, *92*, 353-362.
38. Runions, A.; Fuhrer, M.; Lane, B.; Federl, P.; Rolland-Lagan, A.-G.; Prusinkiewicz, P. Modeling and Visualization of Leaf Venation Patterns. *ACM Trans. Graph.* **2005**, *24*, 702-711.
39. Rusinkiewicz, S.; Levoy, M. QSplat: A Multiresolution Point Rendering System For Large Meshes. In *Proceedings of the 27th annual conference on Computer graphics and interactive techniques*, ACM Press/Addison-Wesley Publishing Co.: 2000; pp 343-352.
40. BIMForum. Level of Development Specification for Building Information Models. <http://bimforum.org/wp-content/uploads/2013/08/2013-LOD-Specification.pdf> (last access: July 2015)
41. Côté, J.-F.; Fournier, R.A.; Egli, R. An architectural model of trees to estimate forest structural attributes using terrestrial LiDAR. *Environmental Modelling & Software* **2011**, *26*, 761-777.
42. Raumonon, P.; Kaasalainen, M.; Åkerblom, M.; Kaasalainen, S.; Kaartinen, H.; Vastaranta, M.; Holopainen, M.; Disney, M.; Lewis, P. Fast Automatic Precision Tree Models from Terrestrial Laser Scanner Data. *Remote Sensing* **2013**, *5*, 491-520.
43. Runions, A.; Lane, B.; Prusinkiewicz, P. In *Modeling trees with a space colonization algorithm*, Eurographics workshop on natural phenomena, 2007; The Eurographics Association.
44. Rutzinger, M.; Pratihast, A.; Oude Elberink, S.; Vosselman, G. Detection and Modelling of 3D Trees from Mobile Laser Scanning Data. *Int. Arch. Photogramm. Remote Sens. Spat. Inf. Sci* **2010**, *38*, 520-525.
45. Leiterer, R.; Morsdorf, F.; Schaepman, M.; Mücke, W.; Pfeifer, N.; Hollaus, M. In *3D Vegetationskartierung: Flugzeuggestütztes Laserscanning für ein operationelles Waldstrukturmonitoring*, Arbeitskreis-Treffen des AK "Fernerkundung" der DGfG und AK "Auswertung von Fernerkundungsdaten" der DGPF, October, 2012; Bochum (D).
46. Koch, A.; Heipke, C. Semantically Correct 2.5D GIS Data — The Integration of a DTM and Topographic Vector Data. *ISPRS Journal of Photogrammetry and Remote Sensing* **2006**, *61*, 23-32.
47. Hernando, A.; Tejera, R.; Velázquez, J.; Núñez, M. Quantitatively defining the conservation status of Natura 2000 forest habitats and improving management options for enhancing biodiversity. *Biodiversity and Conservation* **2010**, *19*, 2221-2233.
48. Fairweather, S.E. Forest Inventory: A Solid Foundation for Stand Density Management <http://extension.oregonstate.edu/douglas/sites/default/files/documents/forestry/SDM/SteveFairweatherPaper.pdf> (last access: Sept. 2015)

49. Korhonen, L.; Morsdorf, F. Estimation of Canopy Cover, Gap Fraction and Leaf Area Index with Airborne Laser Scanning. In *Forestry Applications of Airborne Laser Scanning*, Maltamo, M.; Næsset, E.; Vauhkonen, J., Eds. Springer Netherlands: 2014; Vol. 27, pp 397-417.
50. Leiterer, R.; Mücke, W.; Hollaus, M.; Pfeifer, N.; Schaepman, M.E. Operational forest structure monitoring using airborne laser scanning. *Photogrammetrie - Fernerkundung - Geoinformation* **2013**, *2013*, 173-184.
51. Wikipedia. Carl Linnaeus. https://en.wikipedia.org/wiki/Carl_Linnaeus (last access: September 2015).
52. Vauhkonen, J.; Tokola, T.; Packalén, P.; Maltamo, M. Identification of Scandinavian Commercial Species of Individual Trees from Airborne Laser Scanning Data Using Alpha Shape Metrics. *Forest Science* **2009**, *55*, 37-47.
53. Vauhkonen, J.; Ene, L.; Gupta, S.; Heinzl, J.; Holmgren, J.; Pitkänen, J.; Solberg, S.; Wang, Y.; Weinacker, H.; Hauglin, K.M., *et al.* Comparative testing of single-tree detection algorithms under different types of forest. *Forestry* **2011**.
54. Kaartinen, H.; Hyyppä, J.; Yu, X.; Vastaranta, M.; Hyyppä, H.; Kukko, A.; Holopainen, M.; Heipke, C.; Hirschmugl, M.; Morsdorf, F., *et al.* An International Comparison of Individual Tree Detection and Extraction Using Airborne Laser Scanning. *Remote Sensing* **2012**, *4*, 950.
55. Amon, P.; Riegl, U.; Rieger, P.; Pfennigbauer, M. In *UAV-Based Laser Scanning To Meet Special Challenges in Lidar Surveying*, GEOMATICs INDABA, 64 Jones Road, Kempton Park 1627 South Africa, August 11 - August 13, 2015; 64 Jones Road, Kempton Park 1627 South Africa.
56. Mandlbürger, G.; Hollaus, M.; Glira, P.; Milenkovic, M.; Wieser, M.; Riegl, U.; Pfennigbauer, M. In *First Examples from the RIEGL VUX-SYS for Forestry Applications*, Silvilaser 2015, La Grande Motte, France, September 28-30, 2015; La Grande Motte, France, p 4.

Appendix A - Scientific Articles

Article I

Article

Forest Delineation Based on Airborne LIDAR Data

Lothar Eysn ^{1,*}, Markus Hollaus ¹, Klemens Schadauer ² and Norbert Pfeifer ¹

¹ Institute of Photogrammetry & Remote Sensing, Vienna University of Technology, Gußhausstraße 27-29, A-1040 Vienna, Austria; E-Mails: mh@ipf.tuwien.ac.at (M.H.); np@ipf.tuwien.ac.at (N.P.)

² Department of Forest Inventory at the Federal Research and Training Center for Forests, Natural Hazards and Landscape, Seckendorff-Gudent-Weg, A-1130 Vienna, Austria; E-Mail: klemens.schadauer@bfw.gv.at

* Author to whom correspondence should be addressed; E-Mail: le@ipf.tuwien.ac.at; Tel.: +43-1-588-011-2249; Fax: +43-1-588-011-2299.

Received: 18 January 2012; in revised form: 7 March 2012 / Accepted: 8 March 2012 /

Published: 20 March 2012

Abstract: The delineation of forested areas is a critical task, because the resulting maps are a fundamental input for a broad field of applications and users. Different national and international forest definitions are available for manual or automatic delineation, but unfortunately most definitions lack precise geometrical descriptions for the different criteria. A mandatory criterion in forest definitions is the criterion of crown coverage (CC), which defines the proportion of the forest floor covered by the vertical projection of the tree crowns. For loosely stocked areas, this criterion is especially critical, because the size and shape of the reference area for calculating CC is not clearly defined in most definitions. Thus current forest delineations differ and tend to be non-comparable because of different settings for checking the criterion of CC in the delineation process. This paper evaluates a new approach for the automatic delineation of forested areas, based on airborne laser scanning (ALS) data with a clearly defined method for calculating CC. The new approach, the ‘tree triples’ method, is based on defining CC as a relation between the sum of the crown areas of three neighboring trees and the area of their convex hull. The approach is applied and analyzed for two study areas in Tyrol, Austria. The selected areas show a loosely stocked forest at the upper timberline and a fragmented forest on the hillside. The fully automatic method presented for delineating forested areas from ALS data shows promising results with an overall accuracy of 96%, and provides a beneficial tool for operational applications.

Keywords: forest definition; canopy cover; crown coverage; vegetation mapping; airborne laser scanning; forest classification; land cover; canopy height model

1. Introduction

In recent years, the increasing use of forest products derived from airborne laser scanning (ALS) data as well as many ongoing projects related to this topic show the high demand for this research field. Different products like, e.g., estimated tree heights [1–3], growing stock estimations [4,5], or forest structure analyses [6,7] are of interest for a broad field of applications and users (e.g., forestry, biologists, risk management for natural hazards). An overview of current methods for extracting forest parameters from ALS is given in Hyyppä *et al.* [8]. The results determined from these applications are highly dependent on the fundamental input parameters' size and position of the delineated forest areas. The delineation of these areas is therefore a crucial task. The size of forested areas is also of interest for governmental authorities (e.g., taxation, financial support of the European Commission) and, in a broader sense, for politics (e.g., greenhouse gases, Kyoto protocol).

The delineation of forests has a long tradition in remote sensing. In the past, mainly aerial images were used for a manual or semi-automated extraction of forested areas. Shadow effects limit this task, particularly for detecting small forest clearings and the exact delineation of forest borders. Additionally, the quality of the results of a manual delineation is subjective and variable between analysts and may lead to inhomogeneous, maybe even incorrect datasets. In particular, in loosely stocked areas, the delineated results show low quality. To classify an area as forest or non-forest, different national forest definitions are available [9], beside a global definition of the Food and Agriculture Organization of the United Nations (FAO) [10,11]. To delineate forested areas, an exact geometric forest definition is required. Unfortunately, the current forest definitions are imprecise in most cases. For example, the criterion of crown coverage (CC) is fundamental and mandatory. With regard to the forest definition given by European Commission, the criterion of minimum area is the second important criterion. CC, also known as vertical canopy coverage [12], or forest canopy cover, is defined as the proportion of the forest floor covered by the vertical projection of the tree crowns [13]. Most of the common forest definitions lack precise geometric descriptions for calculating CC (e.g., the reference size and shape for which the amount of projected crown area is calculated). Therefore, the results of current forest delineations are often not comparable and make the CC a doubtful criterion. In recent years, fully automated methods for a forest delineation, based on aerial images or ALS data, have been proposed. They can overcome the limitations of manual delineation in most instances and produce user independent results in short evaluation times.

Radoux *et al.* [14], for example, use different very high resolution multispectral satellite images to delineate forest stands in Belgium. They use an automatic segmentation to delineate homogeneous land cover objects, based on the orthorectified images from IKONOS-2 and SPOT-5. Unfortunately, no criteria of a forest definition are treated.

Mustonen *et al.* [15] evaluate the applicability of a canopy height model (CHM), derived from ALS data, for an automatic segmentation of forest stands in Finland. Additionally, they evaluate a segmentation based on the CHM combined with aerial images. For the delineation of stands based on

the CHM, the height information of forest stands is used as a fundamental input. The authors mention that the use of other parameters, such as number of stems per hectare or canopy cover, both derived from ALS, could be an improvement. However, the method of Mustonen *et al.* [15] focuses on delineating forest stands inside forested areas.

Wang *et al.* [16,17] use aerial images together with ALS data for the automatic delineation of forested areas in Switzerland. They use a green vegetation index, derived from the red and green spatial bands of orthophotos, in combination with a height thresholded canopy height model (CHM), derived from ALS data, to classify forest candidate pixels from the images. In a next step, they apply an image segmentation to find homogeneous, independent regions. By checking the curvature of each segment based on the CHM, forested areas are found. Unfortunately, Wang *et al.* do not treat the criterion of CC, which is a mandatory criterion in the Swiss forest definition [18].

Straub *et al.* [19] delineate forested areas in Germany, based on the normalized digital surface model (nDSM) derived from ALS data. Furthermore, they use point density maps to derive a normalized image, which is thresholded to find areas (pixels) covered by vegetation. Based on these areas, they classify into forest vegetation and non-forest vegetation. For this classification, the criteria height, CC, area and width are used. The reference areas for checking the CC criterion are extracted by intersecting vegetation pixels above 3 m with a grid of 20×20 m. In the resulting, individually shaped areas, pixels lower than 5 m in the nDSM are summed. The relation between reference area and summed pixels represents the amount of CC. Regions with a CC value greater than 50% are connected and checked against the minimum area criterion of 1,000 m². Finally, the minimum width is checked by “skeletonization” and by analyzing profiles of the resulting areas. Unfortunately, Straub *et al.* [19] do not explain why they use a square shaped grid with a grid size of 20×20 m for checking the CC criterion. As discussed in Eysn *et al.* [20], different settings for the grid size lead to different results.

As summarized in the three examples from Finland, Switzerland and Germany, forest is delineated with different methods and parameter settings from ALS data and orthophotos. This is critical because delineation results based on different definitions need to be compared. For example, the Global Forest Resources Assessment (FRA) is based on data (e.g., the amount of forested areas) that countries provide to the FAO in response to a common questionnaire every 5 to 10 years. The FAO analyzes this information and presents the current status of the world’s forest resources and their changes over time [21]. Because taxation is also strongly related to the amount of forested areas, a clear forest definition and consequently technically correct forest delineation are crucial.

In the approach here presented, the forested areas are automatically delineated, based on ALS data and considering the forest definition of the Austrian national forest inventory (NFI). As shown in Eysn *et al.* [20], different settings for reference size and shape within the CC calculation process lead to different delineation results. Therefore, the focus is laid on implementing the criterion of CC in a comprehensible, geometrically clearly defined way to be able to produce comparable delineation results. The used forest definition is mainly based on the five criteria (1) minimum tree height (2) minimum CC (3) minimum forest area (4) minimum forest area width and (5) land use [22]. In the approach here presented, criteria one to four are treated.

The remaining parts of this paper are organized as follows: Section 2 describes the selected study areas and the used data. Section 3 describes the methodology and implementation, whereas results are

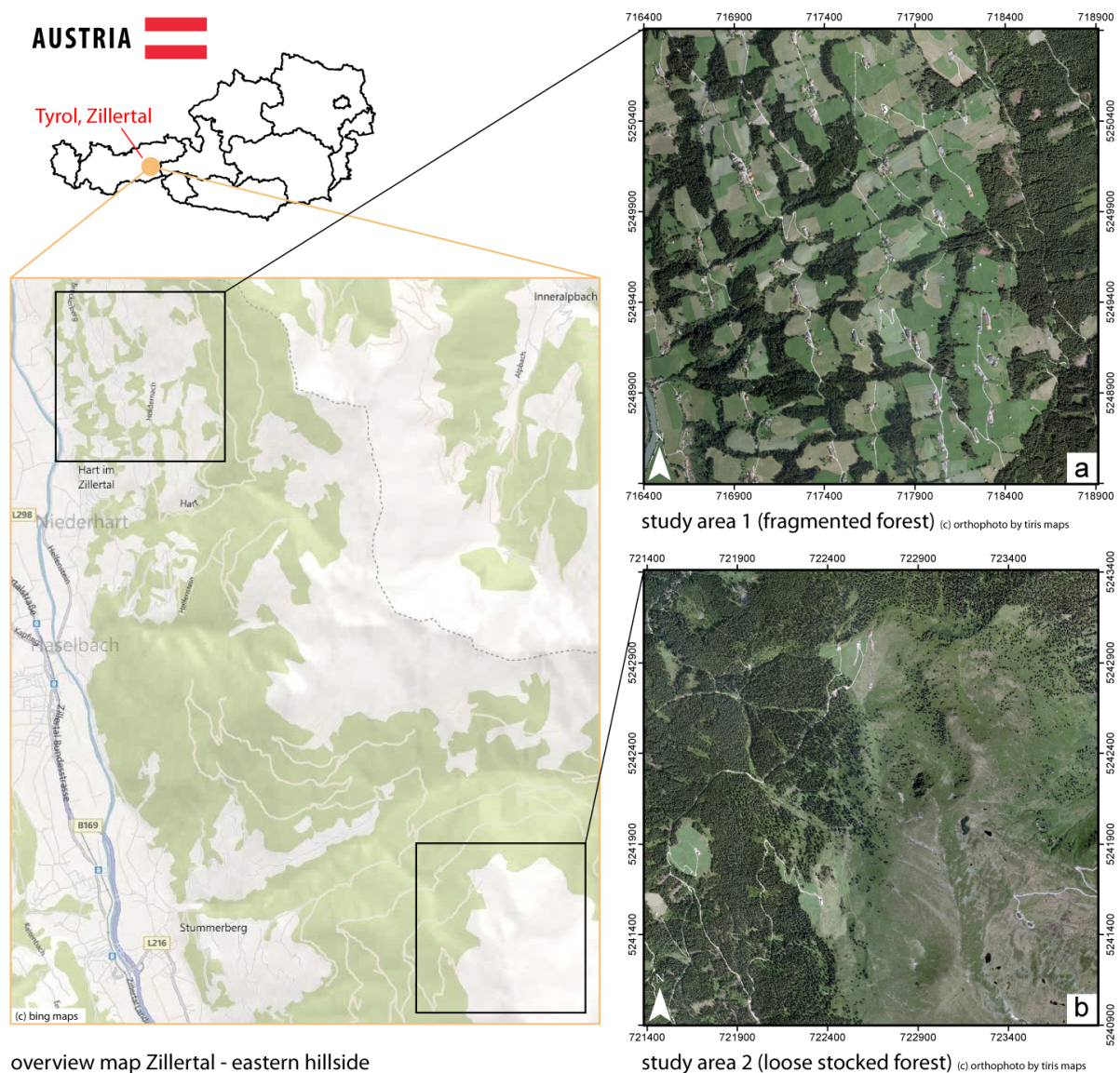
presented and discussed in Section 4. Finally, concluding remarks are given in Section 5. This special issue paper is based on two conference papers by Eysn *et al.* [20,23].

2. Study Areas and Data

2.1. Study Areas

In this contribution, two different study areas in the Zillertal, which is located in the eastern part of the federal state of Tyrol, Austria, are investigated. Each study area covers an area of $2.5 \times 2.5 \text{ km}^2$ and shows different structures and amounts of forested land (Figure 1).

Figure 1. Study areas in Zillertal, Tyrol (a) orthophoto of study area 1: fragmented forest on the hillside and (b) orthophoto of study area 2: loosely stocked forest at the upper timberline. The coordinates are given in UTM32N.



Study area 1 consists of a fragmented forest with patchwork forest stands on the hillside (Figure 1(a)) with elevations from 600 to 1,600 m above sea level (a.s.l.) Study area 2 consists of a loosely stocked

forest at the upper timberline (Figure 1(b)) with elevations from 1,800 to 2,000 m a.s.l. The dominant tree species in both study areas are coniferous trees such as Norway Spruce (*Picea abies*) and European Larch (*Larix decidua*). Beside the forested areas, artificial objects, such as buildings and power lines, can be found in the study areas.

2.2. Airborne Laser Scanning Data

Topographic data were acquired using the discrete Airborne Laser Terrain Mapper ALTM 3100, manufactured by Optech Inc. The data acquisitions were done in the framework of a commercial terrain-mapping project, fully covering the Federal State of Tyrol. The ALS data and the digital terrain model (DTM) were provided by the “Amt der Tiroler Landesregierung, Gruppe Landesbaudirektion, Abteilung Geoinformation”. For the two study areas, the ALS data were acquired during multiple flight campaigns in 2008 under leaf-off and leaf-on canopy conditions without snow cover. The mean point density is about 5 echoes/m² for study area 1 and 4 echoes/m² for study area 2. The ALS data were delivered as XYZ coordinate triples (georeferenced in UTM-32), organized in flight strips, and classified to first echoes (FE) and last echoes (LE). Single echoes are classified as LE. For further calculations, FE and LE were merged and the data organized in 2.5 × 2.5 km tiles. Details of the ALS data used are summarized in Table 1. For the DTM generation the hierarchic robust filtering approach described in Kraus and Pfeifer [24] was applied. The DTM has a spatial resolution of 1 × 1 m².

Table 1. Characteristics of the ALS data used.

ALS Data Characteristics	Study Areas	
	(1) Fragmented Forest	(2) Loosely Stocked Forest
Avg. echo density (m ⁻²)	~5	~4
Available point cloud data format	discrete - xyz	discrete - xyz
Period of acquisition	multiple in 2008	multiple in 2008
Avg. flying height above ground (m)	~1,500	~1,000
Vegetation status	leaf off and on	leaf off and on
Laser scanner system	Optech ALTM 3100	Optech ALTM 3100
Laser wavelength (nm)	1,064	1,064

2.3. National Forest Inventory Data

For the delineation of forested areas, a statistical relationship between tree height and crown radius are computed, based on measurements of crown radii from the Austrian national forest inventory (NFI). The NFI data were acquired by the Department of Forest Inventory of the Federal Research and Training Center for Forests, Natural Hazards and Landscape (BFW), in the framework of the ongoing NFI. The delineation of forested areas in alpine regions is most critical in sparsely stocked forests, which mainly occur at the upper timberline at high elevations. Therefore, a subsample of measured trees in Tyrol, Austria was chosen for describing the crown radii for trees with low competition according to a border situation. Only trees of the species European Larch (*Larix decidua*), Swiss Stone pine (*Pinus cembra*) and Norway Spruce (*Picea abies* L.) were selected because they are relevant and representative of loose areas around the upper timberline in the study areas. Thus, dense stands and

trees of lower social classes according to Kraft [25] were excluded. A short description of the data used is given in Table 2.

Table 2. NFI data description used for the statistical models between crown radius, tree height and elevation.

	Coniferous Trees (n = 1972)	
	Mean	Std. Dev.
Crown radius (m)	3.14	0.97
Tree height (m)	26.50	7.20
Elevation (m)	1,137	426

3. Methods

The delineation of forested areas is commonly a large area application. Performing this task on a pure pointcloud basis would be very extensive because of the large amount of data, which arises when working with high-density laser point data. Therefore, the focus of this work was to develop a method based on the rasterized ALS data. In addition to the ALS point clouds, most of these base products, such as DTM and the digital surface model (DSM), are available with a spatial resolution of 1×1 m for all federal states in Austria.

As described in Section 1, only the geometrical criteria of the Austrian NFI (min. area, min. height, min. width and min. crown coverage) are used for the delineation of forested areas. Land use criteria are not considered in this study. It has to be clarified that land use and legal restrictions are in most cases not deducible from ALS data. Other data sources, such as the cadastre, are needed to gather this information. From a hierarchical point of view, the four geometrical criteria of the Austrian NFI have equal rights. To apply these criteria to remote sensed data, a hierarchy has to be defined with respect to a processing chain. For instance, it would make no sense to check the minimum forested area if there is no potential area detected yet. In this approach, the hierarchy is defined as follows: (1) min. height, (2) min. CC, (3) min. area and (4) min. width, whereas (3) and (4) are checked in an iterative process.

3.1. Derived Base Products

In a preliminary working process, two base products were calculated from the pointcloud. The first one is the nDSM, which is derived by subtracting the DTM from the DSM. The nDSM, also known as CHM, is a very suitable product for the delineation of forested areas because it directly shows object heights (e.g., tree heights). In order to process the DSM, a land-cover-dependent derivation approach, described in Hollaus *et al.* [26], was chosen. This approach makes use of the strengths of different algorithms for generating the final DSM by using surface roughness information to combine two DSMs, which are calculated based (i) on the highest echo within a raster cell and (ii) on moving least squares interpolation (*i.e.*, moving planes interpolation). The second base product is a slope adaptive echo ratio (sER) map, which is calculated, based on the 3D point cloud using FE and LE ALS data. As described in Höfle *et al.* [27,28], the sER is defined as the ratio between the number of neighboring echoes in a fixed search distance of 1.0 m measured in 3D (a sphere) and all echoes located within the same search distance in 2D (a cylinder). The sER is a measure for local transparency and roughness of

the top-most surface and is well suited for the elimination of artificial objects in the forest delineation process (see Section 3.2). The base products derived have a spatial resolution of $1 \times 1 \text{ m}^2$ and have been processed consistently for all study areas using the OPALS software [29].

3.2. Removing Artificial Objects

Since all elevated objects, e.g., buildings, forests, power lines and cable cars, are present in the nDSM, a pre-processing step is required to extract a vegetation mask that includes potential forested areas. As shown in previous studies [27,30], the sER can be used to differentiate between buildings and forested areas. A sER value of 100% means that the echoes within the 2D search radius describe a planar surface (e.g., roofs), whereas a sER value lower than 100% means that the echoes are vertically distributed within the 2D search area, thus indicating penetrable objects, *i.e.*, forests. A specialty of the sER is that the outer edges of buildings as well as power lines appear as pixel lines with values lower than 100% in the sER maps (see figure in Section 4.2). This is the case because echoes that are vertically distributed on walls of buildings and in the area of power lines wrongly indicate penetrable objects. Therefore, an empirically determined threshold of 85% is applied to the sER map for eliminating artificial objects. Furthermore, morphological operations (opening, closing) are applied to remove the remaining building borders and power lines. The resulting vegetation mask provides a fundamental input for the delineation of forested areas.

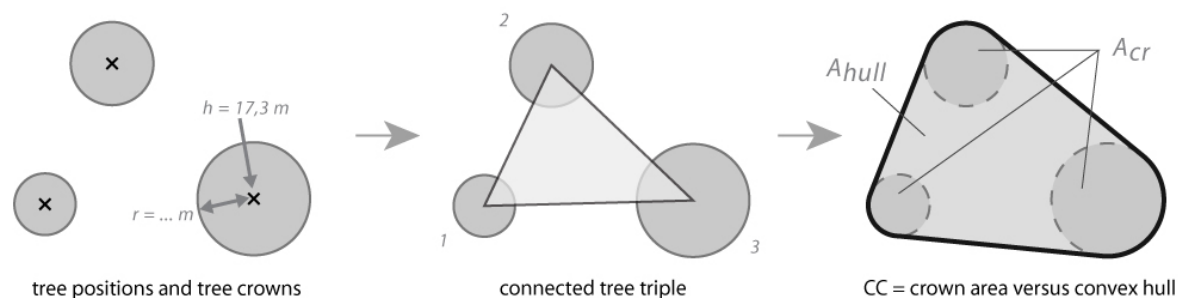
3.3. Minimum Height Criterion

The minimum height criterion is not well defined in the Austrian NFI, since it is dependent on an “*in situ* reachable tree height”. Depending on this *in situ* reachable tree height, which obviously has to be defined by user-dependent expert knowledge, the minimum tree height can be set to 2–7 m. Reachable tree heights cannot be obtained from ALS data directly. However, as the goal of this approach is a user independent result, a minimum tree height of 2.0 m is used for the automatic delineation process. The minimum height criterion is applied by height thresholding the nDSM within the vegetation mask.

3.4. Minimum Crown Coverage Criterion

The parameter CC defines the vertically projected crown area of trees within a certain reference area. Current automatic methods for calculating CC maps are commonly based on a moving window approach. The kernel size of the moving window, which defines the reference area, is a fundamental parameter. Since there is no exact definition of the size and the shape of the reference area available in the NFI, different results are derived if different kernel sizes and shapes (e.g., square, circle) are applied [21]. Another limitation of the moving window approach is that smoothing effects occur at the border of a forest and at small clearings. To overcome these limitations, a new unambiguous approach for determining CC is presented. The method developed aims to define the criterion of CC with a clear geometrical definition, which is based on ALS and NFI data. The basic idea is to express CC as a relation between the sum of the crown areas of three neighboring trees and the area of their convex hull (Figure 2).

Figure 2. ‘Tree triples’ approach: three trees are connected for calculating the CC. The amount of CC is the relation between the area covered by crowns and the area of their convex hull.



3.4.1. Potential Tree Positions

The potential tree positions are detected with a local maxima filter applied to the nDSM. A circular kernel with an empirically determined size of 5×5 m [23] is used to determine potential tree positions. The chosen properties of the local maxima filter are optimized for trees at the timberline, because those areas are the most critical ones for the CC criterion. The detected positions are restricted, to be found within valid areas of the vegetation mask, as well as within valid areas of the height-thresholded nDSM.

3.4.2. Tree Crown Estimation

The crown radii R_i are assessed using the following empirical function, describing the relationship between tree height and crown radius:

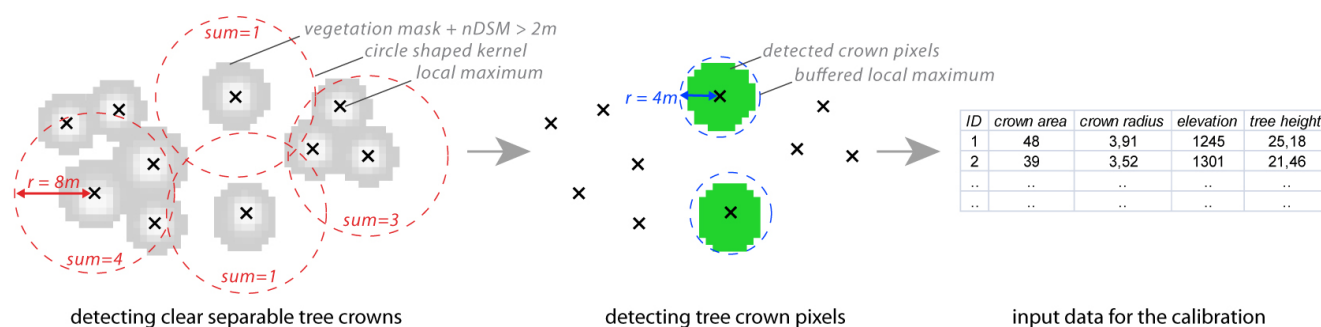
$$R_i = a + b \cdot t_i + c \cdot e_i \quad (1)$$

The input parameters for this function are the tree heights t_i (z-value of the nDSM at the detected potential tree position) and the elevation of the tree e_i (z-value of the DTM at the detected potential tree position). The coefficients a , b and c are calibrated, based on sample crowns. For this calibration the following two possibilities are investigated:

- Measurements of crown radii from the NFI are used for the calibration. For this study the function was calibrated for trees near the timberline. Tree crowns, tree heights and elevations of sample trees, measured within multiple field campaigns of the Austrian NFI (Section 2.3), are used to calibrate the coefficients a , b and c in Equation (1). The calibrated function is applied to the detected tree positions to estimate the crowns for all trees within the study areas.
- Clearly separable tree crown samples are automatically extracted from the nDSM to calibrate the function. The main idea is to extract only trees which are located at least 8 m away from any other detected tree. The distance of 8 m is empirically determined for the study areas and represents the largest tree crown diameter found in the study areas. Based on the tree crowns of those filtered trees the function is locally calibrated (Figure 3). The sample trees are detected with a moving window approach, based on a binary raster map of the local maxima. Pixels in the resulting map, where the sum of all pixels within a circular kernel with a radius of 8 m is one, provide positions of trees with a clear, separable crown. The broadest crown diameter is

found by applying the NFI calibrated function to the detected local maxima. The positions found are buffered by half of the previously-used kernel size and are intersected with the height thresholded nDSM ($nDSM \geq 2$ m) and the vegetation mask. The resulting binary map shows the crown pixels of the identified sample trees. For each tree, the crown area is extracted from the map, and furthermore the average crown radius is derived. Additionally, the tree height and elevation of each sample tree is extracted from the nDSM and the DTM respectively at the position of the corresponding local maximum. For each study area the coefficients of Equation (1) are estimated by solving the system of linear equations based on the crown radii provided, tree heights and elevations of the sample trees. Finally, for each study area the locally calibrated function is applied to derive the crown radii for all trees.

Figure 3. Extraction of clearly separable tree crowns from the nDSM for a local calibration.



To validate the estimated crowns for both possibilities, the derived crown areas are compared to the source map. The source map for the calculations is the height-thresholded nDSM ($nDSM > 2$ m) intersected with the vegetation map. In the source map, all pixels fulfilling the selected threshold are assumed to represent a crown pixel. For each study area the sum of these pixels represents the amount of land covered by tree crowns. To perform a clear validation of the estimated tree crowns, only crown pixels from detected trees should be investigated; otherwise crown pixels of non-detected trees or artificial objects such as buildings and power lines would distort the validation. For that reason the detected local maxima positions are buffered by half of the biggest tree crown diameter found in the study areas to limit the crown pixel to the tree crowns that are represented by detected local maxima. These remaining crown pixels are summed and represent the reference crown area. Furthermore, the areas of the estimated crowns are also summed for each study area and calibration method and compared with the reference crown area.

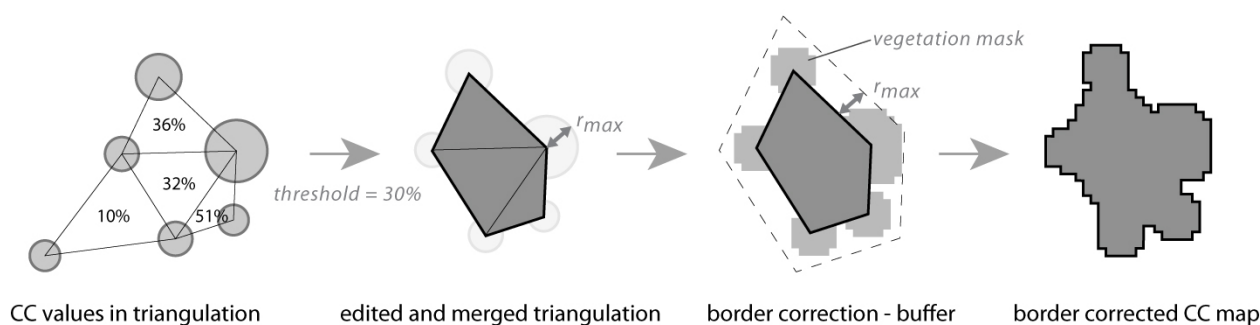
3.4.3. Tree Triples

To connect three neighboring trees, a Delaunay triangulation is applied to the previously-detected tree positions. Since the nearest neighbor graph is a subgraph of the Delaunay triangulation, the three closest standing trees are connected and the minimum inner angles of the triangles are maximized to provide non-sharp-angled triangles, if possible. Further details on Delaunay triangulations can be found in Fortune [31] or Isenburg *et al.* [32]. The Delaunay triangulation is calculated using libraries of the software CGAL [33].

3.4.4. CC Calculation

In a next step, the sum of the crown areas A_{cr} of three neighboring trees and the area of their convex hull A_{hull} is calculated for each tree triple. For this purpose, a tool was implemented in Python [34], which imports a triangulation, calculates the parameters A_{cr} and A_{hull} and returns the CC value for each tree triple. For overlapping tree crowns within a tree triple, the area of the union of crowns is used for A_{cr} . The derived CC values are assigned to their associated triangles. In a next step, the selected CC threshold of 30% is applied to the triangulation and triangles, which do not fulfill the threshold, are removed. As the exported result is an edited triangulation with triangles fulfilling the CC criterion, the borderlines of the derived map represent the tree stem axes and not the convex hulls of the tree triples (Figure 4). For this reason, a borderline correction is applied by buffering the resulting map by the maximum available crown radius found in the study area. In order to prevent an overestimation of the derived potential forest mask, the buffered area is intersected with the vegetation mask and the resulting areas are added to the valid areas of the edited triangulation. The result of these calculations is a potential forest mask that considers the minimum height criterion as well as the minimum CC criterion.

Figure 4. Border correction of the CC map.



3.5. Minimum Area Criterion

The minimum area criterion is applied by using standard GIS-queries. The areas of all valid polygons are calculated for the potential forest mask fulfilling the height- and CC-criterion. Firstly, gaps within polygons are checked. If the gap is smaller than 500 m², the gap is filled. Secondly, the polygons themselves are checked. All polygons that do not fulfill the minimum area criterion of 500 m² are erased.

3.6. Minimum Width Criterion

The minimum width criterion of 10 m is applied by using morphologic operations (open, close) based on the intermediate result fulfilling the criteria height, CC and area. For this operation, a circular kernel with a radius of 5 pixels (pixel size 1 × 1 m) is used to eliminate narrow forested areas that do not fulfill the criterion. This operation is also related to the area criterion, because the removal of narrow areas leads to changes of the forested areas. Therefore, an iterative process of checking minimum area and width is applied.

3.7. Validation

The validation of the final forest mask is performed for the study area 1 (fragmented forest) by comparing the automatically-delineated mask to a reference mask. The reference mask is manually interpreted, based on an orthophoto, using the criteria of the Austrian NFI. The orthophoto was acquired in July 2009 and has a spatial resolution of 0.2 m.

To validate the automatically delineated forest mask with respect to the footprint areas of buildings covered by the forest mask, a building layer is created by manually delineating buildings, based on an orthophoto. Because the acquisition date of the orthophoto differs from the acquisition date of the ALS data, the delineated buildings might be incorrect, or even incomplete, as a result of changes. Therefore, the sER map was used as an additional input within the delineation process to update the building polygons, as necessary. Buildings within densely forested areas might be overgrown and therefore not visible in the orthophoto or sER map. To acquire information about such buildings, the cadastre is used as a third input to gain completeness. For both study areas, the delineated building polygons are intersected with the final forest mask. The remaining building polygons are analyzed.

4. Results and Discussion

4.1. General Considerations

The crowns in the derived base products of ALS tend to be overestimated, because the base products are commonly raster-based and the exact size of the modeled crowns depends on the spatial resolution of the models and on the method applied to calculate the DSM.

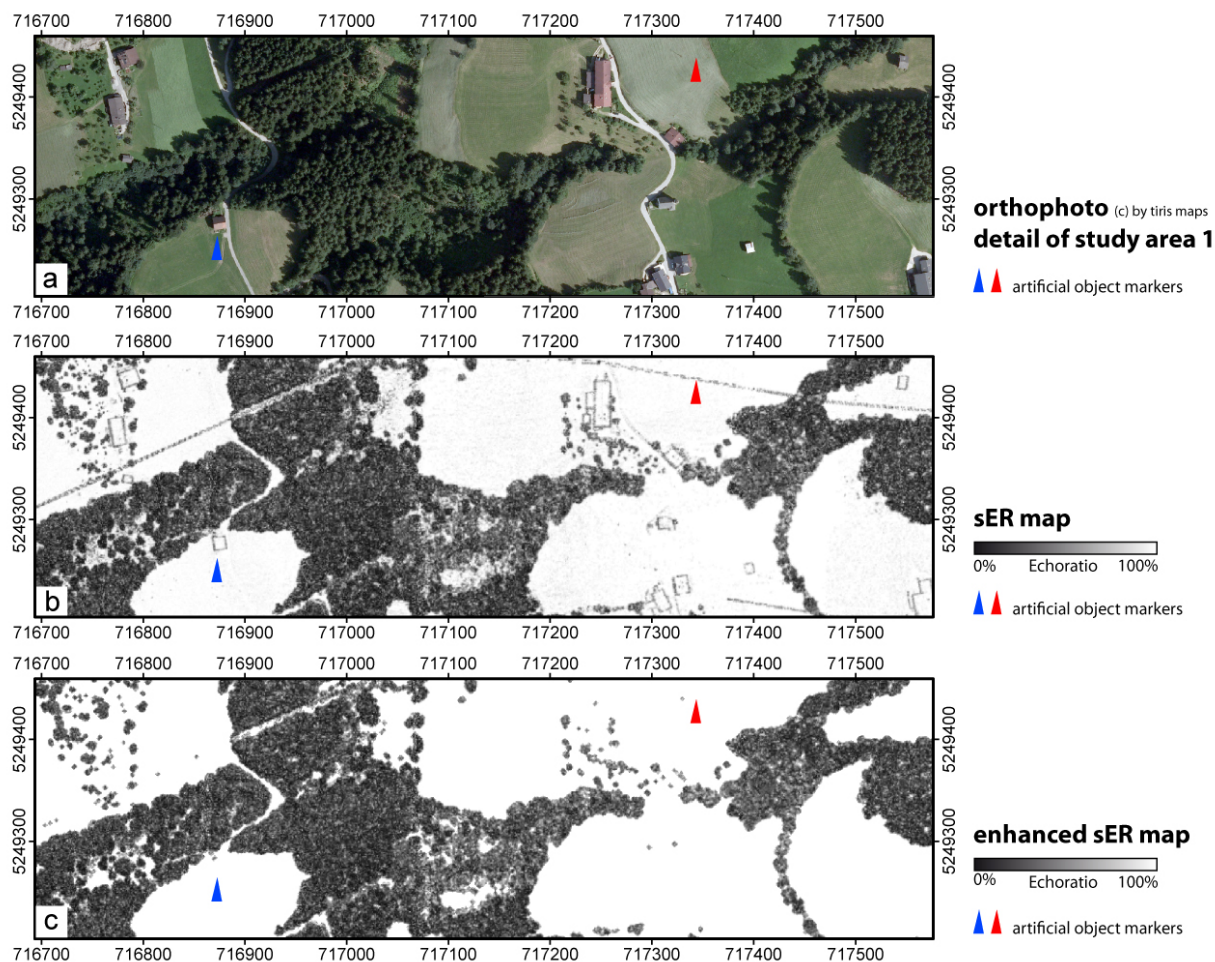
Reference forest maps for large areas, especially those with a high degree of detail, are hard to obtain from other remote sensing data or from *in situ* measurements. In particular, for loosely stocked forests, manually-delineated forest maps based on orthophotos are very limited in quality and always depend on the operator. Therefore, the validation of the automatically delineated forest mask could only be performed for the fragmented study area, since no manually interpreted reference map is available for the loosely stocked study area.

In the following sections, the results of the previous calculations are presented and discussed:

4.2. Removing Artificial Objects

The results of the method described in Section 3.1 are shown in Figure 5 for study area 1. Figure 5(b) shows the original sER-map with colored markers pointing to selected artificial objects. Figure 5(c) shows the enhanced sER-map. The applied processing chain leads to suitable results for eliminating artificial objects and for deriving the vegetation mask. Buildings, power lines, cable cars, *etc.* are removed from the sER-map in most instances, while green areas with a sER value lower than 85 are retained. The vegetation mask obtained is used as a spatial limitation for further processing steps.

Figure 5. Removing artificial objects based on the sER map for the study area 1. The colored markers point to selected artificial objects (a) orthophoto (b) sER map (c) enhanced sER map with removed artificial objects. The coordinates are given in UTM32N.



4.3. Forest Delineation

4.3.1. Detection of Potential Tree Positions

A manual inspection of the automatically detected potential tree positions based on the nDSM and the orthophoto shows suitable results (Figure 6(b)). Due to the limitation of the maxima search of the vegetation mask, no erroneous tree positions at building borders, roof ridges or power lines are available. Because of the small kernel size of 5×5 pixels, multiple local maxima are sometimes found within the area of large single tree crowns. In particular, within densely forested areas, the detected local maxima do not represent the exact tree stem positions and the tree detection rate can be low. Single and clearly separable trees in loosely stocked areas, e.g., near the timberline, are correctly detected in most cases. In general, it can be stated that the completeness of detected local maxima depends on the chosen kernel size, the kernel shape and the tree crown shape. With respect to the estimation of CC, inexact or non-detected trees below dominant trees within a dense forest play a negligible role. Since the CC criterion of forest inventory definitions is commonly in the range of 5%

to 50%, the most critical areas are covered with sparse, loosely stocked forests, where primarily single trees are present. Such trees are clearly separable even with a rather simple local maxima filter.

4.3.2. Tree Crown Estimation

For the detected local maxima, the corresponding tree crowns were calculated, based on the calibrated equations determined from NFI data and the nDSM respectively. For each sample tree the crown radius, the tree height and the DTM height were used. The calibrated coefficients of Equation (1) for calculating the crown radii can be found in Table 3.

For the calibration based on the nDSM without NFI data, Equation (1) was calibrated with sample trees detected in the nDSM. For the loosely stocked forest (study area 2), 1,633 tree crowns, and for the fragmented forest (study area 1), 843 tree crowns could be extracted from the nDSM. The extracted tree crowns are found in loosely stocked areas as well as in denser forested areas. A visual inspection of the extracted sample crowns with an orthophoto shows a good agreement for the detected crowns and the distribution of the samples around the study areas (Figure 6(a)). Only tree crowns, where just a single local maximum was detected within a tree crown, were extracted by the algorithm. The calibrated coefficients for each study area can be found in Table 4.

The validation of the estimated tree crowns for the fragmented study area 1 shows an overestimation of 5% and an underestimation of 25% if the tree crown model is calibrated, based on the nDSM and the NFI data respectively (Table 5). The underestimation of the crowns, estimated based on NFI data, might occur from the very widespread tree samples used in different situations. Additionally, these samples are limited to three tree species which might be more specific to the timberline than to the hillside. Furthermore, the tree samples used are distributed over the entire federal state of Tyrol. Therefore, the calibrated model represents an average tree crown size.

For the loose stocked study area 2, the crown estimation based on the nDSM shows an overestimation of 10%, with the estimation based on NFI data showing an underestimation of 10%. The overestimation might be due to the fact that in the loosely stocked area more trees are detected than in denser areas and tree crowns of single trees in the open terrain tend to be larger than in dense areas, due to the improved sunlight conditions.

The calibrated functions are plotted in Figure 7 for both study areas. Elevations of 1,500 m a.s.l. and 2,000 m a.s.l. are chosen for the fragmented and loosely stocked study areas respectively for plotting the functions. In contrast to the NFI function, the loosely stocked study area the calibrated function based on the nDSM shows a better agreement than the function for the fragmented study area. The bigger difference of the functions for the fragmented area shows the limitations of a NFI function that was calibrated for a usage at the upper timberline when used in other areas. This also corresponds to the huge underestimation of 25% of the NFI function applied to the fragmented study area. A locally calibrated function can overcome these limitations.

Since the calibration based on the nDSM is not always sufficient (e.g., if too few sample trees are extracted in the current study area: if the equation systems of the samples are non-solvable) the calibration based on NFI data is equally necessary. A combination of both might be a good solution. If the local calibration of the function fails, the NFI calibration is used or *vice versa*. If no NFI data are available or only the nDSM calibration should be used, an extension of the current study area can help

if the calibration based on the nDSM fails. With an increasing area, the probability to find single trees increases. Since the crowns, estimated based on the nDSM, fit better for our study areas, the corresponding functions are used for the tree crown estimation in the delineation process.

Figure 6. Tree crown estimation based on the nDSM (a) extracted sample tree crowns (in red) for the loosely stocked forest as an overlay of the orthophoto (b) detected tree positions and estimated tree crowns based on the calibrated function as an overlay of the orthophoto (c) estimated tree crowns and filtered tree triples (CC > 30%) as an overlay of the z-coded nDSM. The coordinates are given in UTM32N.

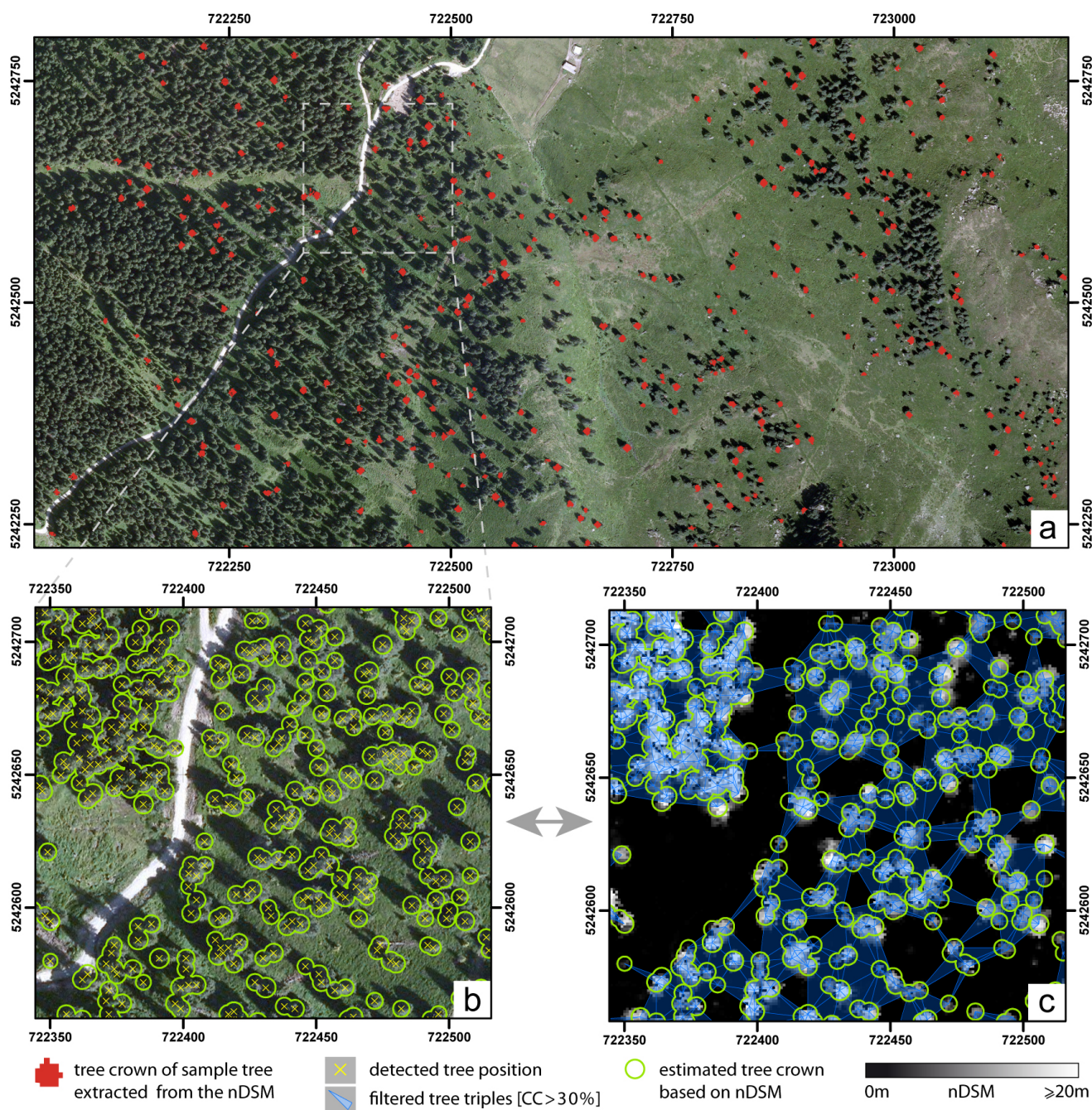


Table 3. Results of the tree crown estimation based on NFI data. Only trees of the species European Larch (*Larix decidua*), Swiss Stone Pine (*Pinus cembra*) and Norway Spruce (*Picea abies L.*) were used for the calibration. The estimated coefficients refer to Equation (1).

Calibration Based on NFI	Estimated Coefficients Based on Selected Conif. Trees
Coefficient a	0.85462
Coefficient b	0.06511
Coefficient c	0.00045

Table 4. Results of the tree crown estimation based on the nDSM. The coefficients of Equation (1) were calibrated by using the crown radii, tree heights and elevations of the detected sample trees.

Calibration Based on nDSM	Study Areas	
	(1) Fragmented Forest	(2) Loosely Stocked Forest
Coefficient a	3.34278	1.92791
Coefficient b	0.03902	0.04771
Coefficient c	-0.00040	0.00032
Nr. of detected sample trees	843	1,633

Figure 7. Comparison of the calibrated functions.

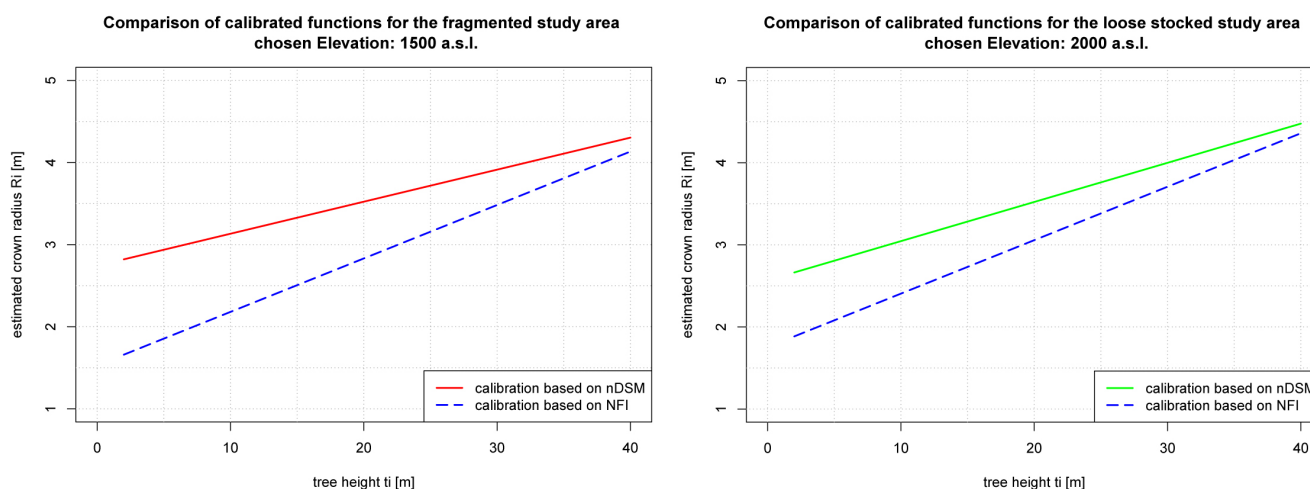


Table 5. Tree crown validation—estimated tree crown areas using different calibration methods.

Crown Area Calibrated with...	Study Areas	
	(1) Fragmented Forest	(2) Loosely Stocked Forest
Reference crown area (ha)	203.07 [100%]	171.57 [100%]
...with nDSM (ha)	212.50 [105%]	189.21 [110%]
...with NFI data (ha)	153.05 [75%]	154.85 [90%]

4.3.3. Tree Triples

The Delaunay triangulation of the potential tree positions shows conclusive results for the connection of tree triples. The detected tree triples are reliably filtered and eliminated, depending on

the selected CC threshold (Figure 6(c)). In particular, in loosely stocked areas at the forest timberline, this method provides a suitable and reproducible potential forest mask. This mask is a fundamental input for the final delineation of forested areas based on a forest definition. Because the tree detection rate is limited in dense stocked forests, the “CC map” based on tree triples shows less detail for such areas. As this method is optimized for loosely stocked forests, it does not provide a highly detailed crown coverage map for dense forests. However, this lower detail in dense areas has no effect on the forest area delineation, because common forest definitions use a CC threshold lower than 50% and therefore the focus is only on looser stocked forests.

4.3.4. Final Forest Mask

In Figure 8 the results for the automatic delineation of the forested areas are. The delineation result for the loosely stocked forest (Figure 8(a)) shows a very jagged forest mask at the upper timberline. Since there is no clearly defined forest border, as in denser forested areas at lower elevations, this result is feasible. Only forested areas are detected by the algorithm, since none of the 22 existing buildings are considered as forest. Single trees on the open terrain as well as areas that are too loosely stocked are reliably excluded from the forest mask. Compared to a manual interpretation, the presented approach is fully automated, the results are independent from the operator and therefore reproducible.

The resulting forest map for the fragmented forest (Figure 8(b)) shows a good agreement with a manual inspection of the forested areas based on an orthophoto and the nDSM. A validation with the manually delineated reference mask shows a producer’s accuracy of 97% and a user’s accuracy of 94% for the classified forest areas (Table 6). The overall accuracy is 96% with a Kappa of 0.92. Due to the applied minimum area criterion, small forest patches with an area less than 500 m², are removed, and forest clearings with an area less than 500 m² are assigned to the forest area. As the preliminary output of the tree triples approach represents the forests borderline along the tree axis, the borderline-corrected forest area delineates the real forest area with good accuracy (Figure 9). Narrow forest areas are eliminated by applying the minimum width criterion (Figure 9, Marker 1). Figure 9, Marker 2 shows an area planted with fruit trees that was wrongly detected by the algorithm. Since the method presented only uses geometrical criteria, additional parameters such as tree species or land use would be needed to tackle this problem. The validation of the automatically delineated forest mask with respect to the footprint areas of buildings covered by the forest mask shows that 68 of 319 existing buildings in the fragmented study area intersect with the forest mask (Table 7). In detail, only nine buildings are 100% covered by the forest mask. A manual inspection of these buildings shows that these buildings are considered as forested area if (a) they are surrounded by single trees (Figure 9, Marker 3), or (b) they are completely covered by vegetation (Figure 9, Marker 4). It is assumed that this problem also occurs with the method presented by Straub *et al.* [19]. 30 buildings are covered lower than 10% by the forest mask (Figure 9, Marker 5). These buildings are partly covered by vegetation and are closely located to the forest border. 29 buildings are covered greater than 10% by the forest mask.

Figure 8. Results of the automatic forest delineation (a) delineated forest area (in red) for the loosely stocked study area overlaid on the z-coded nDSM; (b) delineated forest area (in red) for the study area with the fragmented forest overlaid on the z-coded nDSM. The coordinates are given in UTM32N.

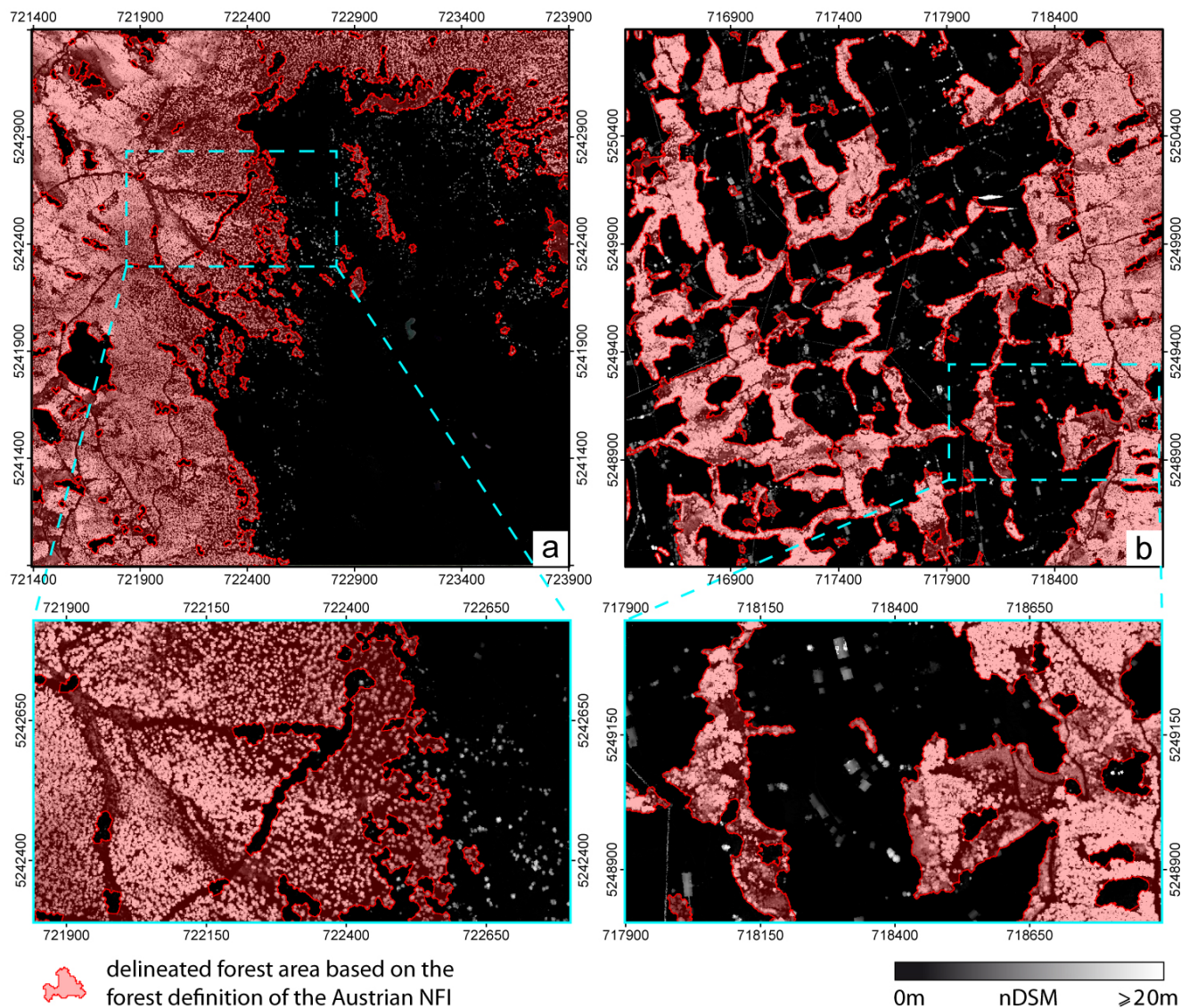


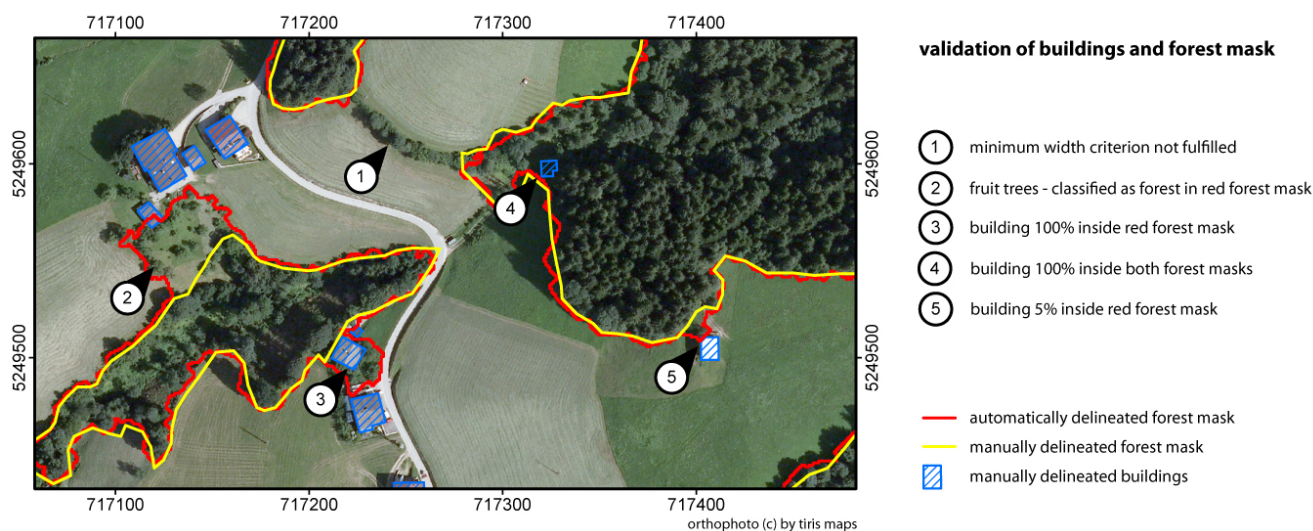
Table 6. Error matrix and descriptive measures showing the comparison of the manual and the corresponding automatic classification for study area 1 (fragmented forest).

Classified Data	Reference - Manually Delineated Forest Mask			User's Accuracy (%)
	Non-Forest (ha)	Forest (ha)	Totals (ha)	
Non-forest (ha)	345	7	352	98
Forest (ha)	17	248	265	94
Totals (ha)	362	255	617	
Producer's accuracy (%)	95	97		
Overall accuracy: 96%		Kappa: 0.92		

Table 7. Validation of the automatically delineated forest mask with respect to the footprint areas of buildings covered by the forest mask.

Buildings vs. Forest Mask	Study Areas			
	(1) Fragmented Forest		(2) Loosely Stocked Forest	
Buildings inside study area	319	[100%]	22	[100%]
Buildings intersecting with forest mask	68	[21%]	0	[0%]
Buildings 100% inside forest mask	9	[3%]	0	[0%]
Buildings <10% inside forest mask	30	[9%]	0	[0%]
Buildings >10% inside forest mask	29	[9%]	0	[0%]

Figure 9. Validation of the automatically delineated forest mask with respect to a manually delineated forest mask and manually delineated buildings. The coordinates are given in UTM32N.



5. Conclusions

The results of the approach here presented show the high potential of an automatic delineation of forested areas, based on airborne laser scanning and national forest inventory data. The method presented delivers repeatable and objective results. Compared to a manually delineated reference mask, the method presented delivers a Kappa of 0.92 for the fragmented study area. The overall accuracy of 96% obtained shows good agreement with the overall accuracy of 97% obtained by Straub *et al.* [19]. The applied workflow considers the four geometrical criteria of the Austrian national forest inventory. Therefore, the criterion of land use and other special restrictions need to be considered in further investigations. The criterion of land use could be investigated by a combination of high-resolution aerial images or with a cadastre. The ‘tree triples’ approach provides a clearly defined reference size for calculating the crown coverage and overcomes limitations such as smoothing effects or dependency of the kernel size and shape of the moving window approach, especially in loosely stocked forests. The crown coverage value is calculated for each tree triple independently and therefore an interaction with neighboring triples is not considered. A possible improvement of the method presented would be to intersect the triangles of a triangulation of tree positions with a map of

the estimated tree crowns. The area of interest for the crown coverage calculation of each triple would then be the triangle connecting three trees, and not the convex hull of the estimated crowns. Since fragments of artificial objects may remain in the vegetation mask, further steps need to be done for the elimination of these fragments. In addition, buildings that have been removed in the vegetation mask may be considered fully or partly as forest if they are surrounded by trees. For example, infrastructure GIS layers or the cadastre could be a sufficient input to tackle these issues. The local maxima detection could be improved, especially for dense forests, by applying a more complex detection method [35–37]. The estimation of tree crowns based on the tree height shows consistent results, especially at the upper timberline. The estimation of crowns could be improved by a local calibrated function for mixed and deciduous forests. This could be achieved by using a tree species map, e.g., derived from full-waveform airborne laser scanning data as presented by Hollaus *et al.* [30]. Further investigations in optimizing the local calibration of the function based on the normalized digital surface model need to be done. A different approach for assessing the tree crowns could be based on a segmentation of the crowns, e.g., based on the normalized digital surface model [38–40]. However, acquiring reference measurements from field data for large areas as well as the manual orthophoto interpretation is still challenging. Therefore, the reliable and fully automatic method presented for delineating forested areas from airborne laser scanning data provides a beneficial tool for operational applications. Finally, we recommend extending the available forest definitions with clear geometric definitions of the parameter crown coverage. In particular, the reference area is often missing in current forest definitions. Due to the new possibilities that are provided by airborne laser scanning data, such geometric definitions can be easily considered within the forest area delineation workflow.

Acknowledgments

This study was partly undertaken within the project NEWFOR, financed by the European Territorial Cooperation Alpine Space, and LASER-WOOD (822030), funded by the *Klima- und Energiefonds* in the framework of the program *NEUE ENERGIEN 2020*. The EO data were kindly provided by the department of Geoinformation of the Tyrol state government (Amt der Tiroler Landesregierung, Gruppe Landesbaudirektion, Abteilung Geoinformation), Austria. The forest inventory data were kindly provided by the Department of Forest Inventory at the Federal Research and Training Center for Forests, Natural Hazards and Landscape, Vienna, Austria.

References

1. Næsset, E.; Bjercknes, K.-O. Estimating tree heights and number of stems in young forest stands using airborne laser scanner data. *Remote Sens. Environ.* **2001**, *78*, 328-340.
2. Holmgren, J.; Persson, Å. Identifying species of individual trees using airborne laser scanner. *Remote Sens. Environ.* **2004**, *90*, 415-423.
3. Hyypä, J.; Inkinen, M. Detecting and estimating attributes for single trees using laser scanner. *Photogramm. J. Fin.* **1999**, *16*, 27-42.
4. Hollaus, M.; Wagner, W.; Schadauer, K.; Maier, B.; Gabler, K. Growing stock estimation for alpine forests in Austria: A robust lidar-based approach. *Can. J. Forest Res.* **2009**, *39*, 1387-1400.

5. Næsset, E.; Gobakken, T. Estimating forest growth using canopy metrics derived from airborne laser scanner data. *Remote Sens. Environ.* **2005**, *96*, 453-465.
6. Sherrill, K.R.; Lefsky, M.A.; Bradford, J.B.; Ryan, M.G. Forest structure estimation and pattern exploration from discrete-return lidar in subalpine forests of the central rockies. *Can. J. Forest Res.* **2008**, *38*, 2081-2096.
7. Næsset, E. Predicting forest stand characteristics with airborne scanning laser using a practical two-stage procedure and field data. *Remote Sens. Environ.* **2002**, *80*, 88-99.
8. Hyyppä, J.; Hyyppä, H.; Leckie, D.; Gougeon, F.; Yu, X.; Maltamo, M., Review of methods of small-footprint airborne laser scanning for extracting forest inventory data in boreal forests. *Int. J. Remote Sens.* **2008**, *29*, 1339-1366.
9. Lund, H.G. *Definitions of Forest, Deforestation, Afforestation, and Reforestation*; Available online: <http://home.comcast.net/~gyde/DEFpaper.htm> (accessed on 28 November 2011).
10. Zhu, Z.; Waller, E. Global forest cover mapping for the United Nations Food and Agriculture Organization Forest Resources Assessment 2000 program. *Forest Sci.* **2003**, *49*, 369-380.
11. FAO/FRA. Definitions of Forest and Forest Change. In *Forest Resources Assessment Programme*; FAO: Rome, Italy, 2000; p. 15.
12. Korhonen, L.; Korpela, I.; Heiskanen, J.; Maltamo, M. Airborne discrete-return lidar data in the estimation of vertical canopy cover, angular canopy closure and leaf area index. *Remote Sens. Environ.* **2011**, *115*, 1065-1080.
13. Jennings, S.B.; Brown, N.D.; Sheil, D. Assessing forest canopies and understorey illumination: Canopy closure, canopy cover and other measures. *Forestry* **1999**, *72*, 59-59.
14. Radoux, J.; Defourny, P. A quantitative assessment of boundaries in automated forest stand delineation using very high resolution imagery. *Remote Sens. Environ.* **2007**, *110*, 468-475.
15. Mustonen, J.; Packalén, P.; Kangas, A. Automatic segmentation of forest stands using a canopy height model and aerial photography. *Scand. J. Forest Res.* **2008**, *23*, 534-545.
16. Wang, Z.Y.; Boesch, R.; Ginzler, C. Integration of High Resolution Aerial Images And Airborne Lidar Data for Forest Delineation. In *Proceedings of The ISPRS XXI Congress*, Beijing, China, 3–11 July 2008; pp. 1203-1208.
17. Wang, Z.; Boesch, R.; Ginzler, C. Forest delineation of aerial images with “Gabor” wavelets. *Int. J. Remote Sens.* **2011**, *33*, 2196-2213.
18. Brassel, P.; Brändli, U.-B.; Lischke, H.; Duc, P.; Keller, M.; Köhl, M.; Herold, A.; Kaufmann, E.; Paschedag, I.; Schnellbacher, H.-J.; et al. *Swiss National Forest Inventory: Methods and Models of the Second Assessment*; Swiss Federal Research Institute WSL: Birmensdorf, Switzerland, 2001; p. 336.
19. Straub, C.; Weinacker, H.; Koch, B. A Fully Automated Procedure for Delineation and Classification of Forest and Non-Forest Vegetation Based on Full Waveform Laser Scanner Data. In *International Archives of the Photogrammetry, Remote Sensing and Spatial Information Sciences*; ISPRS: Vienna, Austria, 2008; Volume 37, pp. 1013-1019.
20. Eysn, L.; Hollaus, M.; Schadauer, K.; Roncat, A. Crown Coverage Calculation Based on ALS Data. In *Proceedings of 11th International Conference on LiDAR Applications for Assessing Forest Ecosystems (Silvilaser 2011)*, Hobart, Australia, 16–20 October 2011; p. 10.

21. Food and Agriculture Organization of the United Nations Global Forest Resources Assessments (FRA). Available online: <http://www.fao.org/forestry/fra/en/> (accessed on 4 December 2011).
22. Gabler, K.; Schadauer, K. *Methoden der Österreichischen Waldinventur 2000/02: Grundlagen, Entwicklung, Design, Daten, Modelle, Auswertung und Fehlerrechnung*; Schriftenreihe des Bundesforschungs- und Ausbildungszentrum für Wald, Naturgefahren und Landschaft; BFW-Berichte: Vienna, Austria, 2006; No. 135.
23. Eysn, L.; Hollaus, M.; Vetter, M.; Mücke, W.; Pfeifer, N.; Regner, B. Adapting Alpha-Shapes for Forest Delineation Using ALS Data. In *Proceedings of 10th International Conference on LiDAR Applications for Assessing Forest Ecosystems (Silvilaser 2010)*, Freiburg, Germany, 14–17 September 2010; p. 10.
24. Kraus, K.; Pfeifer, N. Determination of terrain models in wooded areas with airborne laser scanner data. *ISPRS J. Photogramm.* **1998**, *53*, 193-203.
25. Kraft, G. Beiträge zur Lehre von Durchforstungen, Schlagstellungen und Lichtungshieben, 1884.
26. Hollaus, M.; Mandlbürger, G.; Pfeifer, N.; Mücke, W. Land Cover Dependent Derivation of Digital Surface Models from Airborne Laser Scanning Data. In *ISPRS Commission III Symposium PCV2010*, Saint-Mandré, France, 1–3 September 2010; p. 6.
27. Höfle, B.; Mücke, W.; Dutter, M.; Rutzinger, M.; Dorninger, P. Detection of Building Regions Using Airborne Lidar—A New Combination of Raster and Point Cloud Based GIS Methods. In *Proceedings of GI_Forum 2009: International Conference on Applied Geoinformatics*, Salzburg, Austria, 7 July 2009; pp. 66-75.
28. Rutzinger, M.; Höfle, B.; Hollaus, M.; Pfeifer, N. Object-based point cloud analysis of full-waveform airborne laser scanning data for urban vegetation classification. *Sensors* **2008**, *8*, 4505-4528.
29. OPALS. *Orientation and Processing of Airborne Laser Scanning Data*; Available online: <http://www.ipf.tuwien.ac.at/opals/> (accessed on 07 November 2011).
30. Hollaus, M.; Mücke, W.; Höfle, B.; Dorigo, W.; Pfeifer, N.; Wagner, W.; Bauerhansl, C.; Regner, B. Tree Species Classification Based on Full-Waveform Airborne Laser Scanning Data. In *Proceedings of 9th International Silvilaser Conference*, College Station, TX, USA, 14–16 October 2009; pp. 54-62.
31. Fortune, S. Voronoi Diagrams and Delaunay Triangulations. In *Computing in Euclidean Geometry*; Hwang, F.K., Du, D.Z., Eds.; Lecture Notes Series on Computing; World Scientific Publishing Co.: Singapore, 1992; Volume 1, pp. 193-233.
32. Isenburg, M.; Liu, Y.; Shewchuk, J.; Snoeyink, J. Streaming Computation of Delaunay Triangulations. In *Proceedings of ACM SIGGRAPH 2006*, Boston, MA, USA, 30 July–3 August 2006; pp. 1049-1056.
33. CGAL. *Computational Geometry Algorithms Library*; Available online: <http://www.cgal.org/> (accessed on 20 May 2011).
34. PYTHON. *Python Programming Language*; Available online: <http://www.python.org/> (accessed on 20 May 2011).
35. Reitberger, J.; Schnörr, C.; Krzystek, P.; Stilla, U. 3D segmentation of single trees exploiting full waveform lidar data. *ISPRS J. Photogramm.* **2009**, *64*, 561-574.

36. Brandtberg, T. Classifying individual tree species under leaf-off and leaf-on conditions using airborne lidar. *ISPRS J. Photogramm.* **2007**, *61*, 325-340.
37. Monnet, J.-M.; Mermin, E.; Chanussot, J.; Berger, F. Tree Top Detection Using Local Maxima Filtering: A Parameter Sensitivity Analysis. In *Proceedings of 10th International Conference on LiDAR Applications for Assessing Forest Ecosystems (Silvilaser 2010)*, Freiburg, Germany, 14–17 September 2010; p. 9.
38. Baatz, M.; Schäpe, A. Multiresolution Segmentation: An Optimization Approach for High Quality Multi-Scale Image Segmentation. In *Angewandte Geographische Informationsverarbeitung XII. Beiträge zum AGIT-Symposium Salzburg 2000*; Strobl, J., Blaschke, T., Griesebner, G., Eds.; Karlsruhe, Herbert Wichmann Verlag: Salzburg, Austria, 2000; p. 12.
39. Höfle, B.; Hollaus, M.; Lehner, H.; Pfeifer, N.; Wagner, W. Area-Based Parameterization of Forest Structure Using Full-Waveform Airborne Laser Scanning Data. In *Proceedings of SilviLaser 2008*, Edinburgh, UK, 17–19 September 2008; p. 8.
40. Solberg, S.; Naesset, E.; Bollandsas, O.M. Single tree segmentation using airborne laser scanner data in a structurally heterogeneous spruce forest. *Photogramm. Eng. Remote Sensing* **2006**, *72*, 1369-1378.

© 2012 by the authors; licensee MDPI, Basel, Switzerland. This article is an open access article distributed under the terms and conditions of the Creative Commons Attribution license (<http://creativecommons.org/licenses/by/3.0/>).

Article II

crown coverage calculation based on ALS data

Lothar Eysn¹, Markus Hollaus¹, Klemens Schadauer² and Andreas Roncat¹

¹ Institute of Photogrammetry and Remote Sensing, Vienna University of Technology, Gußhausstraße 27-29, 1040 Vienna, Austria, <le, mh, ar @ipf.tuwien.ac.at>

² Department of Forest Inventory at the Federal Research and Training Center for Forests, Natural Hazards and Landscape, Seckendorff-Gudent-Weg, 1130 Vienna, Austria, <klemens.schadauer@bfw.gv.at>

Abstract

The objective of this paper is to present and evaluate a new geometrically unambiguously defined approach to calculate forest canopy cover, also known as crown coverage (CC) from airborne laser scanning (ALS) data based on national forest inventory (NFI) data. The CC is defined as the proportion of the forest floor covered by the vertical projection of the tree crowns. Most forest definitions lack in precise geometrical definitions for the calculation of CC and therefore, the results of common calculation methods differ and tend to be incomparable. To demonstrate the effect of such an unclear defined, common CC calculation method, CC maps, generated from moving window algorithms using different kernel shapes and sizes, are calculated and analyzed for three study areas in Tyrol, Austria. The new unambiguously approach, the tree triples method, is based on defining CC as a relation between the sum of the crown areas of three neighbouring trees at a time and the area of their convex hull. The approach is applied for the same study areas and is compared with forest masks that are generated from moving window algorithms using different kernel shapes and sizes.

Keywords: forest definition, canopy cover, forest border delineation, vegetation mapping, LiDAR

1. Introduction

The delineation as well as the classification of forests has a long tradition in remote sensing. Considering different forest definitions (e.g. Austrian forest law, FAO) forested land can for example be composed of tree crowns, forest gaps, forest streets or harvested areas. It is often difficult to derive this complex land use class “forest” from remotely sensed data in a reliable and comprehensible way. In different forest definitions the criterion of crown coverage (CC) is a fundamental and obligatory parameter for classifying forested areas. For example the international forest definition of the United Nations Food and Agricultural Organization (FAO) defines a forest as land of at least 0.5 ha with a potential tree height of at least five meters and a CC greater than 10% (FAO/FRA, 2000). CC, also known as canopy coverage or forest canopy cover, is defined as the proportion of the forest floor covered by the vertical projection of the tree crowns (Jennings et al., 1999). In (Korhonen et al., 2011) vertically measured crown cover is referred as vertical canopy cover (VCC). The current paper considers VCC. An unclear defined detail is the treatment of gaps within the projected tree crowns itself. The traditional definition of canopy cover includes an “outer edge” or “envelope” of a crown, inside of which the cover is thought to be continuous, but in practice the “outer edge” is sometimes very difficult to observe (Korhonen et al., 2006). For the current paper those crown gaps are not considered.

To evaluate the amount of CC for an area, in-situ measurements or remote sensing techniques can be used. In-situ measurements are time consuming and are mainly operated for sample plots while remote sensing techniques overcome the limitation of plot-wise sampling and provide the possibility to analyze large areas. As terrestrial measurements deliver the ground truth for most

of the remote sensing techniques, in-situ samples are a fundamental input for cross validations. A comparison of common terrestrial measuring techniques can be found in (Korhonen et al., 2006). An often applied method for assessing an area's CC is the manual interpretation of orthophotos. This technique is however costly, limited by shadowing effects and the quality of the results are dependent on the interpreter. It is therefore difficult to obtain objective quantitative measurements that are suitable for comparisons with remotely based CC measures (Holmgren et al., 2008). A different approach is to define the amount of CC as a relation between two trees. Depending on the threshold of CC, the tree species and the tree crowns size a maximum distance between two trees can be determined (Hauk and Schadauer, 2009). This method, which is originally based on the work of Hasenauer (Hasenauer, 1997), is currently used for the manual delineation of forested areas at the Department of Forest Inventory at the Federal Research and Training Center for Forests, Natural Hazards and Landscape (BFW) in Austria.

As an alternative to the manual photo interpretation the technique of airborne laser scanning (ALS) was established for assessing an area's CC (Holmgren et al., 2008; Korhonen et al., 2010). ALS, as an active remote sensing technique, is not influenced by shadowing effects or different sun illumination conditions, is able to deliver reliable information even for small forest gaps and is well suited for estimating CC. The normalized digital surface model (nDSM), calculated by subtracting the digital terrain model (DTM) from the digital surface model (DSM) provides an excellent data source for calculating the CC. Using the nDSM, a height threshold can be applied to decide whether a pixel is covered by tree crowns or not. In a next step the CC can be calculated by dividing the reference area by the tree crown covered area. As reference area forest stands or moving windows with user defined circular or squared kernel shapes are commonly in use. Unfortunately, due to the lack of precise geometric descriptions of the CC (i.e. reference size and -shape) the derived results are often not comparable and make the CC to a doubtful criterion. Therefore, this study aims at defining a novel, geometrically clear defined method for an automatic calculation of CC based on ALS and NFI data. In this approach CC is defined as a relation between the sum of the crown areas of three neighbouring trees at a time and the area of their convex hull. The new method is applied for three study areas in Tyrol, Austria considering the forest definition of the Austrian national Forest inventory (NFI). This study is part of the research project "LASER-WOOD" funded by the Klima- und Energiefonds in the framework of the program "NEUE ENERGIEN 2020". As LASER-WOOD is an ongoing project this paper describes first results of the ongoing investigations.

The remaining parts of this paper are organized as follows: Section 2 describes the selected study areas and the used data. In Section 3 the methodology and implementation is explained. Section 4 shows results and their discussions whereas in Section 5 concluding remarks are given.

2. Study area and dataset

2.1 Study area

In this contribution three different study areas in Austria are investigated. The study areas are located in the "Zillertal" which is located in the eastern part of the federal state of Tyrol. Each study area covers an area of 2.5 x 2.5 km and shows different structures and amounts of forested land (Figure 1). Study area 1 consists of a loose stocked forest at the upper timberline (Figure 1a) with elevations from 1800 to 2000 m above sea level (a.s.l). Study area 2 consists of a fragmented forest with patch-wise forest stands on the hillside (Figure 1b) with elevations from 600 to 1600 m a.s.l. Study area 3 consists of a mainly dense forest with different age classes (Figure 1c). The elevations for study area 3 reach from 700 to 1500 m a.s.l. The dominant tree species in all three study areas are coniferous trees. Beside the forested areas buildings and power lines can be found in the study areas.

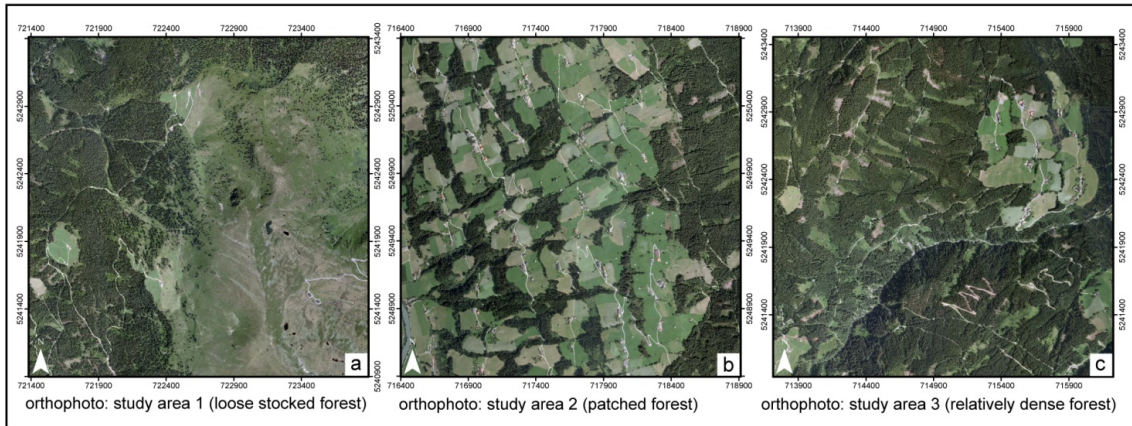


Figure 1: Orthophotos of the study areas. (a) Study area 1 shows a loose stocked forest at high elevations. (b) Study area 2 shows a patched, fragmented forest. (c) Study area 3 shows a relatively dense forest with different age classes.

2.2 ALS data

The used ALS data was acquired using an Optech Inc. ALTM 3100 laser scanner during multiple flight campaigns in 2008 under leaf-off and leaf-on canopy conditions. The mean point density is about 4 echoes / m² for study area 1, 5 echoes / m² for study area 2 and 9 echoes / m² for study area 3. Further details can be found in (Eysn et al., 2010a).

2.3 Derived base products

The ALS data has been processed and filtered using the hierarchic robust filtering approach (Kraus and Pfeifer, 1998) to obtain DTM's. For the processing of the DSM a land cover dependent derivation approach (Hollaus et al., 2010) was chosen. By subtracting the DSM from the DTM a normalized digital surface model (nDSM) was created as a fundamental base product for calculating the CC and delineating forested areas. Additionally a slope adaptive echo ratio (sER) map (Höfle et al., 2009), as a measure for local transparency and roughness of the top-most surface, was derived. To eliminate buildings and other artificial objects, the sER map was corrected with morphological operations and thresholding to a so called "vegetation mask". Further information on this correction can be found in (Eysn et al., 2010b). The spatial resolution of the derived products is 1 x 1 m².

3. Methodology and Implementation

3.1 Moving window approach

As described in the Introduction the automatic inspection of the criteria CC is crucial and unfortunately not clearly defined. Especially for larger scale applications like the automatic delineation of forested areas based on ALS data the moving window approach leads to varying results. To demonstrate the effect of different parameters for kernel shapes and -sizes on the resulting CC maps, multiple variations of these two parameters have been analyzed. To be able to compare the results, the sum of areas fulfilling different CC thresholds are compared with each other.

As a basis for these calculations a combination of a height thresholded nDSM and the vegetation mask is chosen. Pixels with a nDSM value greater than 2.0 m and an sER value less than 85% are assumed to be crown covered and are set to one. Pixels not fulfilling these criteria are set to zero. The height threshold is set to consider the minimum height criterion of the Austrian

NFI. Based on the derived binary, “preliminary vegetation map” the CC values are calculated with a circle- and square-shaped kernel with different kernel sizes using the software OPALS (OPALS, 2011). The used kernel sizes are defined as a radius (in pixels) from 1 to 40 Pixels. For example a kernel radius of 3 the square shaped kernel is a 7x7 matrix. The centre pixel of the kernel is calculated by the mean of all pixels covered by the kernel and represents the CC for this Pixel. To be able to check the results of these calculations against different forest definitions, several CC thresholds are applied to the calculated CC maps. For this study CC thresholds from 10 % to 100 % with steps of 10 % were chosen. The results of this processing step are binary maps which represent so called potential forest masks. Finally, the potential forest mask’s size within the study area is determined. For visualisation purposes those areas are plotted against the kernel sizes corresponding to the selected CC thresholds (see Figure 3).

3.2 Tree triples approach

The developed method for the calculation of CC aims at defining the criteria of CC with a clear geometrical definition which is based on ALS data and NFI data. The basic idea is to express CC as a relation between the sum of the crown areas of three neighbouring trees at a time and the area of their convex hull (see Figure 2).

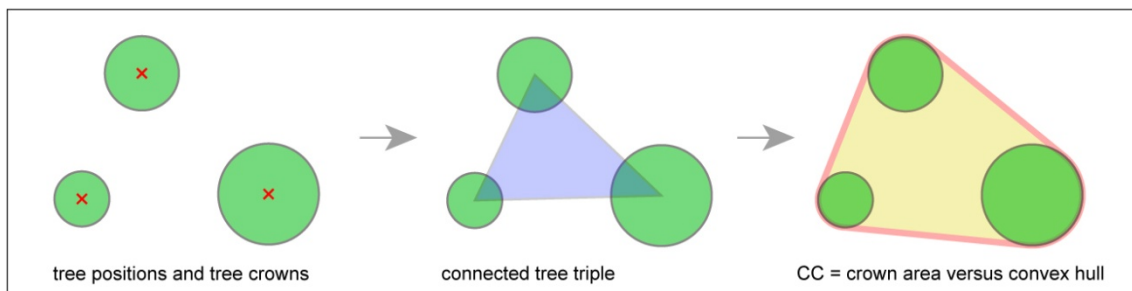


Figure 2: tree triples approach: three trees at a time are connected. The amount of CC is the relation between the area covered by crowns and the area of the convex hull.

As described in (Eysn et al., 2010b) the tree positions are detected with a local maxima filter based on the nDSM and the vegetation mask. To consider the minimum height criterion of the Austrian NFI a height threshold of 2.0 m is applied to the maxima search. The crown diameters are assessed using empirical functions, which act as a relationship between tree height and crown radius. These functions are calibrated based on measurements of crown radii from the Austrian NFI, whereas for this study the function was assimilated for trees near the timberline. Further details can be found in (Eysn et al., 2010b). To find the tree triples for calculating the CC, a Delaunay triangulation is applied to the detected local maxima. The Delaunay triangulation is calculated using libraries of the Open Source software CGAL (CGAL, 2011). In a next step the sum of the crown areas A_{cr} of three neighbouring trees at a time and the area of their convex hull A_{hull} is calculated for each tree triple. For this purpose a tool was implemented in Python (PYTHON, 2011) which imports a triangulation, calculates the parameters A_{cr} and A_{hull} and returns a CC value for each tree triple. For overlapping tree crowns within a tree triple the intersected crown area is used for A_{cr} . Tree triples respectively their triangles are removed if the selected CC threshold is not fulfilled. The result of these calculations is a potential forest mask which considers the minimum height criterion as well as the minimum CC criterion. As the exported result is a triangulation with triangles fulfilling the CC criterion and not the convex hulls of the tree triples, the borderlines of the derived potential forest mask represent the tree stem axes. For this reason the resulting map is buffered by the half of the maximum available

crown diameter found in the study area. In order to prevent an overestimation of the derived potential forest mask the buffered area is intersected with the vegetation mask.

3.3 Comparison of the two approaches

To be able to compare the results of the two different approaches, a final forest mask, based on the potential forest mask, is derived for both methods. This is necessary because the moving window approach delivers raster based information, the tree triples approach delivers triangle based information which makes a direct comparison difficult.

For both methods the final forest mask is calculated considering the geometrical aspects of the forest definition of the Austrian NFI. For the moving window approach different final forest masks are calculated because of the different kernel sizes and –shapes. The minimum height (set to 2.0 m) and the minimum CC (set to 30 %) is already handled in the potential forest mask. The minimum area criterion is applied by vectorizing the potential forest mask and by deleting single polygons or filling forest gaps with an area less than 500 m². In a next step the minimum width criterion (set to 10 m) is applied by morphological operations. As areas might have changed due to deletion according to the minimum width criterion, the minimum area criterion is checked a second time after this step.

4. Results and Discussion

4.1 general considerations

The definition of CC claims a strictly vertical projection of the tree crowns. In ALS the laser beam vectors are inclined in most instances (except at nadir) and the criteria of a vertical projection is not strictly maintained. However, in typical ALS surveys the off-nadir angles are at maximum 20°, so this effect should remain relatively small. In addition, however, the penetration ability of an ALS pulse may be limited through small canopy gaps, and vary somewhat with the technical acquisition settings (Korhonen et al, 2010). The crowns in the derived base products of ALS tend to be overestimated because the base products are widely raster based and the exact size of the modelled crowns depend on the spatial resolution of the models.

In the following sections the results of the previous calculations are presented and discussed:

4.2 Moving window approach

The results of the moving window method for the three study areas are presented in Figure 3. For each study area the results are separated by the used kernel shape and the different CC thresholds (colored curves). The vertical axis represents the sizes of the resulting areas or potential forest masks in relation to the whole extent of the study area while the horizontal axis represents the different kernel sizes. The values on the vertical axis are normalized between 0 % and 100 %. For example, a kernel size of 0 (which means just one pixel) results in a potential forest mask similar to the vegetation mask. If the window size is not correlated with the resulting areas of fulfilled CC thresholds, all curves of the different CC threshold should be strictly horizontal. If the study area would be covered by a forest by 100%, all curves should be strictly horizontal lines which overlap at 100%.

The CC threshold curves for study area 1 are wide spread compared to the results of the other study areas which seems to be a cause of the loose stocked forest pattern. For study area 2 and study area 3 the curves are narrower. This findings show, that a decrease of the forest density leads to an increased effect of different CC thresholds on the found area.

The result of study area 1 shows a strong variation of the resulting areas between kernel size 1 and kernel size 8 for most of the selected CC thresholds. For kernel sizes from 9 to 40, the resulting forest masks seem to be more independent on the kernel size. In study area 2 (patched forest) a strong variation of the resulting areas is given for a larger range of kernel sizes compared to study area 1. It can be deduced, that the gradient and the curvature of the different curves reflect the kernel size dependency of the resulting potential forest masks for different selected CC thresholds.

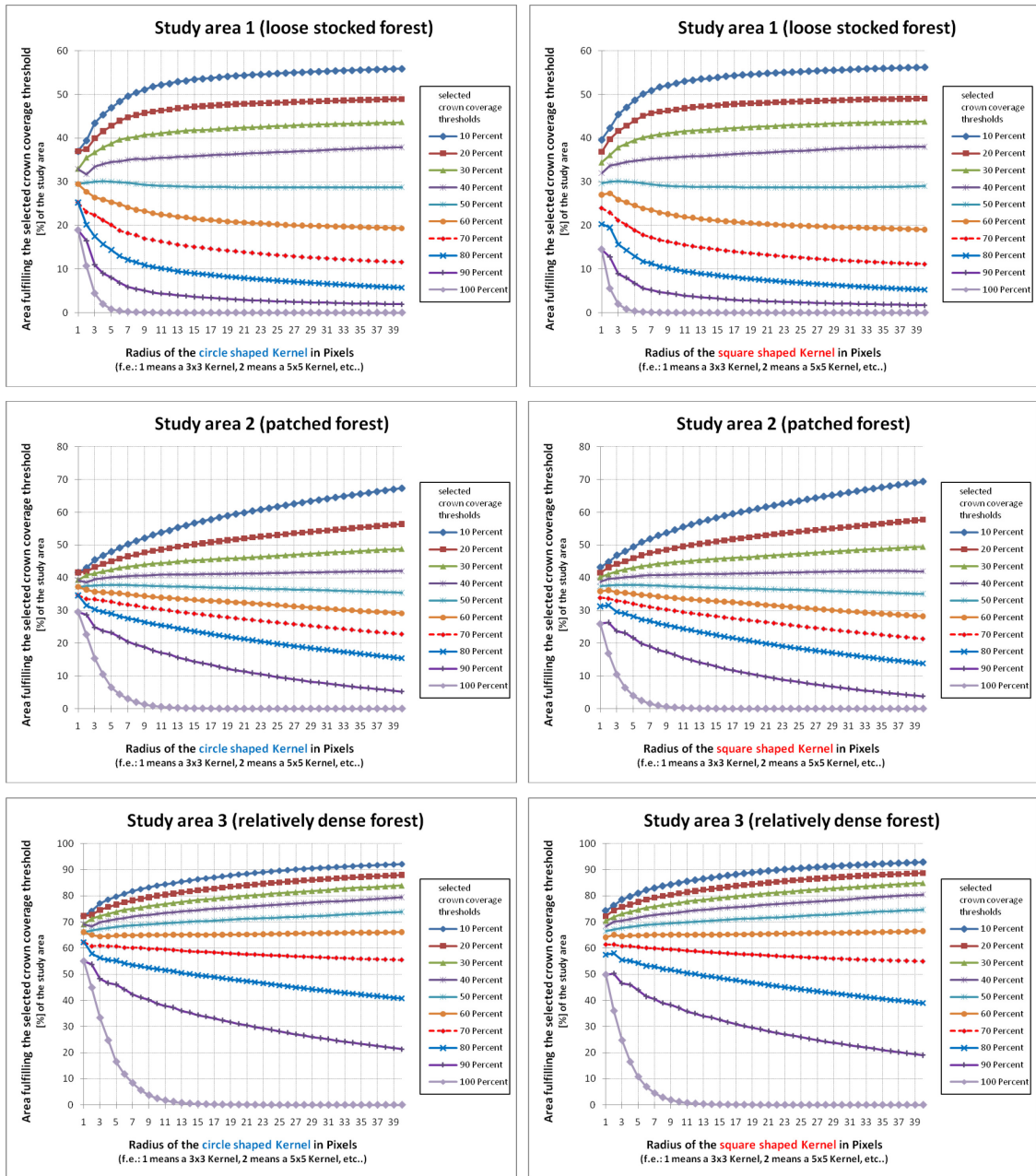


Figure 3: Resulting sizes of the potential forest masks of three different study areas using the moving window approach with varying kernel sizes. In the left column the results for a circle shaped kernel with different CC thresholds is shown for all three study areas. In the right column the results for a circle shaped kernel with different kernel sizes and different CC thresholds are shown.

4.3 Tree triples approach

A manual inspection of the automatically detected potential tree positions based on the nDSM and the vegetation mask shows suitable results (Figure 4b). Due to the limitation of the maxima search using the vegetation mask mainly maxima in vegetated areas are found. Because of the small kernel size of 5 x 5 pixels multiple local maxima are sometimes found within the area of single tree crowns. Especially within dense forested areas the detected local maxima do not represent the exact tree stem positions and the tree detection rate can be low. Single and clear separable trees in loose stocked areas are correctly detected in most instances. It can be assumed that the amount of detected local maxima is highly correlated with the chosen kernel size. In relation to the inspection of CC, not exact or non detected tree positions within a dense forest play a minor role since the criterion of CC is most critical for sparse, loose stocked forest areas where primary single, clearly separable trees are present.

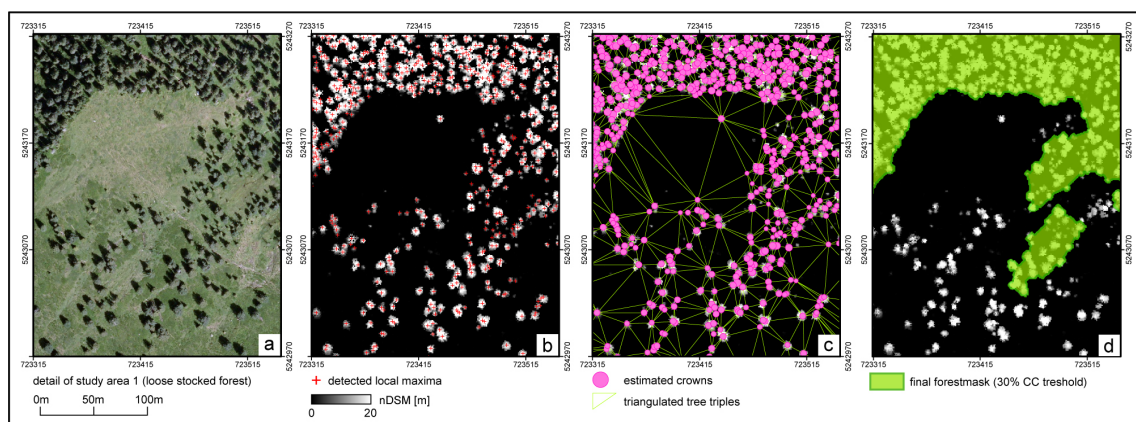


Figure 4: Intermediate results of the tree triple approach; a) orthophoto of a subset of study area 1 b) detected local maxima c) detected tree triples plus estimated crowns d) final forest mask fulfilling the criteria of the Austrian NFI.

For the detected local maxima the corresponding tree crowns were calculated based on the calibrated formulas determined from NFI data. To validate the estimated crowns, the derived crown areas are compared to the source map. The source map for the calculations is the height thresholded (nDSM > 2 m) combined with the vegetation map. In the source map, all pixels fulfilling the selected thresholds are assumed to represent a crown pixel. For each study area the sum of these pixels represent the amount of land covered by tree crowns. The areas of the estimated crowns are also summed up. The comparison of these resulting sums (see Table 1) shows a good estimation of the tree crowns (see Figure 5b) for a loose stocked forest (delta = 3,9 %) while the estimation is worse (see Figure 5d) for a relatively dense forest (delta = 21,8 %). It can be assumed, that the overall smaller estimated sum of crown areas for the relatively dense forest can be explained by limitations of the local maxima search or because the calibration of the relation tree height versus tree crown was performed for mainly trees at the upper timberline.

Table 1: Validation of the estimated tree crowns in comparison to the source map

	\sum crowns source map [%]	\sum estimated crowns [%]	delta [%]
study area 1 (loose stocked forest)	28,5	24,6	3,9
study area 2 (patched forest)	36,5	24,3	12,2
study area 3 (rel. dense forest)	64,9	43,1	21,8

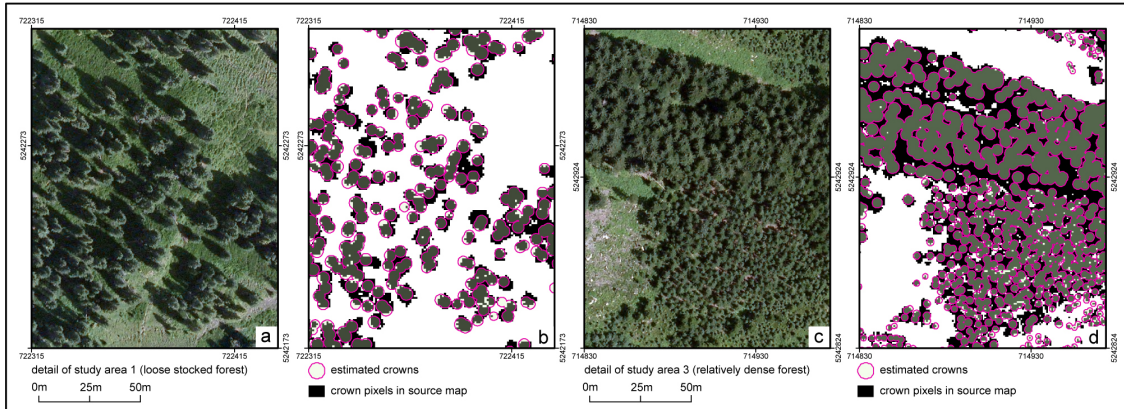


Figure 5: comparison of estimated crowns with the source map; a) orthophoto of a subset of study area 1 b) estimated tree crowns in a loose stocked forest c) orthophoto of a subset of study area 3 d) estimated tree crowns in a relatively dense forest

The Delaunay triangulation of the potential tree positions shows conclusive results for the connection of tree triples (see Figure 4c). The derived tree triples are reliable filtered and eliminated depending on the selected CC threshold and provide, especially at loose stocked areas at the forests timberline, suitable results for the potential forest mask. This mask is a fundamental input for the delineation of forested areas based on a forest definition and therefore, the less detail of this “CC map” at relatively dense forested areas plays a minor role since the focus is on loose stocked areas.

The final forest masks for the comparison of the different approaches are calculated based on the forest definition of the Austrian NFI. Due to the applied minimum area criterion small forest patches with an area less than 500 m² are removed and forest clearings with an area less than 500 m² are assigned to the forest area. Narrow forest areas are eliminated by applying the minimum width criterion. The results of the calculated final forest masks are plotted in Figure 6. The results of study area 1 show almost similar curves for the circle- and square-shaped kernel while the study area 3 shows differing curves with increasing kernel size. It can be assumed that an increasing density of a forested area combined with an increasing kernel size leads to more different results in the resulting final forest mask. Compared to the tree triples approach, the results for the patched and relatively dense forest show almost similar results if a kernel size of 9 to 12 m is chosen, while the results differ for the loose stocked forest. The results show big differences with de- and increasing errors at increasing kernel sizes. Those big differences reflect the limitations of the moving window approach since the results are high correlated with the kernel size.

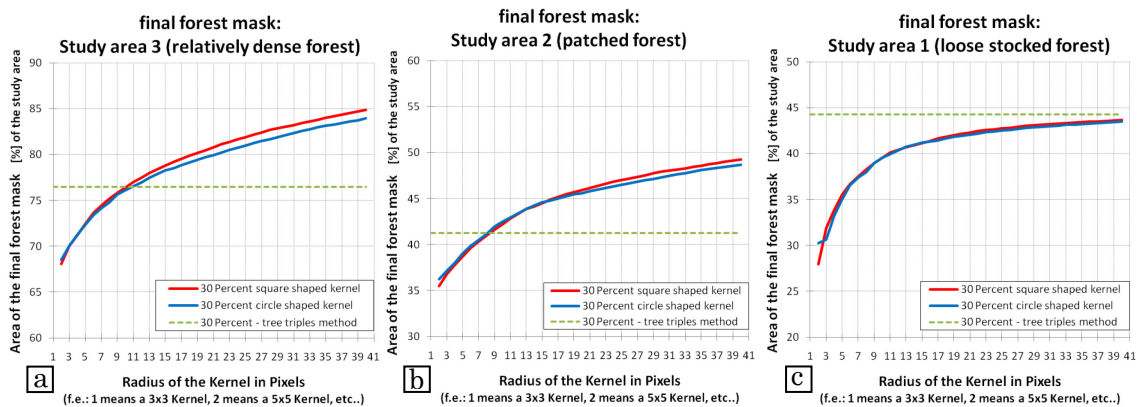


Figure 6: comparison of the resulting forest masks for the moving window approach and the tree triples approach; a) loose stocked forest b) patched forest c) relatively dense forest

5. Conclusion

This study shows the high potential of ALS data for assessing CC and consequently for deriving a forest mask for large areas. A clear geometrical definition for the calculation of CC is necessary since CC is a fundamental criterion in most forest definitions and the results of the moving window method are differing due to its high dependency on the kernel size. It could be shown, that a decrease of the forest density leads to an increased effect of different CC thresholds on the found forest area. Especially at the upper timberline, different kernel sizes and CC thresholds lead to different results. The tree triples method can overcome the limitations of the moving window approach especially at loose stocked forests. The local maxima detection works reliable for such forest areas. The local maxima detection could be improved, especially for dense forests, by applying a more complex detection method. The estimation of tree crowns based on the tree height shows consistent results at the, related to CC, critical area at the upper timberline. The estimation of crowns could be improved by a local calibrated transfer function. In future studies, the method will be firstly investigated for mixed and deciduous forests and secondly a validation with forest inventory will be performed. However, acquiring reference measurements from field data for large areas as well as the manual orthophoto interpretation is still challenging and therefore a reliable method for calculation CC from ALS data is a big effort.

Acknowledgements

The ALS data and orthophotos for the test areas Zillertal were kindly provided by the department of Geoinformation of the Tyrol state government (Amt der Tiroler Landesregierung, Gruppe Landesbaudirektion, Abteilung Geoinformation). A great deal of gratitude goes out to our colleague Christian Ginzler at the Federal Institute for Forest, Snow and Landscape Research (WSL) for the constructive discussions on this topic. The forest inventory data is kindly provided by the Department of Forest Inventory at the Federal Research and Training Center for Forests, Natural Hazards and Landscape, Vienna, Austria. This study is done within the project LASER-WOOD (822030), funded by the Klima- und Energiefonds in the framework of the program "NEUE ENERGIEN 2020".

References

- CGAL Computational Geometry Algorithms Library, <http://www.cgal.org/>, last access: 20.05.2011
- Eysn, L., Hollaus, M., Mücke, W., Vetter, M. and Pfeifer, N., 2010a. Waldlückenerfassung aus ALS Daten mittels alpha-Shapes. In: *Dreiländertagung - 30. Wissenschaftlich-Technische Jahrestagung der DGPF*, Vienna, Vol. Publikationen der Deutschen Gesellschaft für Photogrammetrie, Fernerkundung und Geoinformation e.V., Band 19 (2010): 552 - 560.
- Eysn, L., Hollaus, M., Vetter, M., Mücke, W., Pfeifer, N. and Regner, B., 2010b. Adapting alpha-shapes for forest delineation using ALS Data. In: *10th International Conference on LiDAR Applications for Assessing Forest Ecosystems (Silvilaser 2010)*, Freiburg, Germany, Vol.: 10 p.
- FAO/FRA, 2000. Definitions of forest and forest change, Forest Resources Assessment Programme, Rome 2000, 15.
- Hasenauer, H., 1997. Dimensional relationships of open-grown trees in Austria. *Forest Ecology and Management*, 96, 197-206.
- Hauk, E. and Schadauer, K., 2009. Instruktion für die Feldarbeit der Österreichischen Waldinventur 2007 – 2009 Vienna, 201 p.
- Höfle, B., Mücke, W., Dutter, M., Rutzinger, M. and Dorninger, P., 2009. Detection of building regions using airborne LiDAR – A new combination of raster and point cloud based GIS methods. *GI_Forum 2009 - International Conference on Applied Geoinformatics, Salzburg*, 66-75.

Hollaus, M., Mandlbauer, G., Pfeifer, N. and Mücke, W., 2010. Land cover dependent derivation of digital surface models from airborne laser scanning data. In: *ISPRS Commission III Symposium PCV2010*, Saint-Mandré, France, Vol. Proceedings of the International Archives of the Photogrammetry, Remote Sensing and Spatial Information Sciences Volume XXXVIII: 6-6.

Holmgren, J. et al., 2008. Estimation of crown coverage using airborne laser scanning. In: *SilviLaser 2008, 8th international conference on LiDAR applications in forest assessment and inventory*, Heriot-Watt University, Edinburgh, UK, Vol.: 50-57.

Jennings, S.B., Brown, N.D. and Sheil, D., 1999. Assessing forest canopies and understorey illumination: canopy closure, canopy cover and other measures. *Forestry*, 72(1), 59-59.

Korhonen, L., Kaartinen, H., Kukko, A., Solberg, S. and Astrup, R., 2010. Estimating vertical canopy cover with terrestrial and airborne laser scanning. In: *10th International Conference on LiDAR Applications for Assessing Forest Ecosystems (Silvilaser 2010)*, Freiburg, Germany, Vol.

Korhonen, L., Korpela, I., Heiskanen, J. & Maltamo, M., 2011. Airborne discrete-return LiDAR data in the estimation of vertical canopy cover, angular canopy closure and leaf area index. *Remote Sensing of Environment* 115(4): 1065-1080.

Korhonen, L., Korhonen, K.T., Rautiainen, M. and Stenberg, P., 2006. Estimation of forest canopy cover: a comparison of field measurement techniques. *Silva Fennica*, 40(4), 577-588.

Kraus, K. and Pfeifer, N., 1998. Determination of terrain models in wooded areas with airborne laser scanner data. *ISPRS Journal of Photogrammetry and Remote Sensing*, 53(4), 193-203.

OPALS Orientation and Processing of Airborne Laser Scanning Data, <http://www.ipf.tuwien.ac.at/opals/>, last access: 18.05.2011

PYTHON Python Programming Language, <http://www.python.org/>, last access: 05.05.2011

Article III – German version

The English translation can be found here: [Article III English](#)

Waldlückenerfassung aus ALS Daten mittels α -Shapes

L. EYSN¹, M. HOLLAUS¹, W. MÜCKE¹, M. VETTER^{1,2} & N. PFEIFER¹

1) TU Wien, Institut für Photogrammetrie und Fernerkundung, Gußhausstraße 27 – 29, 1040 Wien;

2) TU Wien, Centre for Water Resource Systems, Karlsplatz 13, 1040 Wien;

E-Mail: le@ipf.tuwien.ac.at

Für die Aufnahme von topographischen Informationen wird verstärkt flugzeuggetragenes Laserscanning (engl. Airborne Laser Scanning, ALS) eingesetzt. Dabei eignet sich ALS als aktive Fernerkundungsmethode besonders für die Abtastung von bewaldeten Gebieten. Speziell in Forstanwendungen ist die aus ALS Daten abgeleitete Höheninformation der Vegetation eine fundamentale Eingangsgröße, die der Berechnung vieler Forstparameter (Baumhöhen, Stammvolumen, Biomasse) zugrunde liegt. Zusätzlich haben sich ALS Daten als Input für eine, auf Objekthöhen basierte, Waldabgrenzung bereits bewährt. Bis dato werden hauptsächlich Orthophotos für eine manuelle bzw. semi-automatisierte Waldabgrenzung verwendet, wobei schattige Bereiche die Detektierung von Waldrändern und vor allem Waldlücken stark beeinträchtigen. Hier zeigt ALS ein großes Potential und bietet in den meisten Fällen gegenüber einer manuellen Bildinterpretation deutliche Vorteile. Im Rahmen dieser Arbeit wird ein vollautomatischer Ansatz präsentiert der Waldlücken in einem automatisierten Prozess aus ALS Daten extrahiert. Die Abgrenzung der Waldlücken erfolgt durch eine Kombination aus Rasteroperationen und einer Punkt-basierten α -Shape Ableitung, die mit Open Source Software realisiert wurde. Die Methode wird für ein rund 5 km² großes Waldgebiet am Achensee in Tirol angewandt. Die automatisch ausgewiesenen Waldlücken zeigen eine sehr gute Übereinstimmung mit manuell abgrenzbaren Waldlücken und zeigen das hohe Potential der vorgestellten Methode für eine großflächige automatische und damit objektivere Waldlückenerfassung.

1 Einleitung

In der Forstwirtschaft ist die Erfassung und Überwachung der horizontalen Bestandesstruktur essentiell für die Bewertung und Analyse des Waldlebensraumes. Dabei sind Informationen über die räumliche Verteilung und Struktur von Waldlücken ein wesentlicher Bestandteil für die Zustandsbewertung (MAIER UND HOLLAUS, 2006; 2008). Die Gründe für das Entstehen von Waldlücken bzw. Löchern im Kronendach sind vielfältig, wie zum Beispiele durch Schlägerung, Windwurf oder Schädlingsbefall, ihr Auftreten gibt aber Auskunft über die dynamischen Prozesse, denen der Wald unterworfen ist. Diese Waldlücken ermöglichen einen verstärkten Lichteinfall, was folglich zu einer Verjüngung des Bestandes führt. Ebenso erhalten Spezies, die zuvor durch Lichtmangel unterdrückt waren, die Chance sich durchzusetzen. In waldökologischen Untersuchungen und in Biodiversitätsstudien, welche sich mit Entwaldung, Fragmentierung oder Degradation des Waldes beschäftigen, nehmen die Waldlücken eine wichtige Indikatorenstellung ein (EUROPEAN COMMISSION, 2008). Durch großflächigen Schädlingsbefall oder lokale Windwurfschäden kann das natürliche Schutzpotenzial eines alpinen Waldes negativ beeinflusst werden, was zu Förderung von Hangrutschungen, Steinschlägen oder der Ausbreitung von Lawinenabrissgebieten im Wald führen kann (MAIER ET AL., 2006). Die terrestrische Erfassung und Überwachung solcher Gebiete vor allem im Hochalpinen Raum ist

nur unter großem manuellen Aufwand möglich und mit erheblichen finanziellen Belastungen durch Personaleinsatz verbunden. Eine zeit- und kosteneffiziente Kartierung und Quantifizierung von Waldlücken über große Gebiete kann daher nur mit Methoden der Fernerkundung aus der Luft erfolgen. Der Großteil der entwickelten oder praktisch erprobten Ansätze stützt sich dabei auf die Auswertung und Interpretation von Luftbildern bzw. Orthophotos, zumeist im sichtbaren, aber auch im infraroten Teil des Spektrums (z.B. BLASCHKE UND HAY, 2001; GREENHILL ET AL., 2003). Die Abhängigkeit der Luftbilder vom Sonnenstand und der sich daraus ergebende Texturverlust in abgeschatteten Bereichen sind besonders bei der Kartierung von Waldlücken nachteilig. Hohe Bäume am Rand der Lücken werfen abhängig von der Aufnahmesituation besonders lange Schatten und machen eine Interpretation oder Auswertung in diesen Bereichen schwierig bis unmöglich. Flugzeuggetragenes Laserscanning (engl. Airborne Laser Scanning, ALS) zeigt gerade in diesen Gebieten seine besondere Stärke. Als aktive Messmethode kommt ALS ohne die Inanspruchnahme von Sonnenlicht aus und ist daher nicht durch Schattenwirkung eingeschränkt (KRAUS, 2003). Durch die direkte Messung von Objekthöhen und seine Fähigkeit zur Durchdringung der Baumkrone durch kleine Öffnungen im Blätterdach, ist ALS sehr gut für die strukturelle Erfassung von Vegetation geeignet. Aufgrund dieser Vorteile hat sich ALS unter anderem in der Forstwirtschaft als gängige Methode zur großflächigen Datenaufnahme etabliert (HOLLAUS ET AL., 2009; NÆSSET, 2004; NÆSSET ET AL., 2004). Zusätzlich haben sich ALS Daten als Basis für die auf Objekthöhen basierte Waldabgrenzung bereits bewährt (KOUKOULAS UND BLACKBURN, 2004).

In der vorliegenden Arbeit wird ein Ansatz zur vollautomatischen Erfassung von Waldlücken aus ALS Daten präsentiert. Diese Arbeit ist Teil des Forschungsprojektes Laser-Wood (Abschätzung der oberirdischen Waldbiomasse aus Laserscanning- und Waldinventurdaten), finanziert durch den Österreichischen Klima- und Energiefonds. In Kapitel 2 wird das Untersuchungsgebiet sowie die vorliegenden ALS Daten beschrieben, in Kapitel 3 wird die entwickelte Methode erläutert und in Kapitel 4 werden die Resultate dargestellt und diskutiert. Abschließend beinhaltet Kapitel 5 eine qualitative Bewertung der Ergebnisse und gibt einen Ausblick über mögliche Verbesserungen und Entwicklungen.

2 Testgebiet

Als Testgebiet steht der Bezirk Schwaz in Tirol mit einer Fläche von 1843 km² zur Verfügung. Für die vorliegenden Untersuchungen wird ein rund 5 km² großes Waldgebiet an der südöstlichen Seite des Achensees analysiert. Dieses Teiluntersuchungsgebiet liegt im Rofengebirge und ist Teil der nördlichen Kalkalpen. Dominierende Baumarten im Untersuchungsgebiet sind die Fichte, die Weißkiefer und die Rotbuche, wobei im Bereich der Waldgrenze ausgedehnte, auf felsigen Böden wachsende Latschenbestände vorherrschen. Die Seehöhe variiert zwischen 980 m ü.A. im Bereich des Achensees und 2041 m ü.A. des Klobenjochs. Das Gebiet ist geprägt durch steile Hänge (mittlere Neigung ca. 35°) hin zum Achensee, schroffen Gesteinsformationen und mehreren eingeschnittenen Wildbächen (siehe Abb. 1.). Im Uferbereich des Achensees sind am Fuße dieser Wildbäche deutlich Schwemmfächer erkennbar. Der im Tal dichte, überwiegend mit hohem Nadelgehölz bestockte Wald wird mit zunehmender Seehöhe lockerer und geht in einen dichten Latschenbestand über der bis in die Kampfzone ragt (siehe Abb. 1.).

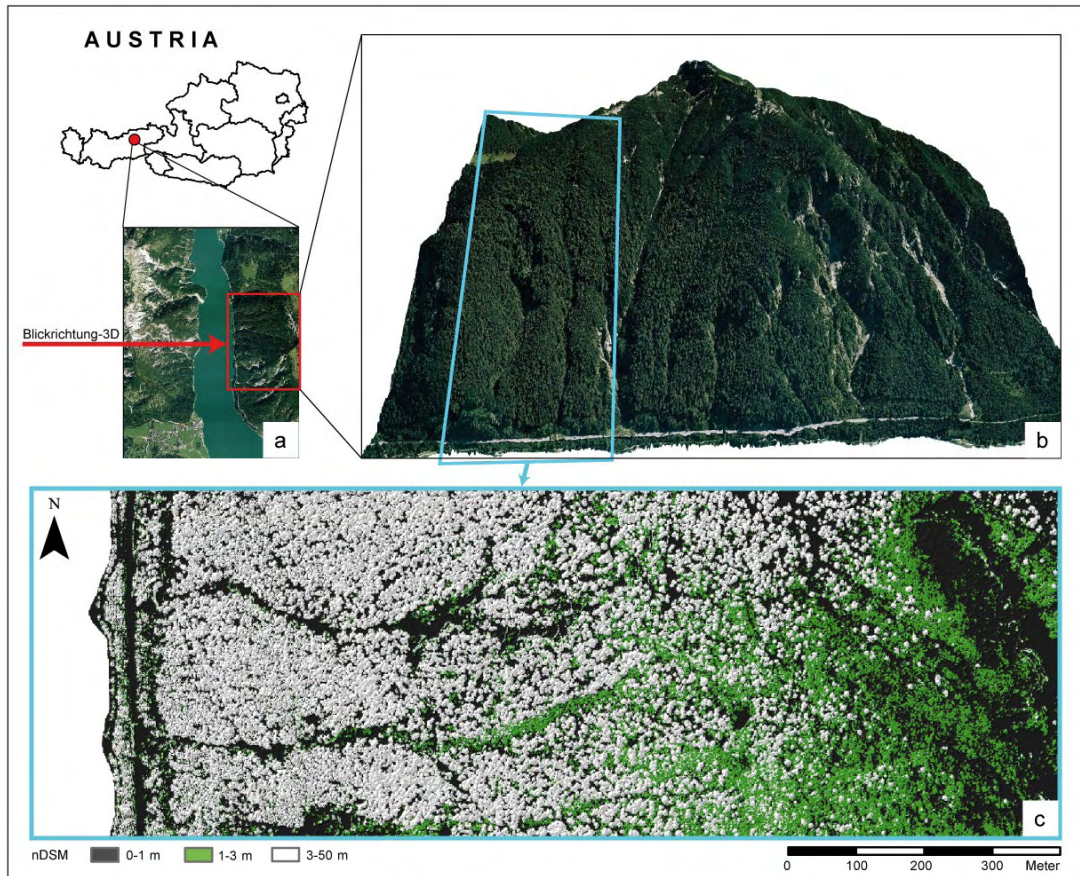


Abb. 1: Übersicht über das Testgebiet Achensee. a) Luftbild des Achensees – Das Testgebiet (rot umrandet) befindet sich im Osten des Sees (Bildquelle Google Maps); b) 3-D Ansicht des Testgebietes (Blick Richtung Osten); c) farbcodiertes nDSM eines Ausschnitts des Testgebietes. Bestockte Flächen über 3 m Höhe (weiß codiert) werden von Westen nach Osten hin lockerer und gehen in geschlossene Latschenbestände (grün codiert) über.

Im Rahmen des Projektes Laser-Wood wurden die georeferenzierten ALS Punktwolken sowie die mittels hierarchisch robuster Filterung berechneten Geländemodelle (engl. digital terrain model, DTM) mit 1 m Gitterweite vom Amt der Tiroler Landesregierung zur Verfügung gestellt. Die Aufnahme der Laserdaten erfolgte im Mai 2007 mit einem ALTM 3100 Laserscanner der Firma Optech. Dieses Messsystem sendet Laserpulse mit einer maximalen Frequenz von 167 kHz im infraroten Bereich des Spektrums (1064 nm) und kann dabei bis zu vier diskrete, aufeinanderfolgende Reflexionen detektieren. Im Testgebiet betrug die durchschnittliche Flughöhe über Grund 1200 m und die durchschnittliche Punktdichte 5.4 Pkt/m².

Aus den Punktwolken wurde ein Oberflächenmodell (engl. digital surface model, DSM) mit einer Gitterweite von 1 m berechnet. Dabei wurde abhängig von der Oberflächenrauigkeit der höchste Punkt pro Rasterzelle ermittelt bzw. gleitende Schrägebenen durch eine lokale Punktwolke geschätzt (HOLLAUS ET AL., 2010). In einem weiteren Schritt wurde ein normalisiertes Oberflächenmodell (engl. normalized digital surface model, nDSM) mit einer Auflösung von 1 m als Basis für die Abgrenzung der Waldlücken berechnet (siehe Abb. 1). Die Berechnung des DSMs und des nDSMs erfolgte mittels OPALS (2010).

3 Methode

Weltweit gibt es viele unterschiedliche, regional angepasste Definitionen für Waldflächen und Waldlücken. Dies führt bei der Abgrenzung von Waldflächen sowie bei der Detektion von Waldlücken zum Teil zu stark voneinander abweichenden Ergebnissen die eine nationale Vergleichbarkeit erschweren bzw. verhindern. Im folgenden Kapitel wird auf die in der vorliegenden Arbeit angewandten Definitionen näher eingegangen. In Kapitel 3.2 wird die angewandte Methode zur Waldlückenerfassung beschrieben. Für die Umsetzung der beschriebenen Schritte werden die Open Source Software Module GRASS und CGAL angewandt (GRASS DEVELOPMENT TEAM 2010, CGAL 2010).

3.1 Definitionen

Waldfläche

Zur Ableitung der potentiellen Waldmaske kommt die Walddefinition der österreichischen Waldinventur (ÖWI) in einer stark vereinfachten Form zur Anwendung. Laut ÖWI muss eine als Wald deklarierte Fläche folgende Kriterien erfüllen: Mindestfläche 500 m², Mindestbreite 10 m, Mindestüberschirmung 30%, Mindesthöhe 2-7 m. Zusätzlich hängt die Waldklassifizierung von der vorliegenden Nutzung (z.B. Forststraße) ab. Diese Abhängigkeit wird für die folgenden Analysen vernachlässigt. Folgende Parameter zur Waldflächen-abgrenzung werden festgesetzt:

- *Mindesthöhe:* Im östlichen Teil des Testgebietes findet man felsige Strukturen und ein Latschenfeld vor, die in dieser Arbeit als Vereinfachung vernachlässigt werden. Die im nDSM ersichtliche Bewuchshöhe dieses Bereiches liegt bei ca. 3 m. Die Mindesthöhe wird aus diesem Grund auf 3 m festgesetzt. Es sei jedoch darauf hingewiesen, dass Latschen- und Grünerlenbestände unter Einhaltung der in der ÖWI vorgegebenen Kriterien normalerweise als Wald zu zählen sind.
- *Mindestfläche:* Die in der ÖWI angegebene Waldmindestfläche von 500 m² wird berücksichtigt.
- *Überschirmungsgrad:* Es wird ein Mindestüberschirmungsgrad von 30% festgelegt, wobei die Berechnung des Überschirmungsgrades mit einer vereinfachten Beziehung zwischen Baumhöhe und maximal erlaubtem Baumabstand erfolgt (siehe Kapitel 3.2).

Waldlücke

Als grundlegende Definition einer Wald- bzw. Bestandeslücke dient die Definition der ÖWI, wobei die Wuchsklasse "Lücke" als eine lokal abgrenzbare flächige Öffnung im Kronenschluss bezeichnet wird. Die Abgrenzung einer Lücke zum benachbarten geschlossenen Wald erfolgt laut ÖWI mit dem abgeloteten Trauf der Krone (HAUK UND SCHADAUER, 2009). Die zulässige Fläche einer Lücke muss zwischen 50 m² und 500 m² liegen. Zusätzlich muss ein Überschirmungsgrad von kleiner 30% gegeben sein. In der vorliegenden Arbeit wird folgender Parameter berücksichtigt:

- *Mindestfläche:* Neben der Definition nach ÖWI werden für Versuchszwecke noch zwei weitere Klassen eingeführt (500 m² bis 1 ha bzw. 1 ha bis ∞).

3.2 Waldlückenerfassung

Die vorgestellte Waldlückenerfassung setzt sich aus den folgenden zwei Arbeitsschritten zusammen:

- Im ersten Arbeitsschritt wird eine „potentielle Waldmaske“ abgeleitet um eine Grundlage für die weiterführende Waldlückenerfassung zu schaffen.
- Im zweiten Arbeitsschritt werden Waldlücken innerhalb der abgeleiteten potentiellen Waldmaske extrahiert und nach ihrer Größe klassifiziert.

3.2.1 Potentielle Waldmaske

Wie in Kapitel 3.1 definiert wird eine Fläche unter Berücksichtigung mehrerer Parameter als Wald klassifiziert. Aktuell wird die operationelle, manuelle Abgrenzung von Wald unter Zuhilfenahme von Tabellenwerken vorgenommen, wobei ein Mindestüberschirmungsgrad von 30% durch einen maximal zulässigen Baumabstand (welcher wiederum abhängig von Baumart und Kronendurchmesser ist) gewährleistet wird. Im Rahmen des Projektes Laser-Wood wurde die Beziehung Überschirmungsgrad versus maximal zulässiger Baumabstand (Stammabstand) durch das Bundesforschungs- und Ausbildungszentrum für Wald, Naturgefahren und Landschaft (BFW) in einer vereinfachten Formel, Baumartenunabhängig auf die Baumhöhe umgelegt, wobei die Baumhöhen (die aus ALS-Daten zuverlässig ermittelt werden können) als Eingangsgröße für die Berechnung der maximal zulässigen Baumabstände herangezogen werden. Bezogen auf den Überschirmungsgrad bedeutet dies, dass bei Baumabständen kleiner als der jeweils maximal erlaubte Baumabstand ein Überschirmungsgrad größer 30% stets gegeben ist. Als Vereinfachung wird die im Untersuchungsgebiet vorherrschende mittlere Baumhöhe von ca. 25 m herangezogen um den maximalen Stammabstand von 24 m zu berechnen.

Für die Ermittlung der Stammabstände im Testgebiet werden zunächst lokale Maxima im nDSM detektiert und diese als Stammpositionen angenommen. Bei der lokalen Maximumsuche wird die definierte Mindesthöhe von 3 m berücksichtigt. Die exportierten Koordinatentripel (Stammpositionen) werden mittels CGAL (Delaunay-Triangulation) trianguliert und mittels α -Shape zu Waldpolygonen aggregiert. Das Ergebnis des α -Shape ist ein Flächenpolygon, das der Kontur der Punktwolke (=Stammpositionen) folgt. Abhängig vom α -Wert (definiert den Radius eines Kreises) folgt das Polygon Einbuchtungen und innenliegenden Löchern mit unterschiedlichem Detail. (EDELSBRUNNER UND MÜCKE, 1994). Im Prinzip werden bei der α -Shape-Berechnung Kanten benachbarter Punktpaare (Kanten aus der Triangulierung), die größer als der Kreis des α -Shapes sind, eliminiert. Für die vorliegende Waldabgrenzung wird ein α -Wert von 12 m angewandt um den maximalen Stammabstand und damit den Mindestüberschirmungsgrad zu gewährleisten. Abschließend werden Flächenpolygone unter 500 m² eliminiert. Das Ergebnis ist eine stark generalisierte Waldmaske die als Grundlage für die weiterführende Waldlückendetektion dient.

3.2.2 Waldlückendetektion

Um die Waldlücken zu detektieren wird in einem ersten Schritt eine binäre Karte aus dem nDSM generiert, wobei potentielle Waldlückenpixel (nDSM <3 m) den Wert eins erhalten. Da laut Definition Waldlücken nur in einer als Wald ausgewiesenen Fläche auftreten können wird die Binärkarte mit der in Kapitel 3.2.1 ermittelten potentiellen Waldmaske verschnitten, wobei

Bereiche außerhalb der Waldmaske eliminiert werden. Im nächsten Schritt werden im Binärbild alle zusammenhängenden Bereiche von potentiellen Waldlückenpixeln mit einer ID versehen, wobei für jede ID die Anzahl der zusammenhängenden Pixel ermittelt wird. Da eine Zelle 1 m² entspricht, kann die Anzahl der gezählten Zellen pro ID als Fläche dieses Bereiches umgelegt werden. Nun wird eine Reklassifizierung aller zusammenhängenden Bereiche hinsichtlich ihrer Fläche vorgenommen. Alle IDs mit Flächen zwischen 50 m² und 500 m² werden der Klasse 0, alle zwischen 500 m² und 1 ha der Klasse 1 und alle größer 1 ha der Klasse 2 zugeordnet. Flächen kleiner 50 m² werden vernachlässigt. In einem weiteren Schritt werden die Koordinaten der Pixelzentren sowie deren Klasse als ASCII-Files, sortiert nach Klassen, exportiert. Die Punktwolke jeder Klasse wird abschließend mittels α -Shape vektorisiert und zu Flächenpolygonen umgewandelt. Dabei werden klassenabhängige α -Werte angewandt um eine klassenabhängige Generalisierung der gefundenen Bereiche zu erzielen. Flächen zwischen 50 m² und 500 m² werden wenig generalisiert und erhalten einen empirisch ermittelten α -Wert (Radius) von 1 m (entspricht der doppelten Pixelgröße). Flächen zwischen 500 m² und 1 ha sowie größer 1 ha werden stärker generalisiert und erhalten einen empirisch ermittelten α -Wert von 4 m (achtfache Pixelgröße).

4 Resultate und Diskussion

Die Lage der anhand des nDSMs gefundenen Stammpositionen wurde visuell mit dem Orthophoto verglichen. Speziell im Bereich der Waldgrenze liegt eine sehr hohe Übereinstimmung mit den visuell am Orthophoto detektierten Stammpositionen vor (siehe Abb. 2,a). Im Bereich von Latschen, Felsen und anthropogenen Objekten mit einer Objekthöhe über 3 m werden im Zuge der lokalen Maximumsuche fälschlicherweise vereinzelt Stammpositionen gefunden. Da der Fokus der vorliegenden Arbeit auf der Waldlückenerfassung liegt, werden diese Verfälschungen vernachlässigt. Die mittels α -Shape automatisch abgeleiteten Flächenpolygone stimmen weitgehend mit der im Orthophoto ersichtlichen Waldfläche überein. An der oberen Waldgrenze werden einzeln stehende Bäume mit Baumabständen größer 24 m mittels α -Shape zuverlässig abgegrenzt (siehe Abb. 2,b).

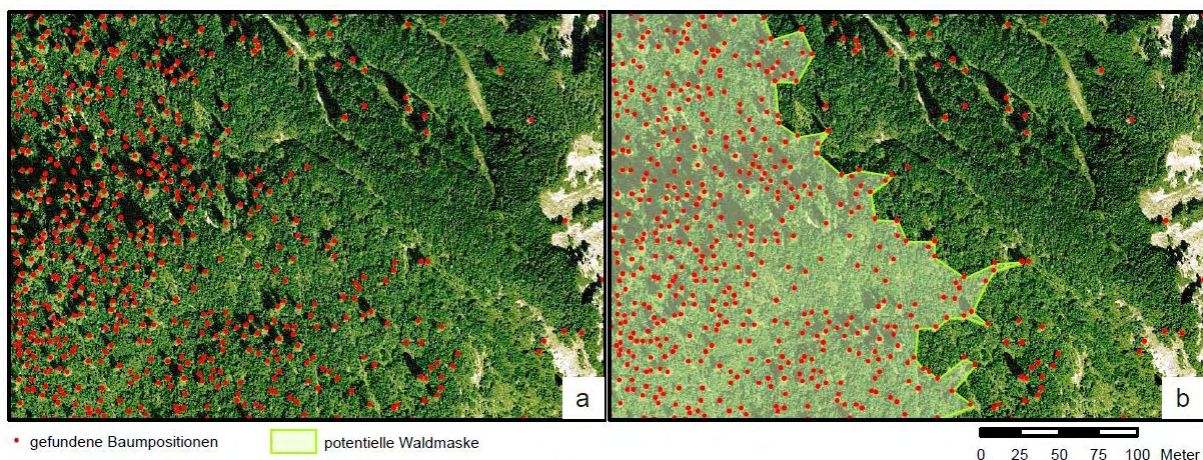


Abb. 2: Automatisch extrahierte Stammpositionen (a) und abgeleitete Waldmaske (b) an der oberen Waldgrenze, überlagert einem Orthophoto (Bildquelle: Google Maps).

Im Vergleich zu einer manuellen Waldabgrenzung im Bereich der oberen Waldgrenze mittels Orthophotos führt die vorgestellte vollautomatische Methode (unter Vernachlässigung der Nutzungsklassifizierung) zu reproduzierbaren Ergebnissen und zu einer deutlichen Reduktion der Auswertekosten. Die abgeleitete Waldmaske wurde als Grundlage für die Waldlückendetektion herangezogen. Die in Abb. 3,b in rot dargestellten Waldlücken repräsentieren die automatisch gefundenen Lücken mit einer Größe zwischen 50 m² und 500 m² die der Definition laut ÖWI entsprechen. Wie zu erwarten nimmt die Anzahl der Lücken mit steigender Seehöhe zu, wobei ab einer Höhe von rund 1700 m ü.A. der Wald unter Vernachlässigung der Latschenfelder in eine lockeren, offenen Bestand übergeht und nur noch vereinzelt Lücken in dieser Klasse detektiert werden können. Die in blau (500 m² - 1 ha) und rosarot (>1 ha) dargestellten Lücken wurden durch die Vektorisierung mittels α -Shape im Gegensatz zu den Lücken der ersten Klasse stärker generalisiert und überbrücken teilweise einzelne Bäume innerhalb der Lücken (siehe Abb. 3,b). Deutlich zu erkennen sind die beiden Wildbäche innerhalb der Waldfläche sowie ein vermehrtes Auftreten der Lücken der mittleren Klasse (500 m² - 1 ha) an der oberen Waldgrenze. Die größten Waldlücken (>1 ha) treten hauptsächlich an der oberen Waldgrenze auf und stellen durch das nach oben hin offene Intervall eine Art Restfläche dar.

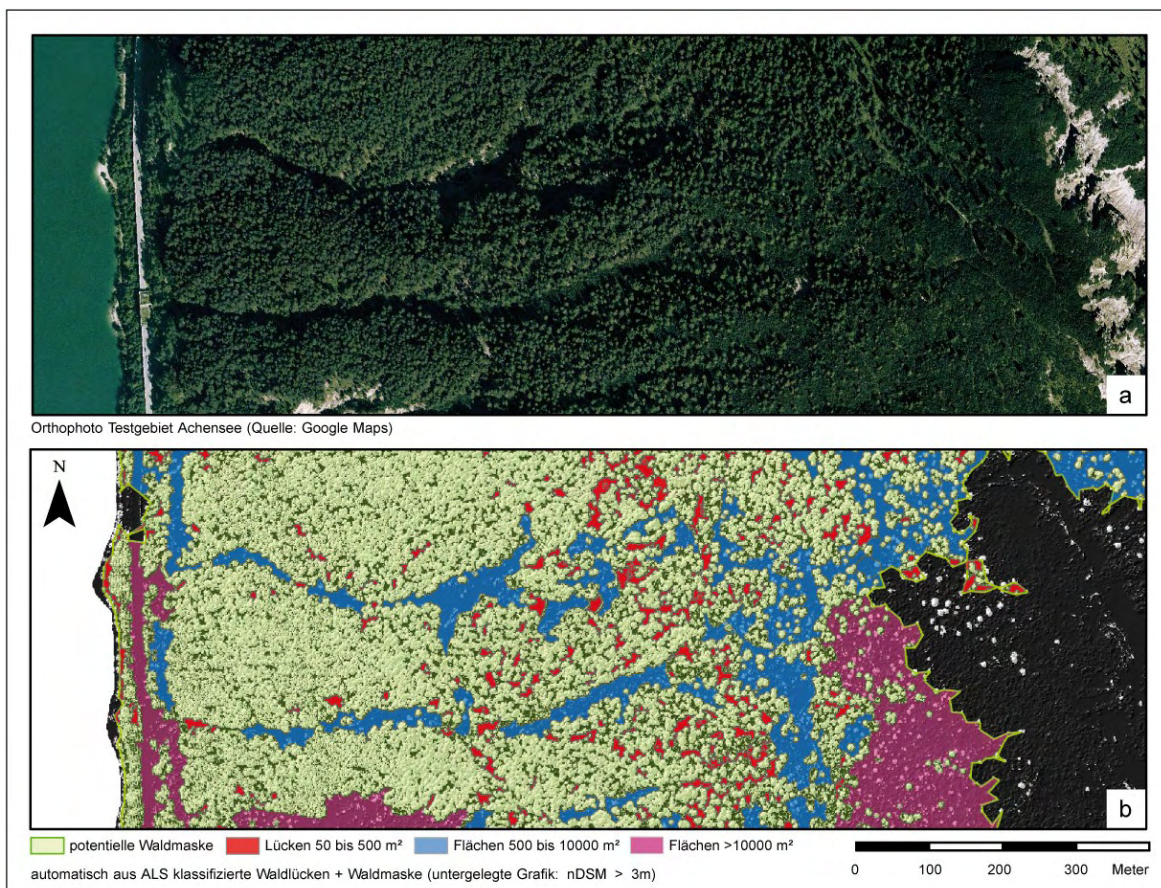


Abb. 3: Ergebnis der automatischen Waldabgrenzung und der Waldlückendetektion. a) Orthophoto (Bildquelle: Google Maps); b) automatisch aus ALS klassifizierte Waldlücken mit unterlegtem, farbcodiertem nDSM und automatisch abgeleiteter, potentieller Waldmaske. In Rot sind Lücken mit einer Größe zwischen 50 m² und 500 m², in Blau jene zwischen 500 m² und 1 ha und in Rosarot jene >1 ha dargestellt.

Generell gilt zu sagen, dass die beiden Waldlückenklassen ($>500 \text{ m}^2$) nicht der Definition der ÖWI unterliegen. Die ÖWI sieht für solche Flächen die Klassifizierung als Freifläche vor.

Die manuelle Auswertung von Waldlücken anhand von Orthophotos ist speziell unterhalb der oberen Waldgrenze aufgrund von vermehrten Objektschatten sehr schwierig bis unmöglich und setzt ein geschultes Expertenwissen voraus. Hier zeigen sich die deutlichen Vorteile der ALS Daten und des vollautomatischen Ansatzes zur Waldabgrenzung und Waldlückendetektion. Es kommt dabei zu einer deutlichen Zeit- und Kostenreduktion bei der Auswertung. Letztendlich werden durch die automatische Auswertung reproduzierbare und objektivere Ergebnisse erzielt.

5 Zusammenfassung und Ausblick

Die in der vorgestellte Methode gezeigte vollautomatische Abgrenzung von Waldflächen und Waldlücken aus ALS Daten zeigt deutliche Vorteile gegenüber einer manuellen Abgrenzung aus Orthophotos und erzielt unter Berücksichtigung der in Punkt 3.1 beschriebenen Vereinfachungen reproduzierbare Ergebnisse. Eine hohe Übereinstimmung mit den im Orthophoto ersichtlichen Waldflächen bzw. Waldlücken wird erzielt. Speziell in schattigen Bereichen des Orthophotos sowie an der oberen Waldgrenze bietet die vollautomatische Abgrenzung aus ALS Daten klare Vorteile. Die Waldlückenklasse 50 m^2 bis 500 m^2 laut Definition nach ÖWI zeigt ein vermehrtes Auftreten der Waldlücken mit steigender Seehöhe. Die stark generalisierte Waldlückenklasse 500 m^2 bis 1 ha zeigt im Bereich des dicht bestockten Bestandes klar den Verlauf der beiden Wildbäche. Eine Kombination dieser Klasse mit der lokalen Geländeneigung, Exposition und Rauigkeit kann in weiterer Folge für Naturgefahrenanalysen herangezogen werden.

Eine Verbesserung der automatischen Waldabgrenzung wird durch eine baumhöhen- und baumartenabhängige Methode angestrebt, wobei weiterführend eine baumartenabhängige Beziehung zwischen Baumhöhe und maximalem Baumabstand notwendig ist. Dies kann durch Verwendung von gewichteten α -Shapes erzielt werden. Dabei werden die Gewichte von den Baumhöhen abgeleitet. Für eine weiterführende Analyse der Dynamik der Waldlücken ist die Verwendung von multitemporalen ALS-Daten notwendig. Durch die Verwendung von full-waveform ALS-Daten samt physikalischer Parameter wird beispielsweise die Baumartendetektion, eine Unterscheidung zwischen anthropogenen und natürlichen Objekten oder eine Klassifikation von Felswänden erleichtert. Für die Definition von Waldlücken nach ÖWI ist eine Erweiterung des zulässigen Flächenintervalls von 50 m^2 bis 500 m^2 um eine weitere Klasse (z.B. 500 m^2 bis 1 ha) sowie die Einführung eines Geometrieparameters (z.B. Mindestbreite) empfehlenswert, da eine 500 m lange und 1 m breite Lücke laut aktueller Definition ebenfalls als Lücke klassifiziert wird. Für eine weiterführende Entwicklung der gezeigten Methode wird eine Überprüfung von Waldmaske und Waldlücken mit manuell aus Orthophotos abgegrenzten Flächen sowie Forstinventurdaten angestrebt.

Danksagung

Die vorliegende Arbeit ist Teil des Projekts LASER-WOOD (822030) und wird finanziert durch den Österreichischen *Klima- und Energiefonds* im Rahmen des Programms "NEUE ENERGIEN 2020". Die Laserdaten wurden vom Amt der Tiroler Landesregierung, Abteilung Geoinformation zur Verfügung gestellt.

6 Literaturverzeichnis

- BLASCHKE, T., & HAY, G. 2001. Object-oriented image analysis and scale-space: Theory and methods for modeling and evaluating multi-scale landscape structure. *International Archives of Photogrammetry and Remote Sensing* vol. 34, 4\W5: 22-29.
- CGAL 2010. Computational Geometry Algorithms Library. www.cgal.org (accessed 1.6.2010).
- EDELSBRUNNER, H., MÜCKE, E., 1994: Tree-dimensional alpha shapes. – *ACM Transactions* 13(1): 43-72.
- EUROPEAN COMMISSION. 2008. The economics of ecosystems and biodiversity interim report. From: http://ec.europa.eu/environment/nature/biodiversity/economics/pdf/teeb_report.pdf
- GRASS DEVELOPMENT TEAM 2010. GRASS 6.5 User Manual. www.grass.itc.it (accessed 1.6.2010).
- GREENHILL, D. R., RIPKE, L. T., HITCHMAN, A. P., JONES, G. A., & G. WILKINSON, G. 2003. Characterization of Suburban Areas for Land Use Planning Using Landscape Ecological Indicators Derived From Ikonos-2 Multispectral Imagery. *IEEE Transactions on Geoscience and Remote Sensing* 41: 2015-2021.
- HAUK, E., SCHADAUER, K., 2009: Instruktion für die Feldarbeit der Österreichischen Waldinventur 2007-2009 (Fassung 18.03.2009), 41-51
- HOLLAUS, M., DORIGO, W., WAGNER, W., SCHADAUER, K., HÖFLE, B. AND MAIER, B., 2009: Operational wide-area stem bolume estimation based on airborne laser scanning and national forest inventory data. *International Journal of Remote Sensing* 30 (19), 5159-5175.
- HOLLAUS M., MANDLBURGER G., PFEIFER N., MÜCKE W., 2010. Land cover dependent derivation of digital surface models from airborne laser scanning data. *International Archives of Photogrammetry, Remote Sensing and the Spatial Information Sciences*. PCV 2010, Paris, France, Vol. 39(3). pp. 6.
- KOUKOULAS, S. AND BLACKBURN, G.A., 2004: Quantifying the spatial properties of forest canopy gaps using LIDAR imagery and GIS. *International Journal of Remote Sensing* 25 (15), 3049-3071.
- KRAUS, K., 2003: Laser-Scanning - ein Paradigmawechsel in der Photogrammetrie. *Bulletin SEV/VSE* (invited) 9, 19-22.
- MAIER, B. AND HOLLAUS, M., 2006: Laserscanning - Ein Wald aus Punkten. *Bündner Wald* 59, 47-53.
- MAIER, B. AND HOLLAUS, M., 2008: Waldstrukturerfassung mittels Laserscanning im Schutzwald. *Die kleine Waldzeitung* 3, 9-11.
- MAIER, B., TIEDE, D. AND DORREN, L.K.A., 2006: Assessing Mountain Forest Strucutre Using Airborne Laser Scanning and Landscape Metrics. In: (Eds.): *Object-based Image Analysis (OBIA06)*, July 4-5, Salzburg, Austria, 6.
- NÆSSET, E., 2004: Accuracy of Forest Inventory Using Airborne Laser scanning: Evaluating the First Nordic Full-scale Operational Project. *Scandinavian Journal of Forest Research* 19, 554-557.
- NÆSSET, E., GOBAKKEN, T., HOLMGREN, J., HYYPPÄ, H., HYYPPÄ, J., MALTAMO, M., NILSSON, M., OLSSON, H., PERSSON, Å. AND SÖDERMAN, U., 2004: Laser scanning of forest resources: the Nordic experience. *Scandinavian Journal of Forest Research* 19 (6), 482-499.
- OPALS, 2010. OPALS - Orientation and Processing of Airborne Laser Scanning Data, <http://www.ipf.tuwien.ac.at/opals/>. Last accessed June 2010.

Article III – English version

Forest Gap Delineation Based on ALS Data Using α -Shapes

ENGLISH TRANSLATION

L. EYSN¹, M. HOLLAUS¹, W. MÜCKE¹, M. VETTER^{1,2} & N. PFEIFER¹

1) TU Vienna, Institute of Photogrammetry and Remote Sensing, Gußhausstraße 27 – 29, 1040 Vienna;

2) TU Vienna, Centre for Water Resource Systems, Karlsplatz 13, 1040 Vienna;

E-Mail: le@ipf.tuwien.ac.at

A common way to acquire topographic information is using the technology of Airborne Laser Scanning (ALS). ALS is an active remote sensing technique and is well suited for acquiring data in forested areas. For forestry applications, local vegetation height information, obtained from ALS data, is a fundamental input for deriving different forestry related parameters as for example tree height, stem volume or biomass. Furthermore, ALS data are a sufficient input for performing an object height based delineation of forested areas. Up to now, a manual or semi-automatically delineation of forested areas is performed by using orthophotos, where shadowed areas can limit the delineation of the forest border and forest gaps. At these areas, ALS shows great potential and, in most cases, is an advantage compared to a manual interpretation of orthophotos. In the presented study, a fully automatic method for extracting forest gaps based on ALS data is presented. The delineation is performed by combining raster operations with a point-based α -Shape detection. An Open Source framework was used to implement the method. The method is applied to approximately 5 km² large forest area located at the Achensee in Tyrol, Austria. The extracted forest gaps show a good agreement with manually interpretable forest gaps, which shows the high potential of the presented method with respect to an area-wide application. Additionally the results are objective and repeatable.

1 Introduction

In the forestry domain, the acquisition and monitoring of the horizontal structure of the forest is essential when it comes to an evaluation and interpretation of the habitat forest. Information about the spatial distribution and structure of forest gaps is a fundamental component of the status quantitation (MAIER AND HOLLAUS, 2006; 2008). The reasons for the development of forest gaps are manifold. For example cutting activities, wind breaks or pest infestation can be a reason. Beside the complex reasons, the occurrence of forest gaps is an indicator about dynamic processes within the forest. The gaps enable more light to come towards the ground, which leads to a rejuvenation of the stand. Furthermore, suppressed species with initially low lightning conditions get the chance to assert them. Within ecologic investigations and biodiversity studies, focusing on deforestation, fragmentation and degradation of the forest, forest gaps are treated as fundamental indicators (EUROPEAN COMMISSION, 2008). The natural protective potential of alpine forest can be negatively affected by pest infestation events or local windbreaks, which leads to an increased potential for landslides, rock falls or an increased spreading of avalanches within the forest (MAIER ET AL., 2006). Especially within the alpine areas, a terrestrial survey and monitoring of affected areas is only possible with great manual effort and high financial costs caused by personnel deployment. Therefore, a time and cost efficient mapping and quantification

of forest gaps within large areas can only be performed by using remote sensing techniques. Most of the existing developed and practically tested methods are based on the interpretation of aerial images or orthophotos, using the visible or infrared part of the spectrum (z.B. BLASCHKE AND HAY, 2001; GREENHILL ET AL., 2003). Aerial images show a high correlation with the lighting conditions of the sun. Shadowed areas result in a limitation of texture and are a drawback for the delineation and mapping of forest gaps. At the forest border, high trees can project long shadows on the ground and the resulting shadowed areas limit the interpretation of the border or can make this task even impossible. Airborne Laser Scanning (ALS) can overcome these limitations as it is an active measurement technique and is not depending on sunlight (KRAUS, 2003). ALS is able to directly measure object heights and to penetrate through small gaps in the canopy. Therefore, ALS is a powerful tool to acquire structural information of the vegetation and made its way to a common large area data acquisition method within the forestry domain (HOLLAUS ET AL., 2009; NÆSSET, 2004; NÆSSET ET AL., 2004). Furthermore, ALS data are proven to be a sufficient input for performing an object height based delineation of forested areas (KOUKOULAS AND BLACKBURN, 2004).

In the presented study a fully-automatic delineation of forest gaps based on ALS data is presented. This study is part of the research project Laser-Wood (Estimation of above ground biomass based on laser scanning and forest inventory), financed by the Austrian Climate and Energy funds. In Section 2 the study area and data are presented, in Section 3 the developed method is explained and in Section 4 the results are presented and discussed. Finally, in Section 5 a qualitative assessment of the results as well as an outlook regarding possible enhancements and developments is presented.

2 Study Area and Material

The study area is located within the district of Schwaz in Tyrol, Austria. A forested area of approximately 5 km² size, located within the so called "Rofengebirge" (part of the Tyrolean limestone Alps) at the South-Eastern bank of the Achensee lake is investigated. The dominant tree species are spruce, white pine and red beech. Additionally, dwarf pines grow on the rocky underground at the upper timberline. The altitude within the study area varies between 980 m above sea level (a.s.l.) at the level of the lake and 2041 m a.s.l. at the highest point. The area is characterized by steep slopes (mean slope is approximately 35°), rugged rock formations and multiple torrents which formed alluvial cones at the bank of the Achensee lake. (Figure 1). The local forest shows a dense coverage at the lower elevated areas, turns into a loosely stocked forest at the upper timberline and finishes in a dense dwarf pine stand at the uppermost elevation (Figure 1).

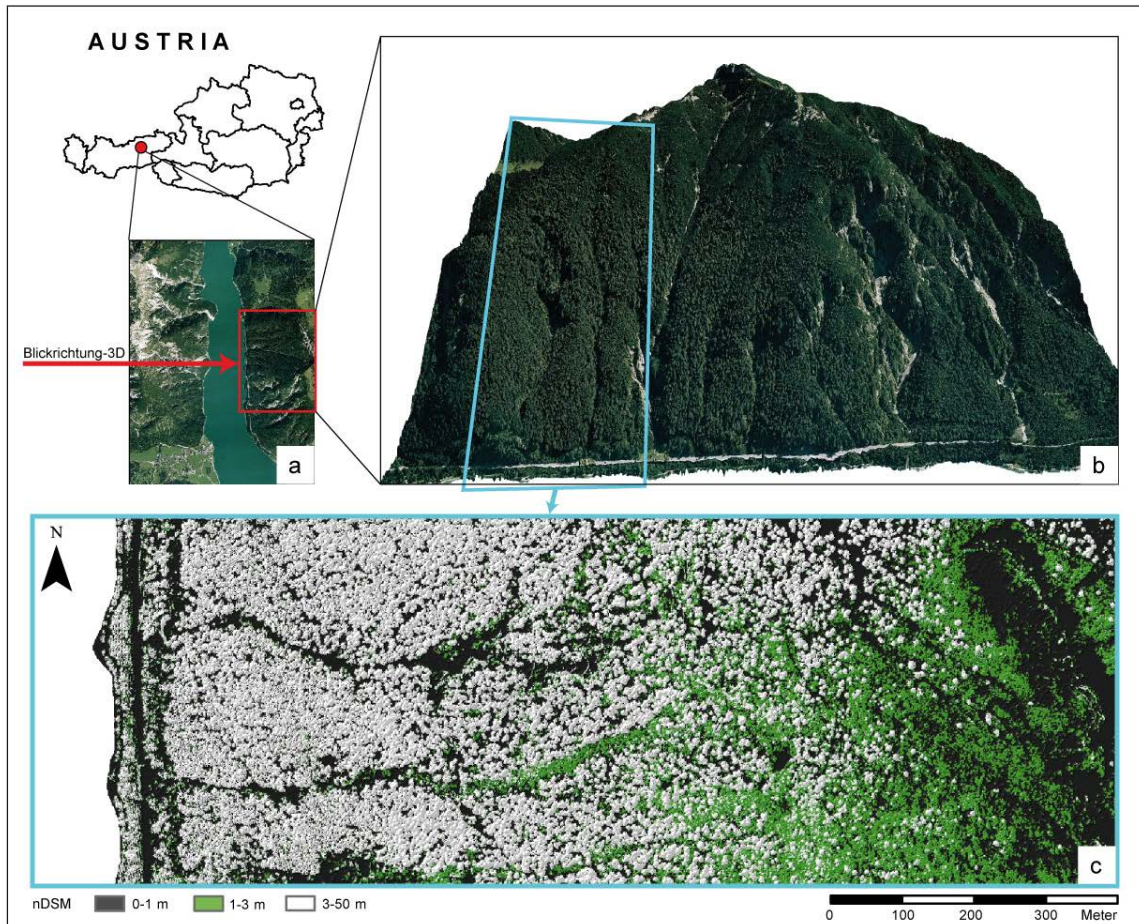


Figure 1: Overview over the study area a) Orthophoto of the lake – The study area (red box) is located at the eastern bank of the lake (Image: Google Maps); b) 3-D view of the study area (view towards East); c) color coded nDSM of a subsection of the study area. Stocked areas with a height greater than 3 m (colored in white) become more loosely stocked from West to East and turn into a dense dwarf pine stand (colored in green).

Within the framework of the project Laser-Wood, georeferenced ALS data as well as a digital terrain model (DTM) with a spatial resolution of 1 x 1 m were provided by the Tyrolean state government. The DTM was derived by using a hierarchical robust filtering approach. The ALS data was acquired in May 2007 with an Optech ALTM 3100 Laser Scanner. The system provides a maximum pulse repetition rate of 167 kHz, uses a laser source in the infrared spectrum (1064 nm) and is able to detect four discrete echoes per shot. The mean flying height above ground was 1200 m and the mean point density is 5.4 points per m². A digital surface model (DSM) with a spatial resolution of 1 x 1 m was derived by using a hybrid approach. Depending on the surface roughness, the highest point per grid cell is used or tilted planes are locally fitted in the point cloud (HOLLAUS ET AL., 2010). Furthermore, a normalized digital surface model (nDSM) with a spatial resolution of 1 x 1 m was derived. The nDSM is used as a base product for delineating the forest gaps (Figure 1). The DSM and nDSM was processed by using the software package OPALS (2010).

3 Method

Worldwide different regionally adapted definitions for the classification of forest area and forest gaps exist, which lead to inconsistent results when these classification tasks are performed and therefore enable only a limited comparability of the results.

In this section the definitions used in this study are explained in more detail. In Section 3.2, the applied forest gap detection method is explained. All steps were carried out using the Open Source Software Modules GRASS and CGAL (GRASS DEVELOPMENT TEAM 2010, CGAL 2010).

3.1 Definitions

Forest area

The delineation of a potential forest mask is carried out by using a simplified version of the forest definition of the Austrian national forest inventory (ÖWI). In the definition of the ÖWI, a forested area is classified as forest if a) a minimum forest area of 500 m² is given, b) a minimum forest width of 10 m is given, c) a minimum crown coverage of 30 % is given and d) a minimum height of 2 to 7 m is given. Additionally the classification depends on the given land use (i.e. forest roads), but this dependency is neglected in this study. The following forest delineation criterions are used:

- *Minimum height:* In the eastern part of the study area rock formations and a dwarf pine stand are given, which are neglected in this study due to simplification. The local nDSM height in this area is approximately 3 m. Therefore, the minimum height criterion is set to 3 m. Following the guidelines of the ÖWI it should be noted, that dwarf pine and green alder stands are normally classified as forest.
- *Minimum area:* The minimum area criterion of the ÖWI (500 m²) is used.
- *Crown Coverage:* A minimum crown coverage criterion of 30 % is used. The calculation of the crown coverage value is performed by using a simplified relation between the local tree heights and a maximum allowed distance between two trees at a time (Section 3.2).

Forest gap

The definition of the ÖWI is used to classify forest gaps and gaps in forest stands. The age class „gap“ is a locally delineable extensively opening of the forest canopy. The delineation of a forest gap within the forest is performed by plumbing down the eaves of the crowns (HAUK AND SCHADAUER, 2009). The accepted gap size must be between 50 m² and 500 m². Additionally, a crown coverage value smaller than 30 % must be given. In the presented study the following criterion is considered:

- *Minimum Area:* Beside the definition of the ÖWI, two additional classes are introduced for experimental purpose (500 m² to 1 ha and 1 ha to ∞).

3.2 Extraction of forest gaps

The presented forest gaps extraction method consists of two steps:

- In the first step a „potential forest mask“ is extracted and is used as a basis for the following gap extraction step.

- In a second step, within the potential forest mask, forest gaps are detected and classified by size.

3.2.1 Potential forest mask

As defined in Section 3.1, a forested area is classified as forest by considering different criterions. A common operational manual delineation of forested areas is performed by using lookup tables defining the minimum crown coverage of 30 % as a maximum possible distance between two neighboring trees. The distance depends on the tree species and crown diameter.

Within the project Laser-Wood, a relation between crown coverage and a maximum possible distance between trees (distance between the stems) was adapted by the Department of Forest Inventory at the Federal Research and Training Center for Forests, Natural Hazards and Landscape. The relation was adapted to use the local tree heights (which can be easily obtained from ALS data) as input for the calculation of the maximum possible distance between two trees. Additionally the relation is simplified to be tree species independent. With respect to the crown coverage criterion this means, that the requested crown coverage threshold of 30 % is fulfilled if the distance between two trees is smaller than the obtained maximum possible distance. For the investigated study area, the process is simplified by using the study areas' mean tree height (25 m) which results in a maximum possible stem to stem distance of 24 m.

The distance check between neighboring stems requires knowledge about the stem positions. Initially, local maxima are detected in the nDSM and stored as potential stem positions. To fulfill the minimum height criterion, only maxima with a local height greater than 3 m are retained. A Delaunay triangulation of the detected stem positions is calculated by using the software package CGAL. Furthermore, an α -Shape is processed to reveal the forest polygons from the triangulation. The results of the α -Shape operation are polygons, which follow the contour of the point cloud (= stem positions). Depending on the α -value (defining the radius of a 2D disc), the polygon tracks indentations and inner holes with different level of detail (EDELSBRUNNER AND MÜCKE, 1994). In principle, the α -Shape method eliminates edges of neighboring vertices (=stems) if the length of the edge is greater than the radius of the α -disc. In the presented study, an α -value of 12 m is used to check the maximum possible distance between stems which is related to the requested minimum crown coverage. Finally, polygons with an area of 500 m² are eliminated to meet the restrictions of the minimum area criterion. The resulting polygons show a generalized forest mask which is used for further processing of the forest gaps.

3.2.2 Forest gap detection

In a first step a binary map of potential forest gap areas is created by thresholding the nDSM with a value of 3 m, whereat Pixels smaller 3 m are set to the value one. These pixels represent potential forest gap areas. By definition, forest gaps can only be inside an area classified as forest. Therefore, the binary map is cropped with the potential forest mask (Section 3.2.1). The area outside the forest mask is eliminated. In a next step, all locally clumped potential forest gap pixels within the binary map are assigned with an ID. For each ID, the number of locally clumped pixels is determined. The determined number per ID can be directly related to the size of this area as one cell represents 1 m². Based on the obtained clumps, a classification regarding the size of the clumps is performed. All IDs with corresponding areas between 50 m² and 500 m² are

assigned to class 0, those between 500 m² and 1 ha are assigned to class 1 and those greater than 1 ha are assigned to class 2. Additionally, areas smaller than 50 m² are neglected. In the next step the coordinates of the pixel centers and their corresponding classes are exported in ASCII-format. Finally, the point cloud of each class is vectorized and transformed to polygons using α -Shapes. The α -value is altered depending on the classification of the input data. This is performed to obtain different generalization levels for different input classes. Areas between 50 m² and 500 m² (class 1) are only little generalized by using an empirically obtained α -value of 1 m, which represents twice the pixel size. Areas between 500 m² and 1 ha (class 2) as well as areas greater than 1 ha (class 3) are more generalized by using an empirically obtained α -value of 4 m, which represents the eightfold pixel size.

4 Results and Discussion

The locations of the detected stem positions within the nDSM were visually checked against an orthophotos. Especially at loose stocked areas at the upper timberline, the detected positions show a good agreement (Figure 2a). Within the areas of dwarf pine stands, rock formations and other anthropogenic objects some stem positions got wrongly detected. Since the focus of this study is on the extraction of forest gaps, these errors are neglected. The automatically derived forest mask shows a good agreement with the forest area interpretable from the orthophoto. At the upper timberline, the α -Shape reliably excluded single trees with tree to tree distances greater than 24 m from the forest area (Figure 2b).

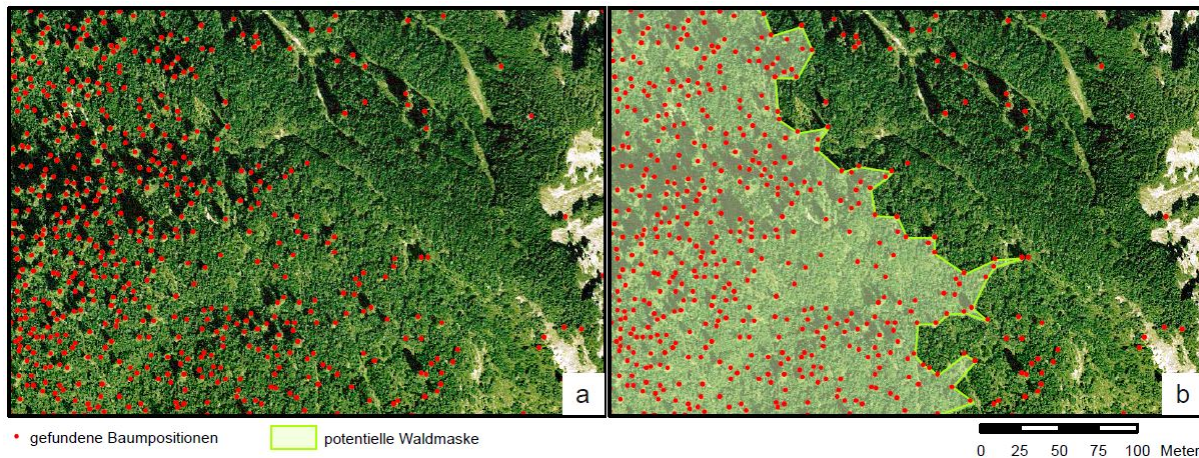


Figure 2: Detail at the upper timberline (a) Automatically extracted stem positions (b) delineated forest area. The results are presented as overlay of the orthophoto (Image source: Google Maps).

Compared to a manual forest delineation based on orthophotos and disregarding the land use component, the presented automatic method delivers reproducible results which leads to a reduction of the processing costs. The extracted forest mask could be used for the detection of forest gaps. In Figure 3b, all automatically extracted gaps with a size between 50 m² and 500 m² (class 1) are presented in red color. These gaps comply with the guidelines of the ÖWI. As expected, the amount of gaps increases with increasing altitude. At approximately 1700 m a.s.l the forest turns into a loosely stocked forest and therefore the amount of detected class 1 gaps

decreases at this area. In Figure 3b, the detected gaps of class 2 ($500 \text{ m}^2 - 1 \text{ ha}$) and class 3 ($>1 \text{ ha}$) are presented in blue and pink color respectively. In contrast to the results of class 1, these gaps are more generalized and partly span over single trees inside gaps. The existing torrents inside the forest as well as an increased amount of class 2 gaps at the upper timberline are clearly visible. The largest gap class (class 3) can be mainly found at the uppermost forest border. As the upper interval of this class is not restricted, the resulting areas can be treated as the remaining area.

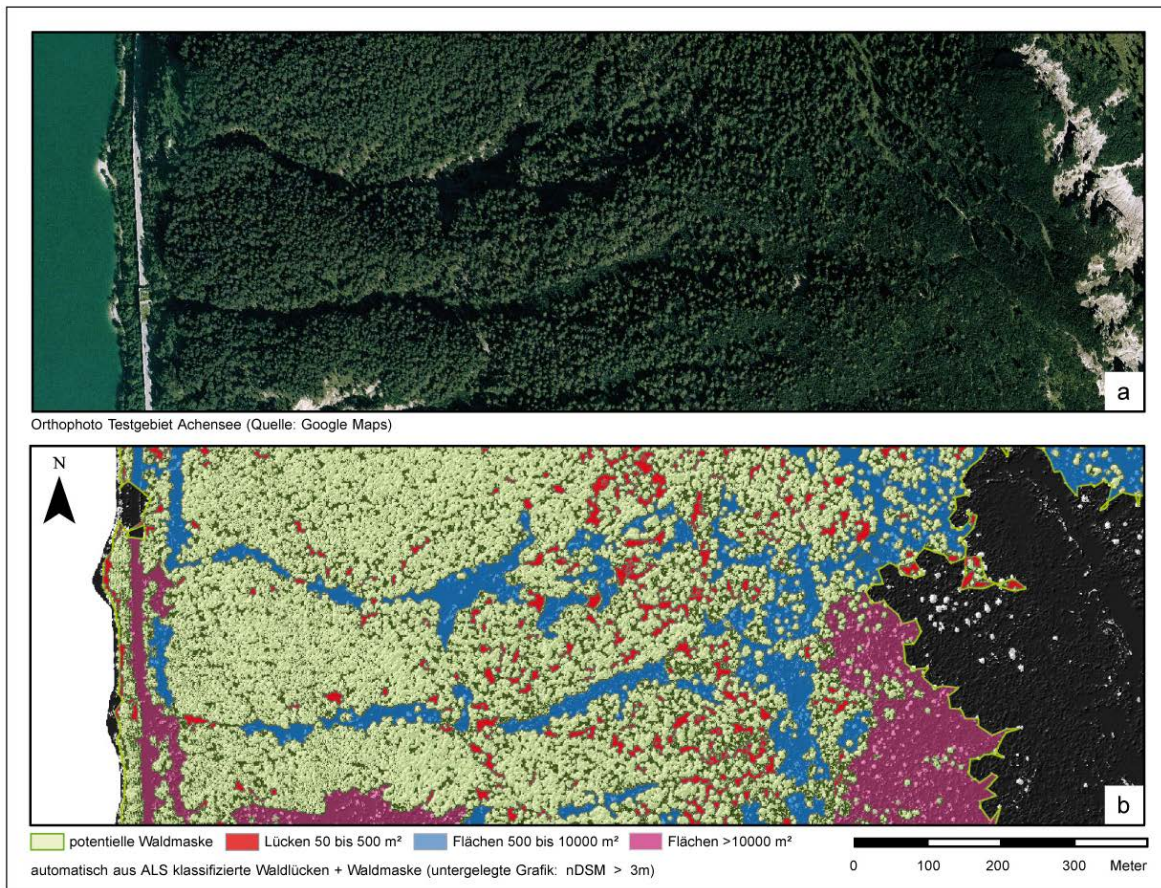


Figure 3: Results of the automatic forest delineation and gap extraction. a) Orthophoto (Image source: Google Maps); b) automatically classified forest gaps as an overlay of the height coded nDSM and the potential forest mask. Red colored gaps are sized between 50 m^2 and 500 m^2 , blue colored gaps between 500 m^2 and 1 ha and pink colored gaps are larger than 1 ha .

In general it should be stated, that the forest gap classes 2 and 3 ($>500 \text{ m}^2$) are not subject of the ÖWI. In the ÖWI such areas are classified as open area. A manual assessment of forest gaps based on Orthophotos can be demanding as shadowing effects limit this task or even make it impossible. Additionally a well-trained human interpreter is a prerequisite for this task. The presented automatic delineation of forest area and forest gaps based on ALS data can overcome this limitation. The results are reproducible and objective and can be obtained at a short amount of time at decreased costs.

5 Summary and outlook

The presented methods for delineating forest area and forest gaps based on ALS data show clear advantages compared to a manual delineation based on Orthophotos. Additionally, the results are, accounting the simplifications stated in Section 3.1, reproducible and show a good agreement with the forest gaps and forest area interpretable in the orthophoto. Especially at shadowed areas in the orthophoto and at the upper timberline the ALS based method shows advantages. The ÖWI forest gap class between 50 m² and 500 m² shows an increased occurrence of gaps with increased altitude. The well generalized forest gaps in the class between 500 m² and 1 ha clearly shows the torrents within the densely stocked forest. Data fusion of this class with local slope, exposition and surface roughness information could be useful for analyzing natural hazards.

The automatic delineation of the forest area could be enhanced by introducing a tree height and tree species dependent method to enhance the relation between tree height and the maximum possible distance between two trees with respect to crown coverage. This could be obtained by introducing a weighted α -Shape methodology, whereat the local weights are deduced from the tree heights. A pursuing study of forest gap dynamics could be realized by using multi-temporal ALS data. The use of full-waveform ALS data including the physical parameters (i.e. intensity) could enable the classification of main tree species, the separation between anthropogenic and natural objects or the classification of rock formations. An extension of the existing gap class (50 m² to 500 m²) with an additional class (i.e. 500 m² to 1 ha), as well as the introduction of a geometric criterion (i.e. minimum gap width) is recommended with respect to the forest gap definition of the ÖWI. The geometric parameter should be mandatory, as the existing definition would also classify a 500 m long and only 1 m wide gap as a forest gap.

Further development of the presented method should include a check of the extracted forest area and forest gaps against manually delineated polygons and forest inventory data.

Acknowledgements

The presented study is part of the research project Laser-Wood (822030), financed by the Austrian climate and energy funds within the framework of the program “Renewable energy 2020”. The ALS data were provided by the Department of Geoinformation, Tyrolean state government.

References

- BLASCHKE, T., & HAY, G. 2001. Object-oriented image analysis and scale-space: Theory and methods for modeling and evaluating multi-scale landscape structure. *International Archives of Photogrammetry and Remote Sensing* vol. 34, 4\W5: 22-29.
- CGAL 2010. Computational Geometry Algorithms Library. www.cgal.org (accessed 1.6.2010).
- EDELSBRUNNER, H., MÜCKE, E., 1994: Tree-dimensional alpha shapes. – *ACM Transactions* 13(1): 43-72.
- EUROPEAN COMMISSION. 2008. The economics of ecosystems and biodiversity interim report. From: http://ec.europa.eu/environment/nature/biodiversity/economics/pdf/teeb_report.pdf

- GRASS DEVELOPMENT TEAM 2010. GRASS 6.5 User Manual. www.grass.itc.it (accessed 1.6.2010).
- GREENHILL, D. R., RIPKE, L. T., HITCHMAN, A. P., JONES, G. A., & G. WILKINSON, G. 2003. Characterization of Suburban Areas for Land Use Planning Using Landscape Ecological Indicators Derived From Ikonos-2 Multispectral Imagery. *IEEE Transactions on Geoscience and Remote Sensing* 41: 2015-2021.
- HAUK, E., SCHADAUER, K., 2009: Instruktion für die Feldarbeit der Österreichischen Waldinventur 2007-2009 (Fassung 18.03.2009), 41-51
- HOLLAUS, M., DORIGO, W., WAGNER, W., SCHADAUER, K., HÖFLE, B. AND MAIER, B., 2009: Operational wide-area stem volume estimation based on airborne laser scanning and national forest inventory data. *International Journal of Remote Sensing* 30 (19), 5159-5175.
- HOLLAUS M., MANDLBURGER G., PFEIFER N., MÜCKE W., 2010. Land cover dependent derivation of digital surface models from airborne laser scanning data. *International Archives of Photogrammetry, Remote Sensing and the Spatial Information Sciences*. PCV 2010, Paris, France, Vol. 39(3). pp. 6.
- KOUKOULAS, S. AND BLACKBURN, G.A., 2004: Quantifying the spatial properties of forest canopy gaps using LIDAR imagery and GIS. *International Journal of Remote Sensing* 25 (15), 3049-3071.
- KRAUS, K., 2003: Laser-Scanning - ein Paradigmawechsel in der Photogrammetrie. *Bulletin SEV/VSE* (invited) 9, 19-22.
- MAIER, B. AND HOLLAUS, M., 2006: Laserscanning - Ein Wald aus Punkten. *Bündner Wald* 59, 47-53.
- MAIER, B. AND HOLLAUS, M., 2008: Waldstrukturerfassung mittels Laserscanning im Schutzwald. *Die kleine Waldzeitung* 3, 9-11.
- MAIER, B., TIEDE, D. AND DORREN, L.K.A., 2006: Assessing Mountain Forest Structure Using Airborne Laser Scanning and Landscape Metrics. In: (Eds.): *Object-based Image Analysis (OBIA06)*, July 4-5, Salzburg, Austria, 6.
- NÆSSET, E., 2004: Accuracy of Forest Inventory Using Airborne Laser scanning: Evaluating the First Nordic Full-scale Operational Project. *Scandinavian Journal of Forest Research* 19, 554-557.
- NÆSSET, E., GOBAKKEN, T., HOLMGREN, J., HYYPPÄ, H., HYYPPÄ, J., MALTAMO, M., NILSSON, M., OLSSON, H., PERSSON, Å. AND SÖDERMAN, U., 2004: Laser scanning of forest resources: the Nordic experience. *Scandinavian Journal of Forest Research* 19 (6), 482-499.
- OPALS, 2010. OPALS - Orientation and Processing of Airborne Laser Scanning Data, <http://www.ipf.tuwien.ac.at/opals/>. Last accessed June 2010.

Article IV

Article

A Benchmark of Lidar-Based Single Tree Detection Methods Using Heterogeneous Forest Data from the Alpine Space

Lothar Eysn ^{1,*}, Markus Hollaus ¹, Eva Lindberg ^{1,2}, Frédéric Berger ³, Jean-Matthieu Monnet ³, Michele Dalponte ⁴, Milan Kobal ⁵, Marco Pellegrini ⁶, Emanuele Lingua ⁶, Domen Mongus ⁷ and Norbert Pfeifer ¹

¹ TU Wien: Department of Geodesy and Geoinformation, Vienna University of Technology, Gußhausstraße 27–29, 1040 Vienna, Austria; E-Mails: Markus.Hollaus@geo.tuwien.ac.at (M.H.); Eva.Lindberg@slu.se (E.L.); Norbert.Pfeifer@geo.tuwien.ac.at (N.P.)

² SLU: Department of Forest Resource Management, Swedish University of Agricultural Sciences, 90183 Umeå, Sweden

³ Irstea, UR EMGR Écosystèmes Montagnards, centre de Grenoble, F-38402 Saint-Martin-d’Hères, France; E-Mails: Frederic.Berger@irstea.fr (F.B.); Jean-Matthieu.Monnet@irstea.fr (J.-M.M.)

⁴ FEM: Department of Sustainable Agro-Ecosystems and Bioresources, Research and Innovation Centre, Fondazione Edmund Mach, Via E. Mach 1, 38010 San Michele all’Adige (TN), Italy; E-Mail: Michele.Dalponte@fmach.it

⁵ SFI: Department of Forestry and Renewable Forest Resources, Biotechnical Faculty, University of Ljubljana, Večna pot 83, 1000 Ljubljana, Slovenia; E-Mail: Milan.Kobal@bf.uni-lj.si

⁶ TESAF: Department of Land, Environment, Agriculture and Forestry, University of Padova, Viale dell’Università 16, 35020 Legnaro (PD), Italy; E-Mails: Marco.Pellegrini@unipd.it (M.P.); Emanuele.Lingua@unipd.it (E.L.)

⁷ UM-FERI: Faculty of Electrical Engineering and Computer Science, University of Maribor, Smetanova ulica 17, SI-2000 Maribor, Slovenia, E-Mail: Domen.Mongus@um.si

* Author to whom correspondence should be addressed; E-Mail: Lothar.Eysn@geo.tuwien.ac.at; Tel.: +43-158-801-122-49; Fax: +43-158-801-122-99.

Academic Editors: Joanne C. White and Eric J. Jokela

Received: 12 March 2015 / Accepted: 8 May 2015 / Published: 15 May 2015

Abstract: In this study, eight airborne laser scanning (ALS)-based single tree detection methods are benchmarked and investigated. The methods were applied to a unique dataset originating from different regions of the Alpine Space covering different study areas, forest

types, and structures. This is the first benchmark ever performed for different forests within the Alps. The evaluation of the detection results was carried out in a reproducible way by automatically matching them to precise *in situ* forest inventory data using a restricted nearest neighbor detection approach. Quantitative statistical parameters such as percentages of correctly matched trees and omission and commission errors are presented. The proposed automated matching procedure presented herein shows an overall accuracy of 97%. Method based analysis, investigations per forest type, and an overall benchmark performance are presented. The best matching rate was obtained for single-layered coniferous forests. Dominated trees were challenging for all methods. The overall performance shows a matching rate of 47%, which is comparable to results of other benchmarks performed in the past. The study provides new insight regarding the potential and limits of tree detection with ALS and underlines some key aspects regarding the choice of method when performing single tree detection for the various forest types encountered in alpine regions.

Keywords: single tree extraction; airborne laser scanning; forest inventory; comparative testing; co-registration; mountain forests; Alpine Space; matching

1. Introduction

The use of remote sensing data and related methods (*i.e.*, biomass estimation, delineation of forested areas) has become a standard in forest management [1–3]. Large area applications such as, for example, harvesting planning or forest stand mapping based on remote sensing products are now widely operational, especially in the northern European countries [4–6]. This development enables high-precision forest management, which is a prerequisite for the sustainable use of one of the key resources within the context of renewable energy. In mountainous regions, and particularly in the Alps, the use of forest resources in remote areas has decreased as valorization is hampered by accessibility constraints that prevent efficient mapping, management, and harvesting. To develop strategies to tackle this shortcoming, the research project NEWFOR (NEW technologies for a better mountain FORest timber mobilization) [7] was introduced to the Alpine Space program of the European Territorial Cooperation. The project aims at enhancing the wood supply chain within the Alpine Space (Alps core area and surrounding foothills/lowlands) to improve forest timber evaluation and mobilization using new remote sensing technologies such as airborne laser scanning (ALS), also referred to as Lidar.

When processing ALS remote sensing data for forest applications, area-based approaches [8–10] as well as single-tree based methods [11–13] can be found in the literature. Area-based methods provide statistically calibrated maps of forest stand parameters such as growing stock, stem density, and stand height, which are useful for large-area forest inventory and long term management planning. They can also be sufficient for harvesting planning in the case of simple forests such as plantations. Meanwhile, in complex alpine forests single tree information is highly valuable. Irregular stands are frequent, and silviculture is driven by the largest trees [14], which might also be used as intermediate support to optimize cable yarding. The spatial distribution of trees and their characteristics (height, species, crown size) are required inputs for growth simulation models [15], for the evaluation of the forest protection

effect against rockfalls [16], or even to identify trees with high biodiversity value [17]. Field inventories (FI) provide the required high level of local detailed information, but the high labor cost as well as accessibility constraint advocate for remote sensing solutions.

To gain such detailed information from ALS data, many studies on single tree detection were carried out by the research community [18–23]. Thus, many different methods are available for operational or scientific use. To gain deeper knowledge about the performance of different single tree detection methods, an international benchmark was carried out from 2005 to 2008 by the European Spatial Data Research Organization (EuroSDR), the International Society for Photogrammetry and Remote Sensing (ISPRS), and the Finnish Geodetic Institute (FGI). The study was published by Kaartinen *et al.* [24,25]. The benchmark was carried out using homogeneous ALS data and FI data from two study areas in southern Finland. A different benchmark based on ALS data from different types of forest was carried out in 2012 by Vauhkonen *et al.* [26] to test six different algorithms under different forest conditions. The investigated study areas are located in Norway, Sweden, Germany, and Brazil. Both studies had a great influence on understanding the performance of single tree detection based on ALS data. While the benchmark of Kaartinen *et al.* [24] focused on the performance of different methods using quite homogeneous dataset from one region, the benchmark of Vauhkonen *et al.* [26] focused on the effect of different study areas and forest types on the detection results of different algorithms. Vauhkonen *et al.* [26] used a very heterogeneous dataset which spans from a plantation of monospecies forest in Brazil to natural mixed forests in Europe.

For the Alps, the previously published benchmark results are only partly applicable as forests in Central Europe are different from forests in Northern Europe or Brazil. For this reason, the present study focuses on testing ALS-based single tree detection methods established in the Alpine Space. Based on a unique dataset covering different study areas, forest types, and structures from different regions in the Alpine Space, different methods are tested and analyzed in a clear and reproducible way. The focus is on the performance of the methods. Investigations on the effect of the heterogeneity of the ALS data (*i.e.*, different point density) on the detection results are not in the scope of this study. To the authors' best knowledge, this is the first benchmark ever performed for different forests within the Alps. This study is based on the single tree detection benchmark carried out within the project NEWFOR [7]. Detailed results are published in the project's final report [27]. The presented study summarizes the findings of the report and provides a discussion of the results.

The dataset used in this study is presented in Section 2. Section 3 provides a brief description of the tested methods as well as a detailed description of the matching procedure and evaluation of the results. In Section 4 results are presented in different levels of information while Section 5 contains the discussion. Finally, conclusions are drawn in Section 6.

2. Data and Materials

In total eight study areas in five alpine countries were investigated, representing different types of forest (Figure 1). For each study area, ALS data as well as detailed FI data were available. The ALS data and FI data used in the presented study were made public. The data are published on the NEWFOR website [28]. The dataset was somehow representative of the currently available operational data within the Alpine Space. This means that the data are heterogeneous as they originate from different sources

who acquired the data for different purposes. For example, the ALS data in Austria were collected with a focus on a nationwide terrain modeling campaign while the data in Slovenia were acquired with a focus on forestry applications. Detailed information about forest parameters is given in Table 1.

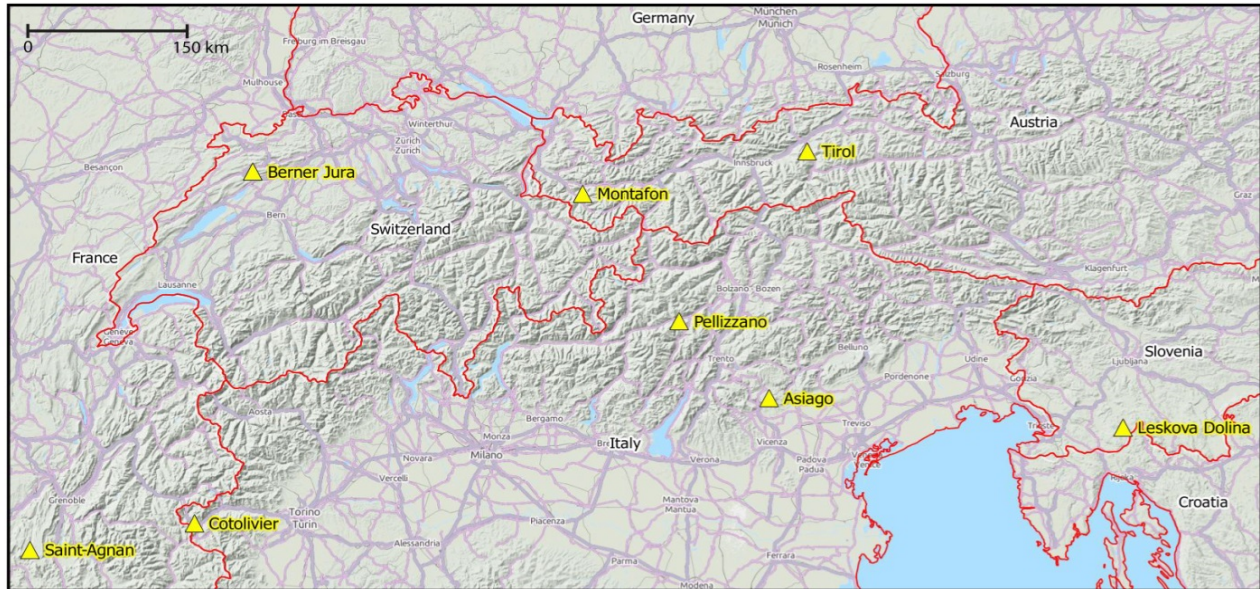


Figure 1. Study areas located within the Alpine Space.

Table 1. Acquisition parameters for the airborne laser scanning data and field inventory data.

Study Area	Country	Localization	Field Inventory			Airborne Laser Scanning		
			Nr. Plots	Total Size (ha)	Date	Date	Density (pts/m ²)	Sensor
Saint-Agnan	France	44°52' N 5°25' E	1	1.0	2010/7	2010/9	13	Riegl LMS-Q560
Cotolivier	Italy	45°2' N 6°46' E	3	0.4	2012/9	2012/7	11	Optech ALTM 3100
Berner Jura	Switzerland	47°9' N 7°4' E	1	0.1	2005	2011/4	5	Leica ALS 70
Montafon	Austria	47°4' N 9°58' E	1	0.3	2009/6	2011/9	22	Riegl LMS-Q560
Pellizzano	Italy	46°18' N 10°46' E	2	0.3	2013/8	2012/9	95–121	Riegl LMS-Q680i
Asiago	Italy	45°49' N 11°30' E	3	0.4	2012/10	2012/7	11	Optech ALTM 3100
Tyrol	Austria	47°23' N 11°44' E	3	1.2	2010/11	2008/7	4–10	Optech ALTM 3100
Leskova	Slovenia	45°39' N 14°28' E	4	0.8	2008/11	2009/10	30	Riegl LMS-Q560

2.1. ALS Data

The ALS data acquisition shows a mixture of different sensors and settings (Table 1). The acquired point densities vary from 5 points/m² in Switzerland up to 121 points/m² in Pellizzano, Italy. The mean flying heights above ground vary from 420 m to 800 m for the different flights. All flights were performed under snow-less conditions.

2.2. FI Data

For all study areas, fully calibrated plots are available. Parameters such as, for example, stem locations, diameter at breast height (DBH), and tree heights as well as information about species composition and number of layers are provided for all plots (Table 2). Since the dataset originates from different institutions and inventory layouts, the size and shape of the inventory plots as well as the acquisition dates are different. Statistical measures are presented in Table 2, while the inventory dates of the FI data are presented in Table 1.

2.2.1. Positioning

The *in situ* absolute georeferencing of all plot locations was performed by GNSS measurements. The plots in Switzerland and Montafon were georeferenced with a total station or photogrammetry. In a post-processing step, each plot location was manually checked and co-registered to remote sensing data. To obtain an interpretable best fit of the tree pattern with the ALS Canopy Height Model (CHM), the tree pattern was visualized and manually moved in Quantum GIS 2.8.1 [29]. The CHM shows the local object heights and can be derived by subtracting the DTM from a surface model. A plot was only manually corrected if the initial position from the field survey showed gross errors. After manual co-registration, the estimated absolute planimetric accuracy of the plot location is ± 2.0 m.

The stem positions were positioned relative to the given plot location with compass bearing and tape or laser range finding. The relative planimetric accuracy of positions varies from ± 0.3 m to ± 1.0 m, depending on the tools used. Vertex systems were used for measuring the tree heights. The vertical accuracy is expected to be ± 1.0 m.

2.2.2. Classification

Four forest types were manually classified by interpreting the height distribution of trees in the FI data and considering the given meta-information. The classes are: (1) Single-Layered Mixed forest (SL/M); (2) Single-Layered Coniferous forest (SL/C); (3) Multi-Layered Mixed forest (ML/M); and (4) Multi-Layered Coniferous forest (ML/C).

Table 2. Statistical description of the forest plots. Only the three main species and species representing more than 5% of the stems are indicated. Corresponding Latin names: spruce (*Picea abies*), fir (*Abies alba*), beech (*Fagus sylvatica*), Scots pine (*Pinus sylvestris*), larch (*Larix decidua*), sycamore (*Acer pseudoplatanus*), elm (*Ulmus glabra*), and poplar (*Populus nigra*). The forest class correspond to single or multi-layered (SL or ML)/mixed or coniferous (M or C).

Plot #	Study Area	Plot Size (ha)	Caliper Threshold (cm)	Stem Density (/ha)	Mean Height (m)	Basal Area (m ² /ha)	Mean Diameter (cm)	Stand Density Index	Coniferous Proportion (%)	Main species	Forest Class
1	Saint-Agnan	1.00	7.5	359	17.1	32.6	30.1	485	56	Fir, beech	ML/M
2	Cotolivier	0.13	4.0	843	18.1	50.5	25.8	889	97	Scots pine, larch, and spruce	ML/C
3	Cotolivier	0.13	4.0	390	16.5	34.3	29.7	514	92	Scots pine and larch	SL/C
4	Cotolivier	0.13	4.0	175	12.9	15.5	24.2	166	59	Larch and sycamore	ML/M
5	Berner Jura	0.10	12.0	340	29.8	67.6	47.7	959	100	Spruce and fir	SL/C
6	Montafon	0.30	10.0	400	13.9	35.7	25.0	401	100	Spruce	ML/C
7	Pellizzano	0.13	5.0	374	25.6	60.1	40.9	823	100	Spruce, larch, and fir	SL/C
8	Pellizzano	0.13	5.0	1870	13.7	68.1	16.7	974	80	Larch, spruce, fir, sycamore, and poplar	ML/M
9	Asiago	0.13	5.0	708	23.6	48.9	29.5	921	100	Spruce and fir	SL/C
10	Asiago	0.13	5.0	851	16.9	56.2	23.7	779	80	Spruce, fir, and beech	ML/M
11	Asiago	0.13	5.0	1344	13.9	37.9	16.0	660	28	Spruce, fir, and beech	ML/M
12	Tyrol	0.40	10.0	317	36.7	59.8	46.6	864	100	Spruce	SL/C
13	Tyrol	0.40	10.0	260	22.0	35.3	39.0	530	29	Sycamore, beech, spruce, and fir	SL/M
14	Tyrol	0.40	10.0	390	23.6	50.5	37.0	733	23	Sycamore, beech, spruce, and pine	SL/M
15	Leskova	0.20	10.0	265	22.9	29.1	34.2	439	76	Fir, spruce, and beech	SL/M
16	Leskova	0.20	10.0	185	24.6	27.6	22.0	359	78	Fir, spruce, and beech	SL/M
17	Leskova	0.20	10.0	585	20.6	38.2	25.5	603	47	Fir, spruce, beech, sycamore, and elm	ML/M
18	Leskova	0.20	10.0	460	24.6	54.0	32.7	708	53	Fir, beech and sycamore	ML/M

3. Methods

The global workflow for the benchmark consisted of the following steps. For each plot the ALS data and rasterized DTMs at 0.5 m and 1 m resolution were provided to benchmark participants. Participants applied their fully-automated tree detection algorithms (Section 3.1) in order to output a list with tree coordinates and heights for each plot. For each participant, this tree list is compared to the FI data with an automated matching procedure (Section 3.2).

3.1. Methods of Participants

In total eight methods were applied to the benchmark dataset (Table 3). The tested methods were chosen as they are common in the Alpine Space and originate from different countries. Most methods rely on local maxima (LM) detection in a rasterized CHM, but also one point cloud-driven method was applied.

Table 3. Overview of the applied methods.

ID	Participant Name	Method	Raster/Point Cloud	Resolution of Raster (m)	Kernel Size (pixel)
1	Irstea	LM + Filtering	R	0.20	11 × 11
2	FEM	LM + Region Growing	R	0.50	5 × 5
3	SFI	LM + Multi CHM	R	NA	3 × 3
4	TESAF	LM + Watershed	R	0.50	3 × 3
5	SLU	Segmentation + Clustering	R + P	0.25	-
6	TU Wien	LM 3 × 3	R	1.00	3 × 3
7	TU Wien	LM 5 × 5	R	1.00	5 × 5
8	UM-FERI	Polyn. Fitting + Watershed	R	1.00	7 × 7

LM: Local Maxima with moving window. The full affiliations of the participants are given on the title page.

3.1.1. Method #1 (LM + Filtering)

The method [30,31] is based on LM filtering within a rasterized CHM. The algorithm consists of five sequential steps:

1. Calculation of rasterized products (0.2×0.2 m resolution) based on the ALS data. The DSM is computed by retaining the highest altitude value of the points located inside each pixel. A DTM is computed by resampling the provided DTM at 0.5 m resolution.
2. Non-linear filtering. Void pixels and artefacts in the DSM are removed with a closing filter. A disk of radius 4 pixels is used as structuring element.
3. Lowpass filtering. A smoothing filter, discrete approximation of a Gaussian kernel with $\sigma = 0.3$ m, is applied to the DSM.
4. Maxima extraction. A LM filtering with sliding window of size 11×11 pixels is applied to extract the LM.
5. Maxima selection. Pixels that are a LM are retained if the value of the corresponding pixel in the CHM is superior to 7.5 m. The CHM is computed as the difference between the non-linear filtered DSM and the DTM.

The remaining maxima are the final tree top candidates. Corresponding coordinates are the pixel centers and heights, which are extracted from the CHM. Algorithm parameters (raster resolution, Gaussian kernel, and LM filtering size) were chosen in the framework of a previous study [31], by using an automatic training process designed to minimize the trade-off between omission and commission errors.

3.1.2. Method #2 (LM + Region Growing)

The method [32] exploits both a rasterized CHM and the ALS point cloud with normalized height. The CHM is computed by assigning each pixel the value of the 95th percentile of the elevations of the first return ALS points. A nearest neighbor interpolation is used for pixels with no corresponding ALS data. The following detailed steps are applied:

1. A low-pass (LP) filter is applied to the rasterized CHM. For the CHM, a spatial resolution of $0.5 \times 0.5 \text{ m}^2$ is used. For the LP filter, a window of 3×3 pixels is used.
2. Seed points $S = \{s_1, \dots, s_N\}$ are defined using a moving window approach. The central pixel of a 5×5 pixel moving window is a seed point if it is (a) the highest point inside the window and (b) higher than 2.5 m.
3. Initial regions are defined starting from the seed points, and a label map L is defined: $L_{i,j} = k$ if (i, j) is a seed point with index k , otherwise $L_{i,j} = 0$.
4. Region growing according to the following procedure:
 - a. consider a label map point $L_{i,j} \neq 0$ and take its neighbor pixels:

$$\{(i, j - 1); (i - 1, j); (i, j + 1); (i + 1, j)\};$$
 - b. a neighbor pixel (i', j') is added to the region n if:

$$(\text{dist}((i', j'), s_n) < \text{Dist}_{\text{Max}}) \& (\text{CHM}(i', j') > (\text{CHM}(s_n) * \text{Perc}_{\text{Tresh}})) \& (L_{i', j'} \neq 0)$$
 with $\text{Perc}_{\text{Tresh}} \in [0, 1]$.
 - c. iterate over all the pixels $L_{i,j} \neq 0$, and repeat until no pixels are added to any region.
5. From each region, extract the first return ALS points, and apply Otsu thresholding [33] to the normalized heights of the extracted points.
6. Take only the first return ALS points higher than the Otsu threshold and apply a 2D convex hull to these points;
7. The resulting polygons are the final tree crowns. The positions of the trees are defined as the position of the highest ALS point inside each crown. The height of the crown is defined as the 95th percentile of the first return ALS points inside the crown.

3.1.3. Method #3 (LM + Multi CHM)

The method is based on iterative CHM generation and LM detection within a moving window of 3×3 pixels for various CHMs. The method is fully automated and processes the data in two general steps, which are (A) sequential identification of potential trees and (B) filtering of the extracted potential trees. Step (A): The ALS point cloud is normalized to local heights by removing the terrain trend using a DTM. From the normalized point cloud, an initial CHM is created by assigning the 95th height

percentile within each raster cell. Based on this CHM, LM are detected and the found positions and heights are stored in a database. For the next iteration, points in the uppermost layer of the normalized ALS data are eliminated. The “eliminating” layer is defined as a band of 0.5 m below the current CHM. Based on the filtered data, a new CHM is created, LM are extracted, and the LM parameters are added to the database. This procedure is carried out sequentially until all points are removed from the normalized point cloud.

Step (B): All detected LM in the database are sorted by decreasing heights. The highest LM is considered a detected tree. For each following LM, the LM is considered a detected tree if there is no detected tree within a 2D distance of 2 m as well as a 3D distance of 5 m.

3.1.4. Method #4 (LM + Watershed)

The presented method [34] is based on the method published in Koch *et al.* [35]. In a first step, a rasterized CHM with a spatial resolution of $0.5 \times 0.5 \text{ m}^2$ is generated from the ALS data. The next processing step consists of a CHM surface smoothing using a Gaussian kernel filter. Focal statistics with a LM detection algorithm are used to extract potential tree tops from the smoothed CHM. The identified trees are then analyzed through a conditional script that considers a minimum distance and height difference from the nearest trees in order to identify and delete potential false positives. The coordinates of the found tree tops are then used as seed points in a watershed algorithm run on the inverse CHM in order to delineate single tree crowns and to generate polygon features with associated information on the canopy area. The method is fully automated and has been implemented as a workflow of geoprocessing tools within the software ESRI ArcGIS 10.2 [36].

3.1.5. Method #5 (Segmentation + Clustering)

In the presented method [37], the delineation is done by segmentation of a correlation surface model followed by ellipsoidal tree model clustering of the ALS data in 3D. The aim of the segmentation is to establish one segment for each tree in the topmost canopy layer. The segmentation method is based on geometric tree crown models and raster maps with 0.25 m cells. For each raster cell, an ellipsoid surface is calculated from different generalized ellipsoids. Correlation coefficients are calculated between the height of the ellipsoid surfaces and the height of the ALS data within the horizontal model radius. The correlation surface (CS) is defined as the highest correlation coefficient for each raster cell. The CS is smoothed and delineated with watershed segmentation.

The aim of the clustering is to establish one cluster for each tree in the topmost canopy layer as well as one cluster for each tree below. The algorithm is based on k-means clustering using ellipsoidal tree crown models. The clustering is done in two steps. In the first step, the ALS data are assigned to different clusters based on the Euclidian distance between the ALS data and the cluster centers. In the second step, an ellipsoid surface is fitted to each cluster and the ALS data are re-assigned to the different clusters based on a distance derived from the ellipsoid surface. Two categories of clusters are defined: Fixed clusters corresponding to trees already identified by segmentation of the CS and additional flexible clusters corresponding to trees below the topmost canopy layer. The top of the clusters is defined as the maximum height above the ground of the ALS data assigned to each cluster. The horizontal position of

the fixed clusters is defined as the horizontal position of the top of the cluster, while the horizontal position of the flexible clusters is defined as the horizontal position of the cluster center.

3.1.6. Method #6 (LM 3×3)

The method is published in Eysn *et al.* [38]. First, a DSM is processed based on the ALS point cloud using a land-cover-dependent derivation approach [39]. This approach makes use of the strengths of different algorithms for generating the final DSM by using surface roughness information to combine two DSMs, which are calculated based on (i) the highest echo within a raster cell, and (ii) moving planes interpolation. Second, a CHM with a spatial resolution of $1 \times 1 \text{ m}^2$ is derived by subtracting the DTM from the DSM. The base products are derived consistently for all study areas using the OPALS [40] software. Finally, the positions and heights of single trees are determined from the CHM using an LM filter based on a moving window (MW) approach. If the center pixel of the MW is an LM, a potential tree is detected. Only detected positions with a CHM height greater than 3 m are considered. A circular kernel with a diameter of three pixels is used (indicator in the assigned name is “ 3×3 ”). For all detected trees, the position and tree height are stored.

3.1.7. Method #7 (LM 5×5)

The workflow is exactly the same as described in Section 3.1.6. Instead of a circular kernel with a diameter of three pixels, a circular kernel with a diameter of five pixels (indicator in the assigned name is “ 5×5 ”) is used for the moving window.

3.1.8. Method #8 (Polynomial Fitting + Watershed)

First, a rasterized DSM is derived from the ALS data. A resolution of $0.5 \times 0.5 \text{ m}^2$ is used if the point density is greater than 10 pts/m^2 ; otherwise the spatial resolution is set to $1.0 \times 1.0 \text{ m}^2$. The height of a grid cell is defined by the highest points within the cell, while inverse distance weighting interpolation is used for defining the heights of the cells with no contained points. The DSM is normalized to a CHM by subtracting a DTM. Morphological opening and closing are performed in order to remove possible outliers. Best fitting second-degree polynomials are estimated in the 7×7 pixel neighborhood of each grid-cell, using the least squares method. Its factors are used to detect concave neighborhoods (potential tree-tops). This approach is also known as local fitting surfaces (LoFS) [41]. Watershed regions are then estimated based on concave markers. A region-adjacency graph is constructed over the obtained regions. Finally, region merging is performed based on geometric attributes of the regions (height, area, and shape compactness) with priorities defined by the measured similarity of best fitting polynomials. In all the test-cases, the same attribute-thresholds are used for identifying regions (nodes of the graph) that were merged. They are defined as follows: Regions with areas smaller than 5 m^2 or heights smaller than 0.2 m are merged under the conditions that the resulting region after the merging does not exceed 150 m^2 , and its compactness does not exceed the value of π . The positions of treetops are defined by the highest points of smoothed CHM (Gaussian filter with standard deviation = 1.0 m) within the corresponding regions, while the original height of the treetop is used for defining the height of the tree.

3.2. Tree Matching Process

A fully automated tree matching procedure for linking the different detection results to the reference FI data is established and applied. Compared to manual interpretation by experienced human interpreters, this methodology enables a clear, objective, and reproducible testing.

3.2.1. Input Data

The input data for the automated tree matching are:

1. Resulting single tree data from benchmark participants (hereinafter referred to as “Test”);
2. Forest Inventory data of the study areas (hereinafter referred to as “Reference”); and
3. Area of Interest of the study areas (hereinafter referred to as “AoI”).

3.2.2. Implementation of the Matching Algorithm

The matching procedure is performed in three general steps (Figure 2). The detailed workflow is presented in Figure 3. The matching between Test trees and corresponding Reference trees is implemented in Python 2.7.8 [42].

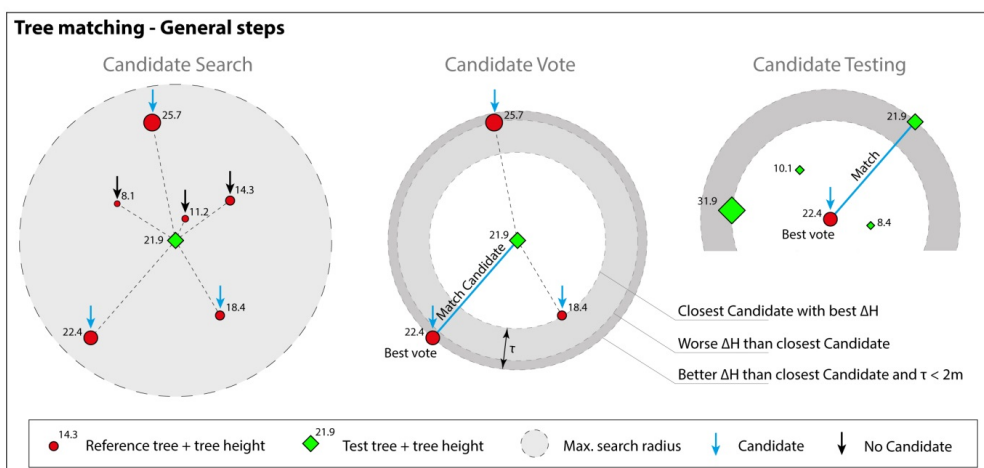


Figure 2. Basic steps of the tree matching workflow.

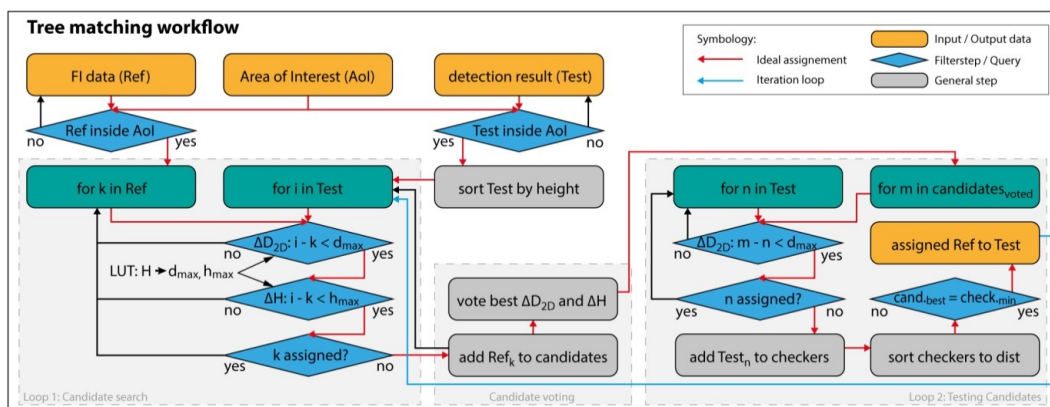


Figure 3. Workflow of the matching procedure.

3.2.3. Candidate Search

Initially, all input data inside an AoI are selected for the matching procedure. The AoI is defined by the surveyed area within the FI. The Test trees are sorted by tree height and the matching procedure starts from the highest Test tree. For a Test tree the restricted nearest neighbor Reference trees within a defined neighborhood are determined. Ideally the neighborhood is defined by the crown area of the Test tree. As this information is not available, circular buffering is used as the 2D neighborhood. In contrast to other methods, which use the nearest neighbor with the smallest 2D or 3D Euclidean distance as a match [26,43], only restricted nearest neighbors are matched. This method introduces a neighborhood criterion ΔD_{2D} and a height criterion ΔH . Both need to be fulfilled to make a tree a candidate for being matched/assigned (Table 4). Additionally, already assigned neighboring Reference trees cannot become candidates. ΔD_{2D} checks the horizontal distance between Test and Reference tree, while ΔH checks the tree height difference. The thresholds of ΔD_{2D} and ΔH vary depending on the tree height of the Test tree. The motive is the following.

The locations of trees are, in case of a terrestrial survey, measured at the bottom of the stem while most detection methods detect the position of the stem at the tree top. If a tree is tilted or shows a curved stem, the locations of tree top and the bottom of the stem differ. This effect normally increases with increasing tree heights. Therefore, with increasing tree heights the ΔD_{2D} criterion is increased up to a value of 5 m. The value of 5 m was chosen to align with the thresholds applied in Kaartinen *et al.* [24]. Additionally, the ΔD_{2D} criterion considers positional errors from the FI survey as well as inaccuracies originating from the tree detection.

The height accuracy of trees measured in a terrestrial forest inventory is believed to be decreasing with increasing tree height. Therefore, when comparing a terrestrially measured tree height to an automatically detected one, this effect should be considered. This is accounted for by increasing the ΔH value with increasing tree heights (Table 4).

Table 4. Height and neighborhood criteria for the candidate search. H_{Test} : Height of Test tree; ΔH : Height difference between Test and Reference; ΔD_{2D} : 2D distance between Test and Reference.

Criterion	Height Test	Distance Test
1	$H_{Test} \leq 10$ m and $\Delta H < 3$ m	$\Delta D_{2D} < 3$ m
2	10 m $< H_{Test} \leq 15$ m and $\Delta H < 3$ m	$\Delta D_{2D} < 4$ m
3	15 m $< H_{Test} \leq 25$ m and $\Delta H < 4$ m	$\Delta D_{2D} < 5$ m
4	$H_{Test} > 25$ m and $\Delta H < 5$ m	$\Delta D_{2D} < 5$ m

The thresholds presented in Table 4 were empirically found by testing different settings on a subset of the dataset while visually interpreting the quality of the matching results. The resulting values are applied to all datasets within this benchmark.

3.2.4. Candidate Voting

Since multiple trees can become candidates in the candidate searching process, the selected candidates are ranked depending on their ΔH and ΔD_{2D} value. Starting from the nearest candidate, all other local

candidates are tested for a better ΔH . If a candidate shows a better ΔH and its ΔD_{2D} is at a maximum of 2.5 m greater than the initial candidate's ΔD_{2D} , the candidate becomes the new best voted candidate (Figure 2). The value of 2.5 m (half of the maximum possible ΔD_{2D}) is introduced to spatially limit possible candidate jumps. This feature is helpful if candidates are clustered and the best fitting tree inside this cluster should be found.

3.2.5. Candidate Testing

Since the tree matching process is more than an isolated problem of matching one Test tree against a group of Reference trees, all other Test trees in the surrounding need to be considered. This is performed by checking the best voted candidate against the surrounding Test trees. If the previously best voted Test tree is the closest tree with the best height difference, these two trees are finally matched.

3.2.6. Products of the Matching Process

The outputs of the matching process are qualitative and quantitative statistical parameters as well as vector layers which can be displayed in a Geographical Information System (Figure 4). The following statistical parameters and vector layers are provided.

Detailed parameters: For each method and plot

- Number of extracted trees N_{Test} and number of Reference trees N_{Ref}
- Number of matched trees N_{Match} and commission errors N_{Com} . $N_{\text{Com}} + N_{\text{Match}} = N_{\text{Test}}$
- Extraction rate \rightarrow Total number (N_{Test}) or rate ($N_{\text{Test}}/N_{\text{Ref}}$) of extracted Test trees by a method
- Matching (assignment) rate \rightarrow Total number (N_{Match}) or rate ($N_{\text{Match}}/N_{\text{Ref}}$) of matched trees
- Commission rate \rightarrow Total number (N_{Com}) or rate ($N_{\text{Com}}/N_{\text{Test}}$) of Test trees that could not be matched
- Omission rate \rightarrow Total number ($N_{\text{Om}} = N_{\text{Ref}} - N_{\text{Match}}$) or rate ($N_{\text{Om}}/N_{\text{Ref}}$) of Reference trees that could not be matched
- H_{Mean} \rightarrow Mean of horizontal modulus of matching vectors (2D vector between Test and Reference)
- V_{Mean} \rightarrow Mean of tree height differences (ΔH between matched Test and Reference)

Global parameters: Using detailed parameters of multiple plots or methods:

- RMS_{extr} \rightarrow Root Mean Square of extraction rates
- RMS_{ass} \rightarrow Root Mean Square of matching rates
- RMS_H \rightarrow Root Mean Square of H_{Mean} values
- RMS_V \rightarrow Root Mean Square of V_{Mean} values
- RMS_{Com} \rightarrow Root Mean Square of commission rates
- RMS_{Om} \rightarrow Root Mean Square of omission rates

The results of the matching process are presented in different levels of information. Exploring the detection results at the method level is displayed in Section 4.2. Section 4.3 shows the results for different forest types. The overall performance of the benchmark is presented in Section 4.4.

In addition to the derived statistical values per plot, the matching rates in different height layers are derived. The tree matches are sorted to the height layers defined by the intervals (in meters) [2, 5],

[5, 10], [10, 15], [15, 20], and [20–∞], which were also used in the benchmark of Kaartinen *et al.* [24]. The matching results in different height layers are derived to get a better understanding of how the different methods perform in understory vegetation.

For all levels of information, the obtained qualitative and quantitative parameters are plotted in two different bar graphs. One bar graph focuses on the different rates found in the matching process, while the other focuses on the spatial accuracy. An example is presented in Figure 5.

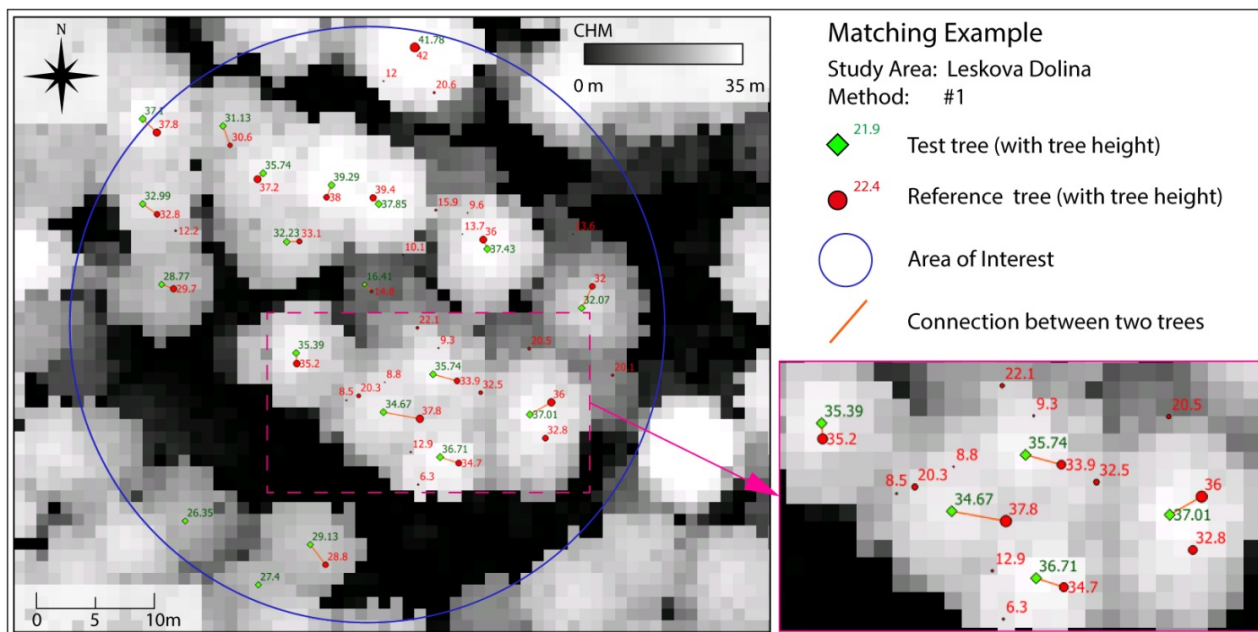


Figure 4. Matching example visualized in Quantum GIS. The detected Test trees (green diamonds), Reference trees (red disks), Area of Interest (blue circle), and the matched connections (orange lines) are displayed together with a height-coded CHM.

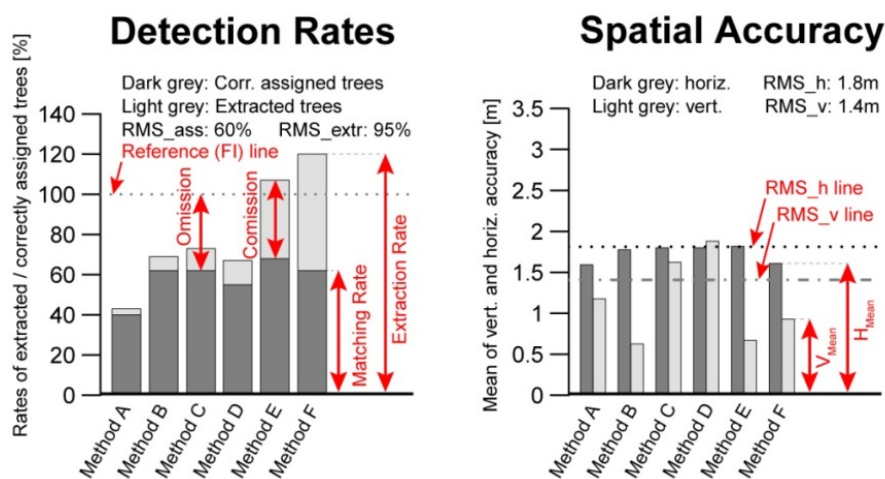


Figure 5. Bar graph examples for detection rates and spatial accuracy.

3.2.7. Validation of the Matching Procedure

The results of the automatic matching are validated by visually interpreting randomly selected matching results in Quantum GIS 2.8.1 [29]. The output vector layers of the matching process are

visualized as an overlay of the CHM. An experienced human interpreter classifies the matching results into four classes: Correctly Assigned (True Positive), Correctly not Assigned (True Negative), Wrongly Assigned (False Positive), and Wrongly not Assigned (False Negative). Descriptive measures are derived and presented.

4. Results

All participants were able to apply their method to the provided dataset. All submitted detection results were checked using the matching procedure described in Section 3.2. In total, 168 results consisting of 10987 detected potential tree positions were investigated.

4.1. Validation of the Matching Procedure

A subset of 699 Test trees, randomly selected from the submitted results, was manually interpreted and classified. The resulting error matrix and descriptive measures are presented in Table 5. An example of a visualized matching result displayed in Quantum GIS 2.8.1 [29] is presented in Figure 4. Nearby trees with matching tree heights get correctly connected in most cases. From the validated tree sample, only 3% were wrongly treated within the matching procedure. The obtained quality of the matching process shows an overall accuracy of 97% and a Kappa of 0.94.

Table 5. Error matrix and descriptive measures for the matching quality check.

Matching Result	Reference—Manual Interpretation			User's Accuracy
	Match	No Match	Totals	
Match	307	8	315	97%
No match	14	370	384	96%
Totals	321	378	699	
Producer's accuracy	96%	98%		
Overall accuracy: 97%		Kappa: 0.94		

4.2. Matching Results at Method Level

The matching results per method indicate how well a method performed for all study areas. In Table 6, the resulting statistical values are summarized.

The highest extraction rate (RMS_{extr} : 154%) was obtained by Method #6 (LM 3×3), while the lowest rate was found by Method #1 (LM + Filtering), showing a value of 51%. Regarding the matching rates, the highest rate (RMS_{ass} : 54%) was found by Method #6. In contrast, the lowest rate was obtained by Method #7 (LM 5×5). Speaking about incorrect detections, the highest commission rate (RMS_{com}) with a value of 113% was produced by Method #6. The best RMS_{com} rate with a value of 9% was found for Method #1. The highest omission rate (RMS_{om}) was found for Method #7, which missed 63% of the given reference trees. The lowest and therefore best omission rates (RMS_{om} : 51%) were found for Methods #5 and #6.

In the spatial accuracy section, the best positional accuracy with a RMS_H of 1.6 m was obtained by Methods #1, #4, and #6. The best height accuracy with a RMS_V value of 0.7 m was found for Method #3.

Table 6. Summarized detection results per method: RMS of selected indicators for all plots.

ID	Method	RMS _{extr.} (%)	RMS _{ass.} (%)	RMS _{com.} (%)	RMS _{om.} (%)	RMS _H (m)	RMS _V (m)
		Extraction Rate	Matching Rate	Commission Rate	Omission Rate	Height Accuracy	Planar Accuracy
1	LM + Filtering	51	45	9	59	1.6	0.9
2	LM + Region Growing	57	43	20	61	1.8	1.2
3	LM + Multi CHM	101	46	61	57	1.7	0.7
4	LM + Watershed	86	49	49	55	1.6	1.1
5	Segment. + Clustering	139	53	95	51	1.7	1.0
6	LM 3 × 3	154	54	113	51	1.6	0.9
7	LM 5 × 5	52	41	16	63	1.8	1.1
8	Polyn. Fitting + Watersh.	54	44	13	59	1.8	1.1

Table 7 shows the matching results (RMS_{ass} values) in different height layers. For the layers 2–5 m and 5–10 m, Method #5 shows the best performance with values of 15% and 17%, respectively, while all other methods detected only half or even a quarter of the trees. For the layer from 10 to 15 m, the clear lead of Method #5 gets lost as Methods #3 and #6 show comparable values. For the uppermost two layers, the performance difference between the different methods is reduced. In the uppermost layer greater than 20 m, RMS_{ass} values from 66% to 82% are found.

Table 7. Root mean square of matching rate per method in different heights.

ID	Method	RMS _{ass.} 2–5 m	RMS _{ass.} 5–10 m	RMS _{ass.} 10–15 m	RMS _{ass.} 15–20 m	RMS _{ass.} > 20 m
1	LM + Filtering	0%	3%	16%	35%	72%
2	LM + Region Growing	0%	5%	15%	30%	72%
3	LM + Multi CHM	0%	3%	32%	46%	68%
4	LM + Watershed	4%	7%	20%	36%	76%
5	Segment + Clustering	15%	17%	32%	45%	76%
6	LM 3 × 3	4%	6%	28%	44%	82%
7	LM 5 × 5	2%	4%	14%	24%	66%
8	Polyn. Fitting + Watersh	2%	9%	16%	40%	73%

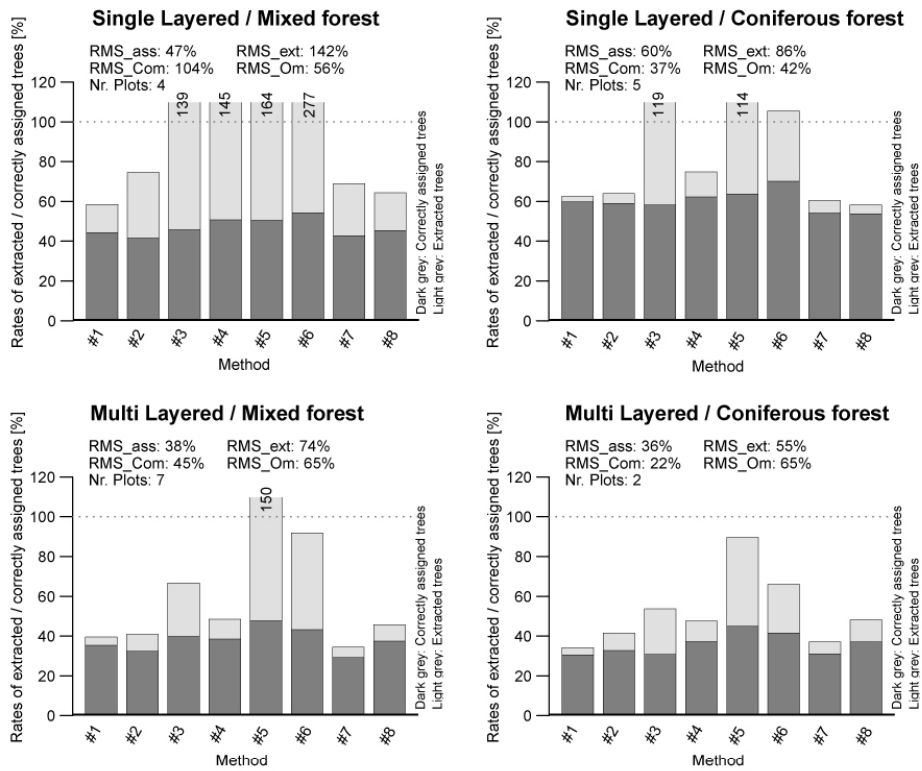
4.3. Matching Results by Forest Type

The detailed matching results by forest type indicate how well the different methods performed for different forest types. A graphical preparation of the matching results sorted to forest type is presented in Figure 6. In Table 8, the statistical parameters are summarized.

The highest extraction rate (RMS_{extr}) of 142% was found for single-layered mixed forests, while the lowest rate of 55% was found for multi-layered coniferous forests (ML/C).

For the matching rates, the highest RMS_{ass} rate of 86% was found for single-layered coniferous forests. The lowest matching rate (47%) was found for single-layered mixed forests.

Detection Rates



Spatial Accuracy

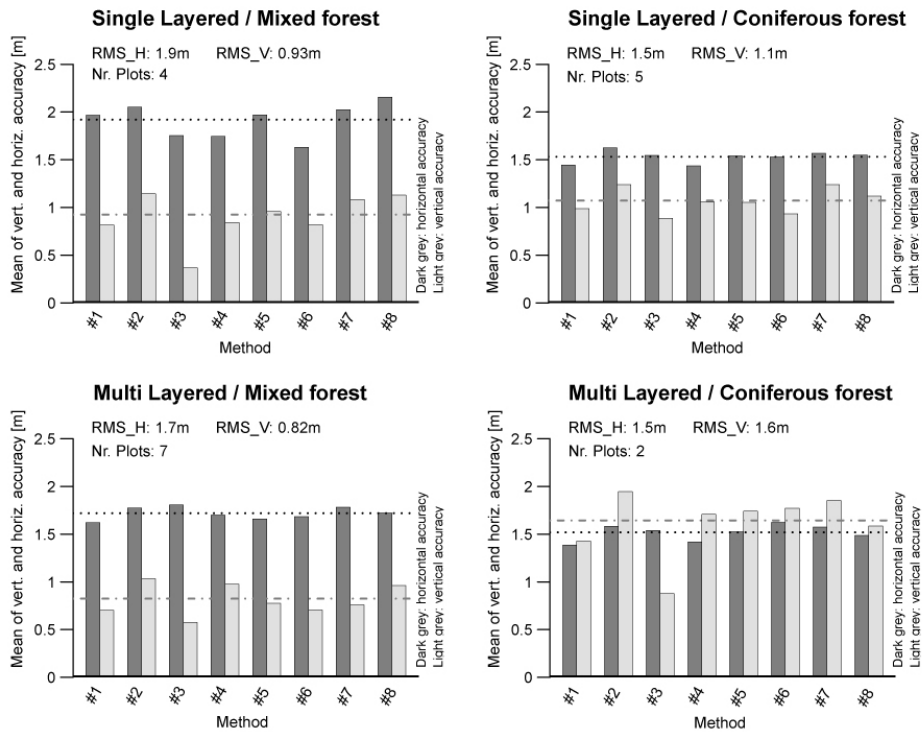


Figure 6. Bar graphs of detection rates and accuracies of the different forest types.

The highest commission rate (RMS_{Com}) of 104% was found for single-layered mixed forests. The lowest RMS_{Com} rate was found for multi-layered coniferous forests with 22%.

The highest omission rate (RMS_{Om}) was found for both types of multi-layered forests, with a value of 65%. The lowest rate was found for single-layered coniferous forests with a value of 37%.

In the spatial accuracy section, the best positional accuracy with a RMS_H of 1.5 m was obtained for coniferous forests. The best height accuracy with a RMS_V value of 0.8 m was found for multi-layered mixed forests.

Table 8. Summarized matching results by forest type—statistical parameters. Forest type: single or multi-layered (SL or ML)/mixed or coniferous (M/C).

Type	Nr. Plots	$RMS_{extr.}$	$RMS_{ass.}$	RMS_{Com}	RMS_{Om}	RMS_H	RMS_V
SL/M	4	142%	47%	104%	56%	1.9 m	0.9 m
SL/C	5	86%	60%	37%	42%	1.5 m	1.1 m
ML/M	7	74%	38%	45%	65%	1.7 m	0.8 m
ML/C	2	55%	35%	22%	65%	1.5 m	1.6 m

4.4. Overall Performance

In this section, the overall performance of the matching results of all eight methods is put together. A graphical preparation of the result is presented in Figure 7. The overall matching rate RMS_{ass} shows a value of 47%. This means that statistically 47% of all available Reference trees could be successfully matched. For the extraction rate RMS_{ext} , a value of 95% was found. The commission error and omission error show values of 60% and 57%, respectively.

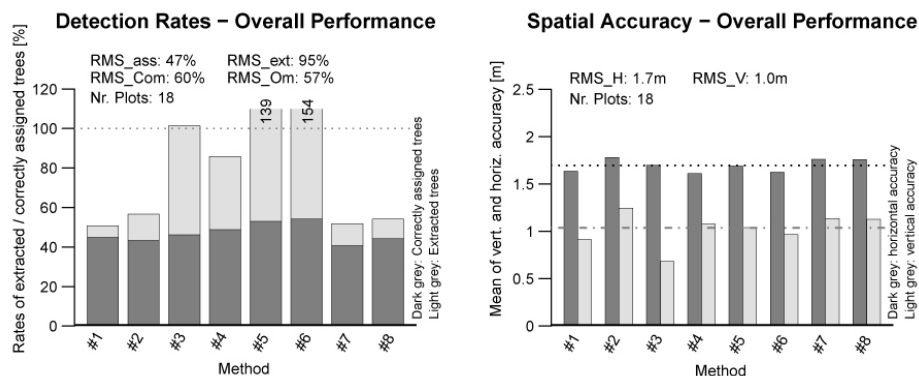


Figure 7. Overall performance of the tested methods.

5. Discussion

5.1. Input Data

For some study areas, the time gap between the ALS flight and the field survey is quite important. In the case of a field survey conducted after the ALS flight, the following errors can be expected:

- false omission errors due to tree growth in diameter (small trees reaching the caliper threshold between the ALS and the field surveys);

- false commission errors due to tree removal;
- false commission errors combined with false omission errors due to tree growth in height, which exceeds the matching threshold.

The opposite errors can be expected when the ALS flight is made afterwards. The time gap is two years in Montafon and Tyrol and six years in Berner Jura. It is one year or less in the other study areas. In mountain areas, tree growth is quite slow so that this factor has a limited impact on the matching process. Indeed the height growth of dominant trees during two years is likely to be lower than the vertical accuracy, which is already handled by the matching process. Besides, the proportion of trees reaching the caliper threshold in between the ALS and field survey is very low, except for young, dense stands. In all plots, the mean diameter exceeds the diameter threshold by more than 10 cm. Unless the diameter distribution is bimodal, the proportion of trees with a diameter close to the threshold is small. In Berner Jura, the forest is a dense, mature stand with no understory, so that the caliper threshold and height growth are not an issue. Regarding tree harvesting or mortality, no changes were reported by the partners who provided the data.

The difference in caliper threshold might also influence the matching results. The smallest trees represent a minor proportion of basal area but a major proportion of omission errors. Foresters usually set the caliper threshold by taking into consideration the inventory objective, the forest structure, and the required field effort. In this benchmark, the caliper thresholds were not *a posteriori* set to the highest value (12 cm in Berner Jura) because this would not be suitable to describe some young, dense plots. When comparing the detection results at the forest type level, it should nevertheless be taken into consideration.

Accurate georeferencing of the input data in a pre-processing step is a prerequisite for correctly comparing remotely sensed data with FI ground truth data. Three main error sources exist when comparing these data. These error sources are (A) positional errors due to inaccurate measurements (georeferencing); (B) irregularities of the local forest (*i.e.*, tilted trees, complex crowns); and (C) errors originating from the detection algorithm. To minimize error source A, forest inventory data is ideally acquired by using a survey grade GNSS system or a total station. A positional check by manually co-registering the inventory data to the remote sensing data in a post-processing step is necessary in most cases. Automated co-registration methods [44–46] can help to support the co-registration process. The reported performance of automated methods varies from 68% up to 92% and depends mainly on the input data and the variability of the forest stands [45]. In the presented study, error A was minimized by using manually co-registered datasets, with an estimated planar accuracy of ± 2.0 m. and ± 1.0 m for the vertical accuracy. The errors B and C are handled within the matching procedure by allowing flexible matching connections with a search radius depending on tree heights. The used FI data are heterogeneous due to different acquisition guidelines and methods. Therefore the data can be considered as imperfect compared to a local standardized FI. However, imperfect data should not have disadvantaged one of the detection methods as all participants faced the same conditions.

The presented matching procedure enables interpreter-independent and reproducible results in a short amount of time. The automatic matching took a few minutes while the manual interpretation within the validation process of the subset took several hours. The Overall Accuracy of 97% indicates that the matching procedure worked sufficiently for the presented dataset.

5.2. Matching Results

In general, the vertical structure of the forest (vertical distribution of tree heights) seems to have a major impact on the detection/matching results of the different methods. This finding is also reported by Vauhkonen *et al.* [26]. The more vertically distributed the trees are, the lower the matching rates are. The matching rates in different height layers indicate that especially in the lower height layers more advanced methods like point cloud-driven 3D clustering (Method #5) can detect more trees than methods that rely on local maximum detection based on a rasterized canopy height model. This finding was also reported in the benchmark study of Kaartinen *et al.* [24]. Method #5 achieved the highest number of small trees extracted.

Matching results combining a high matching rate with a low commission rate indicate a good matching result. The best detection result was obtained within the study area of Berner Jura, which consists of an old forest stand with high trees and no understory vegetation. The lowest detection result was obtained within plot #5 in Pellizzano, which consists of a multi-layered forest with a high amount of trees in different height layers. Only 15% of trees smaller than 10 m could be correctly extracted by the best performing method. In a summarized view, the results show that multi-layered forests are challenging for all tested methods. Maybe new methods as e.g., presented in Vega *et al.* [47] or Kandare *et al.* [48] will help to improve this issue in the future. Vega *et al.* [47] reported an overall performance of 75% for mixed multi-layered mountainous forest in the French Alps, with a 58% detection rate in the dominated tree layer.

Regarding the detection of small trees, it can be assumed that small trees in subdominant layers theoretically get mapped more efficiently at a higher ALS point density. This can be linked to a potentially higher canopy penetration rate. Kaartinen and Hyypä [25] and Reitberger *et al.* [49] conclude that the laser point density has less impact on the individual tree detection. In contrast Wallace, Lucieer, and Watson [43] conclude that high point densities are more significant for single tree detection than the method used. Wallace *et al.* studied a very young, planted stand of Eucalyptus trees using high-resolution UAV Lidar data, which is not comparable to the dataset of the Alpine Space. Therefore, it is assumed that the different point densities given in the presented study should not significantly influence the detection results. Within the pilot area Pellizzano, a maximum ALS point density of 121 pts/m² is given and the inventory data show a high vertical distribution of trees. Even at this high point density, only the worst detection result of all tested areas could be obtained. All study areas have point densities higher than 10/m², except Berner Jura and Tyrol. Both of these have plots of single-layered, mature stands so that the smaller point density is probably not a limiting factor for tree detection. However, investigating the effect of different point density on the detection results was not in the scope of this study.

5.3. Matching Results per Method

The best ratio between a high matching rate and a low commission rate was found for Method #1, which consists of a local maximum search in a canopy height model using a moving window approach. The fact that the algorithm parameters were automatically optimized for this purpose on an independent dataset seems to be an advantage compared to methods where parameters are set according to the user

appreciation. In the lower height layers up to 10 m tree height, only up to 3% of the extracted trees could be correctly matched. Since the method relies on a rasterized canopy height model and filtering of trees smaller than 7.5 m, this rather low value was expected. For the spatial accuracy, the obtained values for the location are comparable to the results of the other tested methods. For the height component, the second best value was achieved with a RMS value of 0.9 m, which is comparable to the values obtained for the best models in the benchmark of Kaartinen *et al.* [24].

Method #2 shows comparable matching rates to Method #1, but with a commission rate twice as high. In the lower height layers up to 10 m tree height, only up to 5% of the extracted trees could be correctly matched. In contrast to Method #1, trees down to a height of 2.5 m could be detected, which might lead to the slightly higher percentage value. However, the method is based on rasterized ALS data and therefore the rather low matching rate in the lower height layers was expected. The spatial accuracy of the method is comparable to the results of Method #1.

High commission rates in the results of Methods #3, #5, and #6 indicate that these methods tend to over-perform, which means they show high commission rates. Methods #3 and #5 are based on 3D operations in multiple canopy height models or directly in the 3D point cloud, while Method #6 is based on local maximum detection in a canopy height model, which uses a small local maxima kernel (3×3 pixels) and no preliminary smoothing. The small kernel tends to find local irregularities in the canopy height model and since these irregularities can be located even inside a single tree crown, the small kernel tends to detect too many potential trees. The result is the highest commission rate within this benchmark. The alternative Method #7 shows better results in terms of commission rate as the rate of the 5×5 kernel is seven times lower than the one from the 3×3 kernel. Methods #3 and #5 seem to be too sensitive in the detection process and the 3D clustering especially tends to detect multiple trees within a given single tree crown. Beside the fact of high commission rates for these methods, Method #5 shows up to 17% of correctly matched trees in the lower layers up to 10 m tree height. Compared to other methods, this is clearly the best result. Method #3 shows the best height accuracy with a RMS value of 0.7 m. Both Method #7 and #3 show the lowest matching rates in the uppermost height layer with trees taller than 20 m. In total, Method #7 shows comparable results to results of Method #1 and is counted as one of the best results within this benchmark.

Method #4 shows a relatively high matching rate of 49% (RMS) but in contrast the commission rate is high. This indicates that the method found many trees that could not be linked to the reference data. In the lower layers below 10 m tree height, up to 7% (RMS) of the available reference trees were correctly matched, while up to 40% (RMS) of the detected trees are sorted to commission errors. The rather low matching value can be explained by the methodology. It uses a smoothed rasterized canopy model, which follows the upper canopy and therefore the detection rate of smaller trees in subdominant layers is believed to be low. In the highest height layer with trees taller than 20 m, a matching rate of 76% (RMS) could be obtained, which is one of the highest values in this benchmark for this height class. The spatial accuracy of the method is comparable to that from Method #1. In general, the spatial accuracy of all methods does not differ very much.

Method #8 shows a high matching rate of 44% paired with a low commission rate of 13%. Based on these values, the results of Method #8 are close to the results of Method #1 and among the best within this benchmark. In the lower levels with tree heights up to 10 m, the method obtained a matching rate of up to 9%, which counts, together with Method #4 and #5, as the best obtained results. In general, a 9%

matching rate in lower height intervals is, compared to the other methods, a good result, but from an overall perspective such a low detection rate is unsatisfying. Like other methods that rely on maximum search in a rasterized canopy height model of the uppermost canopy, the low rate can be explained by the methodology.

5.4. Matching Results per Forest Type

The class of single-layered coniferous forests shows the best results of all tested classes as a high matching rate of 60% combined with a low commission rate of 37% is given. This result seems feasible as coniferous trees have, in most cases, a clearly defined tree crown shape. This means that the tree top appears as a clear peak in the canopy height model. Since most of the tested methods within this benchmark rely on local maximum detection on the canopy height model, the good result for single-layered coniferous forests was expected. The best performing methods for this forest type were Methods #1, #3, and #4.

The class of multi-layered coniferous forest as well as the class of multi-layered mixed forest show the lowest matching rates in this benchmark. Only a matching rate of up to 38% (RMS) could be obtained. The commission rate of the multi-layered mixed forest is twice as high as the rate found for the multi-layered coniferous forest, which shows a value of 22% RMS. The low matching rate can be explained by the methodology of the tested methods. Trees in lower layers are challenging for all tested methods. The higher commission rate for the multi-layered mixed forest can be linked to more complex crowns for deciduous trees, which results in over performing detection results. The best results for the multi-layered coniferous forest were obtained by Methods #2, #4, and #10. For the multi-layered deciduous forest, the best results were obtained by Methods #1, #4, and #8.

The single-layered mixed forest shows a matching rate of 47%, which is the second best matching rate for the classified results. In contrast, a very high commission rate of 104% is given. The high rate can be explained by the fact that deciduous tree crowns tend to be more complex than coniferous ones. Single tree crowns may consist of multiple local peaks in the canopy height model, which may be correctly detected as local maximum but do not represent the tree stem. The best performing methods for this forest type are Methods #1 and #8.

In general, it can be seen that the single-layered forest types show better results than the multi-layered ones. This was expected as forest structure has a significant influence on the results. Between the single-layered coniferous and mixed class, a considerable difference in the matching rates as well as commission rates is noticeable. This confirms the findings of Vauhkonen *et al.* [26], who tested the performance within coniferous and deciduous plots in Germany.

5.5. Overall Performance

The overall performance brings together all matching results from all tested methods. An overall matching rate of 47% (RMS) was found. This value aligns with the benchmark results presented in Kaartinen *et al.* [24], as well as with the results for the study areas in Germany and Norway in the benchmark published by Vauhkonen *et al.* [26]. In contrast, novel methods such as, for example, a purely point cloud-driven method presented in Vega *et al.* [47] enable a higher overall performance, *i.e.*, 75% for mixed multi-layered mountainous forest in the French Alps.

The overall best performing methods are #1, #2, #7, and #8. The other four tested methods show commission errors that are too high. For the spatial accuracy, a horizontal accuracy of 1.7 m (RMS) and a vertical accuracy of 1.0 m (RMS) could be obtained. These values are comparable to other previously carried out benchmarks. The performance of the different methods differs more for the tree detection than for the extracted tree heights. This was also reported by Vauhkonen *et al.* [26].

5.6. Perspectives

The trade-off between omission and commission errors turns out to be a critical point regarding tree detection. Some detection methods are probably intrinsically more efficient because they are able to extract more relevant information from the point cloud, as is expected from point cloud-based methods. However, as exemplified by Methods #6 and #7, which differ only by the LM kernel size, it turns out that the choice of algorithm parameters such as raster resolution, kernel size, and horizontal or vertical exclusion thresholds may have a major impact on detection results. From the image processing point of view, extracting trees is basically separating the signal from the noise. Depending on the forest structure (and on the caliper threshold, which defines the tree object) and on the acquisition parameters, the filters required for tree extraction have to be chosen or at least tuned specifically. In order to improve the detection algorithm available for forest practitioners, it seems important to A) have datasets that allow us to test the robustness of algorithms on a wide range of forest structures, and B) design algorithms able to optimize their setting, either based on internal (Lidar itself) or external (tree allometry) data. For the comparison of results, an automated matching procedure like that presented in this paper is of high relevance. Moreover, the choice of a trade-off criterion between the omission and commission errors would make comparisons easier, but it has to be application-oriented.

6. Conclusions

This study demonstrated that Forest Inventory data can be automatically matched to single tree detection results obtained from airborne laser scanning data. Furthermore, eight single tree detection methods were tested based on a unique dataset of different forest types originating from eight areas within the Alpine Space. The proposed method for automatically matching forest inventory data and remotely sensed data worked efficiently. In general, all tested methods achieve comparable results for the matching rates, but do differ for the extraction rates and omission/commission rates. The tree detection rates show a higher variation than the estimated tree heights. A method based on local maxima detection within a canopy height model using variable-sized moving windows is rated as the best performing algorithm. Complex multi-layered forests were challenging for all tested methods. A point cloud clustering-based method gained the best results for trees in subdominant layers, which is rated as an advantage over raster-based methods. The best detection results were obtained for single-layered coniferous forests.

Future studies should investigate the effect of different point densities on the detection results. Multiple datasets of the same area acquired with different flight parameters (*i.e.*, viewing angles, heights above ground, footprint size) would be necessary to perform this analysis robustly. Such datasets are rarely available. Automated absolute georeferencing between FI data and ALS data (co-registration) as well as an automated classification of FI plots in different forest types (*i.e.*, single-/multi-layered forests)

based on the ALS data would help us to overcome the manual steps performed in the presented study. Finally, the performance of novel, point cloud-driven single tree detection methods [47] should be tested on the unique dataset from the Alpine Space presented herein.

Acknowledgments

This work was funded by the European Commission (project Alpine Space 2-3-2-FR NEWFOR) within the European Territorial Cooperation program “Alpine Space.” The authors would like to thank the NEWFOR partners and the Department of Forests of Canton Bern in Switzerland (KAWA) as well as the Tyrolean Forest Service for providing the data. Furthermore we would like to thank Bernhard Maier, Michael Sautter, and Christian Ginzler for the fruitful discussions. We finally want to thank the anonymous reviewers who contributed constructive and helpful comments and suggestions.

Author Contributions

Lothar Eysn: paper writing; data quality check; tree matching procedure, preparation of results; organization of the benchmark; paper revision. Jean-Matthieu Monnet: paper revision; application of detection method. Markus Hollaus, Norbert Pfeifer, and Frédéric Berger: supervision. Eva Lindberg, Michele Dalponte, Milan Kobal, Marco Pellegrini, Emanuele Lingua, and Domen Mongus: application of their detection method and writing the corresponding method description.

Conflicts of Interest

The authors declare no conflict of interest.

References

1. Hyypä, J.; Holopainen, M.; Olsson, H. Laser Scanning in Forests. *Remote Sens.* **2012**, *4*, 2919–2922.
2. Holopainen, M.; Vastaranta, M.; Hyypä, J. Outlook for the next generation’s precision forestry in Finland. *Forests* **2014**, *5*, 1682–1694.
3. Franklin, S.E. *Remote Sensing for Sustainable Forest Management*; CRC Press; Taylor & Francis Group: Boca Raton, FL, USA, 2001.
4. Wulder, M.A.; Bater, C.W.; Coops, N.C.; Hilker, T.; White, J.C. The role of lidar in sustainable forest management. *For. Chron.* **2008**, *84*, 807–826.
5. Akay, A.E.; Oğuz, H.; Karas, I.R.; Aruga, K. Using lidar technology in forestry activities. *Environ. Monitor. Assess.* **2009**, *151*, 117–125.
6. LidarComm. Second Largest Forest Products Company Realizes Multiple Benefits from LIDAR and Ortho Imagery. Available online: http://www10.giscafe.com/nbc/articles/view_article.php?articleid=432054 (accessed on 9 April 2015).
7. NEWFOR Alpine Space Programme. European Territorial Cooperation 2007–2013. Available online: <http://www.alpine-space.eu/projects/projects/detail/NEWFOR/show/> (accessed on 15 January 2015).
8. Hollaus, M.; Wagner, W.; Schadauer, K.; Maier, B.; Gabler, K. Growing stock estimation for alpine forests in Austria: A robust lidar-based approach. *Can. J. For. Res.* **2009**, *39*, 1387–1400.

9. Holmgren, J. Prediction of tree height, basal area and stem volume in forest stands using airborne laser scanning. *Scand. J. For. Res.* **2004**, *19*, 543–553.
10. Hyyppä, J.; Kelle, O.; Lehtikoinen, M.; Inkinen, M. A segmentation-based method to retrieve stem volume estimates from 3-D tree height models produced by laser scanners. *IEEE Trans. Geosci. Remote Sens.* **2001**, *39*, 969–975.
11. Yao, W.; Krzystek, P.; Heurich, M. Tree species classification and estimation of stem volume and DBH based on single tree extraction by exploiting airborne full-waveform lidar data. *Remote Sens. Environ.* **2012**, *123*, 368–380.
12. Korpela, I.; Dahlin, B.; Schäfer, H.; Bruun, E.; Haapaniemi, F.; Honkasalo, J.; Ilvesniemi, S.; Kuutti, V.; Linkosalmi, M.; Mustonen, J. Single-Tree Forest Inventory Using Lidar and Aerial Images for 3D Treetop Positioning, Species Recognition, Height and Crown Width Estimation. In Proceedings of ISPRS workshop on Laser Scanning and SilviLaser 2007, Espoo, Finland, 12–14 September 2007; pp. 227–233.
13. Dalponte, M.; Bruzzone, L.; Gianelle, D. A system for the estimation of single-tree stem diameter and volume using multireturn lidar data. *IEEE Trans. Geosci. Remote Sens.* **2011**, *49*, 2479–2490.
14. Ancelin, P.; Barthelon, C.; Berger, F.; Cardew, M.; Chauvin, C.; Courbaud, B.; Descroix, L.; Dorren, L.; Fay, J.; Gaudry, P.; *et al.* *Guide des Sylvicultures de Montagne Alpes du Nord Françaises*; ONF/CEMAGREF: Grenoble, France, 2006; p. 154.
15. Lafond, V.; Lagarrigues, G.; Cordonnier, T.; Courbaud, B. Uneven-aged management options to promote forest resilience for climate change adaptation: Effects of group selection and harvesting intensity. *Ann. For. Sci.* **2014**, *71*, 173–186.
16. Dorren, L. *Rockyfor3D (v5.2) Revealed—Transparent Description of the Complete 3D Rockfall Model*; Association ecorisQ: Geneva, Switzerland, 2015; p. 32.
17. Kania, A.; Lindberg, E.; Schroiff, A.; Mücke, W.; Holmgren, J.; Pfeifer, N. Individual Tree Detection as Input Information for Natura 2000 Habitat Quality Mapping. In Proceedings of the Remote Sensing and GIS for Monitoring Habitat Quality—RSGIS4HQ, Vienna, Austria, 24–25 September 2014; p. 3.
18. Brosofske, K.D.; Froese, R.E.; Falkowski, M.J.; Banskota, A. A review of methods for mapping and prediction of inventory attributes for operational forest management. *For. Sci.* **2014**, *60*, 733–756.
19. Lindberg, E.; Hollaus, M. Comparison of methods for estimation of stem volume, stem number and basal area from airborne laser scanning data in a hemi-boreal forest. *Remote Sens.* **2012**, *4*, 1004–1023.
20. Maltamo, M.; Gobakken, T. Predicting Tree Diameter Distributions. In *Forestry Applications of Airborne Laser Scanning*; Maltamo, M., Næsset, E., Vauhkonen, J., Eds.; Springer: Dordrecht, The Netherlands, 2014; Volume 27, pp. 177–191.
21. Saad, R.; Wallerman, J.; Lämås, T. Estimating stem diameter distributions from airborne laser scanning data and their effects on long term forest management planning. *Scand. J. For. Res.* **2014**, *11*, doi:10.1080/02827581.2014.978888.
22. Xu, Q.; Hou, Z.; Maltamo, M.; Tokola, T. Calibration of area based diameter distribution with individual tree based diameter estimates using airborne laser scanning. *ISPRS J. Photogramm. Remote Sens.* **2014**, *93*, 65–75.

23. Næsset, E. Predicting forest stand characteristics with airborne scanning laser using a practical two-stage procedure and field data. *Remote Sens. Environ.* **2002**, *80*, 88–99.
24. Kaartinen, H.; Hyypä, J.; Yu, X.; Vastaranta, M.; Hyypä, H.; Kukko, A.; Holopainen, M.; Heipke, C.; Hirschmugl, M.; Morsdorf, F.; *et al.* An international comparison of individual tree detection and extraction using airborne laser scanning. *Remote Sens.* **2012**, *4*, 950–974.
25. Kaartinen, H.; Hyypä, J. *EuroSDR/ISPRS Project, Commission II “Tree Extraction”; Final Report*; EuroSDR (European Spatial Data Research): Dublin, Ireland, 2008.
26. Vauhkonen, J.; Ene, L.; Gupta, S.; Heinzl, J.; Holmgren, J.; Pitkänen, J.; Solberg, S.; Wang, Y.; Weinacker, H.; Hauglin, K.M.; *et al.* Comparative testing of single-tree detection algorithms under different types of forest. *Forestry* **2012**, *85*, 27–40.
27. Eysn, L.; Hollaus, M.; Monnet, J.-M.; Dalponte, M.; Kobal, M.; Pellegrini, M.; Lindberg, E.; Mongus, D.; Berger, F. *NEWFOR—Single Tree Detection Benchmark—Report*; NEWFOR: Wien, Austria, 2014; p. 87.
28. NEWFOR. The NEWFOR Single Tree Detection Benchmark Dataset. Available online: <http://www.newfor.net/download-newfor-single-tree-detection-benchmark-dataset/> (accessed on 1 February 2015).
29. QGIS Development Team QGIS Geographic Information System. Open Source Geospatial Foundation Project. Available online: <http://www.qgis.org> (accessed on 11 March 2015).
30. Monnet, J.-M.; Mermin, E.; Chanussot, J.; Berger, F. Tree Top Detection Using Local Maxima Filtering: A Parameter Sensitivity Analysis. In Proceedings of Silvilaser 2010, the 10th International Conference on LiDAR Applications for Assessing Forest Ecosystems, Freiburg, Germany, 14–17 September 2010; p. 9.
31. Monnet, J.-M. Using Airborne Laser Scanning for Mountain Forests Mapping: Support Vector Regression for Stand Parameters Estimation and Unsupervised Training for Treetop Detection. Ph.D. Thesis, University of Grenoble, Grenoble, France, 25 October 2011.
32. Dalponte, M.; Frizzera, L.; Gianelle, D. Estimation of Forest Attributes at Single Tree Level Using Hyperspectral and ALS data. In Proceedings of the ForestSAT 2014, Riva del Garda, Italy, 4–7 November 2014.
33. Otsu, N. A threshold selection method from gray-level histograms. *IEEE Trans. Syst. Man Cyber.* **1979**, *9*, 62–66.
34. Sambugaro, M.; Colpi, C.; Marzano, R.; Pellegrini, M.; Pirotti, F.; Lingua, E. Utilizzo Del Telerilevamento Per l’Analisi Della Biodiversità Strutturale: Il Caso Studio Della Riserva Forestale di Clöise (Asiago, VI). In Proceedings of the 17th Conferenza Nazionale ASITA, Riva del Garda, Italy, 5–7 November 2013; pp. 1171–1178.
35. Koch, B.; Heyder, U.; Weinacker, H. Detection of individual tree crowns in airborne lidar data. *Photogramm. Eng. Remote Sens.* **2006**, *72*, 357–363.
36. ESRI ArcGIS Desktop: Release 10.2. Available online: <http://www.esri.com/software/arcgis/arcgis-for-desktop> (accessed on 30 November 2014).
37. Lindberg, E.; Eysn, L.; Hollaus, M.; Holmgren, J.; Pfeifer, N. Delineation of tree crowns and tree species classification from full-waveform airborne laser scanning data using 3-d ellipsoidal clustering. *IEEE J. Sel. Top. Appl. Earth Obs. Remote Sens.* **2014**, *7*, 3174–3181.

38. Eysn, L.; Hollaus, M.; Schadauer, K.; Pfeifer, N. Forest delineation based on airborne lidar data. *Remote Sens.* **2012**, *4*, 762–783.
39. Hollaus, M.; Mandlbürger, G.; Pfeifer, N.; Mücke, W. Land Cover Dependent Derivation of Digital Surface Models from Airborne Laser Scanning Data. In Proceedings of the ISPRS Commission III Symposium PCV2010, Saint-Mandré, France, 1–3 September 2010; p. 6.
40. OPALS Orientation and Processing of Airborne Laser Scanning Data. Available online: <http://geo.tuwien.ac.at/opals> (accessed on 1 February 2015).
41. Mongus, D.; Lukač, N.; Žalik, B. Ground and building extraction from lidar data based on differential morphological profiles and locally fitted surfaces. *ISPRS J. Photogramm. Remote Sens.* **2014**, *93*, 145–156.
42. Foundation, P.S. Python Language Reference, Version 2.7. Available online: <http://www.python.org> (accessed on 15 July 2014).
43. Wallace, L.; Lucieer, A.; Watson, C.S. Evaluating tree detection and segmentation routines on very high resolution UAV lidar data. *IEEE Trans. Geosci. Remote Sens.* **2014**, *52*, 7619–7628.
44. Dorigo, W.; Hollaus, M.; Wagner, W.; Schadauer, K. An application-oriented automated approach for co-registration of forest inventory and airborne laser scanning data. *Int. J. Remote Sens.* **2010**, *31*, 1133–1153.
45. Monnet, J.-M.; Mermin, É. Cross-correlation of diameter measures for the co-registration of forest inventory plots with airborne laser scanning data. *Forests* **2014**, *5*, 2307–2326.
46. Hauglin, M.; Lien, V.; Næsset, E.; Gobakken, T. Geo-referencing forest field plots by co-registration of terrestrial and airborne laser scanning data. *Int. J. Remote Sens.* **2014**, *35*, 3135–3149.
47. Vega, C.; Hamrouni, A.; El Mokhtari, S.; Morel, J.; Bock, J.; Renaud, J.-P.; Bouvier, M.; Durrieu, S. PTrees: A point-based approach to forest tree extraction from lidar data. *Int. J. Appl. Earth Obs. Geoinf.* **2014**, *33*, 98–108.
48. Kandare, K.; Dalponte, M.; Gianelle, D.; Chan, J.C.W. A New Procedure For Identifying Single Trees in Understory Layer Using Discrete LiDAR Data. In Proceedings of 2014 IEEE International Geoscience and Remote Sensing Symposium (IGARSS), Quebec City, QC, Canada, 13–18 July 2014; pp. 1357–1360.
49. Reitberger, J.; Schnörr, C.; Krzystek, P.; Stilla, U. 3D segmentation of single trees exploiting full waveform lidar data. *ISPRS J. Photogramm. Remote Sens.* **2009**, *64*, 561–574.

Article V

Article

A Practical Approach for Extracting Tree Models in Forest Environments Based on Equirectangular Projections of Terrestrial Laser Scans

Lothar Eysn ^{1,*}, Norbert Pfeifer ¹, Camillo Ressel ¹, Markus Hollaus ¹, Andreas Graf ¹ and Felix Morsdorf ²

¹ Research Group Photogrammetry, Department of Geodesy and Geoinformation, Vienna University of Technology, Gußhausstraße 27-29, A-1040 Vienna, Austria; E-Mails: Norbert.Pfeifer@geo.tuwien.ac.at (N.P.); Camillo.Ressel@geo.tuwien.ac.at (C.R.); Markus.Hollaus@geo.tuwien.ac.at (M.H.); Andreas.Grafl@geo.tuwien.ac.at (A.G.)

² Remote Sensing Laboratories, Department of Geography, University of Zurich-Irchel, Winterthurerstrasse 190, CH-8057 Zurich, Switzerland; E-Mail: Felix.Morsdorf@geo.uzh.ch

* Author to whom correspondence should be addressed; E-Mail: Lothar.Eysn@geo.tuwien.ac.at; Tel.: +43-1-588-011-2249; Fax: +43-1-588-011-2299.

Received: 30 August 2013; in revised form: 19 October 2013 / Accepted: 21 October 2013 /

Published: 24 October 2013

Abstract: Extracting 3D tree models based on terrestrial laser scanning (TLS) point clouds is a challenging task as trees are complex objects. Current TLS devices acquire high-density data that allow a detailed reconstruction of the tree topology. However, in dense forests a fully automatic reconstruction of trees is often limited by occlusion, wind influences and co-registration issues. In this paper, a semi-automatic method for extracting branching and stem structure based on equirectangular projections (range and intensity maps) is presented. The digitization of branches and stems is based on 2D maps, which enables simple navigation and raster processing. The modeling is performed for each viewpoint individually instead of using a registered point cloud. Previously reconstructed 2D-skeletons are transformed between the maps. Therefore, wind influences, orientation imperfections of scans and data gaps can be overcome. The method is applied to a TLS dataset acquired in a forest in Germany. In total 34 scans were carried out within a managed forest to measure approximately 90 spruce trees with minimal occlusions. The results demonstrate the feasibility of the presented approach to extract tree models with a high completeness and correctness and provide an excellent input for further modeling applications.

Keywords: 3D tree model; forest inventory; branching structure; tree topology; cylinder model

1. Introduction

In 2014, the European Space Agency (ESA) [1] plans to launch a pair of new satellites (Sentinel-2 and Sentinel-3) which will routinely deliver high-resolution data. These data will benefit services associated with, for example, land management, the agricultural industry and forestry related tasks as monitoring land-use change, forest cover and photosynthetic activity [2]. To be able to validate, develop and compare biophysical Earth observation products from space-borne missions (e.g., ESA's Sentinels), the Project 3D Vegetation Lab was initiated to provide the scientific community with a common benchmarking tool to perform some of these tasks. The aim of this project is to create multi-scale reference datasets for selected forested study areas as well as a scientific toolbox based on a radiative transfer model [3]. A fundamental input for the radiative transfer modeling is a realistic 3D representation of the forest scene located at selected study areas, including tree topology and foliage. Forest scenes modeled at a high level of detail are also necessary to assess detailed forest parameters such as biomass or vertical branch structure. In general, the 3D modeling of a forest scene is very challenging because trees are complex objects and the data acquisition is complicated. In terms of data acquisition within forested areas, airborne methods such as airborne laser scanning or aerial photography show, even at high resolutions, too little detail to facilitate a reconstruction of the forest scene at a high level of detail. Beside the tree stems, branches and possibly leaves need to be modeled for the targeted application of radiative transfer modeling of forest stands with high spatial resolution.

In recent years, terrestrial laser scanning (TLS) became an important method for acquiring 3D data within forests, as the scanners are able to map the vicinity of a viewpoint within very short times. The basis for reconstructing 3D objects from point wise measurements as delivered by TLS is a representative sampling of the smallest objects. In case of a single tree, this means that the stem and all branches need to be sampled "sufficiently" with TLS. Due to the line of sight measuring principle of TLS and the complexity of forest scenes and individual trees, a gapless sampling of the objects is not possible with a justifiable expenditure. Especially in dense forest scenes with a high amount of stems per hectare, high trees with a lot of branching and dense foliage the amount of data gaps due to object occlusions can become very high. Statistical methods have been proposed to deal with partial data gaps due to occlusions by objects [4] but for reconstructing trees to a higher level of detail measurements from multiple viewpoints are necessary.

Faithful geometric reconstructions of larger forest scenes are still rare. As these are required within the project [3], our aim was to develop a practical method that allows a reliable reconstruction of tree structure, also under typical forest environment conditions. In this article, we therefore propose a method that allows geometric reconstruction of the wooden parts of trees (*i.e.*, stem and branches) visible in the TLS scans. A complete model of a tree can be obtained from this reconstruction by augmenting the structure in the upper parts with synthetic models and populating it with foliage [5]. In

contrast to the geometric reconstruction, obtaining biomass or total tree volume is not the objective of the current study.

The presented method relies on manual interpretation but reduces manual modeling to a minimum. The modeling is performed stepwise for each TLS viewpoint. Imperfections of the point cloud through wind or relative orientation errors in the scans are thus also accounted for. The approach is demonstrated for an old, managed forest stand with approximately 90 coniferous trees.

The paper is organized as follows. In Section 2, an overview of related work is given. Section 3 gives information about the study area and data. Detailed information about the method is presented in Section 4. Section 5 describes the implementation and in Section 6, results are presented. Finally, Sections 7 and 8 contain discussion, conclusion and outlook.

2. Related Work

A number of methods for reconstructing trees or parts of trees in 3D were developed and investigated in recent years. Beside methods which rely on simulating trees (*i.e.*, Biliouris *et al.* [6]) many reconstruction methods based on TLS data can be found in the literature. Manual reconstruction methods are challenging and time consuming because the interpreter has to navigate through dense point clouds and the reconstruction of the branching structure in 3D can be tricky. Therefore, different semi-automatic and automatic methods for tree modeling were developed.

Two general approaches can be found in the literature concerning the tree reconstruction: one focusing on tree reconstruction based on single scan data and one based on reconstructing trees based on merged scan data acquired from multiple viewpoints. While the single scan data based methods [4,7] mainly focus on extracting information on the tree's stems, the merged scan data methods can be separated into methods focusing only on the stem [8–11] and methods focusing on reconstructing trees with a high level of detail. Speaking about the latter methods, many authors aggregate the TLS data into voxel space for further analyses.

A semi-automatic tree reconstruction method was presented by Dassot *et al.* [12]. The authors use a merged point cloud from multiple single scans, and firstly isolate the wooden parts of the tree by manually selecting parts of the point cloud in a 3D Software. Using the retro-engineering functions of the software polylines are semi-automatically fit to the wooden tree parts representing the axis of the elements. In a final step, the determined skeleton is split into 25 cm segments and for each segment, cylinders are locally fitted into the point cloud. The handling of data gaps and wind affected point clouds are not treated. The authors conclude that the method is too time-consuming for modeling a large number of trees.

Schilling *et al.* [13] compose two dimensional images automatically by horizontally slicing the voxel data of a tree. Assuming that these slices/images will show circles or ellipses, which represent horizontally cut branches or stems, the authors first apply a Hough transformation to each image to detect circles and ellipses. Then a center point is assigned to each detected object and the detected points of each slice are connected with lines. To eliminate wrong connections, the authors apply search and sorting algorithms to finally extract a skeleton of the tree's topology. With this horizontal slicing primarily vertical structures can be extracted, but the more the structures (*e.g.*, branches) are tilted the

more the slices lose their elliptical shape and their reconstruction is therefore limited. Branches smaller than the data noise scatter or under sampled parts of the tree structure are also limiting this method.

A similar method based on slicing the pointcloud was presented by Delagrangé *et al.* [14]. In each slice, all points are buffered to a disk and centroids are placed in each union surface of the disks. Based on the centroids in all slices, a minimum spanning tree is derived. From the minimum spanning tree, a skeleton and, furthermore, a cylinder model is determined. Problems of imperfect point clouds and data gaps are not treated in this approach.

Vonderach *et al.* [15] use voxelized TLS data to model the wooden parts of a tree with focus on deriving volume and tree height. First, the Authors filter the voxel data using a 3D Kernel to remove noise. A method to find an appropriate filter threshold is presented. The filtered voxel data are separated to horizontal sections showing the surface voxels of stems and branches. As only the “hollow surface” is represented by voxels the Authors fill up the sections with voxels using a voxel intersection approach. A 3D voxel tree model is generated by merging the voxels of all slices. The sum of a mean volume of all layers represents the volume of the tree. The authors conclude that point clouds of high resolution are needed as the algorithm relies on closed surface representations. Large data gaps cannot be bridged and imperfections in the point cloud (e.g., due to registration problems or wind) can lead to erroneous modeling.

Hosoi *et al.* [16] also present a method based on horizontally slicing voxelized TLS data. Voxel sets are identified in each slice by connecting cells using a neighbor-tracing algorithm. In contrast to the method presented by Vonderach *et al.* [15] small gaps in the surface representation are filled by interpolating between valid voxels. The authors apply the method only to larger branches and remain with the pure uncorrected voxels for the small branches. A 3D voxel tree model is generated by merging the voxels of all slices. The handling of larger data gaps and wind affected point clouds are not treated.

Based on TLS voxel data, Bucksch [17,18] derives the center of gravity of TLS points within each voxel to finally connect these points to a graph. To ensure that outliers or noise do not alter the graph erroneous voxels are eliminated by applying a robust test. In a next step, the author simplifies the graph to a skeletonized graph by using a rule based decision tree. In a final step the skeletonized graph is intersected with the TLS point cloud to shift the regular grid based vertices of the graph to the spatial proximity of the irregular TLS point cloud. This method provides a skeleton, which is embedded in the middle of the branch, if the points cover at least half of the circumference. However, larger data gaps cannot be bridged.

Pfeifer *et al.* [19] and Thies *et al.* [20] use a voxel approach as described in Gorte *et al.* [21] to segment the TLS point cloud into segments belonging to individual branches and skeletonize the data as described in Palágyi *et al.* [22] into a wire model. Depending on the chosen voxel size as well as existing gaps in the data the wire model shows missing connections. The authors connect these by applying neighborhood relations. Based on a weighted skeletonized graph the authors use the Dijkstra algorithm to find the shortest path from the stem to the outermost point of each branch. Based on these paths the point cloud is segmented and for each segment cylinders are automatically fitted.

Côté *et al.* [23] classify the TLS point cloud into points belonging to woody tree parts or foliage by filtering the intensity information of the TLS measurements. The authors skeletonize the woody subset of points based on an algorithm presented by Verroust *et al.* [24] to extract the stem and main

branches. The fine branches are modeled by subdividing the foliage subset of TLS points into voxels, deriving local point densities and applying this information to a space colonization algorithm published by Runions *et al.* [25] and Palubicki *et al.* [26]. This method shows realistic looking tree models that only partly fit to the TLS data as only the skeletonized tree parts refer to the input data. Côté *et al.* [23] also mentions the need for filling the gaps with points, which is a manual step.

Cheng *et al.* [27] describe an approach to extract the branch skeleton of a tree from a synthetic range image with subsequent volumetric modeling with cylinders. The authors classify the range image into patches by using the discontinuity of depth and the axis directions derived from the map. For each patch a series of cylinders are fitted and finally the centroids of the fitted cylinders are connected to a hierarchical skeleton. Cheng *et al.* [27] conclude that further tests on real datasets, containing real trees and data gaps, are needed.

Raumonen *et al.* [28] determine small point cloud sets conforming the tree surface from a filtered TLS point cloud and furthermore derive neighbor-relations and a geometrically characterization (*i.e.*, eigenvectors, normal, principle components) for each set. After removing points not pertaining to the tree the authors extract tree components (clusters of the point cloud), as for example the stem, from the previously classified sets by selecting sets with similar properties. By segmenting the tree components using a surface growing approach, connected non-bifurcated parts of the tree as for example parts of a branch are found. Each segment is approximated with a set of cylinders by locally fitting cylinders into the point cloud. In a final step, small gaps between cylinders are filled to complete the model. Raumonen *et al.* [27] conclude that the method is promising but sensitive to the quality of the TLS data. Large data gaps cannot be bridged and imperfections in the point cloud (e.g., due to wind) can lead to erroneous modeling.

We conclude that two types of resulting tree models are found in the literature. The two types are (a) voxel models where filled voxels represent the wooden parts of a tree and (b) geometric models where the wooden parts of a tree are represented with geometric objects as for example cylinders. The voxel models are suitable for estimating tree parameters as for example tree volume but applying them for further modeling as for example needed in [3] can be limited. In contrast obtaining tree volume from geometric models is limited as the tree structure is approximated by geometrical objects. Small anomalies in the tree's surface or rapid diameter changes might be not sufficiently modeled in geometrical models.

Automatic algorithms are sensitive to data gaps or—in more general terms—varying point density. Wind affected scans, causing wavy branches within one scan and multiple branch images in the merged point cloud are problematic for all presented methods. These limitations are also reported by Dassot *et al.* [29]. A first specific solution for the orientation of imperfect scans is stated by Bucksch *et al.* [30]. For most approaches, the number of reconstructed trees is typically smaller than the number of scans used for the data acquisition. The reason is that only single trees or less dense forests were studied.

3. Study Area and Data

3.1. Study Area

A forest stand in a managed forest close to Tharandt in Germany ($50^{\circ}57'45.31''\text{N}$, $13^{\circ}33'54.82''\text{E}$, approximately 397 m above sea level) was selected as study area (Figure 1). The flat elevated site consists of an old homogenous, monospecies coniferous stand with little understory. Mainly very old spruce (*Picea abies* (L.)) trees with heights larger than 30 m and branching starting at the upper tree half can be found in the stand. The investigated area is approximately 100×65 m in size and shows a stem density of approximately 240 stems/ha. The site is additionally permanently equipped with a flux tower and different sensors for monitoring physical and environmental processes within the stand.

Figure 1. Aerial and terrestrial view of the Study area Tharandt.

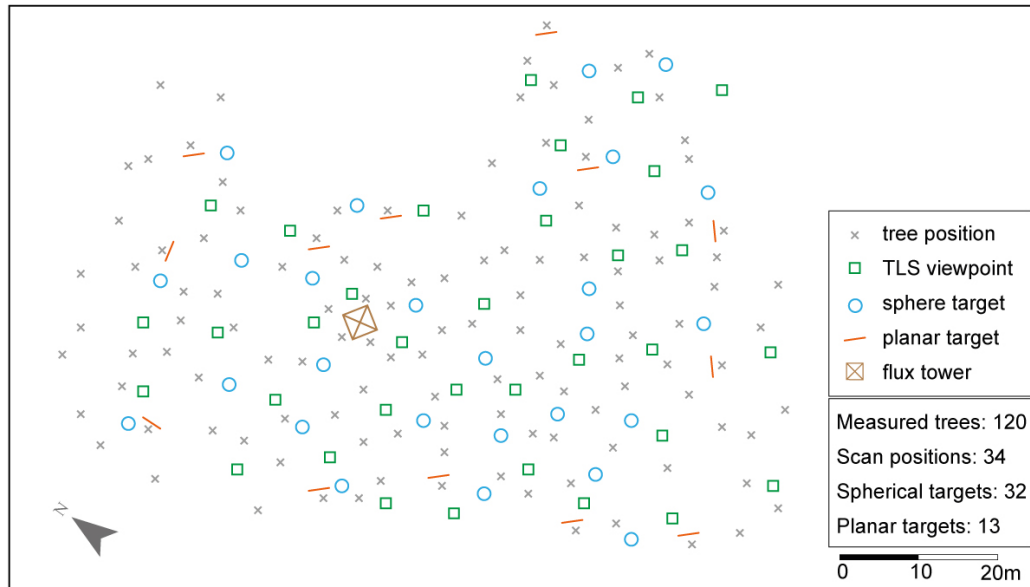


3.2. Terrestrial Laser Scanning Data

The TLS measurements were performed with a phase shift scanner (Z+F IMAGER[®] 5006i) in late September 2011. The scanner was selected because of its large field of view (FoV) (Hz: 360° , V: 310°) and the high scanning speed [31]. The *in situ* measurements were georeferenced based on two geodetic networks of control points. The first order network was realized with control points measured with a total station and RTK-GPS. A traverse, connecting four GPS control points with minor shadowing from the forest canopy, was introduced across the study area to be able to georeference the dataset. The second order network was realized with 32 spherical and 13 planar targets, which were placed across the study area (Figure 2). The planar targets, which consist of a black and white pattern and an identification number, were mounted on trees along the border of the study area. The traverse itself and the positions of all planar targets were measured with a total station. The spherical targets, which were used as tie points, were built from lightweight materials (aluminum and Styropor[®]) and were labeled for better identification purposes in the post processing. The target center can be seen from all

directions, which is not the case for flat targets that need reorientation to the scanner. The spherical targets were mounted stand alone up to approximately 2 m above the forest floor.

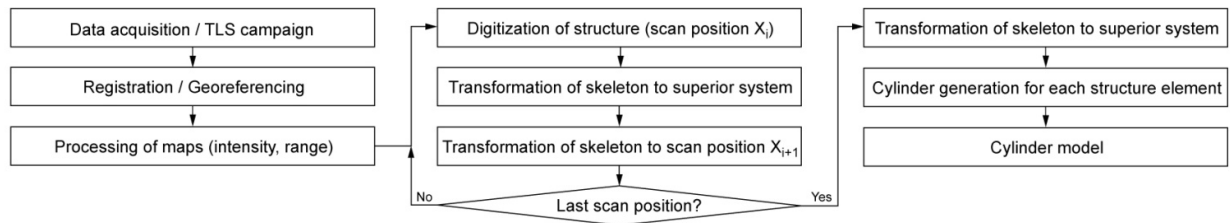
Figure 2. Overview of the scanning geometry.



All TLS measurements were performed from the forest floor without using a lifting platform. The scan resolution was set to “Superhigh” which resulted in a point density of 16 points per cm^2 at a distance of 10 m and a scan time of approximately 7 min per viewpoint when using the complete FoV of the scanner. The layout of the viewpoints for the scanning task was fixed in advance by marking potential viewpoints on site. At least four targets should be visible from each viewpoint and minimum shadowing as e.g., caused by too close tree stems should be given. In total, 34 scan positions, covering the complete study area, were measured in a two day campaign.

4. Methods

The first two steps consist of data acquisition and transformation of all scans from the sensor to the world coordinate system (WCS). In step 3, maps are generated showing the range and intensity measurements in the sensor coordinate system. Step 4 is the digitization of the axis of stem and branches and the radius determination from a single scan. These data are transformed to the WCS in step 5. In step 6, this tree model is transformed into a local coordinate system of another scan and displayed together with the maps in a new run through step 4. The sequence 6-4-5 is repeated for all scans, possibly using each scan a number of times. In this way, the modeled scene is becoming more and more complete. In a last step, the skeletonized tree structure is transformed to the WCS and extruded to a volumetric model. The suggested method is presented in an overview in Figure 3. The important steps will be presented in more detail below.

Figure 3. General workflow of the presented method.

4.1. Registration of the Scans

Based on the GPS and total station measurements a geodetic network is derived with a free adjustment [32], using the GPS control points of the first order network as a reference. Furthermore, all scans are relatively and absolutely georeferenced by a least squares adjustment, using the control points and target positions picked in the different scans. As a result, for each viewpoint the transformation parameters from the scanners own coordinate system (SOCS) to the WCS are obtained. Finally, each scan is exported in SOCS in full resolution containing the coordinates plus intensity information.

4.2. Equirectangular Projection

Starting point of the map generation are the angle, range, and intensity observations of each scan. This can either be exported from the scanner or computed from the SOCS point cloud in the following way for each scan.

Let (x_j, y_j, z_j) be the 3D Cartesian coordinates in the WCS, each of which is corresponding to an intensity value i_j and where $j = 1, \dots, n$ is the number of points in the scan. The scan position, *i.e.*, the point with a range measurement zero, is denoted as (x_0, y_0, z_0) .

$$r_j = \sqrt{((x_j - x_0)^2 + (y_j - y_0)^2 + (z_j - z_0)^2)} \quad (1)$$

$$\alpha_j = \text{atan2}\left(\frac{y_j - y_0}{x_j - x_0}\right) \quad (2)$$

$$\beta_j = \text{asin}\left(\frac{z_j - z_0}{r_j}\right) \quad (3)$$

In these equations, α_j is an azimuth, β_j an elevation angle and r_j the range. They typically do not correspond exactly to the original angle observations because of inclination and arbitrary orientation with respect to the north direction. Computation of the Cartesian coordinates from the angles and ranges is:

$$\begin{pmatrix} x_j \\ y_j \\ z_j \end{pmatrix} = \begin{pmatrix} x_0 \\ y_0 \\ z_0 \end{pmatrix} + \mathbf{R} \times r_j \begin{pmatrix} \cos \alpha_j \times \cos \beta_j \\ \sin \alpha_j \times \cos \beta_j \\ \sin \beta_j \end{pmatrix} \quad (4)$$

where \mathbf{R} is an orthogonal matrix. If the original angles are used, \mathbf{R} describes the rotation from the SOCS to the WCS.

Range and intensity are considered as functions of α and β . The (α_j, β_j) points may be regularly or irregularly distributed. By interpolation using nearest neighbor, moving least squares, or another local

interpolation method, the range map $r(\alpha, \beta)$ and the intensity map $i(\alpha, \beta)$ are generated. Data holes should not be bridged, but a NODATA value should be given. The interpolation is performed in a regular grid providing an image. The images are—by their definition—equirectangular projections of the measured ranges and intensities of each scan. The grid spacing should correspond to the angle increments during scanning in order to maintain the level of information. There is a linear relation between the rows and columns of the image and α and β . The world file mechanism [33] may be used to convert between row, column and α, β . Another convention is that the upper left pixel center = $(0^\circ, 90^\circ)$ for hemispherical scanners and the grid width (in angular units) is stored in the file name.

Alternatively to the range map, the horizontal range map can be computed, which is defined as:

$$r_H(\alpha, \beta) = r(\alpha, \beta) \times \cos(\beta) \quad (5)$$

Vertical lines (straight tree stems) have a constant r_H . Applying normalization (or correction by range) of the intensity is straight forward in this step too:

$$i_N(\alpha, \beta) = \frac{i(\alpha, \beta)}{r^2(\alpha, \beta)} \quad (6)$$

The spatial extent of the interpolated image is prescribed by the FoV of the laser scanner. If the focus is on a small area only, a restriction may be applied. For 360° azimuth coverage, however, a periodic continuation of the acquired data can be useful for viewing purposes:

$$r(\alpha + 360, \beta) = r(\alpha, \beta) \quad (7)$$

This way, a tree that is situated at the beginning and ending of data acquisition is not cut apart, but visible in one piece. This can be used analogously for the intensity maps. For visualization of the range images, a color palette is suggested. The intensity images are visualized with a grey scale palette (as presented in Figure 4).

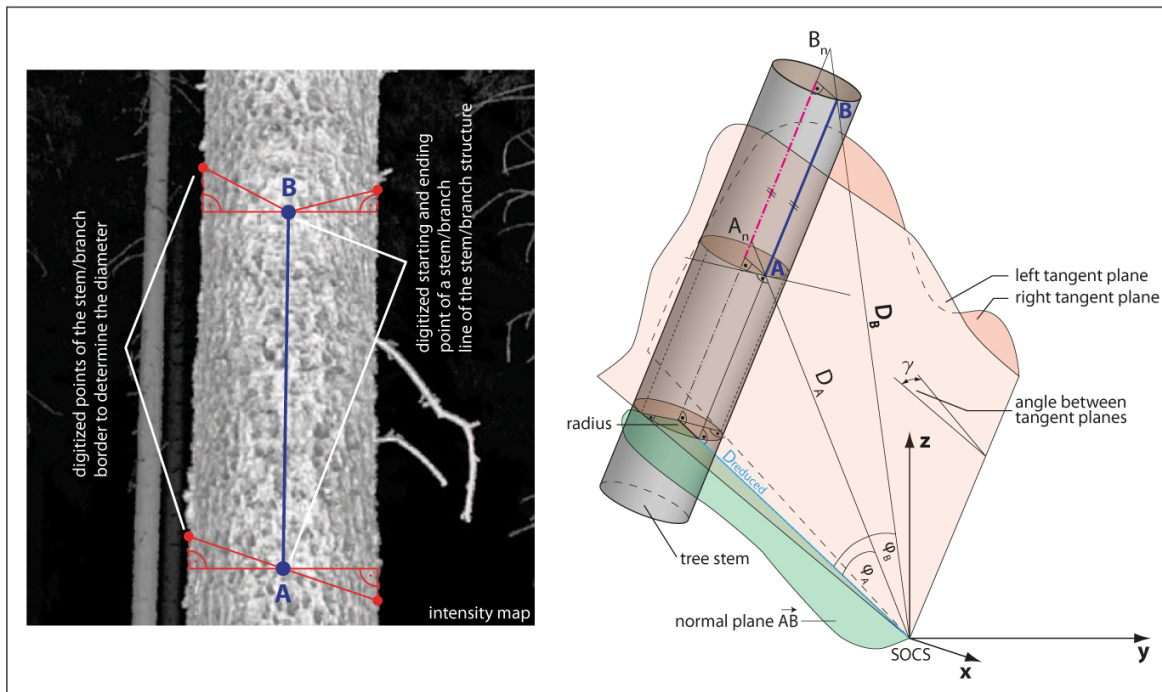
4.3. Digitizing of Tree Axis Radius

The tree shall be described by the axis of the stem and the branches. As they are not necessarily straight but can be curved, multiple, connected line segments are used for modeling. For each segment, the local radius of the tree is defined.

For measuring the tree topology in a single scan a software supporting the digitization of line network, e.g., by providing object snapping, is required, e.g., a CAD or GIS. The basic digitization operation is measuring a line segment along the tree surface. The digitization may be performed in the range or intensity map. At the end points A and B of a segment, a point on the left and a point on the right stem/branch border are measured. These tangent points are used to obtain the diameter of the object. Figure 4 (left) shows the measurement process.

The axis of a branch segment and its radius correspond to a cylinder. The parameters of the cylinder, *i.e.*, axis and radius, need to be determined robustly from the laser scanner measurements and the digitized points.

Figure 4. Method for extracting tree topology based on digitizing in a 2D map. **(Left)** Digitization process based on the 2D intensity map; **(Right)** Geometrical relation for transferring the 2D measurements to 3D space.



By measuring point A and B in 2D, the angles in the scanner coordinate system are determined via the transformation of the image coordinates (row and column) to the angles (α and β). The range is determined by the median of the range map values coming from the identified point and its 8-neighborhood. Therefore, points A and B can be transformed to a Cartesian coordinate system. The same procedure is performed for the tangent points picked at the edges of the object. For the tangent points no range information is determined. Using the left or right tangent points and the scanner's origin the left and right tangential plane is derived (Figure 4 (right)). In a next step the normal plane of the Vector AB, including the scanner's origin, can be derived. Next, the angles φ_A and φ_B are derived and furthermore the distances D_A and D_B are reduced to the normal plane since only in this normal plane a non-distorted radius of the object is deducible. The radius r can be derived using:

$$r = \frac{D_{reduced} \times \sin \frac{\gamma}{2}}{\left(1 - \sin \frac{\gamma}{2}\right)} \quad (8)$$

where $D_{reduced}$ is the shortest distance to the segment and γ is the angle between the tangent planes.

Based on the extracted radius r the Points A and B are shifted to the axis of the object. This axis element is in the middle of the tree, under the assumption of a circular cross section. Additionally the determined radius becomes an attribute of the axis segment.

This procedure is repeated for one map until all visible objects belonging to the tree topology are digitized by the interpreter. Line snapping ensures connection of consecutive axis segments.

4.4. Completion of Tree Model with Multiple TLS Viewpoints

The complete reconstruction of a tree cannot be performed from a single scan position as parts of the tree are occluded. Therefore, the tree topology is extracted stepwise from multiple scan positions. In this way, groups of trees are also completed stepwise. When all visible objects of a scan position are completely digitized, the extracted structure lines are transformed to the WCS. Then they are transformed into the coordinate system of the next scan to be processed for complementing the already extracted topology and new (previously occluded) trees. The lines can then be visualized as an overlay of the range and intensity maps of the new scan position. In addition to digitizing new axis segments, also existing ones may be improved.

4.5. Volumetric Modeling

After all scan positions are processed, the final skeletons of the trees are transformed to the WCS. To generate volumetric models of the digitized tree topology cylinders are generated for each line segment. Based on the starting and ending point of each line the axis of a cylinder is defined. The appropriate line attribute stored with each line is used to define the radius of the cylinder.

5. Implementation

5.1. Derived Base Products

As described above, for all scans an equirectangular projection (EP) based on the observation angles of the scan was created, thereby displaying the distances (range map, RM), intensity information (intensity map, IM), and the map showing the horizontal distances (horizontal range map, HM). Interpolation was performed with OPALS [34]. The spatial resolution of the maps was set to 0.018° which represents the angular step width of the scanning mode “Superhigh”. The maps show the full horizontal and vertical FoV of the scanner whereby pixels assigned to invalid TLS measurements are marked as NODATA. At the right edge of each map, the map was extended by appending the first, left quarter of the map. This should overcome limitations at the borders of the map to avoid having cut objects. For the IM grey scale coded maps and for the HM color coded maps were derived for visualization purposes, but the ranges themselves were also exported into a so called “Rangefile”, containing the ranges in ASCII.

5.2. Extraction of Tree Topology

The extraction of the tree topology was performed by digitizing stems and branches, visible in the intensity map and the map of horizontal ranges. AutoCAD was used for digitizing. While the images can be imported and displayed without problems in AutoCAD, the ranges needed special treatment. Image formats are restricted in AutoCAD, and therefore the full resolution float values of the ranges were imported into an array as an ASCII “Rangefile”. The conversions between the various coordinate systems and the extrusions of the final tree skeletons to cylinder models were performed with VBA scripts.

6. Results

6.1. Registration of the TLS Data

For the first order network a free network adjustment was performed separately for horizontal positions and height using the software package Geosi [35]. Based on the adjusted control points of the first order network and the tie points of the second order network 34 single scans were georeferenced. In each scan, at least six targets were visible for the laser scanner and were measured in the according SOCS during the data acquisition process. In a pre-processing step the 3D coordinates of all visible targets were manually picked in the according SOCS. This was performed using the software “Z+F Lasercontrol 8.2” [36]. The sphere centers were semi-automatically extracted using local sphere-fits within the point cloud. The centers of the planar targets were also semi-automatically extracted using a built in function provided by the software. Based on the reference measurements provided by the total station and the extracted target positions in the scans a 3D bundle block adjustment was performed to finally derive transformation parameters for each single scan. For the relative orientation, 323 targets were extracted from the scan data and were used in the bundle adjustment. For the absolute georeferencing 13 planar targets were used. The average deviation of the planar targets with respect to the total station data shows a value of 5 mm. The relative orientation shows an average target deviation of 4 mm. Each transformation parameter set allowed directly georeferencing of the scans from SOCS to the target system UTM33N. For each viewpoint, the TLS data was exported in ASCII XYZi format in the SOCS, containing the originally measured intensity values for each TLS point.

6.2. Equirectangular Projections

In general, objects close to the upper and lower edge of the maps are distorted. This is a general property of the equirectangular projection as explained by Tissot’s indicatrix. In the IM tree stems and branches are clearly visible. In the upper part of the map, wavy branches are partly visible which were moving due to wind influence during the data acquisition. With increasing distance from the scanners origin, the backscattered intensity decreases which results in darker grey tones for objects more than approximately 30 m away from the scanner. Due to the different reflective properties of the targets the structure of the forest floor and the stems’ bark is visible. Additionally when focusing on living branches the wooden part is distinguishable from the foliage in most cases. The spatial resolution of the processed map is high enough to visualize even small branches of trees, closer than approximately 20 m to the scanner. The beam diameter of the scanner’s laser is approximately 2–7 mm depending on the range. The point spacing of the TLS measurements is theoretically 1.6 mm at a range of 5 m, 4.7 mm at a range of 15 m and up to 8 mm at a range of 25 m. Based on the given scan parameters branches with a minimum diameter d_{min} of 4 mm (scanning range within 5 m), 1 cm (scanning range within 15 m) or 1.5 cm (scanning range up to 25 m) are visible in the maps as continuous pixel bands. Considering the distance calculation as presented in Section 4.3 the minimum reconstructable branch diameter $digit_{min}$ is determined by:

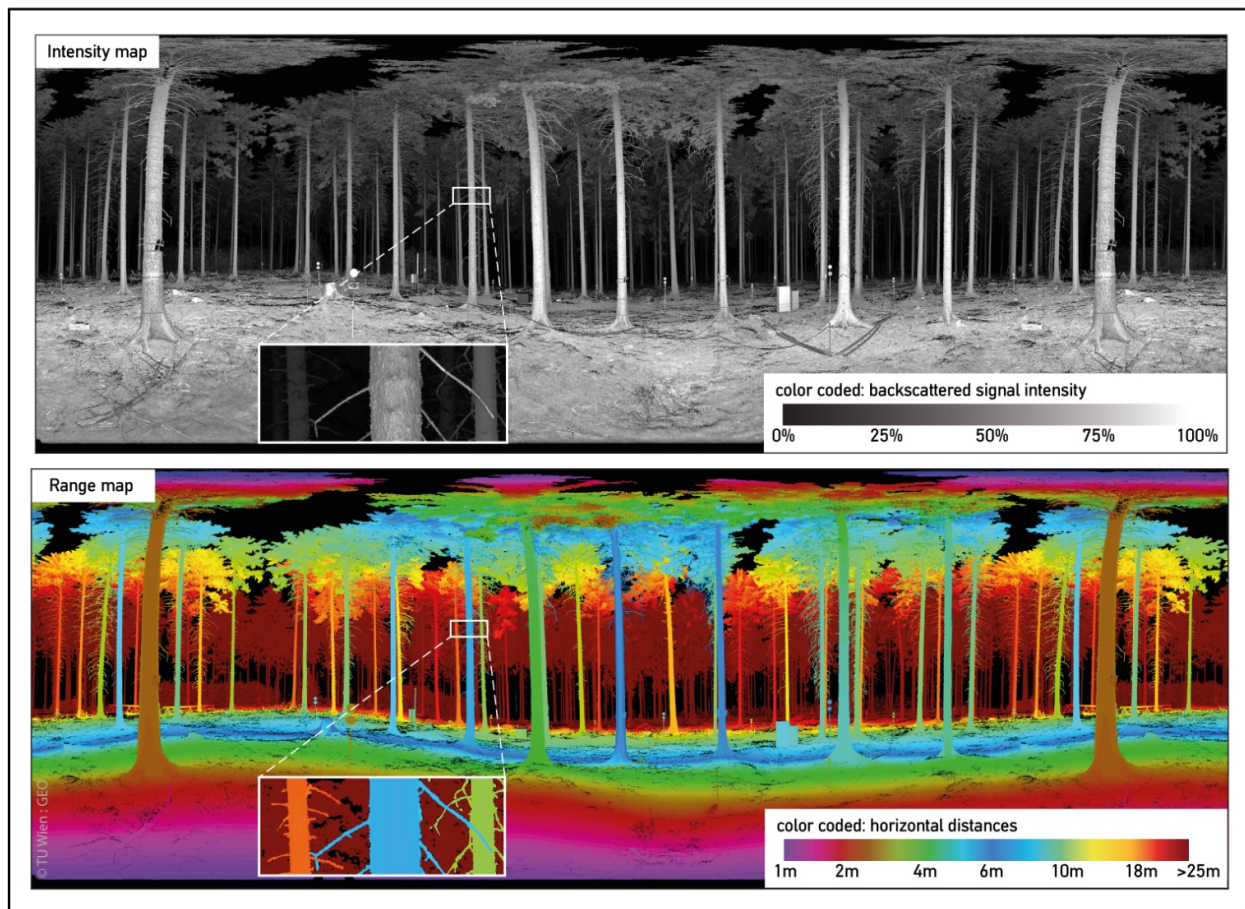
$$digit_{min} = d_{min} \times \frac{5}{9} + d_{min} \quad (9)$$

where $5/9$ is coming from the median distance calculation within the 3×3 kernel. Therefore, the theoretically extractable minimum branch diameter is 6 mm for a distance within 5 m, 1.6 cm for a distance within 15 m and 3.1 cm within a distance of 25 m.

The HM has the same geometrical properties as the IM. The differently colored horizontal distances allow a clearer separation of trees standing at different ranges. This is especially useful if different branches at different ranges partly overlap in the map.

Figure 5 shows the resulting IM and HM of one scan position.

Figure 5. Color coded intensity map and range map (horiz. distances) of a single scan position.

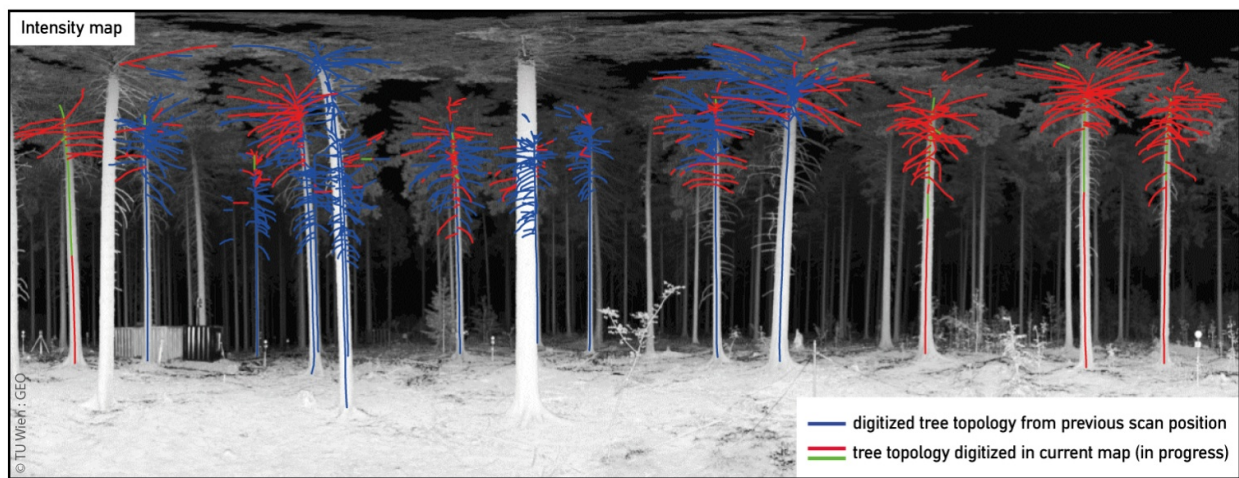


6.3. Digitized Tree Topology

The digitization result for a single scan shows a set of lines, which follow the axes of the stems and branches. To detect and correct misinterpreted points, the interpreter carried out intermediate checks within the digitization process. This was done by transforming the 2D lines to 3D space and visually checking the generated lines. Additionally the newly digitized lines were visually checked after transforming them to another scan position. In the final 2D digitization of one scan position the starting

and ending points of corresponding neighboring lines are correctly connected. Lines that represent a connection between a stem and a branch are correctly intersected with the line that represents the stem. In many cases, partly occluded areas could be bridged over in the digitization process which is attributable to the expert knowledge of the interpreter. In general, the upper part of a tree is easier to digitize if the tree is located more than approximately 6 m away from the scan position. The reconstruction of the top most part of the stem/branch structure is limited due to big data gaps of the TLS measurements and distortions of the maps. Therefore, usually, only segments of branches can be digitized in one scan, but completion of full branches can be done in other scans. Lines from already interpreted scan positions are correctly transformed and furthermore displayed in the target map of a different scan position (Figure 6). The digitized lines were transformed 66 times in total between different scan positions. Corresponding neighboring lines as well as intersected lines of the tree skeletons are correctly connected in 3D after the final transformation into the WCS. The time needed for modeling a single tree is hard to estimate as the digitized trees are composed of lines digitized from multiple scan positions and the trees differ in their appearance. A rough estimate can be given with 30 to 45 min per tree.

Figure 6. Digitized tree topology overlay with the intensity map. The blue color indicates the structure extracted from a previous scan position. Red and green colors indicate lines that are digitized in the current map.

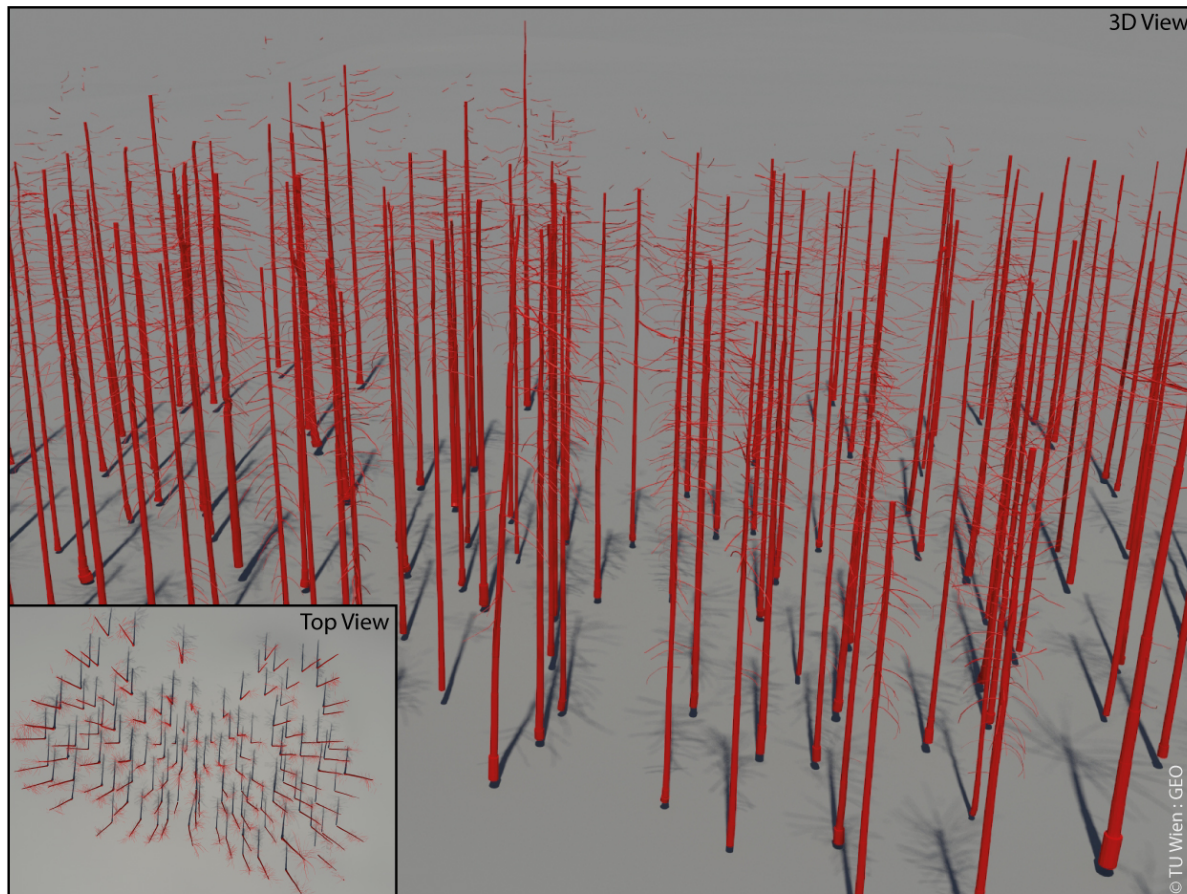


6.4. Volumetric Models

A visual inspection of the volumetric models shows that all cylinders are extruded correctly from the information stored with the 3D lines, containing the corresponding line segment as its axis. In total 38,101 cylinders were extruded from the tree skeletons representing 90 trees (Figure 7). The smallest modeled cylinder shows a diameter of 7 mm, the largest cylinder modeled shows a diameter of 1.05 m. A visual inspection of the final modeled scene and five randomly selected single trees shows that the stems and branches could be modeled approximately up to three quarters of the tree height and the determined cylinders show a good agreement with the corresponding point cloud (Figure 8). In the upper section of the trees, the modeled branches start to get fragmented and in most

cases they are not connected to a stem. For neighboring cylinders, no rapid diameter changes or rapid, unnatural changes of the orientation of the cylinders are visible. Only at the very bottom of some stems a rapid change of the diameter is visible which seems plausible as many tree stems widen up at this area for stabilization purposes.

Figure 7. 3D visualization of the reconstructed forest stand.



6.5. Validation

The quality of the modeled trees is validated based on five randomly selected trees from the scene. Each tree model is tested in two different ways against the corresponding point cloud.

Validation Method 1 investigates the stem diameters of the modeled trees by cutting horizontal slices from the point cloud and the model. The thickness of the slices is set to 1 cm and the spacing between the slices was set to 1 m (Figure 9). For each slice the stem diameter of the model (D_{MODEL}) and the mean stem diameter from the TLS point cloud (D_{TLS}) are determined. D_{TLS} is deduced by deriving the mean value of two stem diameter measurements performed in the sliced point cloud. Figure 9 shows the resulting stem/trunk diameter profiles of the sample trees. In total 71 slices were analyzed. All profiles show decreasing D_{MODEL} and D_{TLS} values with increasing height above ground. The mean of residuals between D_{MODEL} and D_{TLS} shows values between -1.3 cm and 1.7 cm. The standard deviation of residuals shows values between 0.9 cm and 2.0 cm.

Validation Method 2 investigates the 3D deviations between the models of the sample trees and their corresponding TLS point clouds to test the model for completeness and correctness. Since only the wooden parts of the trees should be investigated the point clouds were manually edited in a pre-processing step. In this step, ground points and all points above the first living branch were deleted. Based on the edited point clouds the 3D deviations were derived for each tree. The 3D deviations of sample tree 1 are displayed in Figure 8 colored by a color spectrum. Histograms of the deviations are presented in Figure 10. The mean of deviations for all trees are between 0.2 cm and 0.6 cm. The standard deviations for all trees are between 1 cm and 2 cm.

Figure 8. Extracted tree model of sample tree 1; **(Left)** Extracted tree model *versus* merged TLS point cloud; **(Middle)** Extracted tree model; **(Right)** 3D Deviations.

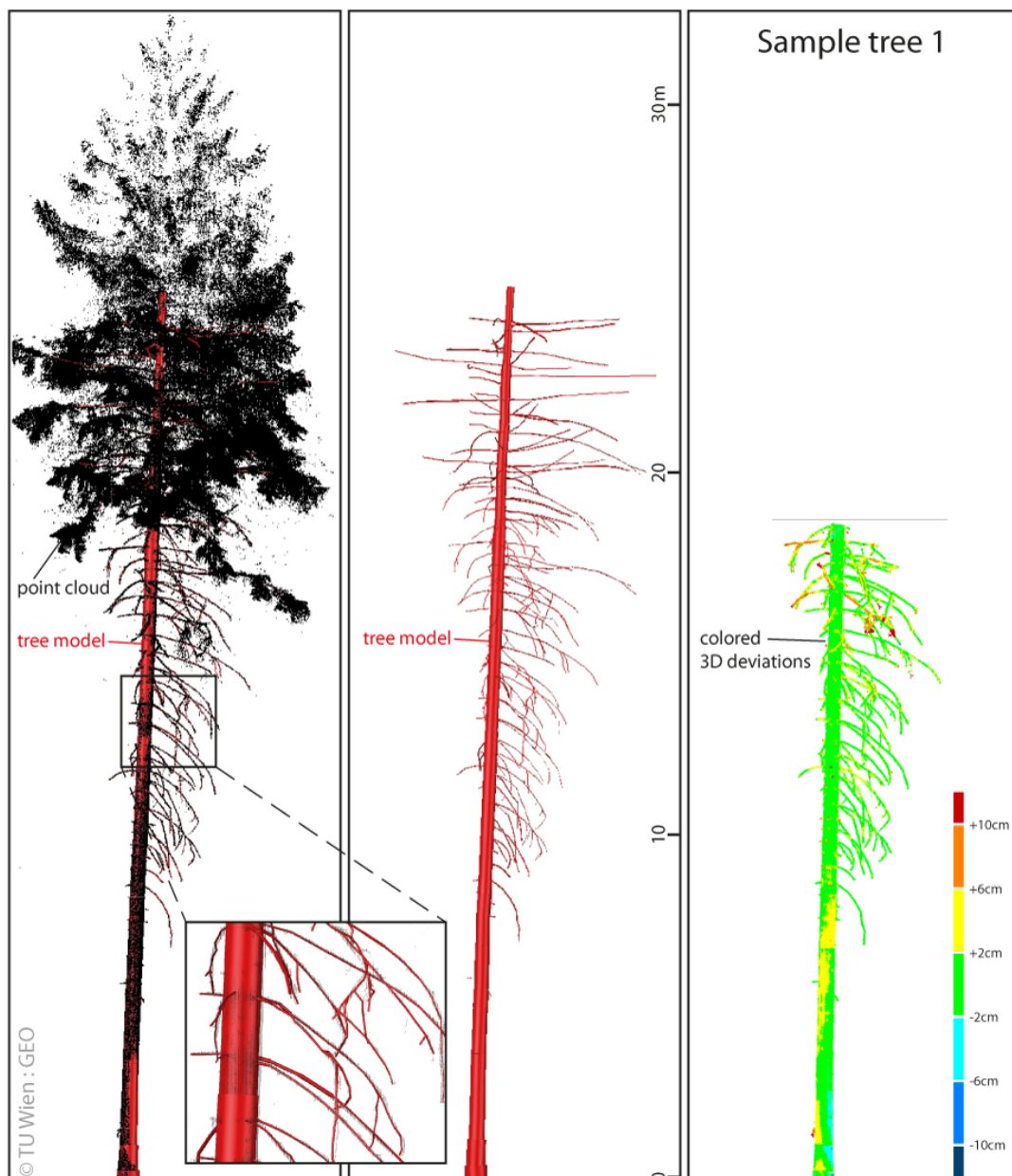


Figure 9. Validation Method 1. Validation of the stem performed for five randomly selected sample trees. Based on horizontal slicing of the point cloud and the model the diameters of the stem are determined. The stem diameters are plotted against the height of the slices above ground as stem profiles.

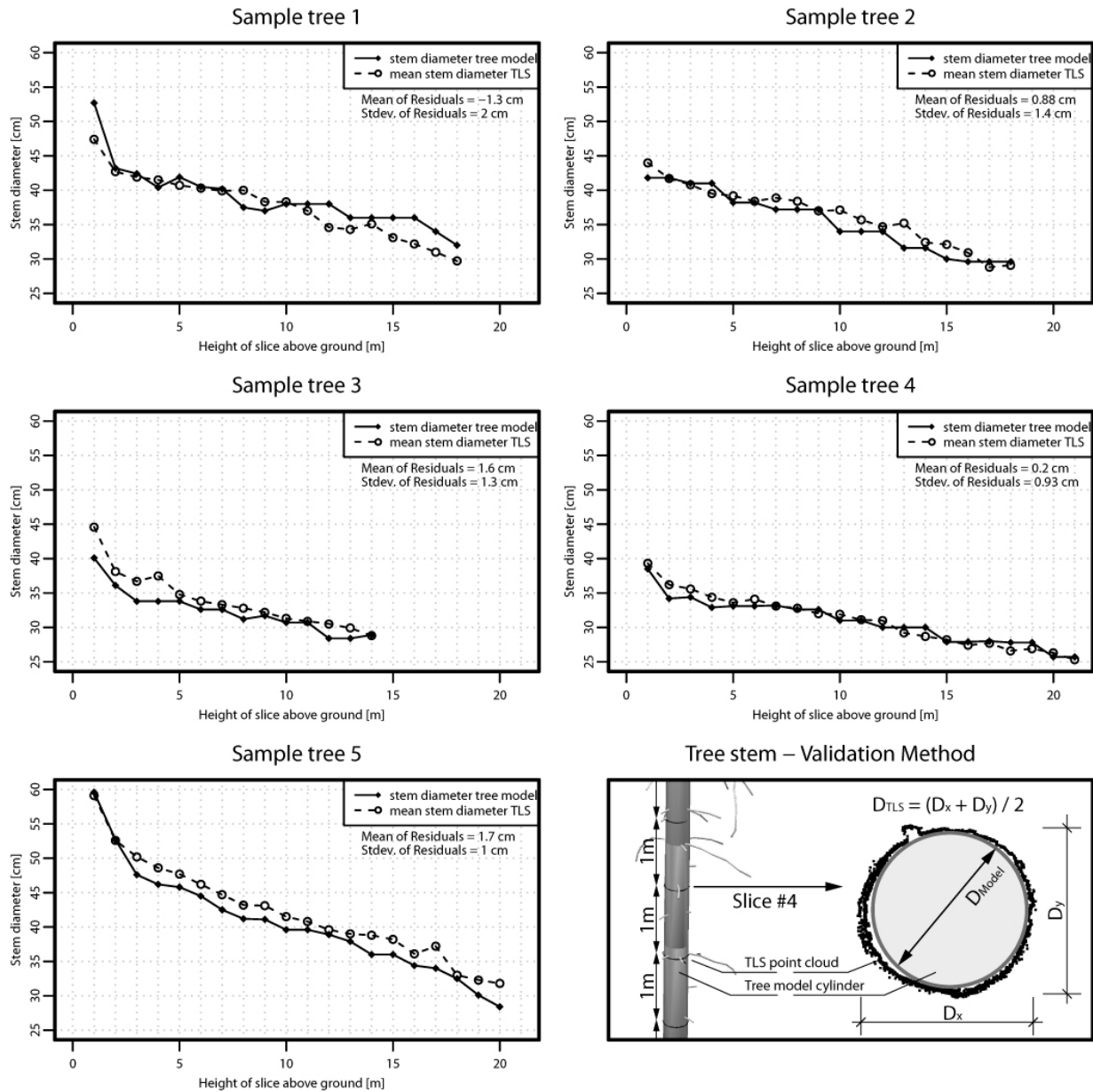
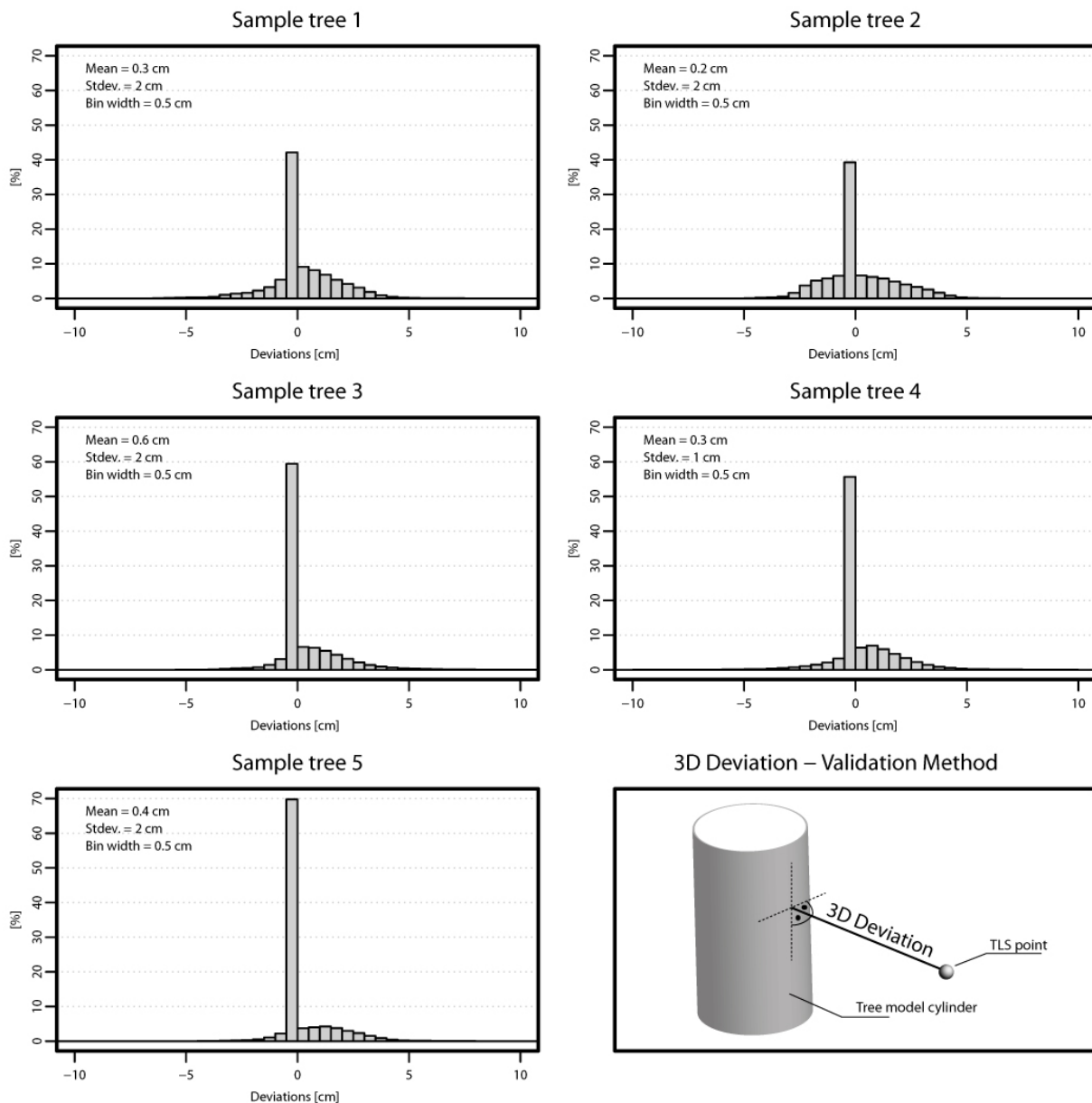


Figure 10. Validation Method 2. Validation of five randomly selected sample trees by investigating the 3D deviations between the TLS point cloud and the model. Histograms of the deviations are presented for each tree.



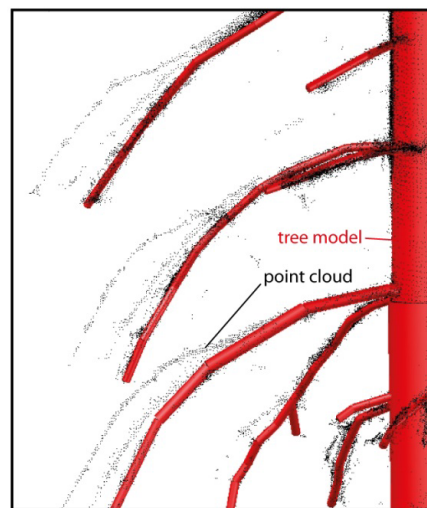
7. Discussion

The result of the presented semi-automatically method shows that the reconstruction of tree topology based on a simple digitization is possible with a high level of detail. As parts of the structure of a tree (stem, branches) are clearly interpretable in the introduced high resolution maps, these maps provide a good basis for extracting the tree structure by digitizing the axis of the structure elements in 2D. This is an advantage compared to the method described by Dassot *et al.* [12]. The digitization can be performed in the intensity map and/or in the range map, using the advantages of the different image information. The intensity map shows the distance corrected backscattered signal intensities and

clearly visualizes the wooden part of a tree. The horizontal distances shown in the range map allow the interpreter to separate tree topology of trees standing at different ranges. The image distortions at the upper part of the maps as well as occlusion effects limit the digitization of the upper tree parts. Therefore, trees standing further away from the scan position are better suited for digitizing the tree's upper part, depending on the visibility. The visibility mainly depends on the density of the scan data and the density of the branches/needles. Other projections or scan positions performed from a lifting platform may help to overcome this limitation. Also the time of the year can make a huge difference for the data acquisition as for example some trees loose their leaves or needles in fall which might be an advantage for the field campaign. Due to the expert knowledge of the interpreter, data gaps can be overcome during the digitization process. Depending on the local situation larger gaps greater than approximately 1 m can be bridged in many cases. This is an advantage compared to fully automatic algorithms as e.g., presented by Pfeifer *et al.* [19], Raumonon *et al.* [28] or Bucksch [17]. It should be noted that the bridgeable gap size is depending on the local situation, *i.e.*, point density, degree of occlusion, wind effects, *etc.*

The tree topology is extracted step wise from multiple scan positions. In this way partly occluded branches and furthermore groups of trees are completed stepwise. Imperfections of the merged point cloud, caused by remaining registration errors, noise or *i.e.*, moving branches which were influenced by wind, are overcome in most cases because of the digitization method (Figure 11).

Figure 11. Tree model *versus* merged point cloud. The merged point cloud, merged from three different scans, shows multiple positions for the same branch due to wind influence.



This is an advantage compared to voxel methods, which are based on a merged pointcloud e.g., [15,16,18]. One of the big benefits of using single scans and their projections is that the inevitable systematic errors (imperfect registration) and random errors (noise) are an unsolvable problem. In forest scans, there are always “phantom points” which are generated from multiple returns and they are along the same line from the scanner. In 3D, these points are visible and problematic, but in 2D projections these all have the same projection and thus they are not visible. Therefore, no filter steps are necessary. This is an advantage over methods that rely on a filtered pointcloud, e.g., [15–17,28].

Additionally, the step wise reconstruction also ensures the quality of the final model. Because the already reconstructed lines are plotted in a new scan, the interpreter visually checks the alignment of the axis with the trees in a new view. Gross errors, e.g., a wrong range measurement, immediately become visible. The cylinders of the extruded volumetric models show no rapid diameter changes or unnatural direction changes and correctly represent the point cloud in its close vicinity in most cases. In contrast to the method presented by Côté *et al.* [23], all branches of the tree models follow the “original” branch structure as no branch colonization algorithm is used. This is also reflected in the validation results presented in Section 6.5. For the tested trees/stems the standard deviation of residuals (Stem diameters Model against stem diameters TLS) varies between 0.9 cm and 2.0 cm. The tested 3D deviation (Tree model against TLS point cloud) shows standard deviations between 1.0 cm and 2.0 cm. The validation proves that the lower part of the trees is modeled correctly and completely. This is also supported by the histogram of 3D deviations presented in Figure 10 and the colorized 3D deviations presented in Figure 8. Primarily wind and registration errors cause large deviations. For the upper part a validation is very challenging and could not be performed within this work. No reference measurements of upper tree parts are available as the trees are too tall. A destructive validation method as for example presented in Dassot *et al.* [12] was not an option, as the trees cannot be cut down. Validating the method by investigating an artificial tree as presented in Raumonon *et al.* [28] was not an option because the simulated point cloud doesn't consider the influence of wind, visibility especially in the upper part of the tree and imperfect point clouds from different TLS viewpoints due to limitations in the registration. Thus, such a simulated point cloud doesn't sufficiently represent the real situation in a dense forest stand with a mean tree height of approximately 30 m. A validation based on tree height and a single DBH measure as presented in Vonderach *et al.* [15] was assumed to be insufficient as the information about completeness and correctness is limited. Furthermore, this publication investigated deciduous trees under leave-off conditions in an urban environment. In general, a comparison between results from different approaches is limited as most authors studied single trees, e.g., [15,18,19,37]. Therefore, a good visibility during the data acquisition was possible resulting in point clouds with a high completeness. In contrast, a dense forest stand is investigated in this study resulting in incomplete point clouds. Another aspect is that many authors study deciduous trees under leave-off conditions. In most cases, the tree heights of the studied trees are much lower than the ones presented in this study, e.g., [12,14–16,18]. Therefore a different scanning geometry and a different point density is given for the upper part of the trees in these studies. A throughout comparison of different modeling approaches is limited since no standard dataset on trees is available nor is there a common method of evaluation. In Raumonon *et al.* [28] a 22 m high Norway spruce (*Picea abies* (L.)) was scanned and further on modeled under leave-on conditions. The tree model and TLS data in Raumonon *et al.* [28] is comparable to the tree models/TLS data from this study. Raumonon *et al.* [28] discuss that the missing data in the upper part of the tree affects the modeling of the upper part, which can be seen in the resulting model. Their resulting model is successfully reconstructed to approximately three quarters of the total tree height. This result is comparable to the results presented in this study.

Regarding modeling of small branches, the minimum modeled diameter is 7 mm. This value is supported by the resolution of the equirectangular maps and the resulting theoretically extractable radius as presented in Section 6.2. Obtaining such a small diameter seems to be realistic for objects

closer than approximately 5 m to the scanner. In general mixed pixels and resulting noise in the TLS measurements limits the modeling of small branches. Wind does not affect the extraction of small branches but it limits their accuracy. It is assumed that a minimum extractable diameter of 1 to 3 cm is realistic for branches larger than 5 m away from the scanner. This value depends on the objects distance to the scanner and the environmental conditions. Similar values are reported in Raunonen *et al.* [28].

Focusing on the TLS data the quality of the acquired data was sufficient for reconstructing the forest scene with a high level of detail. The chosen acquisition and registration strategy delivered well aligned scans, which is crucial for the presented reconstruction method. The resulting tree models look realistic and represent the trees of the dense forest stand up to approximately three quarter of the total individual tree height. Problems with the reconstruction of the uppermost part of a tree are also discussed by other authors (e.g., [19,23,28]). This is mainly caused by imperfections and large data gaps within the point cloud.

The presented method can be improved in a number of ways. A combination with very dense, well aligned airborne laser scanning data acquired by low flying drones or TLS scans carried out from a lifting platform may help to overcome some of the limitations. Alternative map projections may be applied (e.g., stereographic projection for areas close to the zenith). True colored terrestrial laser scans could help the interpreter to distinguish between wooden tree parts and foliage. Given the digitization on the tree surface, larger branches and the stem can be reconstructed by cylinder fitting rather than extracting the radius within the digitization process. Furthermore, the most challenging aspect of automation is obtaining a complete skeleton. Advancing from an approximate skeleton to the axis reconstruction will reduce the need for following curved branches with multiple digitized points. Because of imperfect point clouds (wind, *etc.*), we see a limit in the automation for larger scenes.

In respect to the application of the reconstructed 3D models within the project 3D Vegetation Lab [3], radiative transfer modeling, the accuracy of the presented method is sufficient, as it only covers the stems and major branches. The use of cylinders for tree model representation is well established in radiative transfer modeling, thus the generalization applied in this study is valid. To complete tree models augmenting the structure in the upper parts with synthetic models and populating it with foliage is necessary. For example in Eysn *et al.* [5] shoots were modeled based on triangulating scanner data and cloned across the tree model to simulate the entire tree crown. Additionally radiometric properties can be assigned to the geometric models as shown in Côté *et al.* [37], which provide an appropriate input dataset for radiative transfer modeling.

8. Conclusions

We presented a method for reconstructing 3D tree models based on terrestrial laser scanning data of a forest scene. The trees are modeled by semi-automatically digitizing the wooden parts (*i.e.*, branching and stem structure) in 2D maps. Each tree is described by the axis of its stem and branches and the corresponding radius. The 2D maps are equirectangular projections of the terrestrial laser scanning data showing the range and the intensity measurements of the scanner respectively. The modeling is performed for each viewpoint individually instead of using a merged point cloud, whereas previously reconstructed 2D-skeletons are transformed between the maps. In the final model, the digitized tree skeletons are extruded to cylinders by using the obtained radii.

Due to the requirements of this method to achieve a high completeness and correctness we rely on human interpretation capabilities rather than applying entirely automated approaches. The presented methods therefore focus on enabling simple navigation in the data using 2D maps and incremental completion by using multiple scans. Imperfections of the merged point cloud, caused by remaining registration errors, noise or, *i.e.*, moving branches which were influenced by wind, are mitigated in most cases because of the proposed digitization method. Bridging of gaps may be performed by the operator, but extrapolation or growing of tree structure is not within the scope of this approach.

The main limiting factors for the proposed modeling method are the quality of the TLS data, the visibility of the upper tree parts during the data acquisition and distortions in the 2D maps originating from the chosen projection. These limitations except the last one apply to all reconstruction methods presented in the literature. Summarizing, with the existing approaches our method shares the limitation of reduced visibility in the upper tree parts due to the scan position, it provides better handling of registration errors and wind distortions in the point cloud, a current limitation specific for this method is that areas close to the zenith are not mapped well, and it integrates manual interpretation.

The approach was applied to a terrestrial laser scanning dataset from a managed dense forest stand in Germany. 90 coniferous trees were reconstructed with their stem and branches as visible in 34 single scans. For conifers the occlusions towards the tree tops are limiting the reconstruction. The single trees were modeled up to three quarters of the total tree height. In total 38,101 cylinders were modeled to represent the complete stand. The minimum cylinder diameter modeled shows a value of 7 mm.

The quality of the modeled trees was tested on five randomly picked sample trees. A validation of horizontal slices of the stems by investigating residuals between tree model and scan data shows values between -1.3 cm and 1.7 cm. Additionally a new validation method is proposed to test the models for completeness and correctness. All wooden and defoliated parts of the tree were investigated by deriving the 3D deviations between tree model and point cloud. Standard deviations of the 3D deviations of approximately 1.0 cm were found. In the literature, a high variety of different scanning datasets and validation strategies can be found which makes a qualitative intercomparison challenging. Consequently, there is a need for a standardized validation strategy and input dataset respectively.

In the future the presented method will be developed further, for example by investigating different map projections or automatically extracting the axis of the wooden tree elements from the 2D maps to speed up the digitization process. A standardized benchmark together with other tree modeling approaches is also considered as a future task.

Acknowledgments

This study is partly financed by the ESA funded 3D-VegetationLab project and the project NEWFOR financed by the European Territorial Cooperation “Alpine Space”. We thank Werner Mücke and Franz Blauensteiner for performing the *in situ* TLS measurements.

Conflicts of Interest

The authors declare no conflict of interest.

References

1. ESA European Space Agency (ESA). Available online: <http://www.esa.int/ESA> (accessed on 19 November 2012).
2. ESA European Space Agency (ESA)—Living Planet Programme—Gmes. Available online: http://www.esa.int/esaLP/SEMM4T4KXMF_LPgmes_0.html (accessed on 20 November 2012).
3. ESA 3D Vegetation Lab. Available online: http://due.esrin.esa.int/stse/projects/stse_project.php?id=139 (accessed on 20 November 2012).
4. Lovell, J.L.; Jupp, D.L.B.; Newnham, G.J.; Culvenor, D.S. Measuring tree stem diameters using intensity profiles from ground-based scanning lidar from a fixed viewpoint. *ISPRS J. Photogramm. Remote Sens.* **2011**, *66*, 46–55.
5. Eysn, L.; Ressler, C.; Graf, A.; Hollaus, M.; Mücke, W.; Morsdorf, F.; Pfeifer, N. Extraction of 3D Tree Models Based on Equirectangular Projections of Terrestrial Laser Scanning Data. In Proceedings of SilviLaser 2012, Vancouver, BC, Canada, 16–19 September 2012.
6. Biliouris, D.; van der Zande, D.; Verstraeten, W.; Muys, B.; Coppin, P. Assessing the impact of canopy structure simplification in common multilayer models on irradiance absorption estimates of measured and virtually created *Fagus sylvatica* (L.) stands. *Remote Sens.* **2009**, *1*, 1009–1027.
7. Xinlian, L.; Litkey, P.; Hyyppä, J.; Kaartinen, H.; Vastaranta, M.; Holopainen, M. Automatic stem mapping using single-scan terrestrial laser scanning. *IEEE Trans. Geosci. Remote Sens.* **2012**, *50*, 661–670.
8. Hopkinson, C.; Chasmer, L.; Young-Pow, C.; Treitz, P. Assessing forest metrics with a ground-based scanning lidar. *Can. J. For. Res.* **2004**, *34*, 573–583.
9. Maas, H.G.; Bienert, A.; Scheller, S.; Keane, E. Automatic forest inventory parameter determination from terrestrial laser scanner data. *Int. J. Remote Sens.* **2008**, *29*, 1579–1593.
10. Tansey, K.; Selmes, N.; Anstee, A.; Tate, N.J.; Denniss, A. Estimating tree and stand variables in a corsican pine woodland from terrestrial laser scanner data. *Int. J. Remote Sens.* **2009**, *30*, 5195–5209.
11. Bienert, A.; Scheller, S.; Keane, E.; Mohan, F.; Nugent, C. Tree Detection and Diameter Estimations by Analysis of Forest Terrestrial Laserscanner Point Clouds. In Proceedings of ISPRS Workshop on Laser Scanning 2007 and SilviLaser 2007, Espoo, Finland, 12–14 September 2007; pp. 50–55.
12. Dassot, M.; Colin, A.; Santenoise, P.; Fournier, M.; Constant, T. Terrestrial laser scanning for measuring the solid wood volume, including branches, of adult standing trees in the forest environment. *Comput. Electron. Agric.* **2012**, *89*, 86–93.
13. Schilling, A.; Schmidt, A.; Maas, H.G. Tree topology representation from TLS point clouds using depth-first search in voxel space. *Photogramm. Eng. Remote Sens.* **2012**, *78*, 383–392.
14. Delagrangé, S.; Rochon, P. Reconstruction and analysis of a deciduous sapling using digital photographs or terrestrial-lidar technology. *Ann. Bot.* **2011**, *108*, 991–1000.
15. Vonderach, C.; Vögtle, T.; Adler, P.; Norra, S. Terrestrial laser scanning for estimating urban tree volume and carbon content. *Int. J. Remote Sens.* **2012**, *33*, 6652–6667.

16. Hosoi, F.; Nakai, Y.; Omasa, K. 3-D voxel-based solid modeling of a broad-leaved tree for accurate volume estimation using portable scanning lidar. *ISPRS J. Photogramm. Remote Sens.* **2013**, *82*, 41–48.
17. Bucksch, A. Revealing the Skeleton from Imperfect Point Clouds. Ph.D. Thesis, Delft University of Technology, Delft, The Netherlands, 2011.
18. Bucksch, A.; Lindenbergh, R.; Menenti, M. SkelTre. *Vis. Comput.* **2010**, *26*, 1283–1300.
19. Pfeifer, N.; Gorte, B.; Winterhalder, D. Automatic Reconstruction of Single Trees from Terrestrial Laser Scanner Data. In Proceedings of the XXth ISPRS Congress: Geo-Imagery Bridging Continents, Istanbul, Turkey, 12–23 July 2004; pp. 114–119.
20. Thies, M.; Pfeifer, N.; Winterhalder, D.; Gorte, B.G.H. Three-dimensional reconstruction of stems for assessment of taper, sweep and lean based on laser scanning of standing trees. *Scand. J. For. Res.* **2004**, *19*, 571–581.
21. Gorte, B.; Pfeifer, N. Structuring Laser-Scanned Trees Using 3D Mathematical Morphology. In Proceedings of the XXth ISPRS Congress: GeoImagery Bridging Continents, Istanbul, Turkey, 12–23 July 2004; pp. 929–933.
22. Palágyi, K.; Tschirren, J.; Sonka, M. Quantitative Analysis of Intrathoracic Airway Trees: Methods and Validation. In *Information Processing in Medical Imaging*; Taylor, C., Noble, J.A., Eds.; Springer: Berlin/Heidelberg, Germany, 2003; Volume 2732, pp. 222–233.
23. Côté, J.-F.; Fournier, R.A.; Egli, R. An architectural model of trees to estimate forest structural attributes using terrestrial lidar. *Environ. Model. Softw.* **2011**, *26*, 761–777.
24. Verroust, A.; Lazarus, F. Extracting Skeletal Curves from 3D Scattered Data. In Proceedings of International Conference on Shape Modeling and Applications (Shape Modeling International '99), Aizu, Japan, 1–4 March 1999; pp. 194–201.
25. Runions, A.; Lane, B.; Prusinkiewicz, P. Modeling Trees with a Space Colonization Algorithm. In Proceedings of Eurographics Workshop on Natural Phenomena, Prague, Czech Republik, 4 September 2007.
26. Palubicki, W.; Horel, K.; Longay, S.; Runions, A.; Lane, B.; Mech, R.; Prusinkiewicz, P. Self-organizing tree models for image synthesis. *ACM Trans. Graph.* **2009**, *28*, 1–10.
27. Cheng, Z.; Zhang, X.; Fourcaud, T. Tree Skeleton Extraction from a Single Range Image. In Proceedings of Second International Symposium on Plant Growth Modeling and Applications (PMA '06), Beijing, China, 13–17 November 2006; pp. 274–281.
28. Raumonon, P.; Kaasalainen, M.; Åkerblom, M.; Kaasalainen, S.; Kaartinen, H.; Vastaranta, M.; Holopainen, M.; Disney, M.; Lewis, P. Fast automatic precision tree models from terrestrial laser scanner data. *Remote Sens.* **2013**, *5*, 491–520.
29. Dassot, M.; Constant, T.; Fournier, M. The use of terrestrial lidar technology in forest science: Application fields, benefits and challenges. *Ann. For. Sci.* **2011**, *68*, 959–974.
30. Bucksch, A.; Khoshelham, K. Localized registration of point clouds of botanic trees. *IEEE Geosci. Remote Sens. Lett.* **2013**, *10*, 631–635.
31. Zoller+Fröhlich Technical Data z+f IMAGER 5006i. Available online: http://sluzby.geodis.cz/uploads/dokumenty/laserove_skenovani/Datenblatt_IMAGER5006i_E.pdf (accessed on 22 November 2012).

32. Brinker, R.C.; Minnick, R. *The Surveying Handbook*; Springer-Science+Business Media, B.V.: Dordrecht, The Netherlands, 1995; p. 971.
33. ESRI Understanding World Files. Available online: http://webhelp.esri.com/arcims/9.2/general/topics/author_world_files.htm (accessed on 9 April 2013).
34. OPALS Orientation and Processing of Airborne Laser Scanning Data. Available online: <http://www.geo.tuwien.ac.at/opals/> (accessed on 19 November 2012).
35. IDC Software Package Geosi Netz. Available online: <http://www.geosi.at/index.php?id=78&L=0> (accessed on 22 November 2012).
36. Zoller+Fröhlich Software Package Z+F Laser Control 8.2. Available online: <http://www.zf-laser.com/Z-F-LaserControl.132.0.html> (accessed on 9 April 2013).
37. Côté, J.-F.; Widłowski, J.-L.; Fournier, R.A.; Verstraete, M.M. The structural and radiative consistency of three-dimensional tree reconstructions from terrestrial lidar. *Remote Sens. Environ.* **2009**, *113*, 1067–1081.

© 2013 by the authors; licensee MDPI, Basel, Switzerland. This article is an open access article distributed under the terms and conditions of the Creative Commons Attribution license (<http://creativecommons.org/licenses/by/3.0/>).

Curriculum vitae

ZUR PERSON

Name: Dipl. Ing. Lothar Harald Rüdiger Eysn
Geburtsdaten: 09.04.1980, Wien
Familienstand: verheiratet, keine Kinder
Ehefrau: Dipl. Päd. Daniela Eysn, BEd MA, Lehrerin
Staatsangehörigkeit: Österreich



AUSBILDUNG

- 11/2009 – gegenwärtig **Technische Universität Wien** – Wien
Studium: Dr.-Studium der techn. Wissenschaften Vermessung und Geoinformation
Doktorarbeit „Multi-Scale 3D Modeling and Parametrization of the Resource Forest Based on Airborne and Terrestrial Laser Scanning“
- 10/1999 - 04/2009 **Technische Universität Wien** - Wien
Studium: Vermessung und Geoinformation, Fachrichtung: Geodäsie und Geophysik
Abschluss: Dipl. Ing.
30.04.2009, Diplomprüfung
Diplomarbeit „Untersuchung und praktische Erprobung des terrestrischen Laserscanners FARO Photon 80“
- 09/1994 - 06/1999 **Höhere Technische Bundeslehranstalt** - Saalfelden
Fachrichtung: Hochbau
Abschluss: Matura
22.06.1999, Reife- und Diplomprüfung

BERUFLICHE ERFAHRUNG

- 09/2015 – gegenwärtig **Stadt Wien, MA41 Stadtvermessung** – Wien, *Höherer technischer Dienst, Fachbereiche Technische Vermessung und Photogrammetrie/ 3D Modellierung*
- 11/2009 – 09/2015 **Technische Universität Wien, Department für Geodäsie und Geoinformation, Forschungsgruppe Photogrammetrie** - Wien, *Projekt Assistent*
- 05/2009 - 10/2009 **Vermessungsbüro Dipl. Ing. Robert Wagner** - Wien, *Technischer Mitarbeiter*
- 04/2009 - 06/2009 **Technische Universität Wien, Institut für Photogrammetrie und Fernerkundung** - Wien, *Projektmitarbeiter*
- 09/2004 - 10/2009 **Vermessungsbüro Burkhard Dörflinger** - Wien, *Technischer Mitarbeiter*
- 01/1995 – 09/2004 **Vermessungsbüro Dipl. Ing. Harald Eysn** – Zell am See, *Technischer Mitarbeiter*

